STRUCTURE AND CONFORMATIONS OF HETEROPOLYSACCHARIDES

by

RALPH MOORHOUSE

A thesis presented for the Degree of Doctor of Philosophy at the University of Aston in Birmingham.

December, 1974.

SUMMARY

The various geometrical and molecular forces that can define the conformation adopted by a polysaccharide chain are reviewed. Specific characterised examples are used to illustrate the various general polysaccharide conformational types.

The use of optical rotation, circular dichroism and nuclear magnetic resonance in the investigation of conformations adopted by polysaccharides in solution and the types of junctions that can be involved, are considered.

Various solid state conformations adopted by hyaluronate have been studied by Xray diffraction techniques. A four-fold helical structure having a fibre repeat of 3.39 nm is the more readily obtained form. Initial computer model building studies showed that a double helical structure was one interpretation of the data. Subsequent calculations by colleagues have shown that a single helical structure provides a more favourable interpretation of the results. The conformation of hyaluronate in solution has been examined by various physical techniques. One of these, nuclear magnetic resonance has demonstrated the presence of a novel ordered conformation in solution that is stable to changes in salt concentration, temperature and pH 2.5-7.0. The order can be disrupted by enzymic cleavage or the action of mild alkali. The relationship between such an ordered conformation and the physical and biological properties of hyaluronate are considered.

A preliminary interpretation of Xray diffraction patterns for two bacterial polysaccharides is given.

The uncertainty surrounding their covalent structures is discussed and preliminary computer models corresponding to the various possibilities have been investigated.

Part of the work described in Chapter 2 of this thesis has been published in collaboration with Drs. I.C.M. Dea, D.A. Rees, S. Arnott, J.M. Guss and E.A. Balazs. A reprint is included at the end of the thesis.

CONTENTS

ACKNOWLEDGEMENTS

I should like to express my sincerest thanks to Professor D.A. Rees for his guidance throughout the course of this research. I am most grateful for his patience and understanding during this time.

I am also grateful to Dr. B.J. Tighe for acting as my internal supervisor at the University of Aston.

My thanks are also due to all my colleagues at both Unilever and Purdue University for many stimulating discussions.

I am also grateful to Unilever Ltd., for allowing me to undertake this research and for the provision of such excellent facilities.

CHAPTER 1

General Introduction

INTRODUCTION

Conformational studies on a variety of biopolymers, both in the liquid and solid state, have in some cases been able to further our understanding of chemical and biological properties at the molecular level.

The work described in this thesis attempts to further the knowledge of the conformations adopted, both in solution and in the solid state, by certain polysaccharides of biological or industrial importance.

A. Conformations of monosaccharides

Prior to any consideration of the overall conformations adopted by polysaccharides it is essential to have a full knowledge of the shape adopted by the monomeric units and the disposition and orientation of their pendant atoms.

In the hexose sugars considered here, the predominant form of the molecule is the pyranose ring. However, within this general classification, several forms are possible, all existing without undue distortion of the tetrahedral bond angles. The most common are the Reeves (1949) $^{C}_{1}$ and $^{1}_{C}$ chair forms although several 'boat' forms do exist (Fig. 1.1).

The existence of one form or another is determined by relative free energies (Reeves, 1951), such that any given sugar exists in one or other of the conformations or a mixture, and not in any intermediate form. The preferred ring conformations of most sugars have been firmly established for some time, and are normally one or other of the chair forms, for which $^{C}_{1}(\underline{D})\equiv{}^{1}_{C}(\underline{L})$ is much more common than $^{1}_{C}(\underline{D})\equiv{}^{C}_{1}(\underline{L})$.

(a)

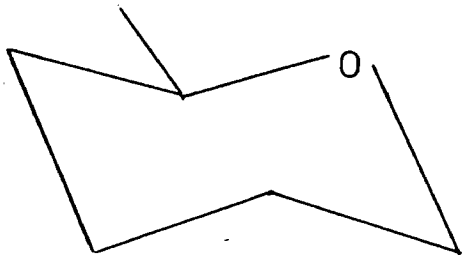

(b)

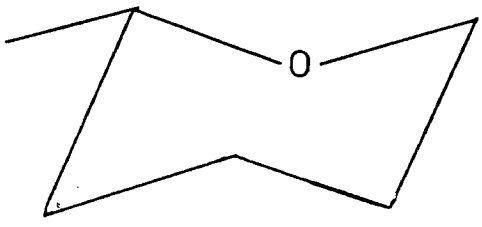

(c)

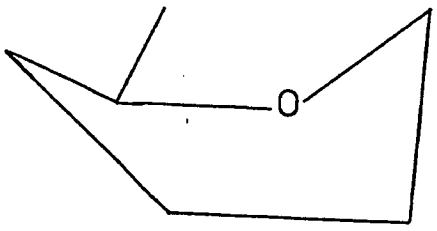

Fig. 1.1 Possible pyranose ring conformations

(a) Reeves C1 chair, (b) Reeves 1C chair,

(c) Reeves B1 boat (several other boat forms exist).

The relative positions of the ring atoms have been fixed by numerous crystal studies and for sugars having the same 'chair' form there tends to be little variance from the norm. Although pyranose rings are commonly assumed to be rigid, bond angles can easily be subject to small distortions as a result of intramolecular attractions and repulsions.

A recent survey of a large number of model carbohydrate crystal structures by Arnott and Scott (1972) showed significant variations in the accurately derived parameters. As a consequence they have derived a standard sugar residue with bond-lengths, bond-angles, and ring conformation-angles that are the most reasonable average of the survey. (Unless otherwise stated all conformational calculations undertaken in this work employed Arnott and Scott coordinates.)

By fixing the position of ring atoms, certain other atoms are also fixed merely by assuming fixed bond lengths and angles. However pendant atoms that can rotate about single bonds have to be treated individually since the particular rotations will depend on the presence, type and influence of neighbouring atoms or groups. In the extreme case, the pendant group can be another sugar ring (Fig. 1.2).

The relationship between such pairs of sugars forms the basis of conformational analysis of polysaccharides.

B. Conformation of polysaccharides

Conformational analysis of polysaccharides and most natural and synthetic polymeric molecules utilises methods descended from the approach used by Corey and Pauling to derive polypeptide conformation.

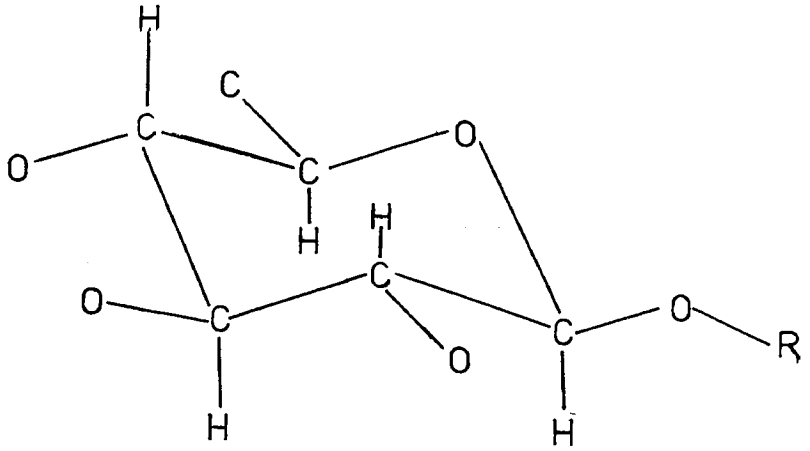

(a)

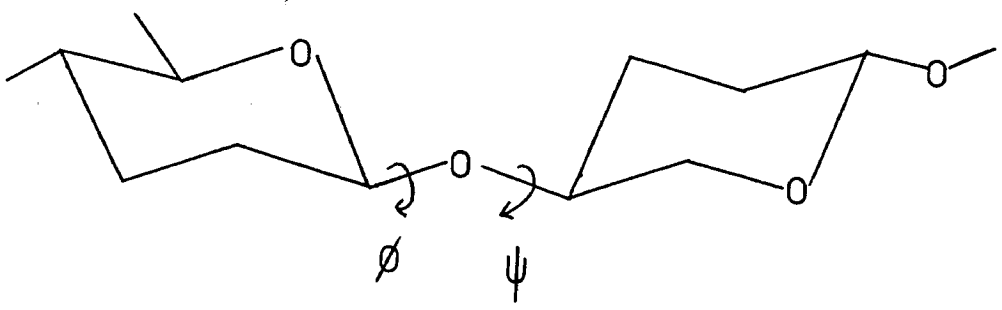

(b)

Fig. 1.2 The positions of all the atoms in (a) (except R) are fixed by the assumption of rigid bond lengths and angles.

R is a pendant atom or group (e.g. another sugar ring) as in (b), whose relative orientation is defined by the dihedral angles ϕ and ψ.

Several reviews on the conformations of proteins and other polymers are available - notable amongst them is the recent work of Flory (1969).

To correlate molecular geometry with, say, biological function, it will usually be adequate to be able to define relative atomic positions with a precision of about 0.01 nm. This accuracy is necessary to identify the more intimate non-bonded and hydrogen bonded contacts within and between molecules. For fibrous polymer systems this precision is not generally attainable by analysis of Xray diffraction intensities alone (James, 1965). This is mainly a consequence of the relatively low resolving power ($>$ 0.02 nm) of Xray data, even from very crystalline fibrous samples. Of course single crystal analysis can and does give the required precision that is used as the basis for the conformational analysis of a polymer.

In its simplest form conformational analysis requires a statement of the stereochemical constraints that can be safely assumed, such as:-

(i) the geometry of the sugar ring and pendant atoms.

(ii) the tendency towards hydrogen bonding resulting from a specified geometry.

(iii) the planarity or otherwise of the amide group in the acetamido sugars.

(iv) particular values for van der Waals radii.

The remaining parameters, the angles ϕ and ψ (Fig. 1.2), defining the glycosidic bridge conformations and the side chain orientations are considered as explicit variables, and are used to systematically derive the best or average conformation. This is usually done

by computer methods similar to those described in later Chapters, although the use of physical models can play an important part in the derivation as will be shown in Chapter 4.

Using expressions available for generating conformations of generalised polymers (Miyazawa, 1961; Mizushima and Shimanouchi, 1961; Némethy and Scheraga, 1965; Sugeta and Miyazawa, 1967), polysaccharide chains may be generated for sugar residues of any sequence and of any length (Rees and Skerrett, 1970), including chains of alternating sugar residues (Anderson et al. 1969). If the linkage conformation is regular (i.e. a repeating di-, tri-, tetra-saccharide etc.), then the polymer chain will describe an extended or helical structure, further, if such a structure can be stabilised by, say, intramolecular hydrogen bonding, then a regular conformation of this kind will be favoured. Alternatively it may be found that the most favourable conformation is one in which, several helices, commonly two or three, intertwine and be similarly stabilised by inter-chain hydrogen bonding.

The most stable conformation is one which satisfies all these criteria, achieved by placing like atoms or groups in almost the same surroundings.

If the intra-molecular forces are very much stronger than the inter-molecular forces, then in the crystalline state, the polymer should assume a conformation close to minimum energy on the conformational energy maps obtained for the isolated molecule (Rao et al. 1967). Conversely if the inter-molecular forces have the greater influence, the conformation of the polymer need not occur near the energy minima but will be within the allowed region i.e. free or almost free of van der Waals compression.

The advantage of calculations of energy functions is that they can be conveniently used to calculate the properties of the random coil as well as to discriminate between alternative ordered conformations (Rees 1972). Such calculations do however have limitations for the random coil in that they only consider interactions between adjacent residues. Consequently clashes are missed between residues that are remote in the covalent sequence and which should disallow many of the more compact overall conformations, by tending to expand the average shape.

It has been shown (Ramachandran et al, 1963; Rees and Skerrett, 1968) that van der Waals repulsion has a dominant influence on many polysaccharide conformations more so, for example, than in polypeptides and polynucleotides. Consequently most of the achievements in the conformational analysis of polysaccharides have been possible because it is relatively easy to rank conformations in order of increasing or decreasing van der Waals repulsion.

It should be realised that to explore the variation in glycosidic angles, pendant group orientation and also to provide some degree of flexibility in the ring bond angles is the ideal. It is also impracticable due to prohibitive computing time required for such an exhaustive analysis. The procedure of Arnott and Scott (1972) does, however, seem to provide the best approach to the 'ideal' situation. This is based on the linked-atom procedure of Arnott and Wonacott (1966), in which bond length, bond angles and conformational angles were explicit parameters. The bond lengths were fixed, the bond angles usually were fixed but might be variable and the conformational angles had variable values based on the analysis of the Xray diffraction pattern, in all constituting a

linked-atom description of the molecular chain. The best values for the structural variables in agreement with measured intensities are obtained - a procedure that has had outstanding success when applied to fibrous polypeptides and nucleic acids (Arnott 1970). Analogous procedures have been proposed and found efficient for refining globular protein conformations (Diamond 1966).

This method for establishing polysaccharide conformations based on fibre diffraction data together with model building 'packages' currently under development by Arnott et al, that consider the molecular chain packed in conjunction with others rather than in isolation, will doubtless become standard procedure in the coming years. The inherent advantage of this type of approach is that because refinement is against measured intensities there is a reduced probability of artefacts being carried over from the starting assumptions. Otherwise this can cause inaccuracies in the molecular chain that are effectively multiplied along the length of the chain.

Polysaccharide chain shapes

Rees (1972) has classified the known and postulated homopolysaccharide chain shapes. However, before defining each shape, it is useful to remember that any regular conformation of a polymer can be described as a helix, which is specified by the two parameters n and h (Fig. 1.3), where

n - is the number of monomer residues per turn of helix

h - is the projected height of each monomer residue on the helix axis.

These parameters are dependent upon the particular values of the glycosidic angles ϕ and ψ, and the fixed geometrical features

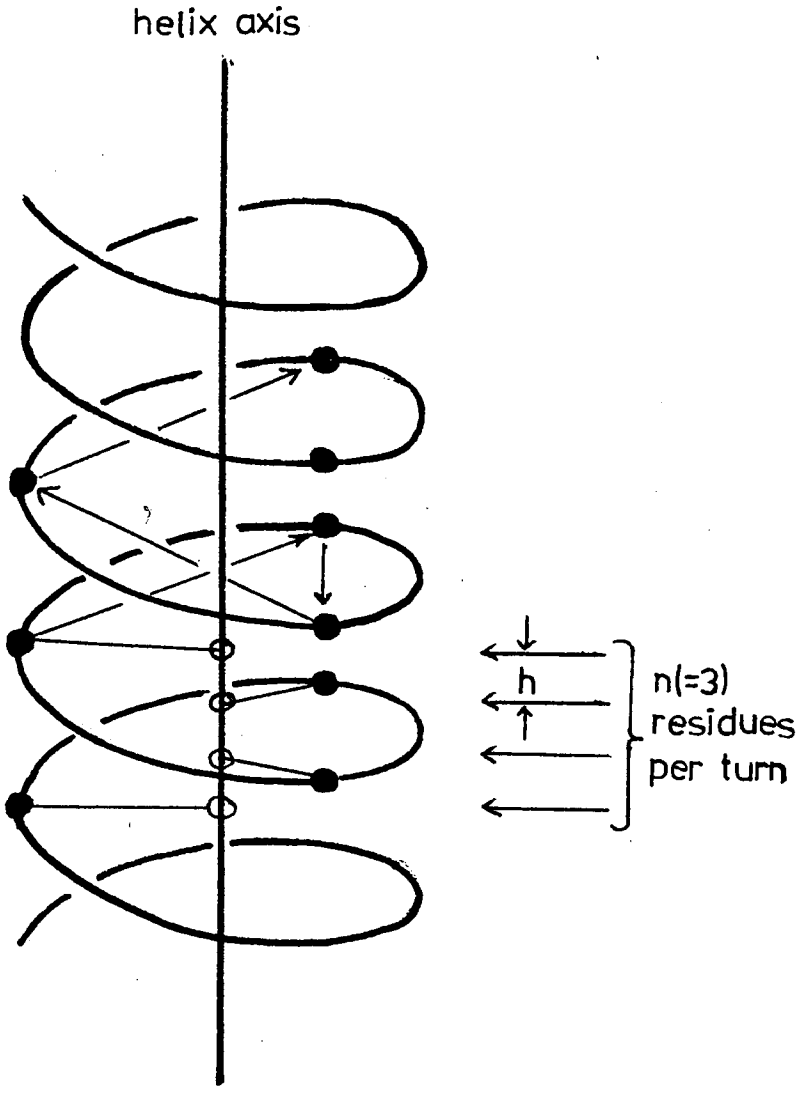

Fig. 1.3 Helix parameters n and h

The filled in circles represent equivalent atoms (e.g. glycosidic oxygens) on successive residues of a regular homopolysaccharide.

of the chain (Ramanchandran, 1963). In the case of a heterosaccharide n and h take on values corresponding to the relevant repeating unit.

The values of n and h considered by Rees (1972) fall into four ranges that are characteristic of various covalent structures (Rees and Scott, 1971) (Fig. 1.4).

(i) Type A - an extended ribbon, having h close to the maximum allowed for the residue, with n in the range $2 \rightarrow \pm 4$ ($-n$, indicates a left handed helix).

The skeletal polysaccharides such as cellulose, β 1,4-xylan and β 1,4-mannan are in this group, suggesting that extended conformations are necessary to form structurally strong materials.

(ii) Type B - a spring-like structure that can exist in various states of extension that vary from close to maximum to almost zero. The allowed n values similarly cover a much wider range (e.g. $2 \rightarrow \pm 10$).

Reserve polysaccharides such as amylose prefer this wider type of conformation. β 1,3-xylan although a wide helix of this type is given more rigidity by forming multiple helices, occurring as triple helices in the cell walls of certain marine algae (Atkins et al. 1969).

(iii) Type C - crumbled ribbon, characteristic of 1,2-linked polymers.

(iv) Type D - a loosely jointed and possibly extended conformation characterised by polymers having the additional degree of freedom conferred by a 1,6-linkage.

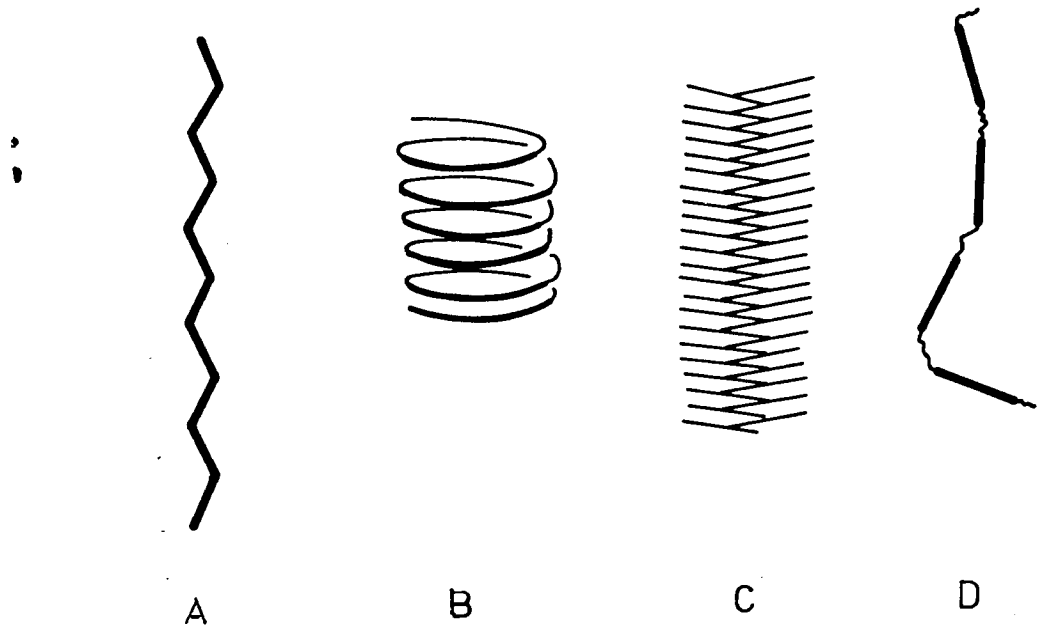

Fig. 1.4 Schematic representation of the types of regular conformation predicted for polysaccharides by conformational analysis in the computer.
Type A, extended and ribbon-like, e.g. β1,4-glucan;
Type B, flexible and helical, e.g. β1,3-glucan;
Type C, crumpled and contorted, e.g. 1,2 glucans;
Type D, loosely jointed and extended, all 1,6 linked polysaccharides.

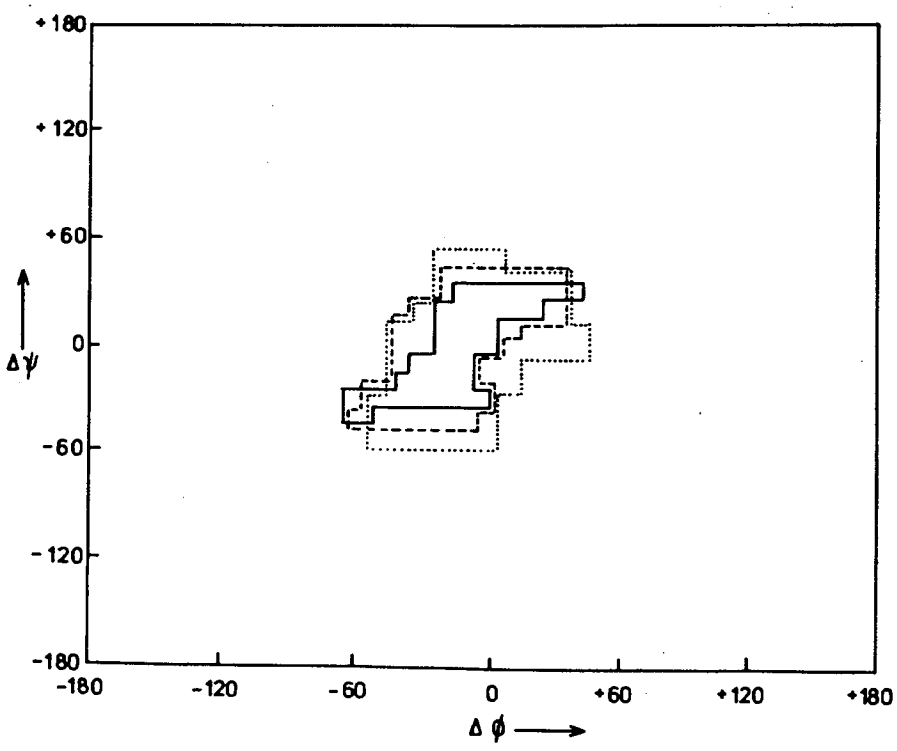

Fig. 1.5 Conformational maps for α-1,4-, α-1,3- and α-1,2-glucans

Allowed conformations are enclosed by continuous, broken and dotted lines respectively, showing the similarity between three different conformation types (cf. Fig. 1.4).

In this work we shall only be interested in Types A and B and combinations thereof.

The conformation adopted by a polymer does not appear to be determined entirely by the interactions between sugar residues (i.e. by ϕ and ψ) since these can be similar for different types (Fig. 1.5), but rather by the dihedral angle across the sugar ring (Fig. 1.6a,b). In their survey of homopolysaccharides Rees and Scott (1971), showed that when the ring dihedral angle was 180° (Fig. 1.6a) then the polysaccharides usually had a range of extended Type A conformations. Alternatively when this angle was close to zero (Fig. 1.6b) a type B conformation was favoured.

Specific examples of characterised helical forms

(a) Cellulose

The most important and variously defined Type A conformation is that of cellulose, the homopolysaccharide of β 1,4D-glucose. Two different crystalline models of cellulose have been reported, the 'straight chain' model of Meyer and Misch (1937) and the 'bent chain' model of Hermans (1943). The axial repeat of cellulose is 1.03 nm and based on the stereochemical knowledge of the time, Meyer and Misch (1937) proposed a two-fold screw axis along the chain in which all the glycosidic oxygens were coplanar (Fig. 1.7a). However it was eventually realised (Carlström 1962) that this structure implied a steric clash between the C(6) and O(2') atoms of contiguous residues. For this reason the 'bent chain' conformation (Fig. 1.7b) originally proposed by Hermans (1943) came into favour by contemporary workers. It also allows a favourable and stabilising, hydrogen bond between the O(3) hydroxyl of one residue and the O(5)' ring oxygen of the next.

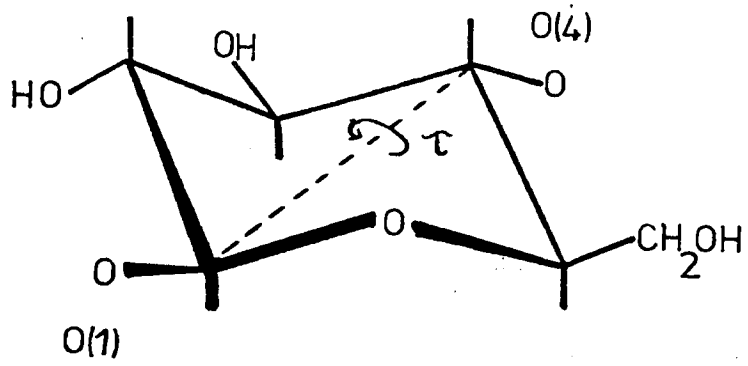

(a)

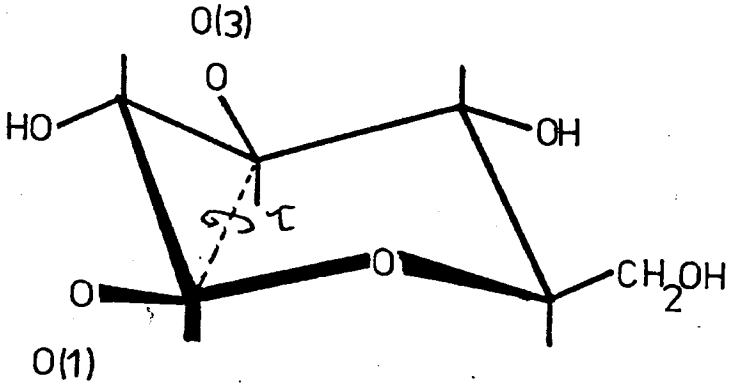

(b)

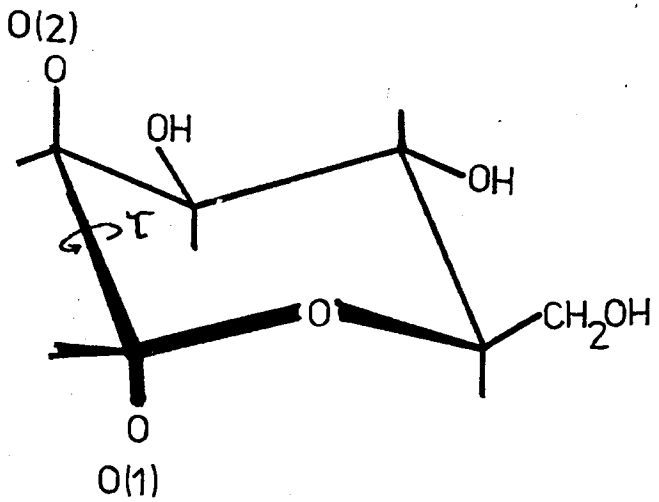

(c)

Fig. 1.6 Dihedral angle across Reeves C1 sugar ring

(a) β1,4-glucose, $\tau \simeq 180°$

(b) β1,3-glucose, $\tau \simeq 0°$

(c) α1,2-mannose, $\tau \simeq 180°$

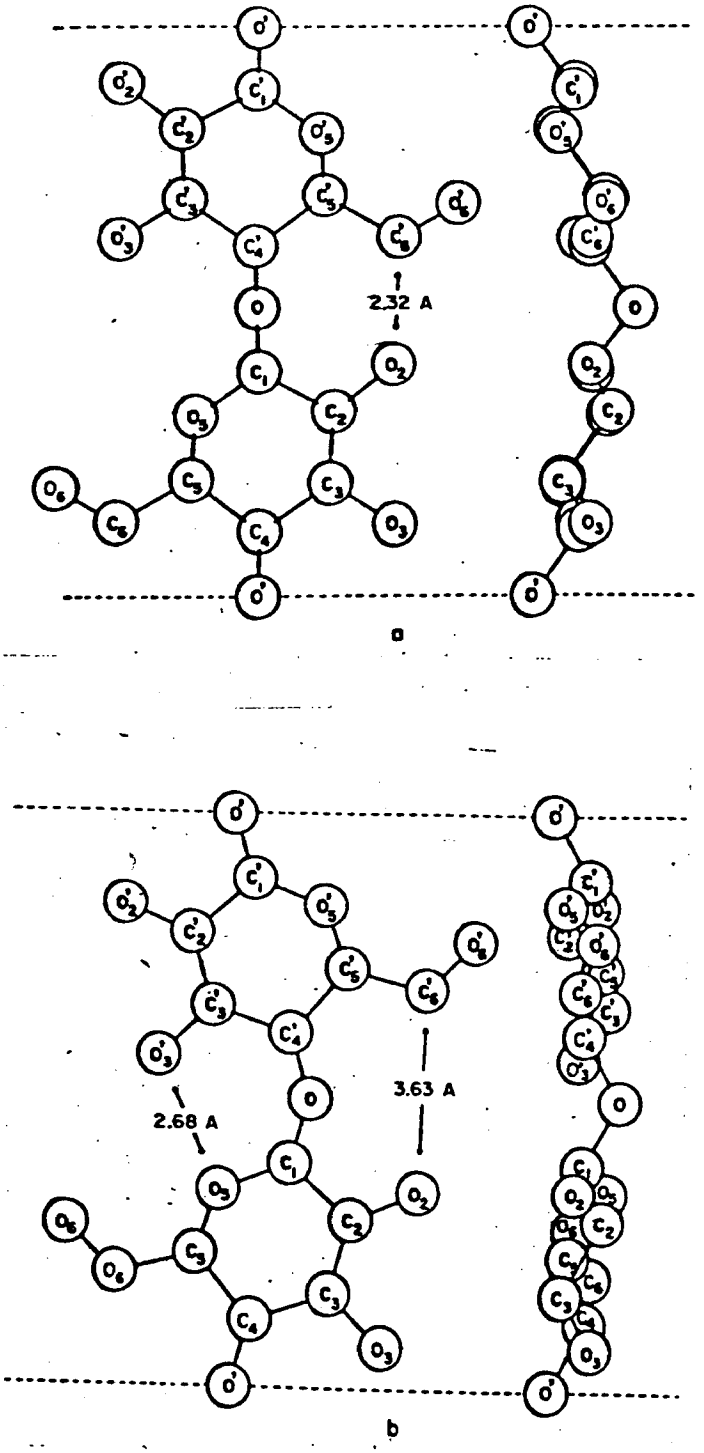

Fig. 1.7 Spatial arrangements of the cellulose chain

(a) Meyer and Misch (1937), 'straight chain';

(b) Hermans (1943), 'bent chain'.

The presence of this type of hydrogen bond has been substantiated by both polarised infra-red spectra of cellulose (Liang and Marchessault 1959) and in the crystal structure of the cellobiose dimer (Brown, 1966; Chu and Jeffrey, 1968). Recent calculations by Sundararajan and Marchessault (1972) further suggests that the bent chain conformation is most favourable and recent work suggests a plausible model in which the chains are packed parallel to each other (Blackwell and Gardner, unpublished).

(b) Amylose

Amylose, a α 1,4-glucan, when complexed with iodine and various other complexing agents, forms a low h type B 6-fold helix loosely termed the 'V' form (Fig. 1.8). The actual diameter of the helix varies according to the amount of water of crystallisation present and the size of the complexing molecule which is held in the centre of the helix (Bumb and Zaslow, 1967; French and Zaslow, 1972; French et al. 1963). The helix is probably left handed (Hybl et al. 1965) and has hydrogen bonds between O(2) and O(6) of adjacent residues on the helix surface but separated by five others in the primary sequence.

Another regular conformation of amylose is produced when the complexing agent is removed from the 'V' form and the product subjected to high humidity. This causes the structure to adopt the more extended 'B' form since the h value has increased

from 0.79 to 1.04 nm. Blackwell et al.(1969) have shown that the helix can be stabilised at this new extension by insertion of a water molecule between the O(2) - O(6) hydrogen bond present in the 'V' form. It has also been suggested that the 'B' amylose chain is extended to 2.1 nm (French, 1969), the observed axial repeat being due to an exactly staggered second parallel chain, intertwined to form a double helix; this model is however difficult to reconcile with hard sphere and energy calculations (Blackwell et al. 1969; Rees, 1972). Using the procedure of Rees (Anderson et al. 1969), Smith (1972) was unable to state categorically that a double helical structure was possible. However, if it is possible to extend the projected residue height by 0.05nm without imposing too great a strain, then a double helical structure would appear to have a conformation closest to the energy minimum.

(c) β 1,3 Xylan

The β 1,3 Xylan structure has a repeat period of 1.8 nm, giving a projected residue height of 0.3 nm for each sugar unit; a more extended version of the amylose type of structure. The hole that existed in the amylose helix is now filled by twisting three strands together in a triple helix. The structure is suitably stabilised by inter-chain bonding by O(2) atoms, one from each chain forming a cyclic triad (Fig. 1.9).

The original work by Atkins et al. (1969) proposed a preference for a right-handed helix, although both are possible. Sathyaneragan and Rao (1970) showed by energy calculations that both left- and right-handed helices had similar energies but that the right handed is slightly favoured by the formation of weak hydrogen bonds with water molecules to bridge the strands (similar to 'B'amylose). Recent

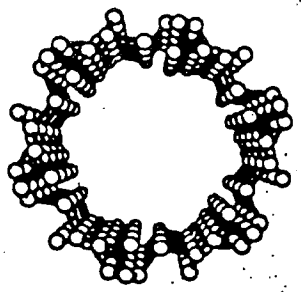

Fig. 1.8 View down amylose 'V' form helix

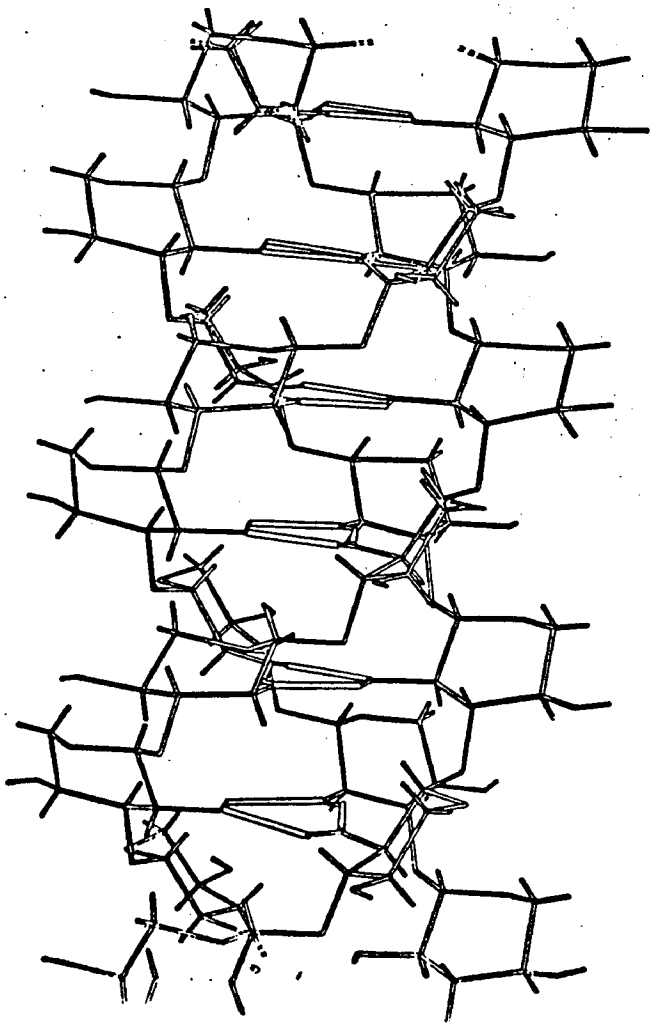

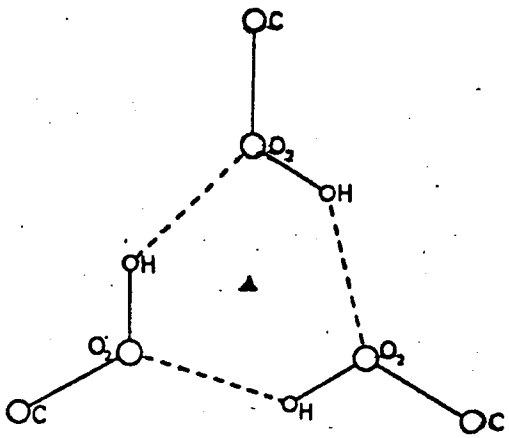

Fig. 1.9 β1,3-xylan triple helix and hydrogen bonding triad.

calculations (Smith, 1972) of the conformational potential energy arising from interactions between and within strands again slightly favour the right-handed conformation.

(d) Alternating Structures

Most of the naturally occuring homopolysaccharides fall into the first two 'Rees-types'. Heteropolysaccharides (i.e. having an alternating repeat unit) have characteristics of both 'types'.

Hyaluronate, that will be discussed in detail in Chapter 2, can be considered as an alternating polymer of β 1,3- and β 1,4-linked glucose units. Computer model building studies (Rees, 1969; Rees et al. 1969) showed that conformation with projected residue heights between 0.72 and 1.02 nm were sterically allowed, indicating a helical conformation probably in between Type A and Type B. It was not surprising, therefore, to find that hyaluronate shows considerable conformational variability, exhibiting a two-fold form (Atkins et al. 1972) that is near a Type A conformation through to a four-fold form that is more compact and sinuous, near to a Type B conformation (Dea et al. 1973; Atkins et al. 1973).

It is possible to consider this variability in the conformations of β 1,4/β 1,3 alternating structures in the following way.

If the polymer is considered to have a repeating unit linked β 1,4 to the next, in which the repeat unit is a disaccharide that is 'locked' such that the β 1,3-linkage can be ignored for the moment. Then, by analogy with β 1,4 linked homopolymers (as this now is) an extended ribbon Type A conformation would be expected. Conversely if the β 1,4-linkage is considered fixed then a conformation near to a Type B helix

would be expected. Therefore, the variability becomes apparent as the β 1,3-linkage gradually alters from its 'fixed' position causing the repeat unit (the disaccharide) to become 'looser' taking on more of the Type B conformation.

The closely related kappa-and iota-carrageenans (Fig. 1.10) which have been studied in some detail (Anderson et al. 1969; Arnott et al. 1974) can be considered to have a similar covalent backbone to hyaluronate (see Chapter 2 Fig. 2.15), and have similar conformational characteristics. Similar to hyaluronate the conformation corresponding to the Xray diffraction data shows a considerable deviation from the type A ribbon in that the helices are more sinuous and of sufficient size to accommodate a second intertwined helix. Kappa-carrageenan is a right-handed three-fold double helix having an axial periodicity of 2.46 nm, iota-carrageenan is similar except that the periodicity is 2.65 nm and that the second identical chain is translated axially 1.328 nm relative to the other. The iota-carrageenan structure is partially stabilised, by a hydrogen bond buried within the double helix that has been demonstrated by its resistance to deuterium exchange (Williamson 1970).
The overall shape of these helices is very much like an extended type B helix with a distinct hole down the centre of the helix (Fig. 1.11). In contrast to amylose the inside of the helix cannot accommodate another molecule, consisting mainly of relatively apolar groups of carbon and hydrogen atoms whose net mutual interactions are strongly attractive and include longer range polar forces as well as van der Waals attractions (Smith 1972).

In summary, the predictions and correlations of conformations, can be made by simple analogy but the method does fail sometimes, particularly with alternating polysaccharides.

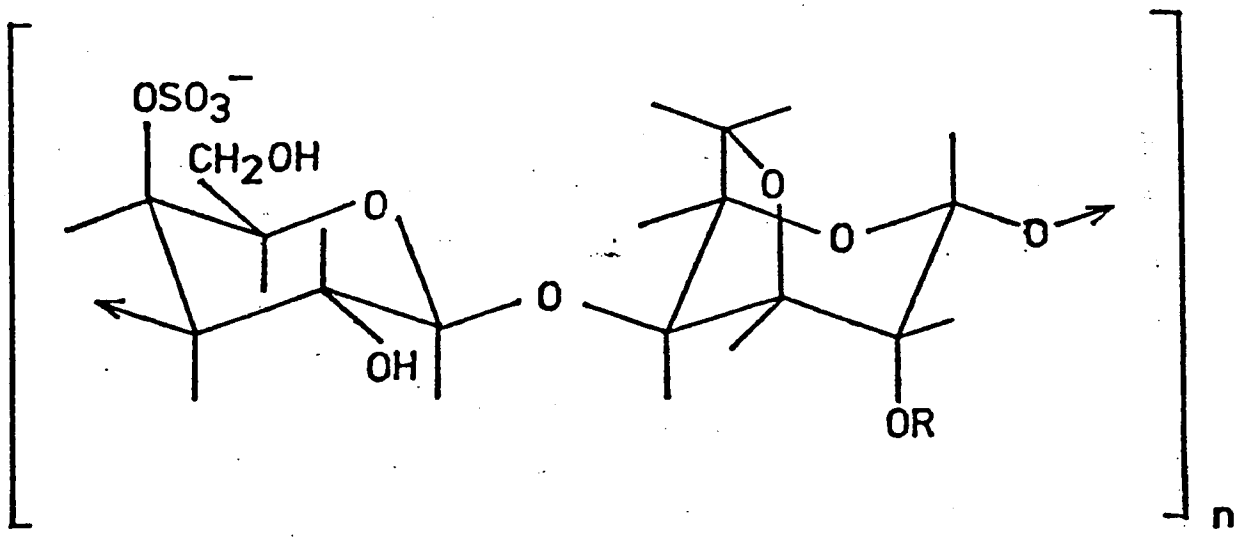

Fig. 1.10 Carrageenan disaccharide repeating units

(a) kappa-carrageenan, R=H.

(b) iota-carrageenan, $R=SO_4$.

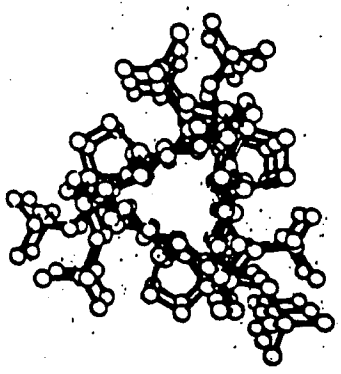

Fig. 1.11 View down iota-carrageenan double helix

This is shown clearly in the carrageenan conformation where the large deviation from the theoretical type A ribbon is confined mainly to the torsion angles about the 3,6-anhydrogalactosyl bond which differs by about 90° from the cellobiose value giving the observed three-fold extended Type B structure.

C. Conformations of Polysaccharides in Solution

The value of Xray diffraction in providing the building blocks for conformational analysis of polysaccharides and other biopolymers is well known. However, the conformation of a bipolymer in the solid state is a special case which on its own can be difficult to reconcile with the conformation *in vivo*. It has been suggested (Brant and Dimpfl, 1970) that solution properties of polysaccharides can be predicted, at least qualitatively from their regular conformation in the solid state. Detailed calculations for 1,4-linked homopolysaccharide systems (Whittington, 1971) indicates that in general this can be true.

The extension of conformational studies to solution has been successfully demonstrated by the use of various chiroptical techniques (McKinnon, 1973; Dea *et al*. 1972) and nuclear magnetic resonance (Bryce *et al*. 1974).

Chiroptical Techniques

(a) Optical Rotation

The measurement of optical rotation at a single wavelength, often at the sodium D-line, has been extensively used in the monosaccharide area and to follow conformational changes in the secondary and tertiary structure of proteins, polypeptides and more recently polysaccharides.

Several workers have formulated empirical rules for the optical activity of sugars notably Hudson (1909), whose rules of isorotation concern anomers of pyranose derivatives. These are based on the van't Hoff super position principle which considers the optical rotation of a molecule as the algebraic sum of the contributions of the various asymmetric centres. The quantum mechanical approach of Kauzmann et al (1961) shows the unsoundness of this approach and suggests that the optical rotation phenomenon arises from the electronic interactions between groups rather than contributions from isolated atoms.

Whiffen (1956) and Brewster (1959) by a consideration of dominant interactions have put this on a quantitative basis by establishing a set of empirical rules which predict values that agree well with those derived experimentally for many compounds including monosaccharides.

Rees (1970) extended this treatment to the optical rotation of disaccharides and higher oligomers including polysaccharides by introducing the concept of linkage rotation(Δ). This represents the optical rotation due to interactions across the glycosidic linkage, in other words a function of the glycosidic conformation angles ϕ and ψ (Fig. 1.2). By an application of Brewster's rules and a consideration of the interactions in chains of four bonded atoms at a time, the linkage rotation can be defined, for residues having the Reeves C1(D) conformation as:

$$[\Delta]_D^{\alpha} = + 105 - 120 (\sin \Delta\phi + \sin \Delta\psi)$$

for the α anomeric configuration and,

$$[\Delta]_D^{\beta} = -105 - 120\,(\sin \Delta\phi + \sin \Delta\psi$$

for the β configuration.

$\Delta\phi$ and $\Delta\psi$ are the ϕ and ψ rotations from the position that eclipses the C-H and O-C bonds (Fig. 1.12).

The expressions for $[\Delta]$ also alter for residues in the L configuration and for those not in the Reeves C1 conformations.

A comparison of observed and calculated rotations for di- and oligosaccharides for which solution conformation could be predicted from Xray and other data showed the validity of these expressions (Rees, 1970). In some circumstances it is possible to relate the nature of conformational changes occuring in solutions by use of this treatment. For example, the helix-coil transition for iota carrageenan segments has been studied and the optical rotations of the two forms calculated (Rees, 1970), from the ϕ and ψ values determined from Xray data (Anderson et al. 1969) and the molecular rotations of the relevant methyl glycosides and disaccharides. The agreement between calculated and observed values was good, providing further support for the hypothesis that the optical rotation shifts observed did in fact originate from a coil to double helix transition (McKinnon et al. 1969; Rees et al. 1969).

These expressions are no longer valid as they stand in the presence of certain chromophores, such as found in acetamido sugars or uronic acids, due to the sensitivity of such chromophores to the conformation.

(b) Circular Dichroism

Circular dichroism and optical rotatory dispersion both arise from the interaction of circularly polarised light with an asymmetric molecule and give essentially similar information. The

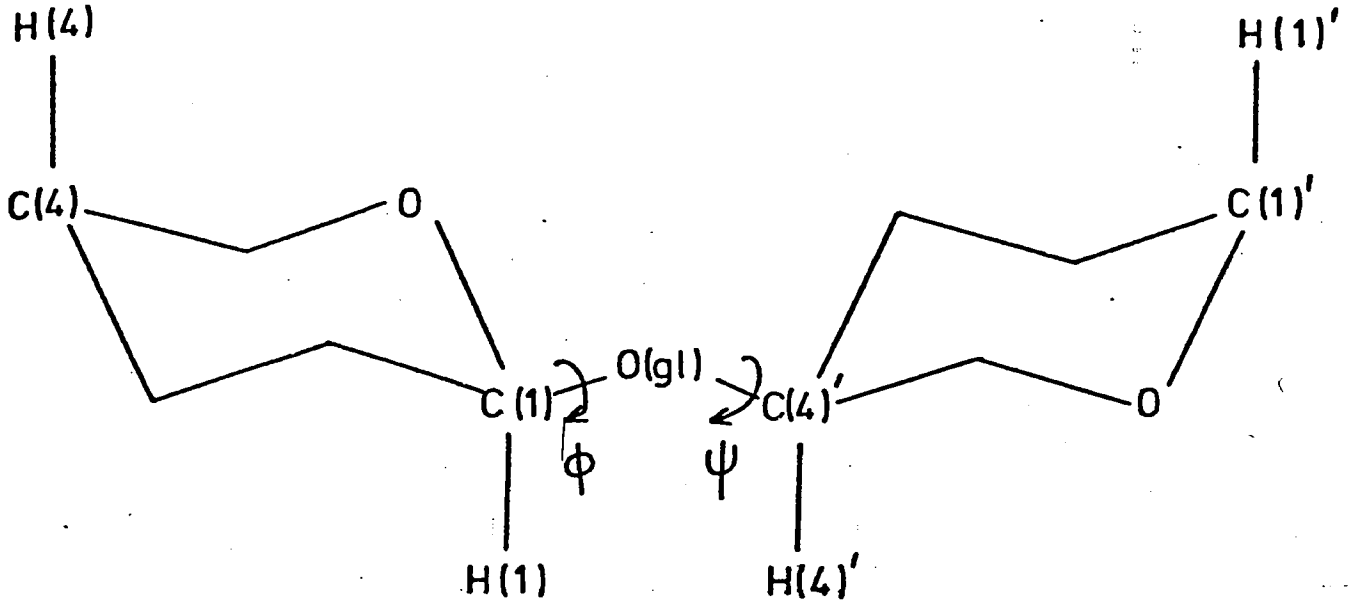

Fig. 1.12 Zeros of ϕ and ψ

$\phi = \psi = 0$ when C(4), C(1), O(gl), C(4)', C(1)' are coplanar, and when C(4) and C(1)' are closest.

$\Delta\phi = \Delta\psi = 0$ when H(1), C(1), O(gl), C(4)', H(4)' are coplanar, and when H(1) and H(4)' are closest.

differential absorption of left and right circularly polarised light results in the light wave becoming elliptically polarised (Fig. 1.13). The angle θ is termed the ellipticity and for comparison purposes, molecular ellipticity $[\theta]$ is usually quoted,

$$[\theta] = \frac{\theta.M}{l.c} \quad \text{deg. cm}^2/\text{d mole}$$

where M is the molecular weight, l the pathlength in mm and c the concentration in gm/cc.

If either the optical rotatory dispersion or circular dichroism curve is known completely, it is possible to calculate the other using the Kronig-Kramers transform(Moscowitz, 1960) since they both have similar electronic origin. The position of the circular dichroism maximum can be estimated by applying the Drude equation to the optical rotatory dispersion curve. The two techniques can be used in conjunction and for an isolated chromophore the forms of the individual contributions are shown in Fig. 1.14.

Although the theory of optical activity is now reasonably well understood in general terms, its use in the prediction and interpretation of spectra is limited (Morris and Sanderson, 1972). For a number of specific transitions, such as the carbonyl $n \longrightarrow \pi^*$ transition, the influence of the spatial distribution of other atoms or groups on the spectra can be considered in terms of certain empirical rules. Probably the best known are the 'carbonyl octant rule' (Moffit, et al. 1961; Crabbe, 1971) and the 'peptide quadrant rule' (Schellman, 1966).

Such rules mainly deal with interpretations in terms of the configuration of rigid molecules but circular dichroism has been

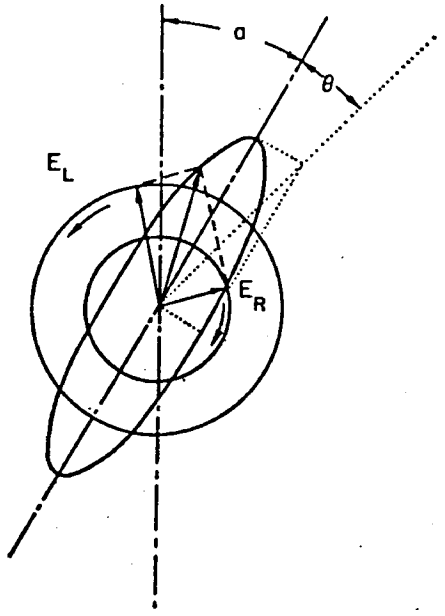

Fig. 1.13 Effect of an optically active absorbing sample on plane polarised light.

α , optical rotation; Θ , circular dichroism ellipticity.

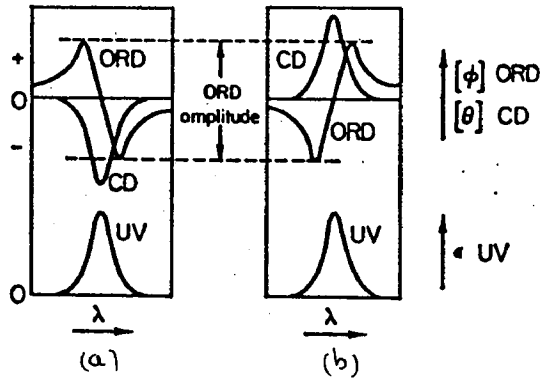

Fig. 1.14 Idealised ultraviolet (uv), circular dichroism (CD), and optical rotatory dispersion (ORD) spectra for an isolated chromophore.

(a) laevorotatory molecule, negative Cotton effect;

(b) dextrorotatory molecule, positive Cotton effect.

successfully extended to the study of conformational distributions in solution. Changes in temperature, cause conformational changes that are reflected in the circular dichroism spectra (Wellman, et al. 1965).

The spectra for proteins and polypeptides arising from the three basic conformations (α-helix, pleated sheet and random coil), can now be interpreted qualitatively and in some cases quantitatively by a comparison between computed and observed circular dichroism curves (Greenfield and Fasman, 1969). The computed curves are formed by a linear combination of the individual curves corresponding to the three basic conformations. In the case of a protein whose three-dimensional structure is known from Xray diffraction studies, and which contains a high degree of secondary structure in solution (e.g. α helix), the computed curves will often fit well with those experimentally observed. Intermediate structures tend to have poorer fits. These results were able to show that circular dichroism appears to be a superior method for determining protein conformations than optical rotatory dispersion.

For polysaccharides the application is limited due to the absence of suitable chromophores. However it has been applied successfully to the uronic acid and acetamido polysaccharides that contain the carbonyl chromophore as the dominant feature. Thus the gelation of alginates (Thom,1973)and pectins (Grant, 1973; Grant et al. 1973) in the presence of calcium ions has been followed by circular dichroism.

For polysaccharides having no accessible chromophores it is often possible to introduce a suitable chromophore by chemical modification (e.g. addition of acetate group). For anionic polysaccharides such as the carrageenans (McKinnon, 1973), the

combination of a suitable cationic dye (e.g. acridine orange or methylene blue) is possible. The dye when bound to the polysaccharide becomes optically active; the associated changes in spectral parameters are termed absorption metachromasy, a topic that has been reviewed in detail by Stone (1969).

The application of circular dichroism to polysaccharides in general has recently been reviewed in some detail by Morris and Sanderson (1972).

Nuclear Magnetic Resonance

Proton magnetic resonance (^{1}H nmr) has had a revolutionary effect on carbohydrate chemistry since its conception about 16 years ago. Although its primary use has been for the elucidation of structures and conformational preferences, more routine applications have been developed. For example, the analysis of composite mixtures and monitoring of reactions.

A review confined to monosaccharides has recently been published (Kotowycz and Lemieux, 1973).

Until recently ^{1}H nmr has not found great use for macromolecules for two reasons:

(i) relatively low machine sensitivity requiring a large sample weight (30-50 mg)

(ii) difficulty in interpreting the spectra obtained due to the presence and number of overlapping signals.

Problem (i) has now been overcome to a large extent by more sophisticated equipment running at higher magnetic field strengths and by use of Fourier Transform methods (Ernst and Anderson, 1966; Ernst, 1966).

Considerable groundwork in the study of amino acids, dipeptides and nucleotides has provided useful knowledge for the interpretation of spectra of biopolymers, this has been reviewed

in detail by Cohen (1969). Sheard and Bradbury (1970) have reviewed the principles involved in ^{1}H nmr with particular reference to the study of biopolymers and their interactions with ions and small molecules.

Early ^{1}H nmr work on polysaccharides seems to have been confined to establishing the proportions of component sugar units and the nature of the glycosidic linkages in the polysaccharides, particularly heparins and related compounds (Inoue and Inoue, 1966; Jaques et al. 1966). More recently Perlin et al. (1970) have compared the 220 M.Hz. ^{1}H nmr spectra of heparin and other glycosaminoglycans, from which they were able to make satisfactory assignments for individual resonance signals. In addition they were able to show that heparin had α-L-iduronate as the major uronosyl component rather than the previously proposed D-glucuronate.

Nmr spectra contain a considerable amount of information. The position of a spectral peak is characteristic of the environment of that group of protons (electronic or chemical), and may be used to identify the nature of the group containing the resonating nucleus. The area of the peak is proportional to the number of nuclei of that particular type in the system (e.g. 3 protons for a $-CH_3$ group) and its fine structure can provide information about neighbouring chemical groups.

Each peak is associated with spin transitions between a pair of energy levels, and the transition probabilities can be related to two nuclear spin relaxation times, T_1 and T_2. If these are measured it is possible, in principle, to obtain details of the molecular dynamics of the system. T_1 and T_2 are sensitive to molecular motion which allows an assessment to

be made of the internal rigidity of macromolecules, in particular T_1 and T_2 decrease as molecular motion becomes slower. The time scale for molecular tumbling is the so called correlation time τ_c, which expresses the time scale on which molecules or parts of molecules lose memory of their previous relative positions and orientations, i.e. lose 'correlation'.

T_1 is the longitudinal or spin lattice relaxation time and describes an exchange of energy between the nuclear spins and the surroundings which, irrespective of their physical state, are known collectively as the 'lattice'.

T_2 is the transverse or spin-spin relaxation time and is a measure of the angular re-adjustment of nuclei.

In this work we shall be interested mainly in T_2 and the position of a peak in the spectrum, namely its chemical shift. Both of these parameters can provide information about the conformational state of a molecule.

T_2 is inversely related to the peak width of the high resolution ^1H nmr spectra, thus, broad peaks are usually indicative of slow motion, that could be an indication of order or immobility in the system.

$$T_2 = \frac{1}{\pi \Delta \nu_{\frac{1}{2}}}$$

where $\Delta \nu_{\frac{1}{2}}$ is the line width at half-height of a particular peak.

The presence of ordered regions in a polypeptide was first reported by Bovey et al.(1959), who observed a broadening or increased line width, of peaks from the backbone protons of poly-γ-benzyl-L-glutamate upon helix formation, and a complete loss of the spectra on aggregation. It should be noted that when rigidity produces

a very broad peak the signal may not be detectable above the instrumental background noise.

In general the changes in line width that accompany order-disorder or helix-coil transitions provide useful information on rate or form of the transition.

(i) If the helix-coil interconversion is rapid, single peaks will be obtained. Thus when helical segments are thought to move or ripple rapidly along the chain there is no position that affords short term rigidity, consequently the observed line width is not noticeably dependent on helix content.

(ii) When the helix and coil states have different environments the line width of the single peak observed will be found to vary with helix content, i.e. as more helix (rigid) is formed the width becomes greater. It is therefore possible to follow the helix-coil transition with, say, temperature in a similar way to optical rotation studies.

(iii) For cooperative transitions in which there is a rapid winding-up or unwinding of, say, a helix, the line width changes observed may well be an all or nothing situation. In other words the spectra is that of the ordered state (helix + coil) or that of the disordered state (random coil) with little in between.

Helix formation, as well as exhibiting broadening, often shows changes in the chemical shift.

If all protons on a molecule were to undergo resonance at identical field strengths and applied frequencies, no conformational information could be obtained. However, fortunately separate nmr

peaks are obtained at different positions, according to the chemical environment of the nuclei. These differences arise because the nucleus is partially shielded from the applied magnetic field by the surrounding electron cloud, which itself varies with the nature of the chemical group containing the nucleus. This displacement of the resonance is the so called chemical shift (δ), a dimensionless constant expressed in parts per million (ppm). It is usually recorded as the fractional displacement from the resonance of a standard peak of a reference compound, such as sodium 2:2-dimethyl-2-silapentane-5-sulphonate (DSS). Thus a particular resonating nucleus can be defined by its chemical shift, for a particular system.

Considerable information on the mobility of a system can be obtained by the use of relaxation times determined by pulsed nmr techniques. By following the decomposition of free induction decays it is possible to separate the relaxation times into separate exponential processes. For systems containing some order, three T_2 times are often observed.

(i) a very long T_2 - due to residual water in the sample (ca. 1 sec).

(ii) a short T_2 - indicative of immobility or order in the system (ca. $<$ 3 millisec.)

(iii) a long T_2 - indicative of mobility or disorder in the system (ca. $>$ 5 millisec.)

Thus providing it is possible to distinguish between these processes, evidence complementary to that from high resolution ^1H nmr can be obtained.

Carbon-13 nmr (^{13}C nmr) is a relatively new and fast growing technique in the study of biopolymer structures. Because

of the low natural abundance of the ^{13}C nucleus coupled with a low inherent sensitivity relative to ^{1}H, ^{13}C nmr experiments tend to be approximately 6000 times less sensitive. Fortunately this problem has been overcome to some extent by the development of computer methods for averaging many signals together with pulsed Fourier Transform nmr (Ernst and Anderson, 1966; Becher and Farra 1972), which resulted in effective sensitivity increases of more than an order of magnitude. With a time-averaged accumulation of data from repetitive pulses spaced typically 1 second apart, it is possible to achieve time savings greater than a hundredfold. Normally macromolecules like polysaccharides are summed over 30,000-60,000 transients, which means overnight or weekend runs. However, because of the larger range of chemical shifts observed for the ^{13}C nucleus, better resolution and ease of resonance assignment is possible.

Recently Bryce et al. (1974) have followed the coil-helix transition in iota-carrageenan segments by ^{13}C nmr. They were able to show that the spectrum disappeared when the polysaccharide was near the limit of conversion to helix as judged by optical rotation. This was interpreted on the basis that the mobility of the residues become so restricted that the relaxation times for the carbon nuclei have been decreased causing broadening and loss of peaks in the same way as for ^{1}H nmr. At 80°C, when the polysaccharide is judged to be entirely random coil, a well defined spectrum consistent with a mobile species is apparent (Fig. 1.15). Such measurements can re-inforce the conclusions obtained from ^{1}H nmr by showing that the ring carbons are experiencing a similar motion restriction to that shown by protons in side groups.

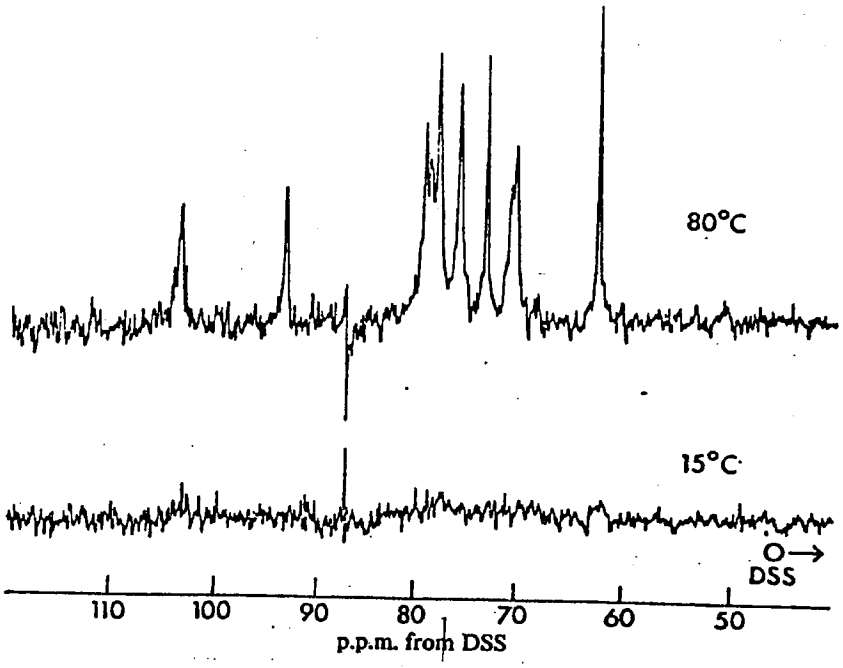

Fig. 1.15 Comparison of ^{13}C nmr spectra for iota-carrageenan segments at 80°C (upper spectrum) and 15°C (lower spectrum), showing loss of signal on conversion to helix.

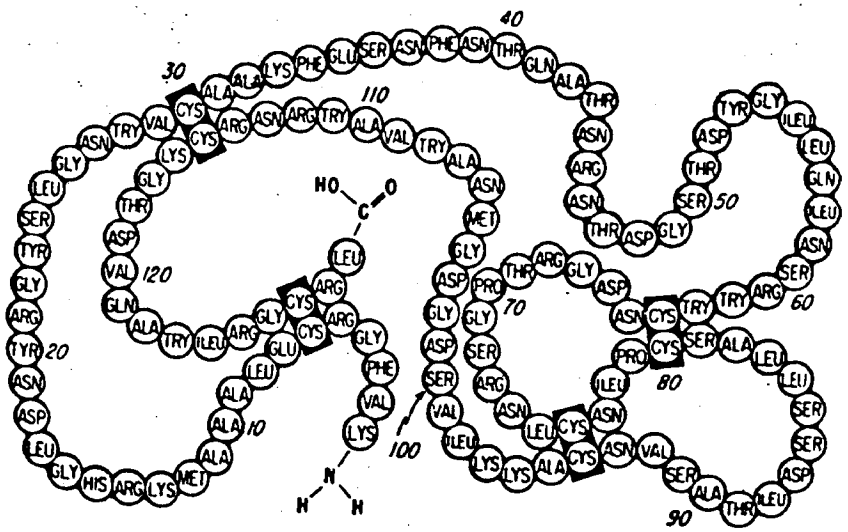

Fig. 1.16 Primary structure of hen egg-white lysozyme showing covalent disulphide bridges between cysteine residues.

D. Conformation Changes of Biopolymers

Conformational transitions in proteins, nucleic acids, and polysaccharides play a decisive role in many biological processes, particularly in control processes. Probably the best known example is the vital role of nucleic acids in cellular reproduction. When the DNA strand duplicates, one strand of the double helix (Watson and Crick, 1953) goes to each daughter cell (Messelsohn and Stahl, 1958) where it serves as the template for the synthesis of the complementary strand.

Such processes often proceed cooperatively i.e. the elementary processes in the individual segments are influenced by the state of the o ther chain segments. In the case of DNA and some polysaccharides there is a strong tendency to assume the form of the neighbouring segment during this process. Such cooperative processes are sensitive to even relatively small variations in external parameters (e.g. temperature, pH, solvent) which can lead to practically complete conformational transition(Engel and Schwarz, 1970). A further characteristic of cooperative processes, is the dependence of the transition upon the chain length, thus the sharpness of the transition increases with the size of molecule (e.g. Zimm and Bragg, 1958, 1959).

Under suitable conditions, many biopolymers have a specific conformation which is stabilised by non-covalent interactions between the segments. An understanding of some of the broader aspects involved can be expected to lead to further development of the theory of conformation and biological function since this function is usually confined to its structural state. Enzymes are a good example in that even small conformational changes generally lead to large changes in enzymic activity (Monod et al. 1965; Kirtley and Koshland, 1967).

Polysaccharide Gels

Polysaccharides in solution frequently form gels of varying strength even when present in very low concentrations (e.g. 0.1% w/v agarose forms a gel capable of maintaining its shape). To do this they form an association of chain segments into zones which are joined into a network by chains that run through two or more zones. Such a network traps water in its interstices according to the classical picture of gelation (Hermans, 1949). Normally one would expect, in dilute solution, that the random coil configuration would predominate. In gel formation, however, certain regions of the polymer chains may have sufficient conformational constraints operative such that they can form regular helical (in its loosest sense) conformations (Flory, 1972), that interact with others to form a 'junction' or 'cross link' in the network. It is the nature of these 'junction zones' that has been the subject of considerable study in polysaccharides.

Junction Zones

Although most of the polysaccharide studies have been concerned with junction zones in gelation, similar junctions have been shown to exist in the non-gelling systems of iota-carrageenan short segments (McKinnon, 1973; Bryce et al. 1974). A gradual increase in the size, number, and lifetime of junction zones leads to the formation of a three dimensional network extending over the entire polymer-diluent system. The lifetime of a junction zone due to the dynamic nature of the individual links, will depend on the availability of more stable, and therefore energetically favoured, links.

There are three main types of junctions:

(i) Covalent, in which a chemical bond is formed between two components of the system. For example, the disulphide bridge between cysteine residues in proteins e.g. lysozyme (Fig. 1.16) contributes greatly to the stabilisation of the tertiary structure. An extreme case is that of keratin, which is so highly cross-linked through disulphide bridges between polypeptide chains that it is almost impossible to extract from the tissues in which it occurs (Seifter and Gallop, 1966).

(ii) Non-covalent, in which factors such as van der Waals forces, hydrogen bonds, hydrophobic and electrostatic interactions are involved. An example of this type of system is the iota-and kappa- carrageenan double helix, in which two chains are held together by hydrogen bonding, van der Waals and polar interactions (Smith, 1972) and possibly cation fixation (Arnott, et al. 1974). In the case of kappa-carrageenan and agarose, the helices are in turn held together in bundles by similar forces to further reinforce the gel network (Fig. 1.17).

(iii) In certain systems, such as microcrystalline cellulose and tobacco mosaic virus gels, the chain microcrystallites or virus particles which have an ordered internal structure, coalesce to form a network (Fig. 1.18). It has recently been proposed that cellulose gels contain single helices, packed or aggregated together to form networks (Arnott et al. 1974a).

Many gels have junction zones that are aggregates of a number of molecules having the character of more than one extreme. For

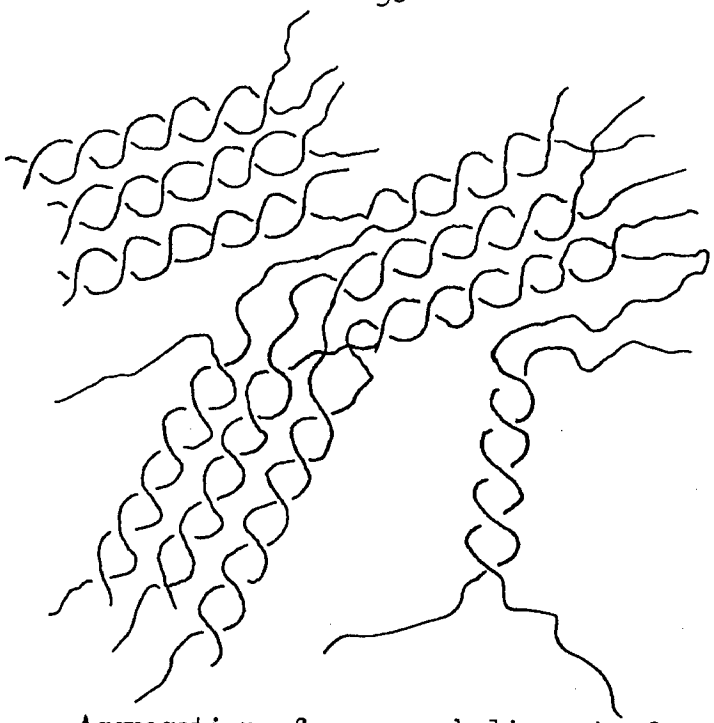

Fig. 1.17 Aggregation of agarose helices to form network

Fig. 1.18 Organisation of virus particles in a Tobacco Mosaic Virus gel.

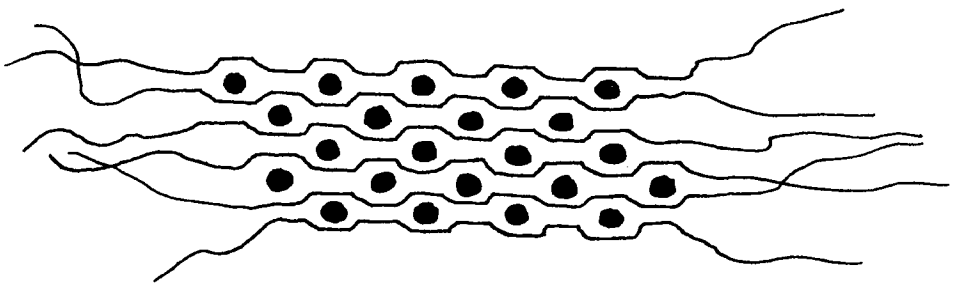

Fig. 1.19 The "egg-box" model for an alginate junction zone

example, alginate and pectin gels (Grant et al. 1973) have junction zones that have been interpreted in terms of microcrystallites stabilised by cooperative binding of calcium ions between the chains - the so called 'egg box' model of chain association (Fig. 1.19).

A further stabilising force that can sometimes be considered is that arising from the solvent or surrounding dissimilar medium, which represents a special type of inter-molecular interaction. An example of this is shown by the agarose double helix which is stabilised by a column of water molecules within the helix (Arnott et al. 1974c).

General Characteristics

The cooperative nature of many of the processes mentioned is demonstrated by the 'all or nothing' behaviour i.e. two limiting structures occur either completely ordered (within the limitations of the molecule) or completely disordered - there is no substantial amount of intermediate state at thermodynamic equilibrium. Thus formation of this type of junction has an energy barrier of nucleation (i.e. to bring two acceptable parts of the molecule together), followed by a rapid 'zipping up' of the ordered region to produce a lower favourable energy level.

Gels having non-covalent junction zones are frequently reversible i.e. the ordered regions can be 'melted' out and reformed, carrageenan and agarose are examples of this kind. Similar reversible transitions have been shown for the protein, gelatin. Such interconversions often involve a conformational transition that can be detected and characterised by spectroscopic methods already described.

CHAPTER 2

Some conformations of hyaluronate in the solid state

A. INTRODUCTION

This chapter will consider the structure of hyaluronate in the solid state, as found by Xray diffraction. Model building studies will be described. A comparison will be made between this work and that of others. Finally, an indication will be given of subsequent results from collaborators who had access to more sophisticated computational techniques than available here.

1. Origin

Hyaluronate belongs to the glycosaminoglycan family of polysaccharides which are present in the intercellular matrix of the connective tissue of most vertebrates. It is also present in some bacterial capsules. The concentrations in various tissues or fluids are listed in Table 2.1.

	Percent of net weight
Human vitreous	0.2
Human adult skin	0.03-0.09
Human synovial fluid	0.14-0.36
Human umbilical cord	0.3
Rooster comb	0.75
Bovine brain	0.015
Normal urine	0.002
Tumours	
Rous sarcoma	0.1
Mesothelioma	0.2-0.7
Streptococcal cultures	0.01-0.1

Approximate Concentration of Hyaluronate in Some Tissues and Fluids (From Laurent, 1970)

Table 2.1

The glycosaminoglycans are important for the associations in which they participate, both with their own kind and with other types of molecule. For example, they may be involved in cell aggregation (Pessac and Defendi, 1972a,b), in the structure and elasticity of connective tissue of all types (Balazs, 1970a) including skin, cartilage, heart valves and arterial walls, in joint lubrication (Hammerman, 1970) and in various parts of the eye. There are indications that their interactions with serum lipoproteins might be involved in the initiation of arteriosclerosis (Iverius, 1972; Srinavasa, et al. 1972).

2. Structure and Physical Properties

Hyaluronate prepared from human umbilical cord is believed to be a regular, unbranched, polymer of the type (-A-B)n, where A is β-D-glucuronic acid and B is 2-acetamido-2-deoxy-β-D-glucose (N-acetyl glucosamine). The linkages A→ B and B → A are β1,3 and β1,4 respectively (Fig 2.1), both pyranose rings being considered to be in the energetically favourable Reeves C1 conformation.

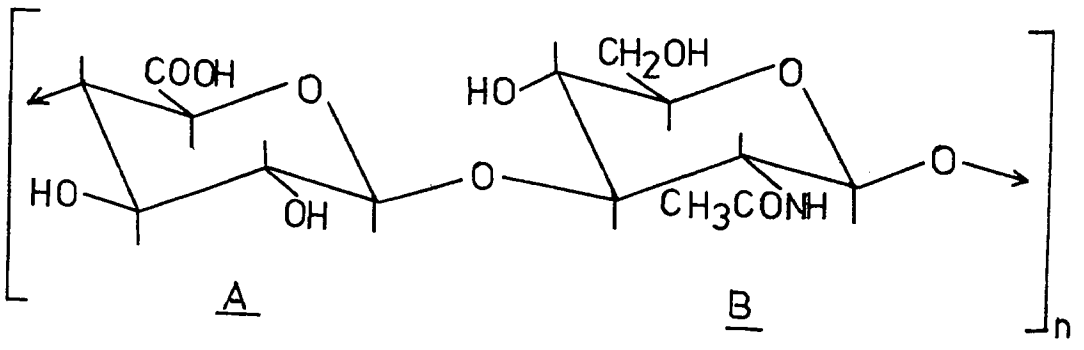

Fig. 2.1 Hyaluronic acid repeating unit

The linkages have been determined by identification of

the fragments released by acid hydrolysis and by enzyme degradation; this has been reviewed in some detail (Brimacombe and Webber, 1964; Jeanloz, 1956; Meyer, 1958). Additional evidence for the structure was provided by methylation analysis (Hirano and Hoffman, 1962; Jeanloz and Jeanloz, 1964) and by synthesis of the repeating unit (Flowers and Jeanloz, 1964). While extensive structural studies have not been performed on hyaluronate from tissues other than umbilical cord, the results of many investigations have indicated that they, too are composed of glucuronic acid and N-acetyl glucosamine in equimolar amounts (Meyer, et al. 1956; Laurent, 1957a; Balazs, 1958; Preston, et al. 1965).

Hyaluronate is the simplest glycosaminoglycan for two reasons. First, as far as is known its covalent structure is entirely regular and repeating whereas other members usually deviate to some extent from this perfectly alternating arrangement. Second, it seems to occur in tissues as the free polysaccharide, or at least with very little covalently bound protein, rather than as a side chain is a more complex conjugate e.g. Chondroitin sulphate in proteoglycan.

The physical properties of hyaluronate isolated from different tissues, however vary greatly. Fessler (1960) indicates that hyaluronate from human umbilical cord and synovial fluids are similar, and differ from those of sheep and ox synovial fluids, in particular in the dependance of relative viscosity on shear rate. It is not known (Swann, 1968) whether these differences are a consequence of a different molecular architecture of hyaluronate in the different tissues or an artefact caused by such factors as the method used to isolate and purify the materials examined (Balazs,1958).

Meyer (1970) has suggested that heterogeneity and variability in glycosaminoglycans exists to a far higher extent than can be demonstrated by existing separation and analytical techniques. He defines heterogeneity as hybrid molecules, i.e. replacement of one glycosyl group in the carbohydrate chain by another as well as differences in the linkage region. Variability is defined as the existence of differences in number and sequence of exo groups such as sialyl, fucosyl, and sulphate. Heterogeneity and variability have been demonstrated in all glycosaminoglycans with perhaps hyaluronate as the exception. Polydispersity has been demonstrated for hyaluronate and in some tissues it may be covalently linked to protein (Preston, et al. 1965; Hardingham and Muir, 1972; Hascall and Heinegard, 1974) but in general is usually considered to be free or at least not covalently linked. Most preparations are quoted as having very low protein content after mild extraction procedure.

3. Preparation of hyaluronate

Hyaluronate can be conveniently prepared from various solid tissues (umbilical cord, rooster comb, skin etc.) or tissue fluids (synovial fluid, vitreous), in a pure form (Laurent, 1957a; Swann, 1969; Varga, 1955) with less than 0.5% protein content and with a molecular weight of $1\text{-}3\times10^6$. Mild extraction usually involves water or salt solution followed by precipitation with an organic solvent e.g. ethanol or a quaternary ammonium compound such as cetylpyridinium chloride (CPC) (Scott, 1970). Protein is usually removed by ultrafiltration or pronase digestion (Swann, 1968; Scott, 1970), chromatography or ion exchangers and adsorbents (Ciffonelli and Mayeda, 1957; Preston, et al. 1965; Swann, 1968), and centrifugation on CsCl-gradient (Silpananta, et al. 1968).

Other charged polysaccharides are usually removed by fractional precipitation with CPC (Scott, 1960).

4. General Rheological Characteristics

Considerable work has been reported on molecular weight determinations of hyaluronates from various sources. Several reviews exist (e.g. Balazs, 1958; Laurent, 1957b; Balazs and Jeanloz, 1965), a selection of values are given in Table 2.2.

Tissue	Molecular weight	Technique	Reference
Human umbilical cord	3.4×10^6	Light-scattering	Laurent and Gergely (1955)
Bovine vitreous body	7.7×10^4 1.7×10^6	Light-scattering Sedimentation and diffusion	Laurent et al. (1960)
Bovine synovial fluid	14×10^6	Light-scattering	Preston et al. (1965)
Human synovial fluid			
Normal	6×10^6	Light-scattering	Balazs, Watson, Duff and Roseman (1967)
Rheumatoid	$(2.7\text{-}4.5) \times 10^6$	Light-scattering	
Rooster comb (main fraction)	1.2×10^6	Ultracentrifugation	Swann (1968a)
Streptococcal cultures	0.115×10^6 0.93×10^6	Sedimentation and viscosity	Blumberg, Ogston, Lowther and Rogers (1958)

Some Published Molecular Weights of Hyaluronic Acids from Different Tissues

(From Laurent, 1970)

Table 2.2

There are distinct differences in the degree of polymerisation of hyaluronate prepared from different sources and indeed it can vary locally within the same tissue (Balazs, 1970b). Obviously

preparation of pure intact polysaccharide of very high degree of polymerisation in 100% yield is extremely difficult to achieve thus published values should be regarded as minimum molecular weights.

That the long polymeric chain is linear and unbranched, was confirmed by Fessler and Fessler (1966) using electron microscopy. They found only long chains having a weight average strand length of 2 - 4μ, which if it was assumed that the strands were stretched hyaluronate molecules they would have a weight average M. wt. of $1 - 2 \times 10^6$, this was in good agreement with ultracentrifuge data and later light scattering and ultracentrifuge data of Cleland (1970). It has been characterised as a 'random coil with some stiffness' when studied at low concentration (< 0.1% dissolved in 0.1 - 0.2 M NaCl pH 6-7) . . . , which was thought to be consistent with an expanded random coil exhibiting non-Newtonian behaviour. The radius of gyration of the molecule was found to be 1500-4000Å, therefore, the chain extends over a very large domain in the solvent. This domain contains $10^3 - 10^4$ times more water than polysaccharide. At a polysaccharide concentration as low as 0.01-0.1% the molecules fill the whole solution and begin to entangle with each other. At higher concentrations the solution contains a continuous three dimensional network of chains and it is no longer possible to recognise single molecules. Fig 2.2.

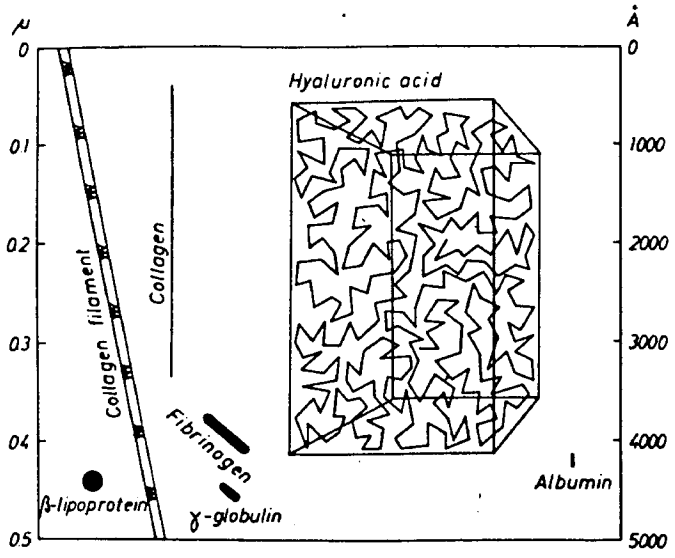

Fig. 2.2 Schematic representation of the volume occupied by the hyaluronic acid molecule.

In natural hyaluronate containing fluids (synovial, liquid vitreous) and in the solution of purified sodium hyaluronate at higher concentrations (> 0.1%), the viscoelastic characteristic of the hydrated biopolymer was emphasised (Balazs and Gibbs, 1970). When aqueous solutions of high molecular weight ($1\text{-}2\times10^6$) hyaluronate (concentrations > 0.3%) are dialysed against 0.1M NaCl pH 2.5, a 'viscoelastic putty' forms (Balazs, 1966). The 'putty' when it contains 1% or more hyaluronate forms a solid which rheologically is quite different from agar or gelatin gels. The viscoelastic characteristics of the putty are highly dependent on strain frequency - it flows slowly under stress and cut surfaces heal when pressed together. In vivo the natural fluid exhibits similar properties in protecting cells against shock (Balazs and Gibbs, 1970). Under slow mechanical loading it behaves as a viscous oil-like lubricant, at higher loading it

transforms to a highly deformable elastic system able to absorb the imposed stress and convert it to an elastic deformation then rebound to the original state when the stress is relaxed.

The rheological characteristics will be discussed more fully in Chapter 3.

5. Other Glycosaminoglycans

The other members of the glycosaminoglycan family are listed with their chemical structure (known or suggested) in Fig. 2.3. In contrast to hyaluronate they tend to have a galactosamine sulphate residue instead of glucosamine, and in some cases, dermatan sulphate, heparan sulphate and heparin, have L-iduronate replacing glucuronate. Further, they all are found bound to protein (proteoglycan).

Chondroitin 4-, and 6-sulphate possess the simpler and more regular structures. Heterogeneity does exist, manifesting itself in several ways (Roden, 1970). In particular,

a) molecular weight polydispersity, in the range 20-60,000

b) variation in degree of sulphation together with the possible occurrence of chondroitin 4-, and 6-sulphate hybrids

c) variation in the polysaccharide composition of the macromolecular proteoglycan, particularly the presence of varying proportions of chondroitin sulphate and keratan sulphate.

Dermatan sulphate differs chemically from the chondroitin sulphates in having α-L-iduronate replacing the β-D-glucuronate (Fransson, 1970). α-L-Iduronate residues would appear to be conformationally unstable; proton nmr studies of dermatan sulphate in solution, above 70°C, suggest that the α-L-iduronate is in the IC chain conformation (Perlin, et al. 1970). However, Xray and molecular model building (Arnott, et al. 1973 ; Atkins and Isaac,

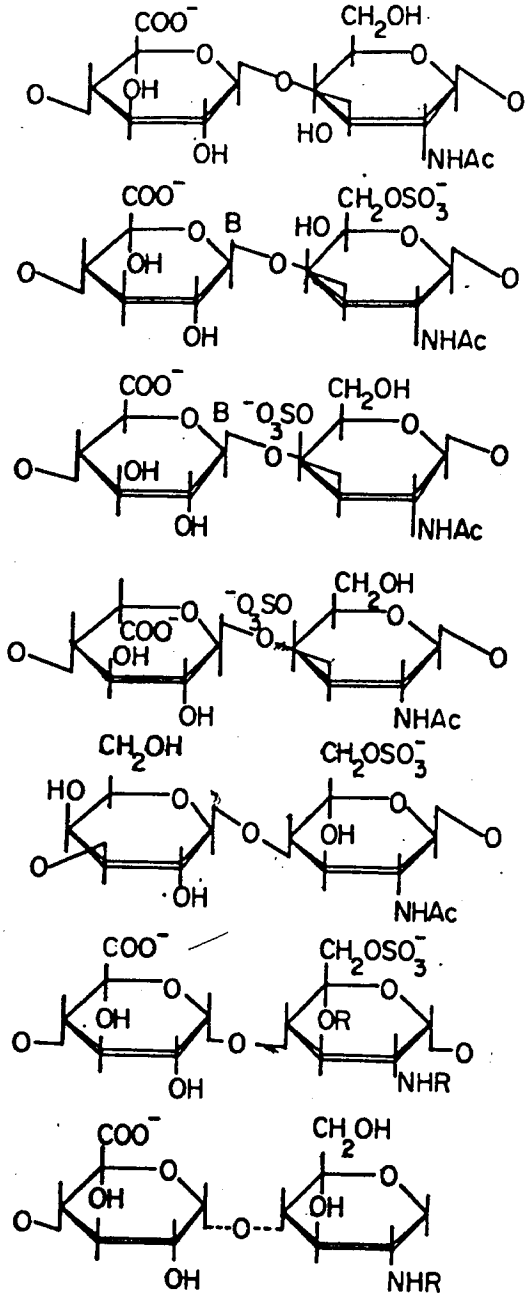

Fig. 2.3 The basic disaccharide repeat units of the glycosaminoglycans.

1973) evidence shows that in the solid state the Cl chain conformation is favoured. Heparan sulphate is probably a block copolymer of uronic acid and glucosamine with parts of the glucosamine N-sulphated and others N-acetylated, having variable sulphate content. Heparin has a high ratio of five sulphates to four saccharide residues, occurring in N-sulphate, O-sulphate and 6-sulphate locations. The glycosidic linkages are thought to be 1⟶4 throughout (Wolfrom, et al. 1964; Perlin, et al. 1972). Keratan sulphate is the odd man out in this series in that it contains no uronic acid residue. Typically, 70% of the N-acetyl-glucosamine residues and 40% of the galactose residues are sulphates although the number of sulphate groups and presumably their distribution may vary (Mathews and Ciffonelli, 1965; Bhavanandan and Meyer, 1967, 1968; Hirano and Meyer, 1971).

6. Early Xray Diffraction Studies on Hyaluronate

The primary structure of hyaluronic acid has already been discussed, the regular repeating structure and high molecular weight of the polymer strongly suggesting that Xray diffraction techniques similar to those used for other regular polysaccharides (Anderson, et al. 1969) should be applicable here. Early attempts had been made to crystallise hyaluronate. Sylven and Ambrose (1955) reported hyaluronate fibres that exhibited birefringence. Using higher molecular weight materials Laurent (1957c) described amorphous Xray diffractograms for hyaluronate and chondroitin. He also noted that there was considerable similarity between these, indicating that the conformational relationship as well as the covalent relationship between the two molecules was not purely organochemical. Bettleheim (1959) crystallised and orientated hyaluronate films and reported a periodicity of 1.19 nm. This

is clearly wrong since Rees (1969) showed by computer model building that the maximum possible extension of a (1eq,3eq-1eq,4eq) linked disaccharide residue cannot exceed 1.02nm. (Fig. 2.4.)

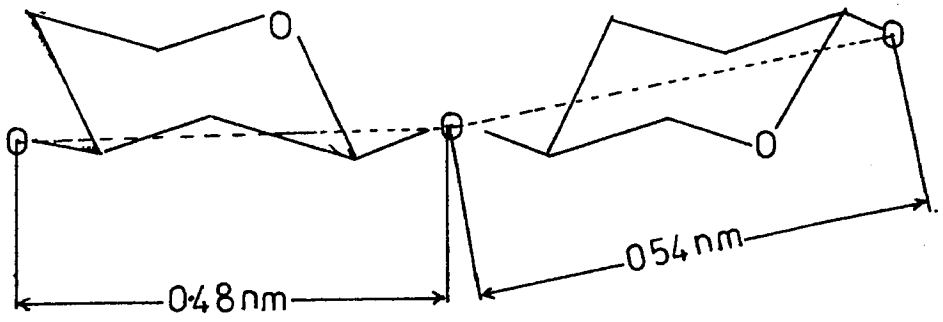

Fig. 2.4 Maximum extension of a 1eq., 3eq., -1eq.,4eq., linked disaccharide

While practical attempts to produce good quality Xray diffraction photographs of hyaluronate did not prove successful until 1971/2, computer model building studies by Rees (1969) were able to make predictions of likely conformations that were very close to those found.

B. METHODS

1. Crystallisation of hyaluronate

Hyaluronate films were produced by drying down a 0.5-1% aqueous solution on a Teflon sheet or glass. Teflon is preferable to glass for ease of film removal. Normally films were formed by slow evaporation in air at room temperature and humidity, the teflon sheet being partially covered to prevent dust etc. settling in the solutions. The films thus formed from high molecular weight hyaluronate tend to be transparent, any excess salt and inorganic impurity, collecting in the centre due to the slow evaporation effectively zone refining the preparation. Such films tend to be tough and easily handled when dry, even when very thin. On the other hand materials with molecular weights $< 2.5 \times 10^5$ tend to form brittle films that crack in the later stages of drying or when being cut.

The films are stretched between 100 and 400% by loading them with between 1 and 10 gm depending on the film thickness and its molecular weight (thick films and/or high molecular weight take higher loads) under relative humidity held at about 80%. The films are highly hygroscopic at relative humidities greater than 70% so much so that samples of low molecular weight and/or quality tend to dissolve or take in so much water that they rapidly 'neck' and break under very low loading. A 'normal' sample also 'necks', usually after 10-20 min at 80% relative humidity a fairly rapid stretching takes place such that with 30-60 minutes stretching is complete and additional loading will produce no further noticeable extension. A diffraction pattern taken at this time would show orientation that improves with time -

normally 24 hrs, after which the crystal form will usually remain stable unless the conditions are changed e.g. humidity or temperature change (but note, metastable crystalline forms 'relax' to more stable forms).

Experimentally the arrangement consists of a narrow strip of the hyaluronate film (approx. 2 mm x 5 mm) glued by its ends with Bostic to a piece of old Xray film or card that has been cut almost completely across its width. When the glue is set the edge of the mounting can be cut away leaving two halves joined by the hyaluronate film (Fig. 2.5). This serves as a useful guide to the extent of extension whilst stretching is taking place. The two ends of the mounting are held by miniature Bulldog clips - one being suspended from the container lid the other holding the weights. The relative humidity is controlled by using saturated solutions of various salts within the closed vessel.

This is the basic technique - experimental points to note are:

(i) If using a very thin film, 2 or 3 pieces stacked together can be used advantageously to provide additional strength.

(ii) No matter what the film thickness, in the case of the first experiment with a new sample, weights should be added gradually allowing sufficient time (say 20 mins) for any extension.

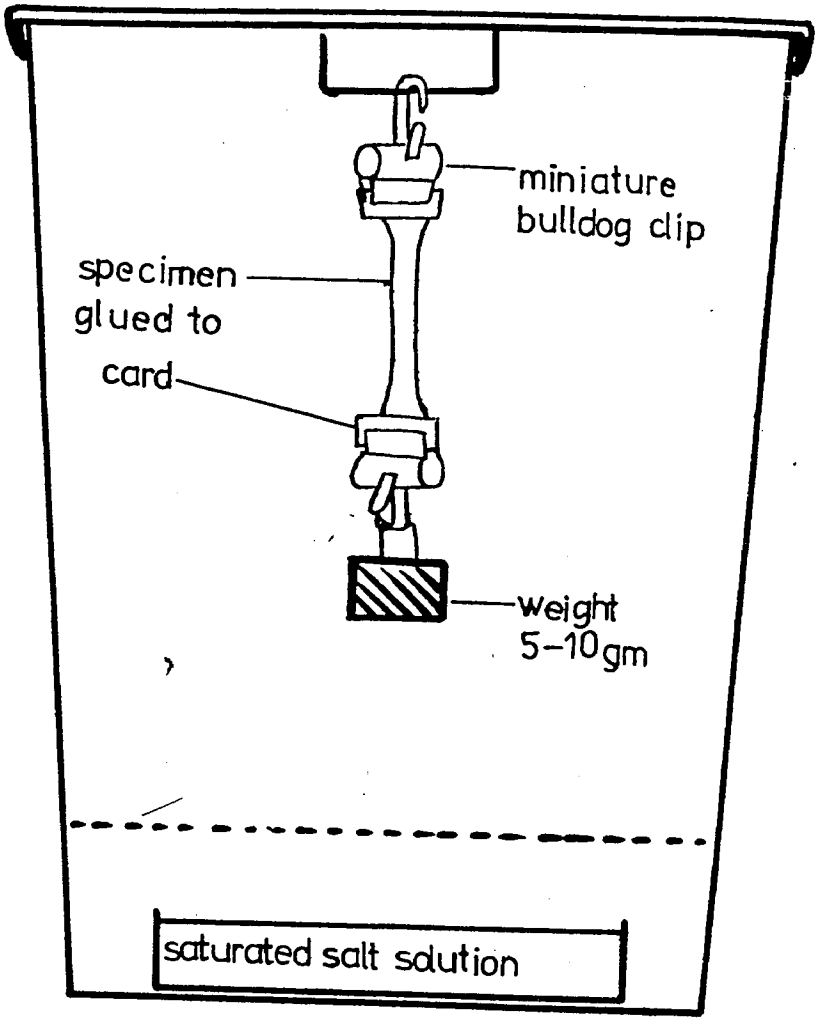

Fig. 2.5 Experimental arrangement for stretching hyaluronate films

(iii) A high proportion of potential failures (i.e. breakages) can be avoided by careful observation of the stretching. If the sample is obviously going to break often it is possible to remove it rapidly to a container at room humidity hence stopping the extension. After equilibrating, the sample can then be returned to the original humidity for further controlled stretching or as often happens equilibration with no further observable stretching.

(iv) The samples should be stretched at constant temperature or at least in a room that does not suffer large temperature variations.

Clearly this technique is rather uncontrolled although (iii) above allows some rather irreproducible control. However in general we and our collaborators at Purdue University have found that samples prepared in the above manner almost always give the same diffraction diagram. This appears to be at variance with results from the Bristol group, this will be discussed later.

Modification of the crystal packing of the sample is sometimes possible either by 'aging' (i.e. leaving for several weeks under tension at the particular humidity) or by 'drying' over silica gel. Temperature is also another factor that can be varied and is reported to have been used in the interconnection of various crystal forms of hyaluronate (Atkins and Sheehan, 1973).

2. Source and Preparation of Samples

Samples used were normally freeze dried preparations and are listed below:

(i) From human umbilical cord; Na^+ salt, # 1117, # 1113, # 1119.

(ii) From rooster comb; Na^+ salt:- C32/2, C34, 'Rooster comb'. These samples (molecular weight $1-2x10^6$) were a kind gift from Dr. E.A. Balazs of Boston Biomedical Research Institute, Boston, Mass., U.S.A. (also (i) above)

(iii) K^+hyaluronate from human umbilical cord bought from BDH Chemicals, Poole, England.

(a) pH 7 solutions

The most convenient way to dissolve this polymer is to gradually add water allowing the polymer to rehydrate and swell gradually using the minimum of stirring and avoiding metal spatulas etc. since dissolved air and some metal ions promote depolymerisation (Harris et al. 1972).

The natural pH of the samples used when dissolved in deionised water was pH 6.5-7.0.

(b) Viscoelastic putty - pH 2.6

A 0.5-1% solution of hyaluronate in deionised water was dialysed against a large volume of a 0.15M NaCl solution at pH 2.6 for 4-5 days at 0-4°C with stirring. The resulting viscoelastic 'putty' was squashed between two pieces of Teflon to spread it out quickly

prior to drying. Alternatively on leaving, a lump of 'putty' will eventually (ca 1 hr.) flow out. The resulting film usually had a brittle central region containing excess salt.

3. Density of fibres

Densities of stretched films were determined by flotation in a chloroform/toluene mixture. The mixture was adjusted until the specimen floated freely throughout the volume of the liquid. The specific gravity of the fluid was then measured using a specific gravity bottle. This technique gives only a rough guide to the density as it is difficult to assess the extent of errors involved, such as the presence of air bubbles, is the sample truly floating freely and also there might be slight specimen solubility in the liquids used.

From the formula

$$d = \frac{n \times M}{V \times N}$$

where n = No. of disaccharides

M = M.Wt. of disaccharide

V = Vol. of unit cell

N = Avogadro's No.

d = Measured density

the number of disaccharides in the unit cell can be calculated making allowance, if desired, for the number of water molecules/ disaccharide .

4. Xray Apparatus

Xray diffraction photographs were taken with flat plate pin hole cameras of similar design to that of Langridge et al. (1960) using leaded glass collimators of approx. 250μ aperture. They were used in conjunction with a Hilger Watts Y.33 semi micro focus Xray generator having a copper target. Air scatter and humidity changes were avoided by constantly flushing the cameras with a slow

stream of helium gas that had been bubbled through a saturated solution of an appropriate salt.

Routine survey photographs using unfiltered radiation needed exposures of 2-4 hours depending upon the thickness of the specimen. For more accurate measurements nickel filtered radiation was used, removing the unwanted CuKβ radiation. As a consequence the exposure time normally had to be increased by a factor of 4 or 5. With long exposure times the double film technique was used, having the advantage that the piece of film nearest the specimen although over exposed near the centre shows up weak reflections, particularly those having 2-3Å spacings.

All photographs were calibrated by dusting the specimen with finely powdered calcite to enable accurate measurements of film to sample distance, normally within the range 3 to 5 cm.

5. Measurement of Diffraction Patterns

The 'x' and 'y' coordinates of all visible reflections were measured within ± 0.2 mm with a steel rule, on a light box, the intensity of each reflection being ranked from strong to weak. In some cases it was found to be advantageous to enlarge the photograph by projection onto a wall. For sharp photographs very little loss of definition occurred and of course it was possible to effectively reduce the measuring inaccuracies. The diameter of the most intense powder ring due to the calibrating calcite(characteristic spacing 0.3035nm) was measured and used to derive accurate fibre to film distance using the formula

$$D = r/\tan 2\theta \qquad -1$$

where D = film fibre distance

r = reflection coordinate i.e. powder ring radius

2θ = Bragg angle

and $$\Theta = \sin^{-1} \frac{d}{2\lambda} \qquad - 2.$$

d = spacing of major calcite reflection = 0.3035 nm

λ = wavelength of CuKα_1 radiation = 0.1542 nm

The reciprocal lattice coordinates, Zeta (ζ) and Xi (ξ) are calculated using the expression from International Tables (1968).

$$\text{Zeta} = \frac{y}{(D^2 + x^2 + y^2)^{\frac{1}{2}}} \qquad - 3.$$

$$\text{Xi} = \left(1 + \frac{D^2 + x^2 - 2D(D^2 + x^2 + y^2)}{D^2 + x^2 + y^2} \right)^{\frac{1}{2}} \qquad - 4.$$

From the meridional and equatorial reflections, the axial and lateral periodicities, d_{Zeta} and d_{Xi}, can be readily calculated from:

$$d_{Zeta} = \lambda/2 \sin \Theta \text{ or approximately} = \frac{\lambda}{Zeta} \qquad - 5.$$

$$d_{Xi} = \lambda/2 \sin \Theta \quad " \quad = \frac{\lambda}{X_i} \qquad - 6.$$

where $\Theta = \sin^{-1} \left(\frac{Zeta}{2}\right)$ or $\sin^{-1}\left(\frac{Xi}{2}\right)$ respectively.

It is however, most useful at this stage to plot out Zeta vs. Xi for each reflection (e.g. Fig. 2.9). From this diagram

one can distinguish layer lines (constant ζ) and row lines (constant ξ).

6. Analysis of Xray Diffraction Patterns

The diffraction pattern can be conveniently analysed according to the following stages:

(i) a preliminary visual examination can classify the pattern in terms of its extent of crystallisation and orientation (Arnott, 1973).

(ii) determination of the axial and lateral periodicities.

(iii) a plot of the reciprocal lattice coordinates ζ and ξ gives possible unit cell dimensions and a clearer picture of systematic layer line absences.

(iv) the unit cell parameters a and b are evaluated using;
(a) a Hull Davey type graph and reciprocal lattice net (Alexander, 1969), and/or
(b) a least squares minimisation (see Methods 7.b).

(v) computer model building can then be related to the above data.

This is shown schematically in Fig. 2.6.

The amount of information obtained in steps (i) - (iv) is considerable. The determination of axial periodicity from the layer line spacing and of the fundamental repeating unit from the meridional reflection often make it possible to distinguish between a number of configurational models suggested by other evidence e.g. chemical and/or computer model building. Combining this data with information about the unit cell dimensions and the density of the material, it is possible to obtain details of the number, size, shape and environment of the molecules in the unit cell. It is also possible in certain cases, to say whether or not

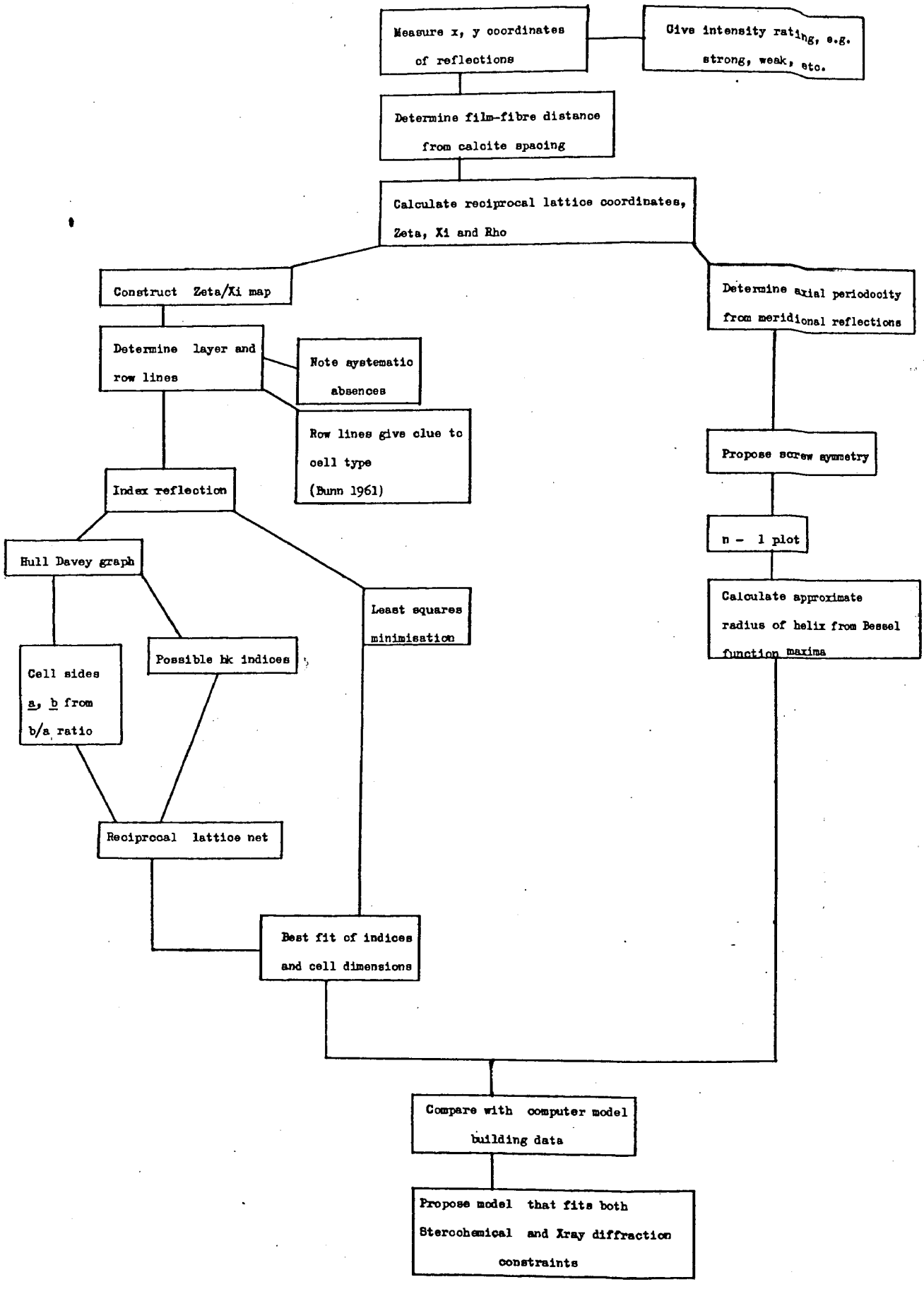

Schematic of possible procedures used in determination of a polysaccharide structure by Xray diffraction and computer model building.

Fig. 2.6

single, or multi-strand helices form the basic unit. Thus it is relatively easy at this level to follow changes to the crystalline polymer due to factors such as humidity changes, metal ion or temperature changes.

7. Determination of Unit Cell Parameters

(a) Use of Hull Davey Chart

Values of d_{hkl} are calculated for each layer line from the expression (6) in previous section. This is strictly true only for equatorial reflection ($l = 0$) but to a first approximation can be used for higher layer lines.

Using the method described by Alexander (1969), the ratio of the cell sides b/a can be determined, together with tentative indices (hk) for each reflection.

For an orthorhombic lattice a and b are determined from,

$$d\xi = d_{hko} = \frac{a}{\left[h^2 + \frac{k^2}{(b/a)^2}\right]^{\frac{1}{2}}} \qquad - 7.$$

(b) Unit cell least squares evaluation

A more convenient method for indexing and/or cell side evaluation is a least squares refinement of the various cell parameters such that the expression

$$\sum_i w_i (\rho_{io} - \rho_{ic})^2 \text{ is minimised} \qquad - 8.$$

where w = weight factor dependent on reliability of a reflection

ρ_o and ρ_c are the observed and calculated reciprocal lattice vector ρ_{hhl}, respectively.

A program was written for this purpose by Dr. W.E. Scott and supplied in an amended version by Dr. P.J.C. Smith, both of Purdue University. The strategy involved for this method can be summarised:

(i) From the row lines in the Zeta/X_i plot, approximate unit cell (a and b) dimensions can be estimated and a trial set of unit cell parameters postulated.

(ii) The type of cell can, in some cases, follow from the relationship between the a and b values as described by Bunn (1961).

(iii) Lists of ρ_{calc} with corresponding indices (hkl) can be calculated for each layer line that corresponds to the trial lattice.

(iv) A comparison of ρ_{calc} for each layer line with ρ_{obs} for each reflection on that line is then made. ρ_{obs} is calculated from

$$\rho = \left(S^2 + \xi^2 \right)^{\frac{1}{2}} \qquad -9.$$

Thus tentative indices can be assigned to each reflection.

(v) Given a collection of measured ρ values and their corresponding weights (w) and indices (hkl), along with initial trial values for a, b, c and γ, the program will least-squares refine any or all of the unit cell parameters so as to minimise the function (8) given above.

8. Computer Model Building

A full description of the processes used have already been described in some detail (Anderson, et al. 1969) consequently only a brief summary will be given here.

The procedure is applicable to any alternating polysaccharide chain consisting of a disaccharide repeat unit (also for homopolymers) without 1,5 or 1,6 glycosidic linkages.

Considering hyaluronic acid the repeat unit can be considered as a backbone (Fig. 2.7) on which other groups are fixed appendages. Following the methods and notations of Sugeta and Miyazawa (1967), the helical parameters, n and h can be expressed in terms of the angles of internal rotation Tau_{ij}, the angles between vectors and bonds ϕ_i, and the interatomic distances r_{ij} (Fig. 2.7). All these quantities are implicit in the starting assumptions, (Rees, 1969a; Anderson, et al. 1969) except Tau_{12}, Tau_{34}, Tau_{45}, Tau_{61} which correspond respectively, to ψ_{BA} ϕ_{AB}, ψ_{AB} and ϕ_{BA}. A short length of the polymer chain is set up in the computer and the combinations of Tau_{34} and Tau_{45} are obtained that are not excluded by van der Waals outer limit criterion. (Table 2.3.)

Table 2.3

Hard sphere limits

Atoms	Outer	Inner		
		normal	Acetamide calculations	three-fold calculations
	nm	nm	nm	nm
C–C	0.32	0.3	0.29	0.18
C–O	0.29	0.27	0.26	0.14
O–O	0.25	0.24	0.24	0.10
C–H	0.24	0.22	0.21	0.11
O–H	0.24	0.22	0.21	0.10
H–H	0.20	0.19	0.18	0.06

Each angle is varied stepwise from 0° to 360° for every value of the other; this allows all interatomic distances to be calculated so that sterically impossible conformation can be repeated. Similarly all possible combinations of Tau_{12} and Tau_{61} are obtained. Each allowed combination of Tau_{34} and Tau_{45} taken with each allowed combination of Tau_{12} and Tau_{61} and with the fixed parameters ϕ_c and r_{ij} already determined, values of n and h are

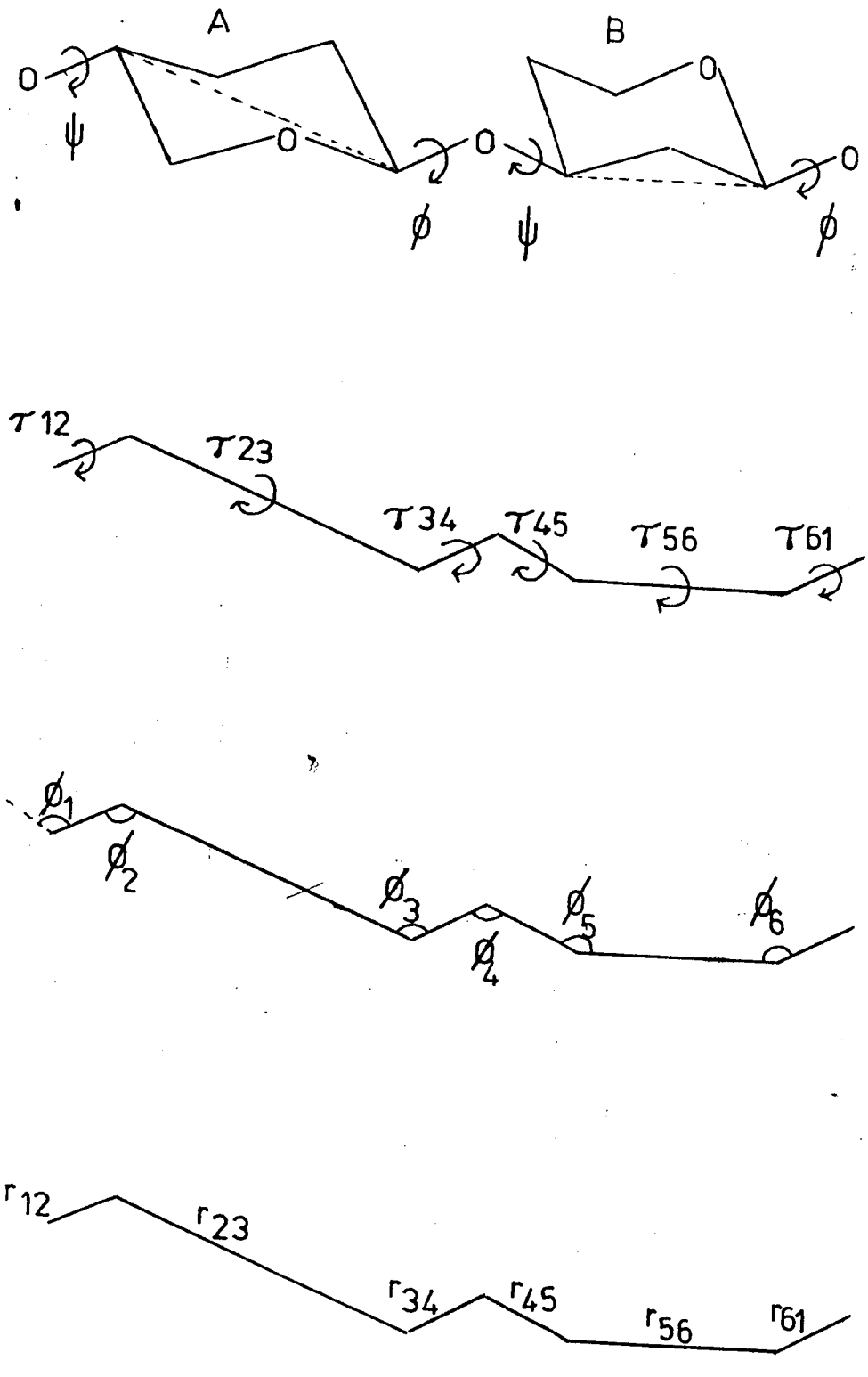

Fig. 2.7 Definition of chain backbone

(a) disaccharide including backbone,

(b) dihedral angles; τ_{23} and τ_{56} are fixed by the geometry of the sugar ring,

(c) fixed angles between vectors and bonds,

(d) fixed interatomic distances.

calculated. The results for this stage are then plotted on n-h graphs (Ramachandran, et al. 1963), holding two angles constant at a time, n and h are found to change smoothly with the torsion angles. The conformations required are at the intersections of the n = ± x curves with the curve corresponding to the value of h (n and h having values consistent with those derived from the diffraction pattern). Often it is then necessary, and desirable, to repeat the calculations for the suggested region in small steps to pinpoint a possible set of angles more accurately. The result is a list of sets of T_{ij} values which will give the measured or postulated n and h.

For each T_{ij} set, a complete turn of helix (or more) can be generated having the corresponding n and h values. Contacts between non adjacent residues and residues in different chains are then checked.

This is the procedure used in studying the various forms of hyaluronate in this chapter, in subsequent chapters modification of this basic procedure to deal with tri- and tetra-saccharide repeats and repeating units involving 1,6 linkages will be discussed. This is only the initial limited approach to molecular model building. Further stages, which involve the consideration of inter-chain packing and refinement of geometrical parameters against the measured Xray intensities, were not done in this laboratory but by our colleagues at Purdue University.

9. Deuteration and Infrared Dichroism

Deuteration was carried out in a gastight sample cell, containing the polysaccharide film, fitted with an inlet for nitrogen, which had been slowly bubbled through deuterium oxide (Prochem; 99.8 g of D_2O/100 g) and an outlet to a calcium chloride tube.

The film sample was held in the cell between barium fluoride windows on a mounting such that the beam only passed through the sample. Deuteration was normally complete after two hours exposure to deuterium oxide vapour.

The cell was attached to a Perkin Elmer 337 double beam recording grating spectrometer having a rotatable polariser mounted in the common beam between the sample and detector.

An adjustable grating was used to reduce the intensity of the reference beam although ideally a cell containing a reference film might have been more representative.

C. RESULTS AND DISCUSSION

1. Diffraction Patterns from Four-Fold Helices

(a) Hyaluronate at pH 2.6 ('putty' form)

Fig. 2.8a shows an Xray diffraction photograph from sodium hyaluronate obtained initially from a film of high molecular weight umbilical cord 'putty', supplied by Dr. E.A. Balazs. He produced the film by pressing the 'putty' between two microscope slides, allowing to air dry before removing. The film was held under stress (5g) at room temperature (ca 22°C) and 80% relative humidity. In the first hour the film stretched about 50% and had doubled in length in about 16 hours. The diffraction photograph shows good crystallinity and orientation, the diagram improving on being held at the above conditions over a number of weeks.

Subsequent photographs were obtained from putties prepared as previously described using high molecular weight umbilical cord hyaluronate (batch # 1119) and rooster comb (batch C34 and C32/2) kindly provided by Dr. E.A. Balazs. Films were produced by initially squashing the 'putty' on a teflon block then allowing to dry at room temperature and humidity. Films were stretched as before, the extension varying from 100 ⟶ 400%. The photographs (Fig. 2.8b) obtained for all

preparations, were essentially identical to the original (Fig. 2.8a) except that they showed higher crystallinity and orientation.

The salient features of the diagram are:-

(i) The strong meridionals on layer lines l = 2,4, plus a somewhat weaker meridional on l = 6, i.e. meridional reflections are present when l = 4n-2 rather than the expected l = 4n (see 1(d) p.79). When the specimen is suitably tilted, the diffraction photographs also show meridionals on all even layer lines up to 14 i.e. to about 0.24 nm resolution.

(ii) The striking absence of low angle reflections on the equator and on layer lines 1 and 2 (Fig. 2.9).

(iii) The lack of horizontal streaking suggests that the helices are antiparallel.

(iv) The axial periodicity from a consideration of the layer line spacings is 3.39 ± 0.02 nm.

Unit Cell Parameters

Indexing of the reflections was on a trial and error basis using one or more of the procedures indicated in the Methods section.

Initial values were obtained using the simplified Hull-Davey chart (Alexander, 1969) (Fig. 2.10) producing a fit for an orthorhombic cell with $\underline{a}$ = 2.24 nm, $\underline{b}$ = 0.98 nm ($\underline{c}$ = 3.39 nm, the fibre axis). However another fit was found by ignoring certain weak reflections that were later found to be due to a small amount of a mixed phase, with $\underline{a}$ = 1.14 nm, $\underline{b}$ = 0.98 nm that was clearly a simpler version of the former.

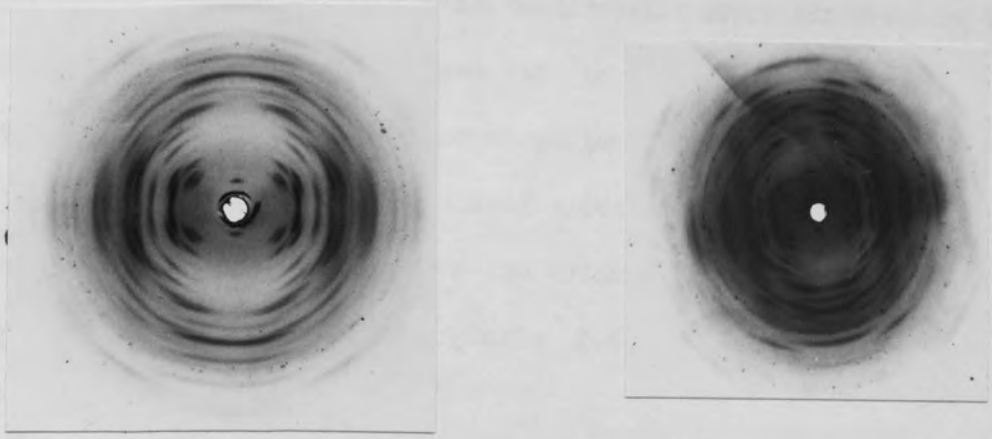

Fig. 2.8 Xray diffraction patterns from hyaluronate

(a) pH 2.5 'putty', original pattern

(b) subsequent patterns.

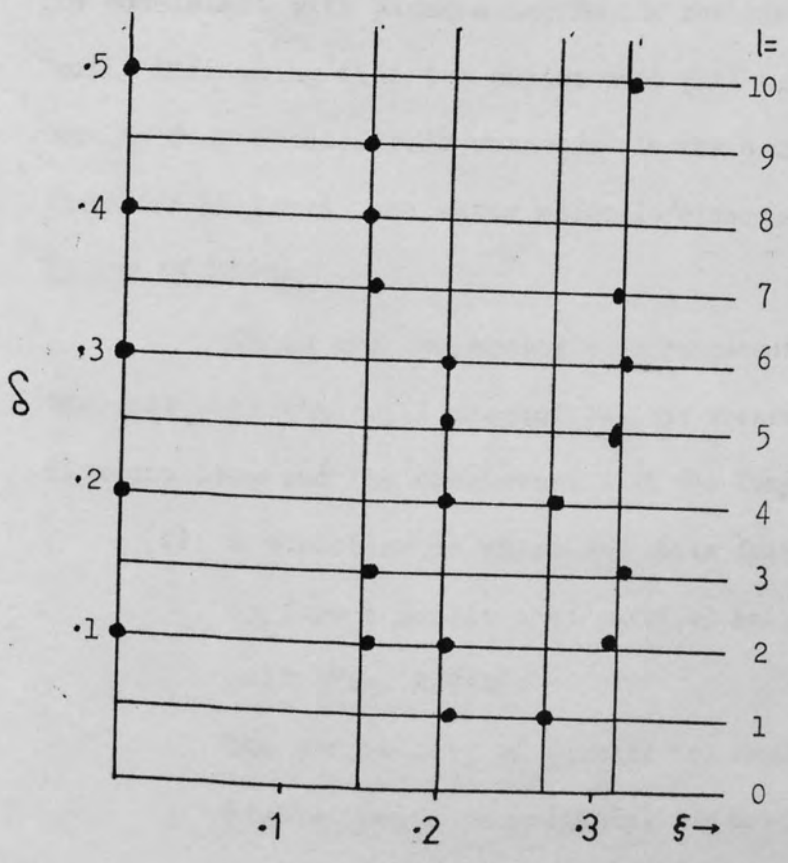

Fig. 2.9 Zeta/Xi map for pattern (b) above

•, indicates reflection.

Obviously there is considerable scope for error in this method but the value obtained can be verified to some extent by a reciprocal lattice net construction (Alexander, 1969).

Subsequently the cell sides were refined using the least squares program CELL to give the orthorhombic lattice with a = 1.153 nm, b = 9.89 nm, c = 3.388 nm (Table 2.4).

Density

Stereochemical calculations, together with the axial repeat from the diffraction pattern, indicate that the most reasonable model for this and the other 4_3 forms would be one having four disaccharide residues per turn of helix. This is reinforced by the density measurements. The weight for ($C_{14}O_{11}NH_{20}Na$), the disaccharide repeat of sodium hyaluronate, is 401.3. The measured density by flotation of the stretched fibres was 1·45 gm/cc. giving an observed mass/repeat unit of 421.5. This is consistent with eight disaccharide residues in each unit cell, indicating that two chains must pass through the cell, each having four disaccharide residues in the c axis repeat distance. There is at least one water molecule/disaccharide.

Choice of Model

There are two probable arrangements of the chains in the unit cell that will account for the presence of eight disaccharides and be consistent with the Xray data

(i) A structure in which one chain drapes around the other to form a double anti parallel helix at the corner of the cell (Fig. 2.24b).

The possibility of packing two chains in a parallel double helix is unlikely, for the following reasons:

In general when two chains pack together around a single

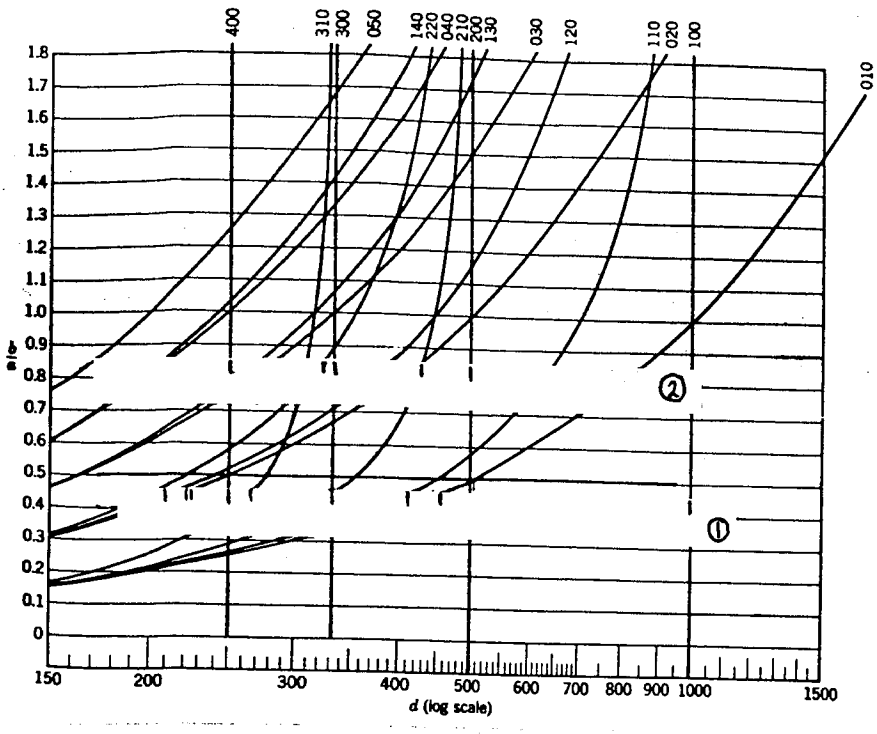

Fig. 2.10 Hull-Davey chart showing two possible fits;

1. b/a = 0.44 giving a = 2.24 nm, b = 0.98 nm
2. b/a = 0.86 giving a = 1.14 nm, b = 0.98 nm

Observed Intensity*	h	k	l	ρ_{obs}	ρ_{calc}
vs	0	2	1	0.2124	0.2044
av	2	2	1	0.2719	0.2681
s	2	0	2	0.1825	0.1832
vs	1	2	2	0.2296	0.2278
s	1	3	2	0.3251	0.3210
s	3	2	3	0.3466	0.3412
av	3	1	5	0.3126	0.3157
w	4	0	5	0.3774	0.3770
av/w	3	3	7	0.4429	0.4498
av	1	3	8	0.3906	0.3940
s	4	0	9	0.4330	0.4368

Table 2.4 Best Fit Comparison of ρ_{obs} with ρ_{calc} for orthorhombic cell; a = 1.153nm, b = 0.989 nm, c = 33.88 nm

* Visual rating: vs = very strong, s = strong, av = average, w = weak

axis they are constrained by space filling considerations to be 180° or close to 180° out of phase. Thus for two parallel chains exactly 180° out of phase all odd layer lines would be absent i.e. there would be a halving of the diffraction pattern as in ι-carrageenan (Anderson, et al. 1969; Arnott et al 1974). The true repeat would thus be 6.78 nm (2 x 3.39) and the resulting model could not be a simple four-fold structure, as proposed. With helices that are almost 180° out of phase, a weakening of odd order layer lines should appear, this is not seen. In the case of an anti parallel double helix there is no simple symmetry relationship between chains and therefore the transform that is sampled is basically that of a single chain.

(ii) A single helical structure having one chain at the corner and one at the centre in which the two chains could be parallel or anti parallel (Fig. 2.24a) although most probably anti parallel by examination of the diffractive diagram.

Computer refinement and packing studies were undertaken to test both cases, by our collaborators at Purdue University, and will be discussed later in this chapter.

The foregoing has been concerned in the main with the diffraction photographs produced from the unusual viscoelastic putty form of hyaluronate that is perhaps a more pronounced form of the solution at pH 7 that also exhibits non-Newtonian viscosity, and computer model building will of course apply equally to all molecular structures having the axial periodicity of 3.39 nm. However it appears that hyaluronate exists in several different conformations and molecular packing arrangements.

b. Hyaluronate at neutral pH

Oriented films were made from neutral pH (6-7) sodium hyaluronate solutions by the technique previously described. The first diffraction pattern was obtained for a film supplied by Dr. E.A. Balazs (Batch No. ~~##~~ 1113 dried in a desiccator). Initially this gave a diffraction photograph that could be considered as a mixed state.

The features of the photograph are:

(i) meridional reflections are consistent with three-fold and four-fold structures having axial periodicities of 2.85 nm and 3.38 nm respectively.

(ii) Strong equatorial reflections were apparent.

(iii) Lack of horizontal streaking again suggests absence of disorder involving 'up-pointing' and 'down-pointing' chains.

Indexing shows the presence of three main forms

a) an hexagonal form, previously reported by Atkins et al. (1972) having $a = b = 1.17$ nm, $c = 2.85$ nm

b) a large orthorhombic cell (Atkins et al. 1974) having $a = 3.42$ nm, $b = 1.17$ nm, $c = 2.85$ nm

c) the orthorhombic form found for the 'putty' sample above

d) a few reflections could be indexed on four-fold orthorhombic forms having $c = 3.72$ (Atkins and Sheehan, 1972).

Thus we have the situation of an intermediate multi-crystalline state which contained the single helical structures a, b and d, that have disaccharide axial periodicities greater than 0.9 nm giving an extended structure, coexisting with a structure having a more squat disaccharide axial periodicity of 0.84 nm that could be interpreted as either a double or single helix.

Interestingly on leaving the specimen under constant tension and relative humidity for a period of weeks it 'relaxed' entirely into form (c) above, suggesting that the other more extended helices were intermediately in the formation of this more favourable squat structure. The interconversion of the various forms of hyaluronate has been interpreted by others (Atkins and Sheehan, 1972), and will be discussed later.

Subsequent experiments on a variety of samples, both in our hands and those of the Purdue Group, have failed to produce the type of diffractive pattern with $\underline{c}$ = 2.85 nm. Routinely the pattern was that of type (c) with perhaps 5% of the reflection but could be indexed on the basis of the hexagonal cell type (a), that usually were lost on aging.

A typical pattern of the mixed sample is shown in Fig. 2.11 with its Zeta/Xi diagram showing row and layer line that lead to the various cells.

On one occasion the hexagonal form (a) was obtained under circumstances that might be described as accidental and harsh. The hyaluronate solution remaining in a test tube after casting a film on a Teflon sheet was left on the bench for several days before it dried and detached itself from the glass. Clearly there was ample opportunity for contamination and degradation. However when a strip of film was stretched at 80% relative humidity a pattern essentially the same as that published by Atkins and Sheehan (1972) was obtained, showing the characteristic rib-like pattern. This is shown in Fig. 2.12 together with Zeta/Xi map. It was indexed on the same unit cell as obtained by Atkins and Sheehan (1972) (Table 2.5). It was interesting to note

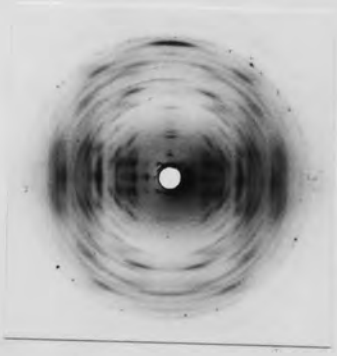

(a)

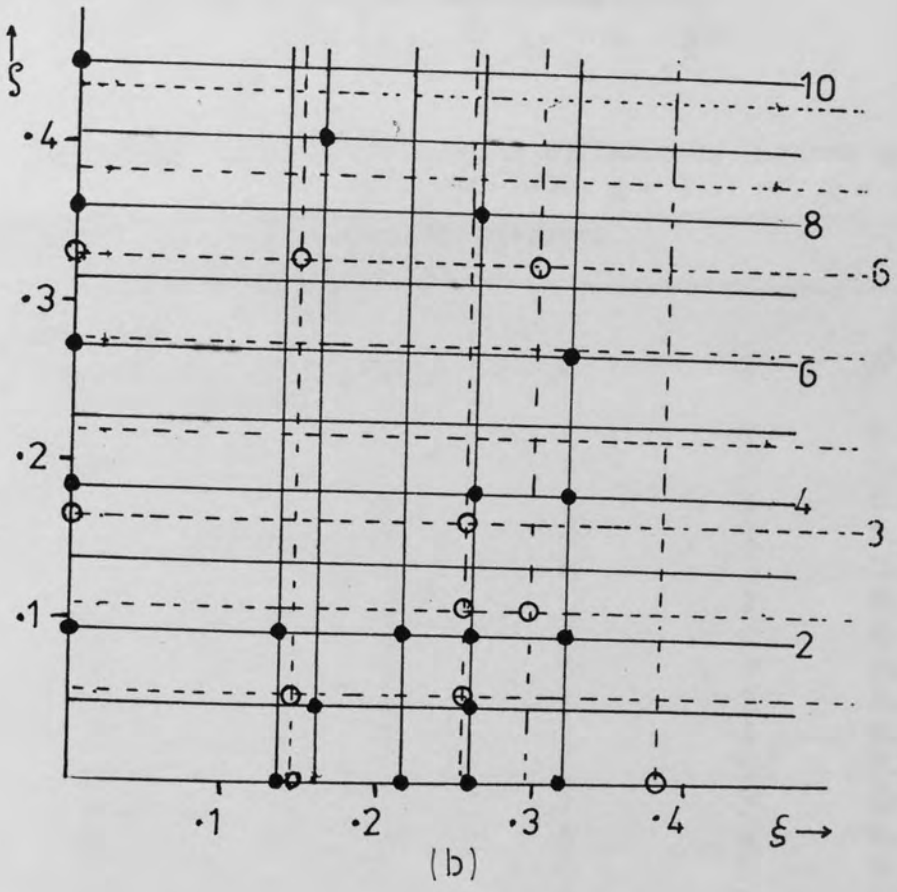

Fig. 2.11 (a) 'Mixed' diffraction pattern from pH 7 hyaluronate

(b) Zeta/Xi diagram for the mixed pattern, showing some of the reflections that index on an orthorhombic cell, a = 1.14 nm, b = 0.989 nm, c = 3.388 nm (solid circles). Also on an hexagonal cell, a = 1.17 nm, c = 2.85 nm (broken circles).

Other reflections (not shown) could be indexed on other reported cells (Table 2.8 p. 94)

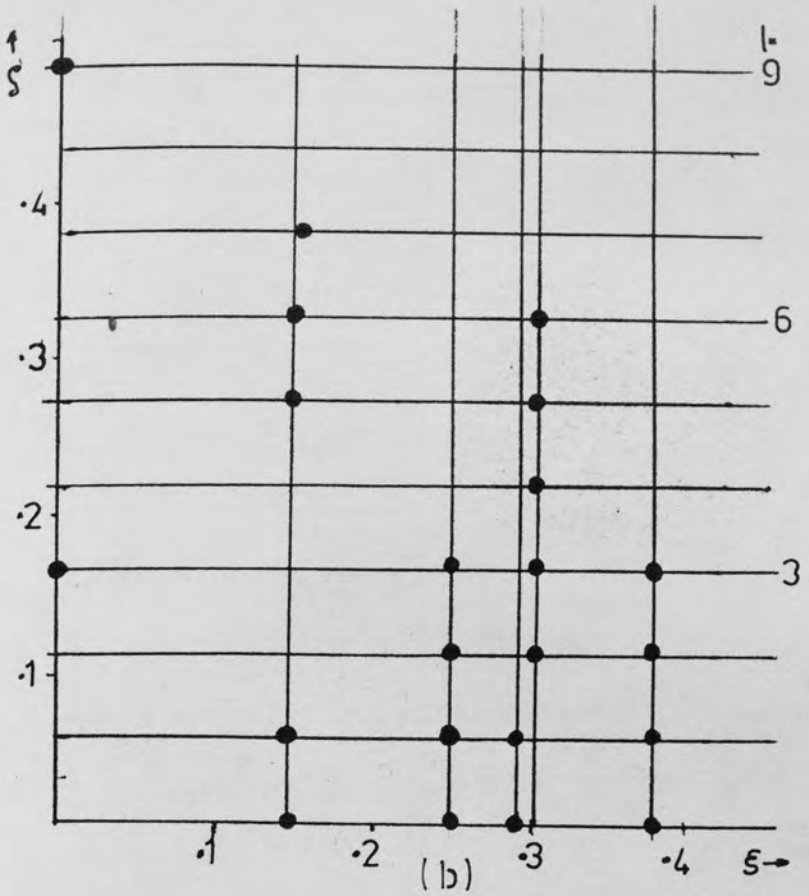

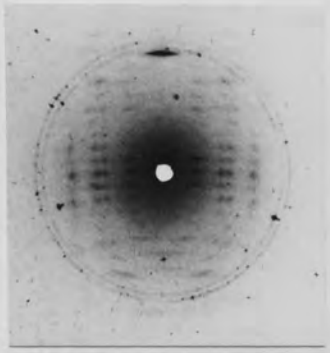

(a)

Fig. 2.12 (a) Hyaluronate diffraction pattern characteristic of hexagonal cell, a = 1.17 nm, c = 2.85 nm.

(b) Zeta/Xi diagram.

Observed Intensity	h	k	l	ρ obs	ρ calc
av	1	0	0	0.1023	0.0982
av	1	1	0	0.1768	0.1701
av	2	1	1	0.2557	0.2620
av	3	0	1	0.2901	0.2967
w	4	0	1	0.3852	0.3905
av	2	1	2	0.2721	0.2692
av	3	0	2	0.3156	0.3094
av	4	0	2	0.4007	0.3992
w	4	0	3	0.4133	0.4067
w	2	2	4	0.3651	0.3681
av	3	0	5	0.3455	0.3430
av	2	2	5	0.3756	0.3820
av	2	1	6	0.3370	0.3345
av	2	2	6	0.3988	0.4001
av	3	0	7	0.3879	0.3836
av	3	1	7	0.4398	0.4310
av	2	2	9	0.4662	0.4642
av	2	2	8	0.4410	0.4411

Table 2.5 Best fit comparison of ρ obs and ρ calc for hexagonal cell a = 1.17 nm, c = 2.85 nm.

that most parts of the specimen, when photographed, showed exclusively the orthorhombic form having c = 3.39 nm. Normally samples do not exhibit this kind of inhomogeneity along their length.

Prolonged keeping had the same effect as for the 'mixed' photograph and the patterns relaxed to the 'normal' four-fold orthorhombic form. Again, this experiment could not be repeated in a more controlled manner, i.e. allowing a film to form by drying slowly on a Teflon sheet.

It must therefore be concluded that the samples, through some accident in their preparative history, were caught in a transient crystalline state prior to their relaxation into the more stable orthorhombic form.

By aging and annealing samples of umbilical cord hyaluronate (Batch ## 1119) previously stretched at 80% relative humidity, two further conformational forms of hyaluronate have been observed.

c. Orthorhombic - 'one-fold'

On leaving a film specimen under tension at the same relative humidity for 2-3 weeks, the structure can become 'one-fold' in that meridionals are observable on every layer line from l=2 to l=10 (Fig. 2.13). The overall pattern indexes on a similar orthorhombic unit cell to those already discussed (see Table 2.6).

Here we have what is essentially an octasaccharide one-fold repeating structure, i.e. 8 sugar residues/turn of helix. Clearly this is an extension of the dissymmetry shown by the four-fold structure previously discussed. Variables causing this dissymmetry that need to be considered are:-

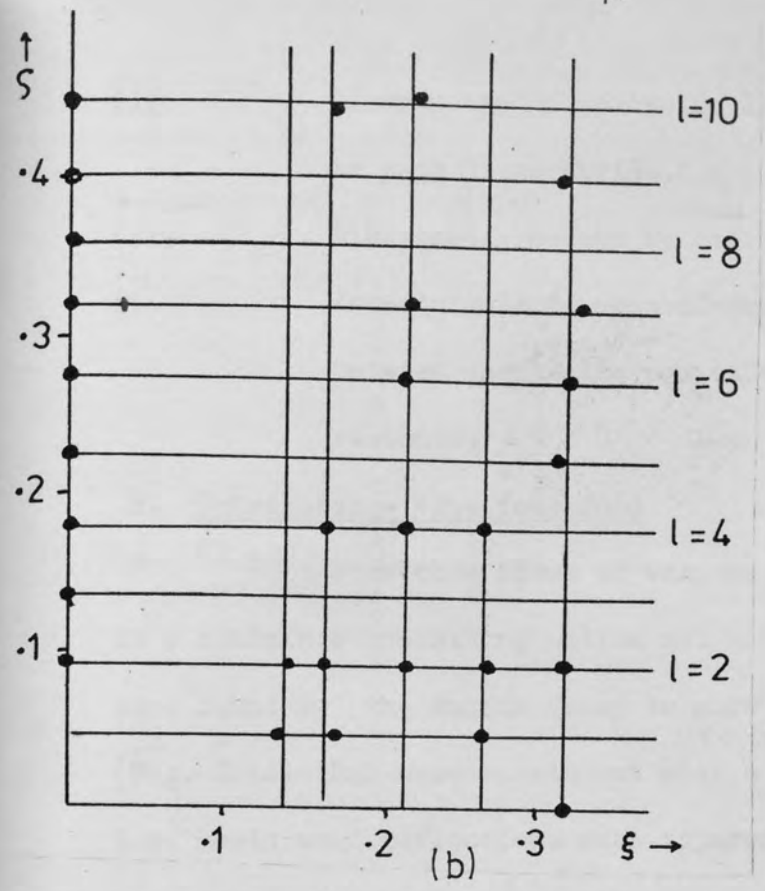

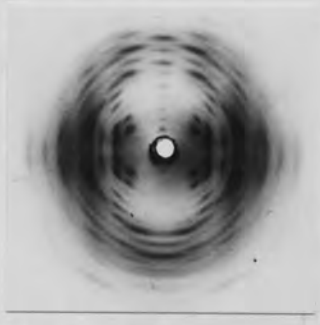

(a)

Fig. 2.13 (a) Diffraction pattern for orthorhombic 'one-fold' cell.

(b) Zeta/Xi diagram.

Observed Intensity	h	k	l	ρ_{obs}	ρ_{cale}
w	1	0	1	0.0947	0.0911
w	1	1	1	0.1378	0.1365
w	2	0	1	0.1759	0.1747
vs	2	2	1	0.2681	0.2680
av	2	0	2	0.1868	0.1823
vs	1	2	2	0.2270	0.2287
vs	1	3	2	0.3242	0.3224
av	2	3	2	0.3526	0.3552
av	3	2	3	0.3441	0.3407
s	0	3	4	0.3203	0.3277
w	3	2	5	0.3676	0.3613
av	3	1	5	0.3159	0.3155
av	1	3	8	0.3984	0.3976
av	2	3	8	0.4266	0.4246
av	0	4	7	0.4591	0.4576
av	2	3	8	0.4256	0.4246

Table 2.6 Best fit comparison of ρ_{obs} and ρ_{calc} for orthorhombic one fold $\underline{a}$ = 1.162 nm, $\underline{b}$ = 0.984 nm, $\underline{c}$ = 3.332 nm

(i) Dissymmetry of acetamide and/or carboxyl residues in <u>each</u> disaccharide.

(ii) Dissymmetry caused by cations and/or water.

(iii) Non-equivalence of conformation angles (ϕ, ψ) between chemically equivalent disaccharide residues.

d. <u>Tetragonal - true four-fold</u>

Stretched films of various hyaluronates when placed in a container containing silica gel and maintaining the tension, were found by the Purdue group to give diffraction photographs (Fig. 2.14) that were consistent with a true four-fold structure i.e. meridional reflections were apparent only on every 4th layer line ($l = 4n$). We have repeated this work and confirm that these patterns can be indexed on the basis of a tetragonal cell of base parameters $\underline{a} = \underline{b} = 0.989$ nm (Table 2.7).

It is interesting to note that this relatively mild treatment involving removal of water from the structure has also removed the dissymmetry present in the other forms. The most reasonable interpretation of the apparent dissymmetry is that the overall distribution of intensities is altered little between the various 4_3 forms suggesting little change in the overall backbone conformation. Thus the lower symmetry of the other forms is unlikely to be traced to the backbone conformation angles. This may have been caused by water and cations between helices rather than interstitial water (which may be difficult to remove without harsher treatment e.g. heat). Also of note, the tetragonal cell has shrunk in one direction only i.e. from 1.153 to 0.989 nm.

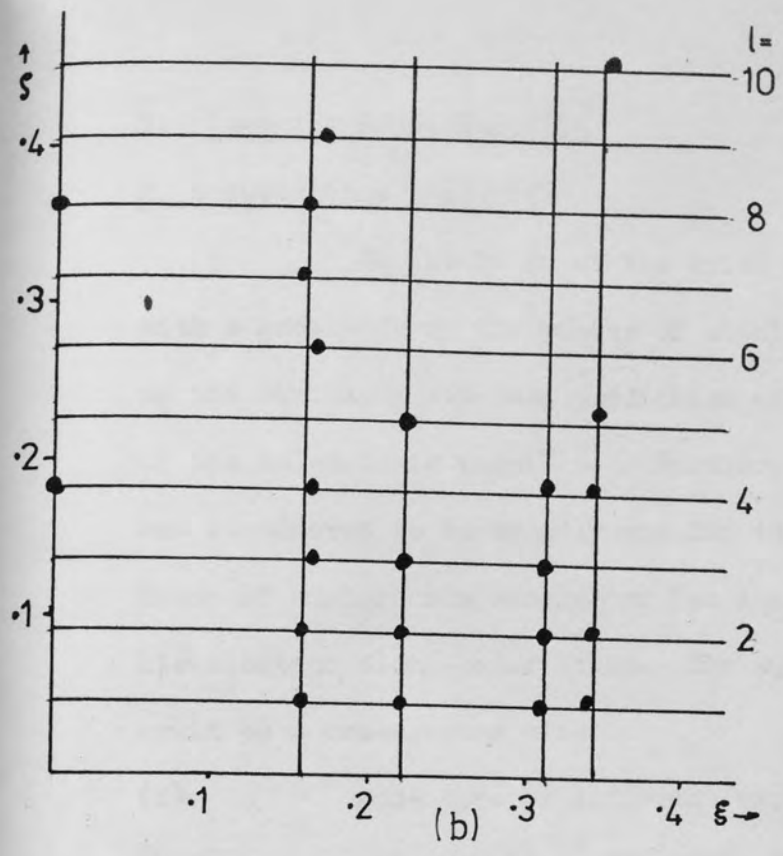

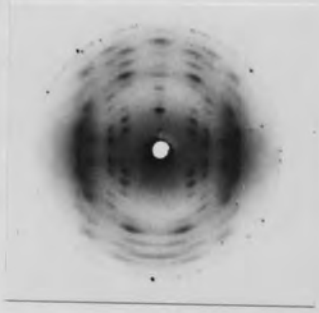

(a)

Fig. 2.14 (a) Diffraction pattern for tetragonal form of hyaluronate.

(b) Zeta/Xi diagram.

Observed Intensity	h	k	l	ρ_{obs}	ρ_{calc}
vs	2	1	1	0.2231	0.2280
vs	3	0	1	0.3048	0.3115
s	2	1	2	0.2336	0.2336
w	3	1	2	0.3269	0.3251
w	2	1	3	0.2418	0.2427
av	2	0	4	0.2318	0.2340
s	3	2	4	0.3826	0.3831
w	2	2	4	0.2998	0.3093
av/w	2	2	5	0.3187	0.3217
av	2	2	7	0.3589	0.3525
av	2	2	7	0.4477	0.4539
av	3	1	8	0.4021	0.3992
av	4	0	9	0.4653	0.4681

Table 2.7 Best fit comparison of ρ_{obs} and ρ_{cale} for tetragonal cell

$\underline{a}$ = 0.989 nm, $\underline{c}$ = 3.396 nm

2. Computer Model Building

4_3 orthorhombic cell

On the basis of the axial repeat period, together with a knowledge of the number of chemical repeating units making up the chains, a reasoned prediction of the backbone conformation of the molecule is possible. Further, the backbone conformation was considered to be broadly similar to those in the other 4_3 forms of hyaluronate because of the similarity of the intensity distribution along layer lines. The apparent lower symmetry could be a consequence of:-

(i) some type of different arrangement of the pendant side groups on alternate disaccharides. The obvious choice being the acetamido group or possibly the carboxyl, and/or

(ii) some irregular distribution of the counterions that are likely to be coordinated within the structure.

Early theoretical computer predictions (Rees, 1969) suggested that a probable molecular structure for hyaluronate would be one having $n \simeq \pm 4$ and $h \simeq 0.8$ nm, with a preference for left-handed helices. Double helices were a strong possibility, particularly as a consequence of the strong structural similarity of the backbone to that of carrageenan ($n = +3$, $h = 0.86$ nm) as shown in Fig. 2.15.

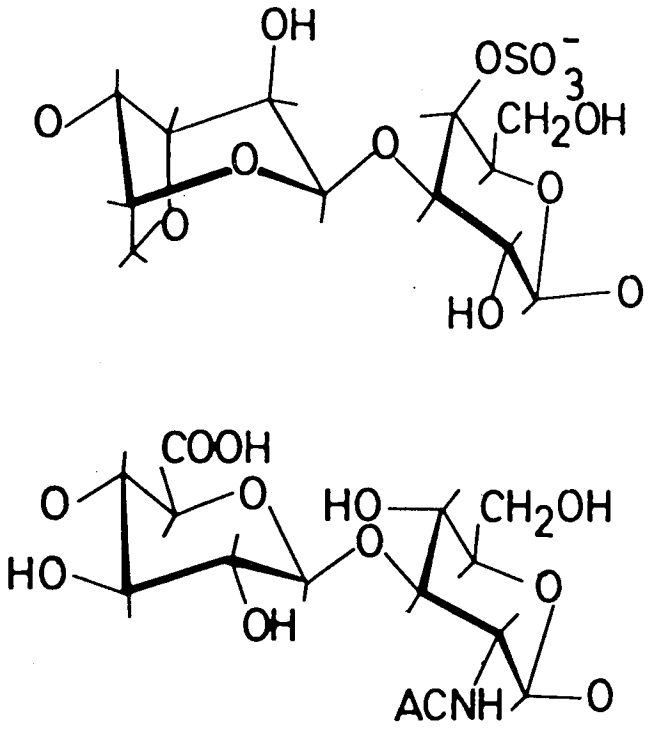

Fig. 2.15 Backbone similarity between kappa-carrageenan (a), and hyaluronic acid (b)

Search for suitable glycosidic angles

From an investigation of all combinations of the glycosidic angles ϕ and ψ for the B-A and A-B linkages (Rees, 1969), only about 10% of the values were 'allowed' (Fig.2.16) as judged by the 'outer limit' criteria (Ramachandran et al, 1963). The conformational maps (the so called hard sphere maps) produced are shown in Fig. 2.16, in which it can be seen that the 'fully' and 'marginally allowed' regions occur as a single main block, with small subsidiary zones.

The conformations at each glycosidic linkages seem to be virtually confined by steric forces to a range of oscillation of

B-A linkage

TAU61= \ TAU12=	0	40	80	120	160	200	240	280	320	360
0	0	0	0	0	0	0	0	0	0	0
20	0	0	0	0	0	0	0	0	0	0
40	0	0	0	0	0	0	0	0	0	0
60	0	0	0	0	0	0	0	0	0	0
80	0	0	0	0	0	0	0	0	0	0
100	0	0	0	0	1	2	0	0	0	0
120	0	0	0	0	1	2	0	0	0	0
140	0	0	0	0	1	2	2	2	1	0
160	0	0	0	0	0	0	2	2	1	0
180	0	0	0	0	0	0	2	2	1	0
200	0	0	0	0	0	0	0	0	0	0
220	0	0	0	0	0	0	0	0	0	0
240	0	0	0	0	0	0	0	0	0	0
260	0	0	0	0	0	0	0	0	0	0
280	0	0	0	0	0	0	0	0	0	0
300	0	0	0	0	0	0	0	0	0	0
320	0	0	0	0	0	0	0	0	0	0
340	0	0	0	0	0	0	0	0	0	0
360	0	0	0	0	0	0	0	0	0	0

A-B linkage

TAU34= \ TAU45=	0	40	80	120	160	200	240	280	320	360
0	0	0	0	0	0	0	0	0	0	0
20	0	0	0	0	0	0	0	0	0	0
40	0	0	0	0	0	0	0	0	0	0
60	0	0	0	0	0	0	0	0	0	0
80	0	0	0	0	0	0	0	0	0	0
100	0	0	0	0	0	0	0	0	0	0
120	0	0	0	0	0	0	0	0	0	0
140	0	0	0	0	0	0	0	0	0	0
160	0	0	0	0	0	1	2	0	0	0
180	0	0	0	0	0	1	2	0	0	0
200	0	0	0	0	0	1	2	1	2	1
220	0	0	0	0	0	0	0	1	2	1
240	0	0	0	0	0	0	0	1	2	0
260	0	0	0	0	0	0	0	0	0	0
280	0	0	0	0	0	0	0	0	0	0
300	0	0	0	0	0	0	0	0	0	0
320	0	0	0	0	0	0	0	0	0	0
340	0	0	0	0	0	0	0	0	0	0
360	0	0	0	0	0	0	0	0	0	0

Fig. 2.16 Hard sphere maps for the B–A and A–B linkages (Rees, 1969), showing only about 10% of 'allowed' values i.e. printed 1 or 2 on map.

approximately 90° about each bond to the oxygen. Using the procedure outlined in the Methods section, a search was made for screw symmetries (n) and projected residue heights (h) that fitted the Xray data, hence fixing the conformational angles.

Initial calculations, using Skerrett coordinates and omitting the acetamido side group, proved disappointing providing few possibilities in the chosen range. Shortening the 'outer-limit' criteria (see Table 2.3, p 63) and recalculating the hard sphere map was more encouraging, giving a small zone of right handed helices of the required n and h, and a larger zone of left-handed helices but having the wrong range of n/h values.

Repeating these calculations with the 'average' coordinates of Arnott and Scott (1972) that are likely to give a more realistic model, confirmed that:

(i) to account for an identity period of 3.37 nm in terms of a sterically acceptable, integral helix, one must have four disaccharide residues/turn of helix.

(ii) there are two, conformationally very different, zones of four-fold helices

(iii) there is no reason to doubt earlier calculations showing that double helices are possible in both these zones (Rees et al, 1969).

However, the opposite conclusion is reached in that it is now found that there is a good left-handed fit, but no integral right-handed helices were found that were stretched enough to match the known translation period. The right-handed

model was subsequently discounted. However, coordinates from both types of model showed (Fig. 2.17) that both gave sinuous strands reminiscent of a single strand of the ι-carrageenan double helix (Anderson et al, 1969; Arnott et al, 1974). On checking contacts between non-adjacent residues and residues in different chains both right and left handed forms gave 'allowable' double helical structures. Initial molecular models that were made of these structures clearly indicated the need to include the acetamido side group in the calculations.

Inclusion of the acetamido group in calculations

To avoid steric clashes it was apparent that the acetamido group was not in the usual trans conformation in which the C-O bond eclipses the $C_{(2)} - H_{(2)}$ bond on the sugar ring (Fig. 2.18). This is the 'ideal' situation that occurs in N-acetyl glucosamine crystals and is postulated for chitin

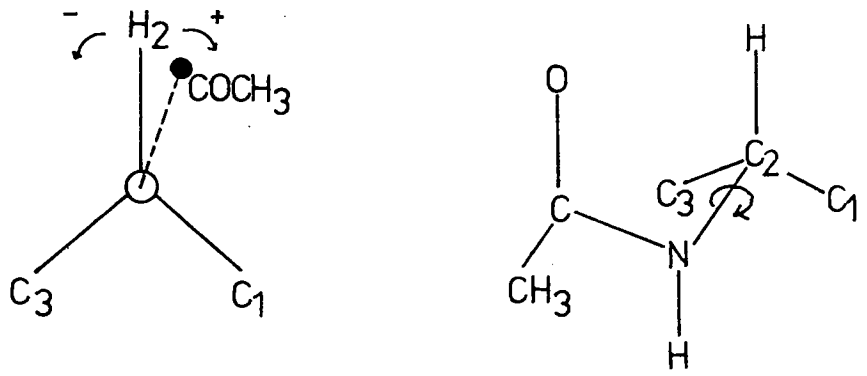

Fig. 2.18 Trans conformation of N-acetyl side group

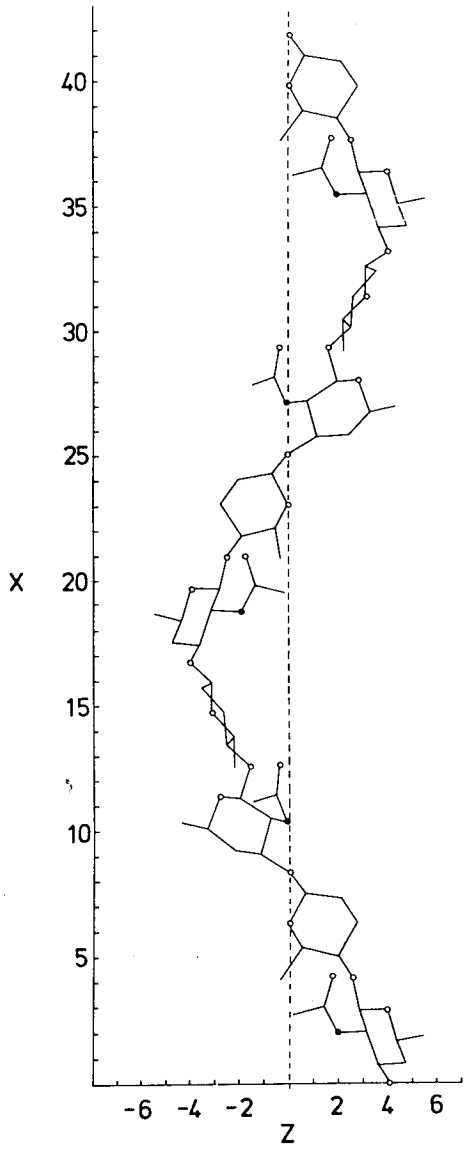

Fig. 2.17 Coordinate plot of left-handed hyaluronate helix, showing its sinuous character. A plot for a right-handed helix shows similar characteristics.

The coordinates for this residue were derived from Pauling-Cory (1953) parameters. The conformation about $C_{(2)}$-N (rather than C(O)-N) was varied systematically over the range that seemed reasonable.

When the contacts, including acetamido groups, were explicitly and accurately considered, the packing of two left-handed helices does become a great deal more restricted. However, by relaxing the 'outer-limit' contact criteria a little (0.01 nm or so) a small zone of 'marginally allowed' structures appeared which had the acetamido group in the 'expected' trans conformation (Johnson, 1966). Since the sampling in multi-dimensional conformational space was in discrete and not very small steps, it is possible that these models could be made 'fully-allowed' by relatively minor adjustments. For example rotation about the $C_{(2)}$-N bond, showed that only on two of the many maps were there any 'fully allowed' conformations, one with a value of $+60^{\circ}$ for the amide dihedral angle and the other with $+40^{\circ}$ that was almost identical. Although this acetamido conformation is unexpected on the basis of precedent, from classical conformational analysis it would be expected to be as stable as any other form.

3. Physical models

At various stages of the calculation Beevers ball and spoke molecular model were built together with CPK space filling models (Appendix 1).

A model of the right handed helix based on Skerrett coordinates revealed considerable problems in placing side groups that had not been included in the calculations so much so

that it was almost impossible to build a CPK model, thus the model was rejected.

The model based on the Arnott and Scott coordinates (Fig. 2.19) clearly showed that the acetamido group had to be displaced from the trans position to avoid steric clashes. A space filling model was also built according to these parameters (Fig. 2.20).

The potential steric clashes due to side groups did however lend support to the suggestion that these groups might be responsible for the apparent lower levels of symmetry observed in some Xray patterns. One could imagine having the acetamido groups in two different rotational states, these being 'paired' in a complementary fashion along the chain. Alternatively (or in conjunction with) the carboxyl groups in the centre of the helix could be in a partially ionised state rather than fully ionised. A precedent for this from another system polycytidylic acid, shows that a polyelectrolyte can exist in a partially ionised state at pH 7 and in so doing form similar conformations to those expected nearer its pK values (50:50 ionisation). This type of situation might be favoured by hydrogen bonding between adjacent carboxyl residues.

The models did, however, show some features that gave rise to some reservations on the validity of the double helix. Fig. 2.20 of the space filling model clearly shows large holes between carboxyl groups more than sufficient for two sodium ions plus some water. Further, a certain amount of bond strain was needed to close-pack the two antiparallel chains together.

Hydrogen bonding possibilities

Certain hydrogen bonding possibilities are evident,

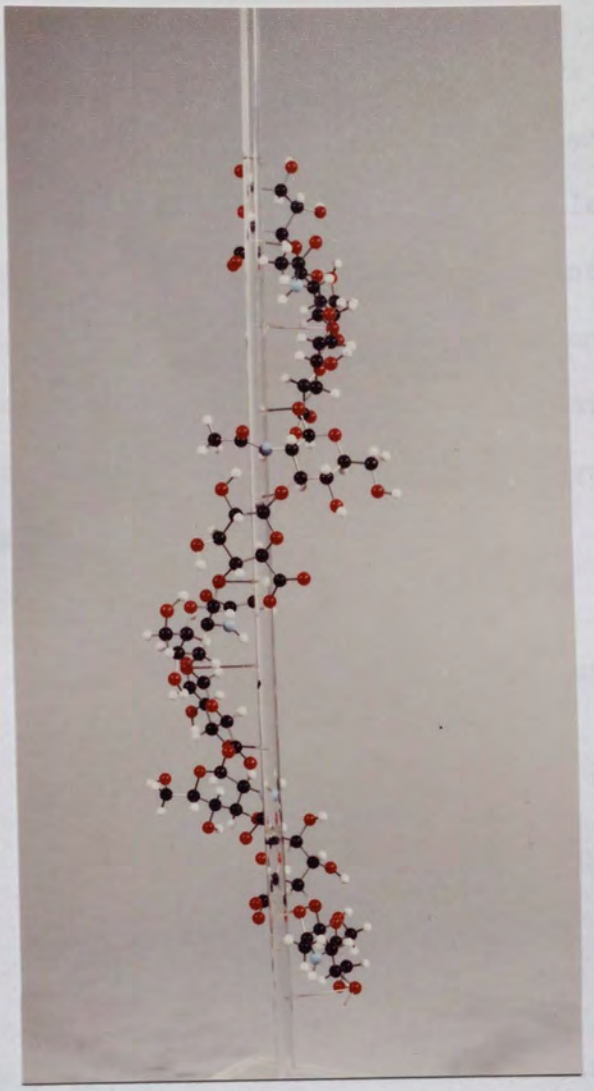

Fig. 2.19 Beevers model of the left-handed hyaluronate single helix

Fig. 2.20 C.P.K. spacefilling model of the left-handed hyaluronate double helix

the most striking being between the C(4) hydroxyl on the N-acetyl glucosamine residue on one chain and the C(5) carboxyl oxygen on the other chain. This is repeated along the length of the double helix and would appear to be the only inter-chain bonding. Intra-chain bonding is possible if some distortion of the acetamide group is induced from the strictly ideal conformation. Assuming the above it seems likely that a string of hydrogen bonds runs along each chain thus,

Intra-chain (atoms on acetamido residue are primed)

N' (2) - - - - - - - - - - $^{-}$OOC-

O' (5) - - - - - - - - - - O(3)

O (2) - - - - - - - - - - O' = C' $^{'}CH_3$

Inter Chain

A further possibility is an additional inter—chain carboxyl-carboxyl bonding sequence at the expense of the N(2) - - - - $^{-}$OOC- bond. This would give the sequence

O'(4) - - - - - $^{-}$OOC-

Strand 1 Strand 2

-COO - - - - - O'(4)

O'(4) - - - - - $\bar{O}$OC-

-COO - - - - - O'(4)

The carboxyl-carboxyl hydrogen bonding being approximately parallel to the longitudinal axis of the chain.

This is, of course, purely speculative and can only be substantiated or disproved by further model building calculations and possibly infra red dichroism studies.

4. Deuteration and Infrared Studies

Deuteration exchange and infrared dichroism studies on film samples have supported the existence of a hydrogen bond in ι-carrageenan (Williamson, 1970).

Using unstretched and stretched films of hyaluronate it was theoretically possible to check the proposed models for particular hydrogen bonding schemes by exposure to deuterium oxide vapour. Any buried hydroxyls would be expected to remain unexchanged.

The spectra before and after exchange (Fig. 2.21) show a suggestion of a residual hydroxyl peak and polarised infrared indicates the possibility of buried hydrogen bonds parallel to the helix axis.

The results of this study were inconclusive mainly due to problems with film thickness (too thick) and can only be taken as an indication.

5. Other conformations of hyaluronate - $\underline{h} > 0.92$ nm

Diffraction patterns of ordered samples of hyaluronate, by various workers, show a variety of preferred helical conformations that are summarised in Table 2.8.

Types (1) to (3) are most readily obtainable in our hands (including Purdue) although types (5), (6) and (8) have been seen as transient species in type (1).

The Bristol group have proposed (Atkins and Sheehan, 1972) a relationship between the various helical types that are claimed to be interrelated and that by varying relative humditiy, pH, temperature and applied stress, all forms may be obtained (Fig. 2.22).

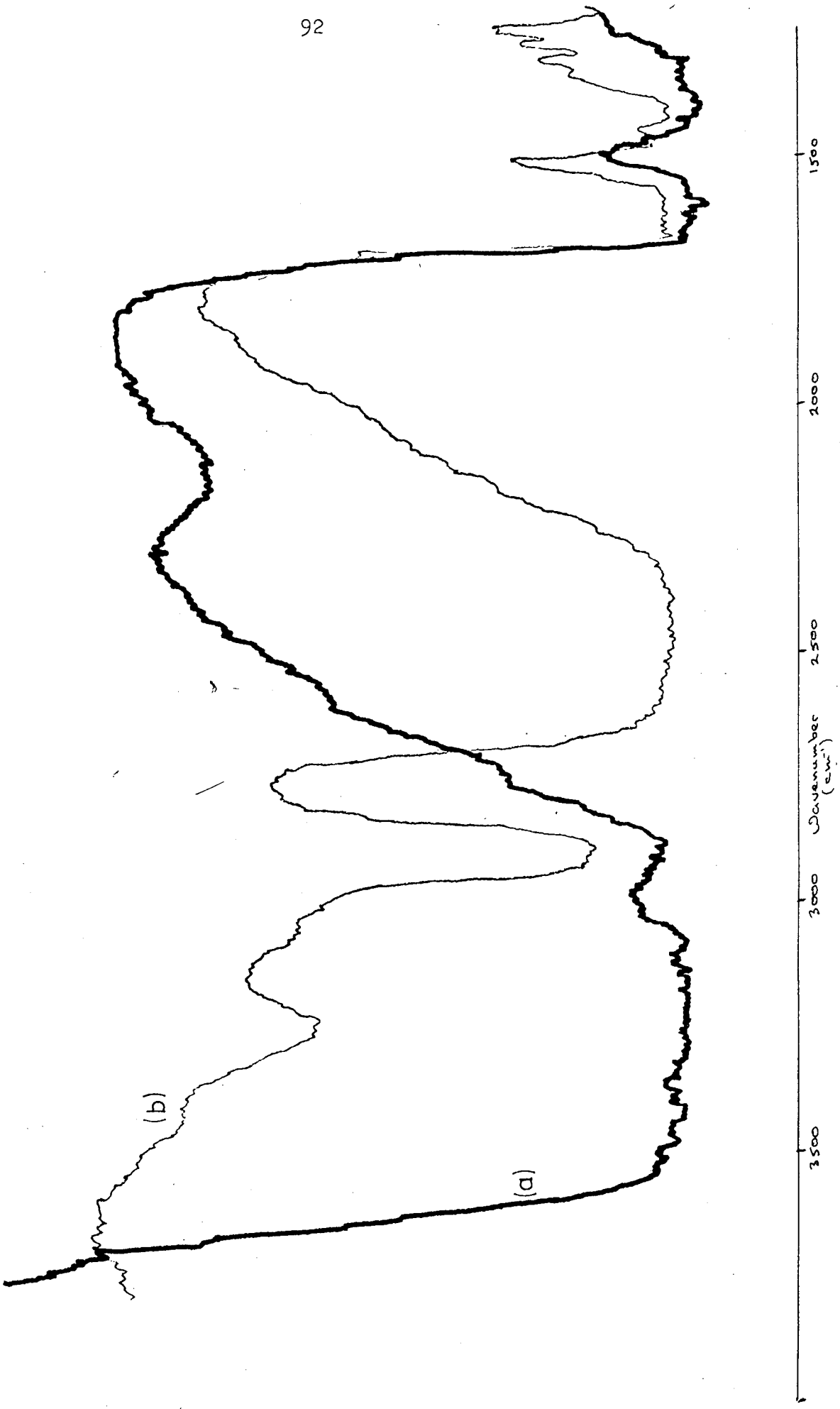

Fig. 2.21 Infra-red spectra of hyaluronate films.

(a) before deuteration; (b) after deuteration.

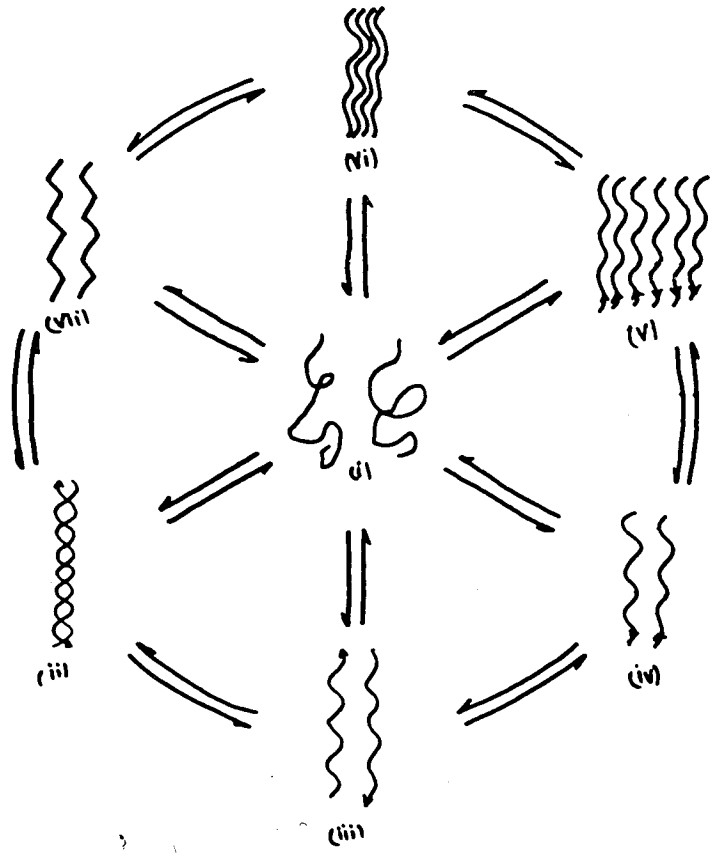

Fig. 2.22 Scheme for the interrelation of hyaluronate conformations (Atkins and Sheehan, 1973).

(i) the chains in dilute solution

(ii) the "double" helix

(iii) the antiparallel untwisted helices

(iv) the three-fold antiparallel helices

(v) the same helices packed closer together

(vi) a more compact state

(vii) a free acid form

It is claimed that each individual state can be obtained by variation of humidity and temperature.

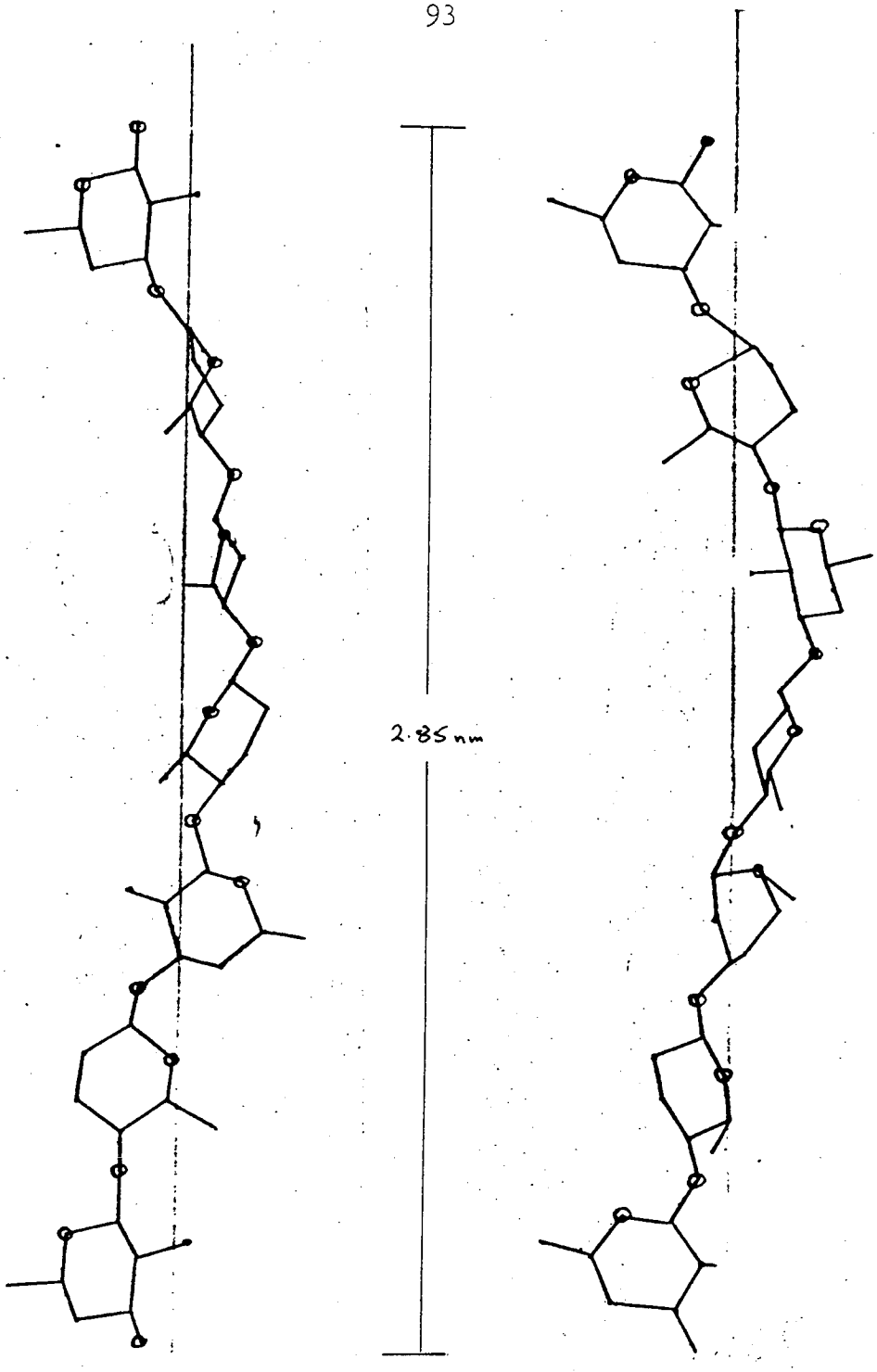

Fig. 2.23 Typical three-fold hyaluronate chain having fibre repeat distance of 2.85 nm. There is a strong similarity to the plot for the four-fold single strand in Fig. 2.17.

Cell type	Salt form	Helix 2_1	Helix 3_2	Helix 4_3	Meridional Symmetry	References
(1) Orthorhombic a=1.153nm, b=0.989nm c=3.388nm	Na^+			0.847	2 fold	This work; repeated/ confirmed at Purdue*
(2) Orthorhombic a=1.162nm, b=0.984nm, c=3.332nm	Na^+			0.833	1 fold	- do -
(3) Tetragonal a=b= 0.989nm c=3.396nm	Na^+			0.849	4 fold	Purdue; repeated/ confirmed by this work
(4) Orthorhombic a=1.10nm, b=0.99nm c=3.30nm	K^+			0.825	2 fold	Bristol+
(5) Orthorhombic a=1.04nm, b=0.90nm c=3.72nm	K^+			0.93	4 fold	Bristol; observed in 'mixed' form by this work and Purdue
(6) Hexagonal a=b=1.17nm, c=2.85nm	Na^+		0.95		3 fold	Bristol; repeated accidentally, confirmed by this work
(7) Hexagonal a=b=1.87nm, c=2.85nm	Na^+		0.95		"	Bristol
(8) Orthorhombic a=1.17nm, b=3.42nm, c=2.85nm	Na^+		0.95		"	Bristol; observed in 'mixed' form by this work
(9) Monoclinic c=1.96nm	Acid		0.98		2 fold	Bristol

Average error ± 0.005nm

Average axial periodicities in nm/ disaccharide

* Arnott et al. at Purdue University

\+ Atkins et al. at Bristol University

Table 2.8

Both the Purdue group and ourselves have difficulty in repeating this work. We found that a wide range of hyaluronate samples of varying source and molecular weight, routinely give diffraction patterns consistent with types (1) to (3) in Table 2. , and that annealing does not alter the interpretation.

If diffraction patterns for types (1) to (3) are consistent with a double helical structure it is difficult to envisage the mechanism proposed by Atkins and Sheehan (1972) by which it unwinds in the solid state to form single helices. Although the three-fold single helix is relatively extended(0.95 nm/disaccharide) it is not fully extended (1.02 nm/disaccharide); therefore could the extended forms be double helices?

Computer model building. Is there a three-fold double helix?

Using the techniques already described it was apparent that many possible models for single strands (having $n \simeq -3$ and $h \simeq 0.95$nm) existed. These turn out to be rather sinuous (Fig. 2.23) and closely related in both form and ϕ, ψ to the four-fold form (Fig. 2.17b).

On testing for double helix formation it was not until the 'outer limit' criterion had been relaxed to a sterically unacceptable level (Table 2.3) that marginally allowed possibility of three-fold double helices.

In the light of this, the double helix has to be reconsidered even though initial refinement calculations at Purdue showed that a unit cell consistent with a single helical structure, having one chain at the corner and one at the centre (Fig. 2.24a) was sterically unacceptable. Consequently the interconversion scheme of Atkins and Sheehan (1972) becomes more tenable if the double helical form is omitted.

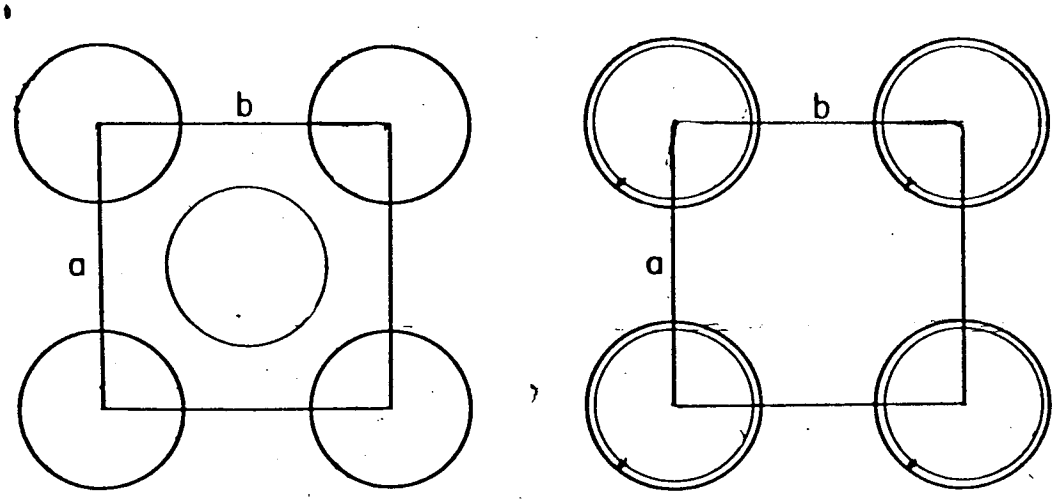

(a) (b)

Fig. 2.24 Chain packing arrangements for the 4_3 helical forms of hyaluronate.

(a) Single helices, one at the corner and one at the centre.

(b) Coaxial double helices at the corner of the cell.

6. Detailed model building - 4_3 helix

From the initial model building and chain packing considerations by ourselves and the Purdue group, the 4_3 helical types 1-3 (Table 2.8) were interpreted in terms of a left-handed antiparallel double helix (Dea et al. 1973) even though the model was not entirely satisfactory in certain aspects that have been mentioned.

We now know that the chain conformation we have produced is essentially correct, however, the chains are not packed in co-axial double helices (Fig. 2.24a) but rather side by side in an arrangement of the type shown in Fig. 2.24a. This has emerged from an elegant approach that was conceived by our collaborators at Purdue University. (Guss et al. 1974.)

Using the observed amplitudes of the diffracted intensities corresponding to the tetragonal lattice, they calculated by Fourier synthesis, the electron density in the unit cell corresponding to the particular phases of diffraction. Initially they disregarded the site of the second chain and calculated phases for a model with only one chain at the unit cell corners. (Fig. 2.25a.) Difference Fourier synthesis to a first approximation reveals additional electron density when the model phases are combined with the observed diffraction amplitudes. This density corresponds to a second antiparallel chain not co-axial with the first but passing through the centre of the unit cell (Fig. 2.25b).

In consequence, it appears that none of the hyaluronate systems studied by Xray diffraction contain double helices. Moreover it is extremely unlikely that the ordered conformation in solution (Chapter 3) which survives substantial changes in salt concentration temperature and pH 2.6-7.0, could be a double helix that fails to survive the gentle crystallisation procedure that yielded helices

Fig. 2.25 Fourier syntheses projections of electron density in hyaluronate. The"valleys" are shaded. Top left shows the electron density perpendicular to the helix axis for a model with one chain at the corners of the unit cell (the model is superposed). Top right is a difference synthesis showing the additional density that appears when the model phases are combined with the observed diffraction amplitudes. This density corresponds to a second anti-parallel chain (shown superposed) passing through the centre of the unit cell. The corresponding model density projected down the helix axis is shown bottom left. The difference density at bottom right confirms that the second chain is in the centre of the unit cell and not coaxial with first as proposed by Dea et al. (1973).

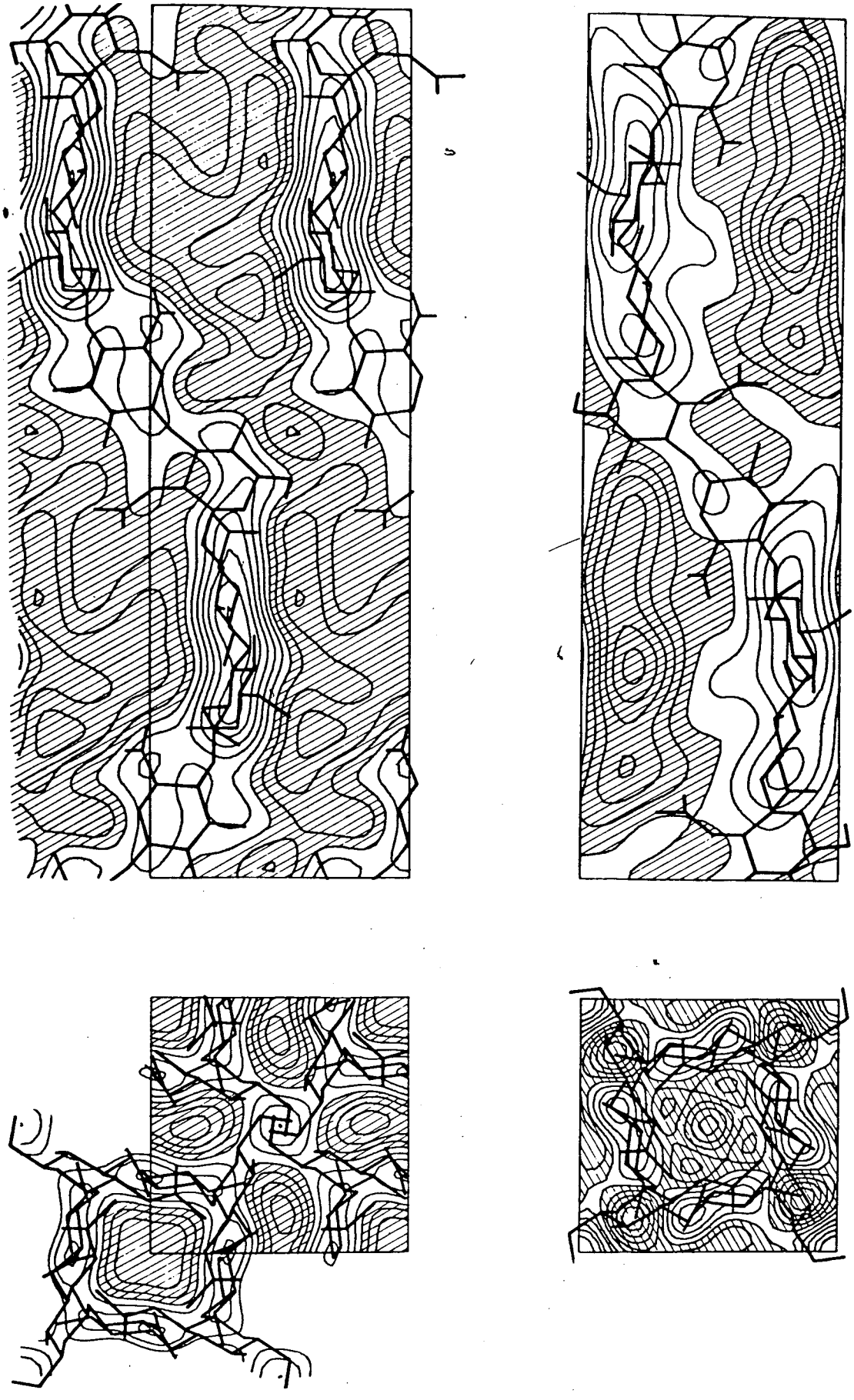

Fig. 2.25

with 4_3 symmetry and h=0.85nm. All the ordered structures formed by hyaluronate therefore, appear to consist of antiparallel, but not co-axial, helices formed, perhaps, by chain folding. Evidence for such a system will be discussed in Chapter 3 together with the biological significance of these results.

Application of stretched films to another polysaccharide system

In the course of the film stretching experiments on hyaluronate a similar technique was applied to films prepared from other systems particularly agarose. This seaweed polysaccharide is an alternating copolymer of 3-linked β-D-galactopyranose and 4-linked 3,6-anhydro-α-L-galactopyranose residues (Araki and Arai, 1967).

Experience with carrageenans has shown that the ability to form crystalline and oriented fibres correlates inversely with aggregation in sols and gels. Hence it was not surprising that unmodified agarose which aggregates rapidly upon gelling did not produce good quality diffraction patterns from drawn fibres. A second approach was to stretch films in the way that had been successful for hyaluronate. This failed as no extension could be obtained. A third approach was more successful.

Agarose gels can be clarified by the addition of dimethyl sulphoxide (DMSO) (Ng Ying Kin and Yaphe, 1972). Films were made by dissolving agarose in DMSO which was removed under vacuum. The films were cut into narrow strips as before and clamped between two spring clips one of which held a weight of 2-5g. The arrangement was immersed in an alcohol/water mixture of varying water content (0-30%) until an extension of 200-300% was obtained. The weighted film was then rapidly removed to an absolute alcohol bath to remove excess water then allowed to air-dry, maintaining the tension throughout.

Diffraction patterns obtained showed well defined layer-lines with a spacing of 0.95 nm and a sharp meridional reflection on the third layer-line. The diffraction pattern has been more fully interpreted by our colleagues at Purdue University as a left-handed double helix of axial periodicity 0.95 nm in which each chain has a three-fold pitch of 1.90 nm and is translated axially relative to its partner by exactly half this distance.

This work is the subject of a joint publication that has been accepted for publication (Arnott et al. 1974c).

CHAPTER 3

Solution Conformations of Hyaluronate

A. INTRODUCTION

The previous chapter has shown the uncertainty that has existed until recently concerning the conformations of hyaluronate in the solid state. For other polysaccharide systems, such as carrageenan and agarose, it has been possible to correlate the solid state conformation with that in the gel state by chiroptical techniques. In these systems a cooperative transition from random coil to double helix occurs, which is characterised by a temperature dependent sharp sigmoidal transition in optical rotation. Circular dichroism studies on the alginate system (a block copolymer of 1,4 linked β-D-mannuronic acid and α-L-guluronic acids) during gelation have shed some light on the conformation adopted by the polymer chains on the formation of junctions involving cation binding (Morris et al, 1973). Both techniques can provide conformational information resulting from changes in both backbone and more localised interaction undergone by side groups.

Nuclear magnetic resonance (nmr) has also found increasing use in the study of conformations and interactions of biological macromolecules (see Chapter 1) ^{1}H nmr can in principle provide exact structural information by a study of chemical shifts and coupling constants of anomeric and other protons (Lemieux and Stevens, 1966). For simple homopolysaccharides and oligomers in solution it has been suggested that the chemical shift of the $C_{(1)}H$ signal, besides being indicative of the orientation of the anomeric $C_{(1)}$-H bond with respect to the glucopyranose unit, is also dependent on the angles of internal rotation between the adjacent units i.e. on chain conformation (Casu et al. 1966; 1968). It is probable that systems studied here are too complicated for similar

conformational investigations, at least with present instrumentation. Thus although Xray Diffraction, Optical Rotation and Circular Dichroism can give more fine detail information than nmr, at least for hyaluronate and similar systems, the use of nmr relaxation times can distinguish between structure and mobility in a molecule. In simple terms, a solution of random coils would be considered 'mobile'. A crosslinked gel, perhaps having double helices as tie points, would be considered mainly as 'immobile' although some 'mobile' character might remain due to the random sections joining the ordered tie points.

For hyaluronate in solution there are three questions to be considered here;

(i) Is hyaluronate ordered in solution?

(ii) Under what conditions can this order be 'melted out' and is this a cooperative process?

(iii) Can the order be interpreted in terms of any particular model such as a double helix?

To answer these questions, the previously mentioned techniques have been used. To familiarise myself with the behaviour of hyaluronate, particularly in chiroptical experiments, it was felt necessary to repeat the published work of others. Parts that are relevant to the discussions presented later are summarised here.

1. Optical Rotation Studies

Variation of Optical Rotation with temperature and pH - (Balazs and Chakrabarti, 1972)

These authors undertook a study of hyaluronate of varying molecular weights, from which the following points emerge:

(i) A sigmoidal transition in the optical rotation is claimed to take place in the region of 50-65°C, that could be indicative of a concerted order-disorder transition of the same kind shown for other polysaccharides.

(ii) The transition is reversible provided 65°C is not exceeded and is shown for high molecular weight samples ($2x10^6$) for both a pH 6-7 solution and a pH 2.6 'putty'. This parallels the observation by Swann (1969), that the viscosity changes reversibly below 65°C and that above this temperature an irreversible undefined change occurs.

(iii) Lower molecular weight material ($1x10^5$) at both pH values, shows no apparent sigmoidal change and is completely reversible in the temperature range 10-90°C.

(iv) Heating the high molecular weight samples above 70°C causes some change such that, on cooling, the optical rotation follows a path similar to that for the low molecular weight sample.

The transitions mentioned are shown in Fig. 3.1 which is reproduced from a lecture slide of Balazs.

Variation of Optical Rotation with Urea Concentration -(Hirano and Kando (1973)).

These workers have studied the change in optical rotation of hyaluronate as a function of urea concentration, interpreting the results in terms of a conformational change.

(i) The specific rotation $[\alpha]_D^{21}$ of hyaluronate in water changes from -62° to -17° in 8M urea.

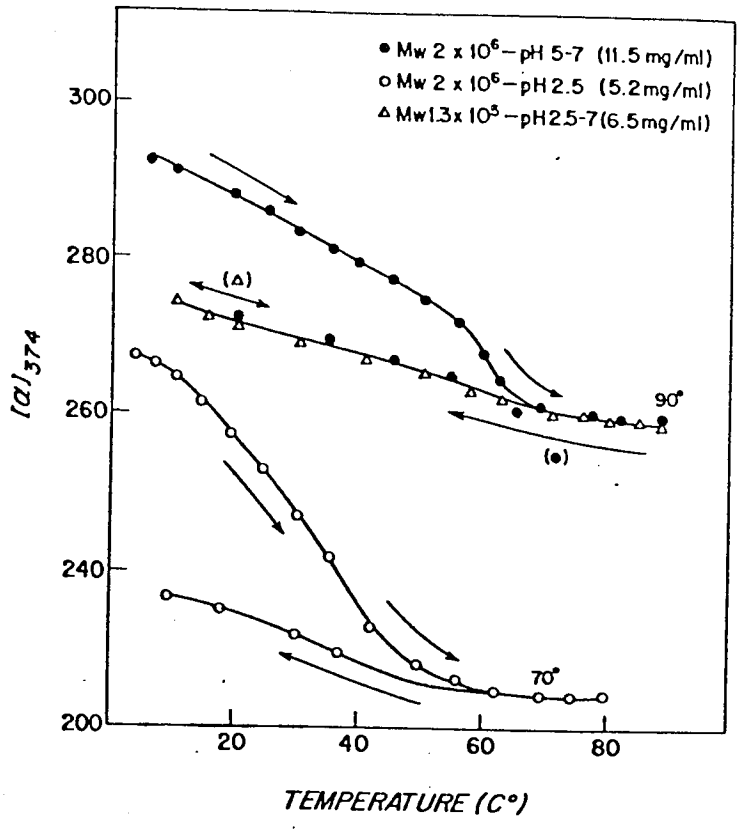

Fig. 3.1 Optical rotation vs. temperature for hyaluronate

(Balazs and Chakrabarti, 1973)

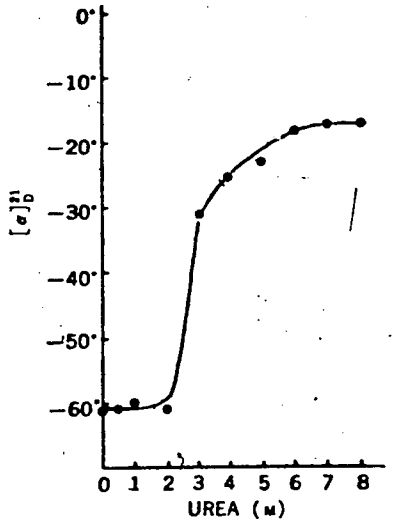

Fig. 3.2 Optical rotation vs. urea concentration

(Hirano and Kando, 1973)

(ii) The sigmoidal curve reproduced in Fig. 3.2 is interpreted as being similar to that exhibited for conformational transitions in proteins and DNA.

(iii) Re-isolated hyaluronate (urea removed by gel filtration) shows an $[\alpha]_D^{21}$ of -54° which is close to that of the original material. This was taken as an indication of the transition being reversible.

(iv) The change in specific rotation is attributed to the dissociation of the hyaluronate double helix into random coils.

2. Circular Dichroism Studies - (Chakrabarti and Balazs, 1973)

Chakrabarti and Balazs in a further study of the chiroptical properties of hyaluronate, have described and discussed several features of the circular dichroism and optical rotatory dispersion spectra and their variation with molecular size, pH and temperature.

(i) The molar optical rotation at 220 nm and ellipticity at 210 nm of both sodium hyaluronate and hyaluronic acid are greatly enhanced in comparison with the monomeric units and oligosaccharides, indicating a 'degree of preferred order'.

(ii) In addition to the normal negative band at 210 nm the circular dichroism shows a positive band around 185-190 nm that is sensitive to concentration in acid solution (pH 1.5 - pH 2.5). No such effect is observed at lower hydrogen ion concentrations.

(iii) Temperature effects were only measured above 200 nm and at two temperatures 4°C and 22°C. Neutral pH and pH 2.5 hyaluronate show no change in the first band at 210 nm whereas there is claimed to be a 2 fold increase in the positive tail of the pH 2.5 sample as the temperature is decreased from 22°C to 4°C (Fig. 3.3).

(iv) Since neither monomers nor oligomers show a positive ellipticity below 200 nm, the major change in sign and position shown below pH 4 is attributed to the conformational change of a single polysaccharide chain or to chain-chain-interactions.

(v) The sensitivity of the ellipticity at 185-190 nm is attributed to a decrease in degree of ionisation of the carboxyl groups, that is tentatively interpreted in terms of an order-disorder transition based on the interconversion of double helix and random coil.

3. Rheological Characteristics

Viscoelastic Nature of Hyaluronate

Many early investigations were carried out on the viscous properties of hyaluronate, especially with regard to the non-Newtonian character of the viscosity in relation to biological lubrication. Ogston and Stanier (1951) showed that bovine synovial fluid has elasticity that is attributable to the hyaluronate content. Balazs (1966) has shown that hyaluronate solutions at pH 2.6 form highly elastic pastes or putties.

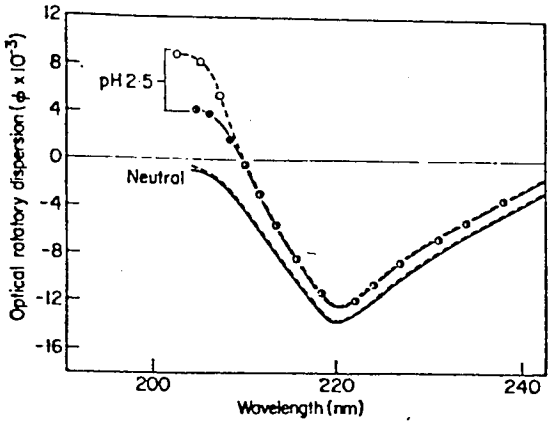

Fig. 3.3 Temperature dependence of rotatory dispersion of hyaluronate at pH 2.5 and neutral pH (--- 0 --- 0 ---), pH 2.5, 4°C; (—— 0 —— 0 ——), pH 2.5, 22°C; (- - - - -) neutral pH, 4°C;(——) neutral pH, 22°C. (Chakrabarti and Balazs, 1973).

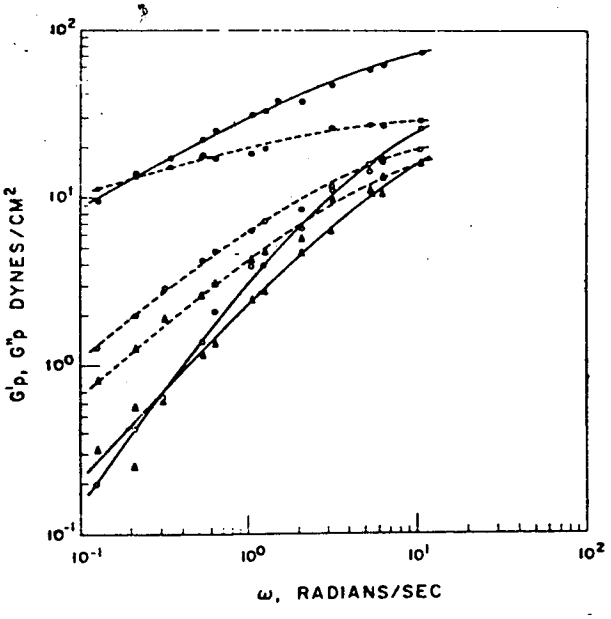

Fig. 3.4 Plots of (——) storage moduli (G') and (- - -) loss moduli (G") for hyaluronate, (Δ) pH 1.5; (●) pH 2.5; (○) pH 7.

The parameters which are used to characterise the rheological properties of viscoelastic materials are the loss modulus G" and the storage modulus G'. G" gives a measure of the energy dissipated as heat within the material - the viscosity, or the damping of the fluid; G' measures the energy stored in the material - the elasticity. It has been shown (Balazs, 1966) that G' reaches a maximum in solutions at pH 2.5, i.e. on formation of the viscoelastic putty. Furthermore the ratio G"/G' is less than unity consequently the pH 2.5 solution appears as a relatively rigid, elastic mass and not as a viscous liquid. For hyaluronate liquids the G"/G' ratio is normally greater than unity. To illustrate the viscoelastic nature of solutions and putties of hyaluronate, Fig. 3.4 is reproduced from Gibbs et al. (1968). These curves can be divided into two regions:

(i) The region below the intersection of the G' and G" curves in which the ratio G"/G' becomes larger than unity and the elasticity, as measured by G', falls rapidly towards zero. The polymer chains are thus able to move through Brownian motion and the samples appear as viscous liquids.

(ii) Above the intersection of G' and G" the elastic modulus predominates and the solutions take on an elastic character.

Rheologically the 'putty' is thus considerably different from the more common type of agar, carrageenan or gelatin gel. The latter types, when subject to stress or shear, break showing no viscous nature. In contrast when the 'putty' is cut, the surfaces heal when pressed together and it flows slowly under stress. In vivo the natural fluid exhibits similar

properties in protecting cells against shock (Balazs and Gibbs, 1970). Under slow mechanical loading it behaves as a viscous oil-like lubricant, at higher loading it transforms to a highly deformable elastic system able to absorb the impossed stress and convert it to an elastic deformation then rebound to the original state when the stress is relaxed.

4. Hyaluronidase

It is convenient to review the mode of action of this enzyme here since it was used in the context of the physical studies to be described in this Chapter.

Hyaluronidase is an endo enzyme that randomly attacks the β1-4 linkage in hyaluronate, chondroitin sulphate and dermatan sulphate. The N-acetyl glucosamine group that is revealed at the reducing end of the chain provides a useful means of assaying the extent of reaction. The main product of the hydrolysis is tetrasaccharide although dimers, hexamers and other species can be present in the final product.

This enzyme has been recently reviewed in some detail by Meyer (1972).

B. METHODS

1. Materials

(i) Hyaluronate samples used in this study were mainly the Balazs samples C34 and C32/2 detailed in the previous Chapter, additional samples used are detailed in the text.

(ii) Oligomers of hyaluronate consisting of tetramer/hexamer and hexamer/octamer mixtures were a kind gift from Dr. A.H. Olavsson, Biochemistry Dept., University of Cardiff.

(iii) Testicular hyaluronidase (EC 3.2.1.35) from ovine testes, activity 1000 NFU/mg was purchased from Boehringer, Mannheim, W. Germany. Additionally for some circular dichroism studies a highly purified enzyme, Leo Hyalas Ref. J:2:20, activity 31000 IU/mg, was used, being a gift from Dr. Olavsson.

2. Solutions for chiroptical studies

(i) pH 6-7 solutions

For optical rotation studies, solutions containing 0.5-1.0% hyaluronate were made up in deionised water or urea solutions of the required molarity, using the method outlined in Chapter 1. Circular dichroism requires much lower concentrations of sample, the normal range being 1-2 mg/ml.

(ii) pH 2.6 putty

For both optical rotation and circular dichroism it was clearly impossible to insert a putty into the

appropriate cell without introducing considerable quantities of air bubbles. Thus it was more convenient to dialyse a solution of hyaluronate at the required concentration in the cell against 0.15M NaCl, pH 2.6, over several days. A similar technique for the introduction of calcium ions into alginate has proved successful (Morris et al, 1973; Thom, 1973).

3. Optical rotation measurements

These were carried out on a Perkin-Elmer 141 spectropolarimeter using 1 cm and 10 cm water jacketed cells. Temperature control was via a circulating water bath that was accurately controlled to ± 0.25°C over the temperature range 10-90°C by a contact thermometer. Adequate time was allowed for the sample to attain equilibrium, a series of readings being taken over a period of 15-20 mins to ensure no change had occurred.

Readings were taken at several wavelengths:- i.e.

365 nm and 436 nm amplify to readings

436 nm and 546 nm have high light intensities that are useful when transmission is poor.

589 nm - the sodium D line for comparison with literature values.

Cell blanks to allow for any variations inherent in the cell were determined over the temperature range being used, with the cell filled with deionised water.

In the hyaluronate/urea experiment the results were corrected for the change of refractive index due to the urea by multiplying by the conversion function (K) (Dintzis and Tobin, 1969) where

$$K = \frac{\eta_{25}^2 + 2}{\eta_T^2 + 2} = \frac{\rho_{25}}{\rho_T}$$

η_{25} and ρ_{25} are the refractive index and density of the solvent at 25°C.

η_T and ρ_T are the equivalent values at a temperature T.

For the case of changing solvent isothermally this expression reduces to:

$$K = \frac{\eta_{H_2O}^2 + 2}{\eta_{solvent}^2 + 2}$$

where η_{water} and $\eta_{solvent}$ are the refractive indices of water and the particular urea solution respectively. Refractive indices were determined in an Abbé Refractometer at 25°C.

4. Circular Dichroism spectra

Circular dichroism spectra were recorded on a Cary 61 spectropolarimeter using 0.1 mm and 0.5 mm pathlength cells and a 10 sec. integration period. Cell blanks were allowed for using a cell filled with deionised water.

Temperature control was by the same system used in the optical rotation measurements.

Wavelength ranges were normally between 260 nm and 190 nm beyond which the machine was usually 'out of light'. Continuous scan experiments used the 100 sec. integration mode and a chart speed of 1 mm/min.

5. Deuterations for nmr

Solutions of hyaluronate (1-5%) were made up in deuterium oxide (Prochem: 99.8g D_2O/100g), freeze dried then redissolved. This process was normally repeated 2-3 times. To ensure that the minimum of atmospheric water was absorbed by the

freeze dried material prior to the addition of deuterium oxide, the freeze drier was allowed to attain atmospheric pressure by passing in dry nitrogen. As soon as the drier was opened (maintaining a positive nitrogen pressure) the dried material was quickly covered with the required volume of deuterium oxide and the sample container sealed with stopper or parafilm. Strict adherance to this procedure gave small HOD peaks in the spectra.

6. NMR Spectra

(i) High resolution ^{1}H nmr spectra were obtained at 100MHz on a Varian XL-100 spectrometer operating in the Fourier transform mode, and at 220 MHz on a Varian HR-220 spectrometer, operating in the continuous wave mode.

(ii) High resolution ^{13}C spectra were obtained at 22.63 MHz on a Bruker WH 90 spectrometer, operating in the Fourier transform mode.

(iii) Pulsed nmr relaxation time (T_2) measurements were made on a Bruker SXP, operating at 60 MHz and using a Carr-Purcell-Meiboom-Gill sequence.

(iv) Integration methods used for determining the fraction of samples contributing to the high resolution spectra have been described (Finer et al. 1974).

(v) Decomposition of free induction decays into separate exponential processes for T_2 measurements were carried out using a computer program supplied by Dr. A.H. Clark of this laboratory.

(vi) The enzyme digestion and alkali treatment studies were followed in the XL-100 by storing free induction decays on magnetic tape and printing out Fourier

transformed spectra subsequently. The time of reading was taken as the beginning of the accumulation period. (5 minutes for the enzyme assay and 10 minutes for the alkali treatment.)

(vii) Where spectra needed examining near the water resonance, this peak was eliminated using the double pulse technique of Benz et al (1972).

The high resolution spectra were recorded by Mr. A. Darke and the pulse measurements by Mr. S. Ablett, URL Colworth/ Welwyn

7. Viscosity Measurements

Viscosities of dilute solutions (ca 0.1% w/v) were measured in an Ostwald viscometer type BS/IP/MU, size M3, sample volume 2.5 ml, water flow time 78 sec., maintained at various temperatures in a circulating water bath.

The readings obtained were the average of several timings.

For more concentrated solutions, the fall of a ball bearing ($\frac{1}{8}$" diameter) through 6 cm of solution in a 5 mm diameter nmr sample tube was timed by Mr. A. Darke, URL Welwyn.

8. Hyaluronidase Treatment

Hyaluronate (ca 1.5 mg/ml) was incubated with various levels of enzyme activity in closed glass tubes at the required temperature

(i) in deionised water with no added NaCl or buffer approx. pH 6.

(ii) in deionised water containing 0.15% NaCl but no buffer pH 5.5 to 6.

No buffer control of the reaction was allowable because

(i) acetate buffer normally used would make the nmr spectra difficult or impossible to interpret due to near coincidence of the peaks due to methyl groups from both hyaluronate and acetate.

(ii) Phosphate buffer tends to inhibit the enzyme.

9. Enzyme Assay

The Good and Bessman (1964) modification of the Morgan Elson reaction was used to determine the release of N-acetyl glucosamine end groups.

(i) A suitable aliquot of the incubation mix (usually 0.1 ml) was pipetted into 0.1 ml potassium tetraborate buffer (7.86g KOH + 17.32g H_3BO_3 in 100 ml H_2O) in ice. The volume was made up to 0.5 ml with deionised water or 0.15M NaCl as necessary.

(ii) The loosely stoppered tubes were heated in a boiling water bath for exactly 3 minutes, then removed back to an ice bath immediately - the assays can be safely left after this stage.

(iii) 3 ml of dimethylaminobenzaldehyde (DMAB) reagent was added (10g DMAB (AR) to 100 ml glacial acetic acid containing 12.5% concentrated HCl, stored at 0°C and diluted 1 to 10 with glacial acetic acid before use).

(iv) The tubes were incubated at 37°C for 20 minutes and the purple colour that develops read at 589 nm against a blank of hyaluronate that had undergone the same processes.

(v) The colour is unstable at 37°C and should be read within 60 minutes or stored at 0°C if left for any longer period.

(vi) The results were compared with a standard curve, using N-acetyl glucosamine as reference compound.

10. Carbon, Nitrogen and Hydrogen analyses

Microanalysis of the various hyaluronates used were determined by the Butterworth Microanalytical Consultancy, Teddington, Middlesex.

The procedure used was to combust the sample in an atmosphere of pure oxygen in a static system. The combustion gases were passed firstly over a catalyst of platinum and an oxidant of copper oxide, then finally over copper metal. The resulting gases carbon dioxide, water and nitrogen were determined by passing through thermal conductivity cells. The temperature of combustion was 925°C for a time of two minutes.

The values obtained are shown in Table 3.1.

Sample	Carbon %		Hydrogen %		Nitrogen %		C:N		C:N $\frac{(a)}{(b)}$
	(a)	(b)	(a)	(b)	(a)	(b)	(a)	(b)	
Balaz C34	34.4	41.9	5.5	5.0	2.8	3.5	12.3	12.0	10.3
N-acetyl glucosamine	43.7	43.6	6.7	6.4	6.1	6.4	7.2	6.8	10.6

(a) - observed

(b) - theoretical

Table 3.1

11. Corrected disaccharide molecular weights and water content

The carbon, hydrogen, nitrogen analyses indicate that some structural irregularity may exist. In particular the nitrogen content seems low, the theoretical C:N ratio is 12.0 while that observed is 12.3.

To quantitate the results obtained it was necessary to determine the water content of the samples and also have a check of the disaccharide repeating structure.

The theoretical molecular weight of the disaccharide unit of Sodium hyaluronate was taken as 401.

(i) Water content allowance

For chiroptical studies the exact concentration is needed for calculations of molar rotation and ellipticity. The theoretical disaccharide weight was corrected for water content based on the carbon analysis results.

$$\text{corrected weight} = \frac{\text{theoretical disacc:weight}}{\text{observed carbon}} \times \text{theoretical carbon}$$

(ii) Disaccharide repeat structure

For the nmr work reported it was necessary to have an accurate knowledge of the chemical structure in particular the N-acetyl methyl content. An average disaccharide molecular weight was therefore calculated by averaging the number of water molecules calculated to be associated with each disaccharide unit.

If n water molecules associated with each disaccharide then,

$$\text{true molecular weight} = 401 + 18n$$

then for determined hydrogen content,

$$\text{observed H\%} = \frac{20 + 2n}{401 + 18n} = *5.53\%$$

* see Table 3.1

$$\therefore n = 2.16$$

where, weight of hydrogens in theoretical unit = 20
Number of hydrogens associated with water = 2n

Similarly for carbon and nitrogen (Table 3.2).

Element	No. of H_2O molecules	Calculated M.Wt.
Hydrogen	2.16	440
Carbon	4.90	489
Nitrogen	5.90	507

Average molecular weight = 479 $\pm$ 18

Table 3.2

For chiroptical studies the disaccharide weight based on the carbon analysis (488) was taken. For nmr work an average (479) of all the values was used. Within experimental error these are the same.

C. RESULTS AND DISCUSSION

Work on other polysaccharide systems in this laboratory has established that the ordered conformation in the solid state can be related to solution behaviour involving a cooperative order-disorder transition (McKinnon 1973).

As outlined in the introduction to this Chapter other workers have used similar techniques and interpreted the changes observed in terms of a coil to double helix transition. In the light of this their work was repeated to optimise conditions prior to further studies.

1. Optical Rotation Studies

Variation of Optical Rotation with temperature - (Balazs and Chakrabarti, 1972)

The reported experiments on the variation in optical rotation with temperature for the pH 2.5 'putty' and pH 7 solution, for heating and cooling cycles have been repeated (Fig. 3.5). In view of the sharp contradiction between these results and those reported by Balazs and Chakrabarti (Fig. 3.1, p 105), the experiments were repeated independently in this laboratory by Dr. A.A. McKinnon. In both sets of experiments commercial hyaluronate (BDH) and material supplied by Balazs (Batches: ## 1119, C34, C32/2) were used and in both cases we find it impossible to reproduce the reported results. Although the overall specific rotation change is similar for the same temperature change, we can find no indication of a sigmoidal transition that would provide evidence for a cooperative process.

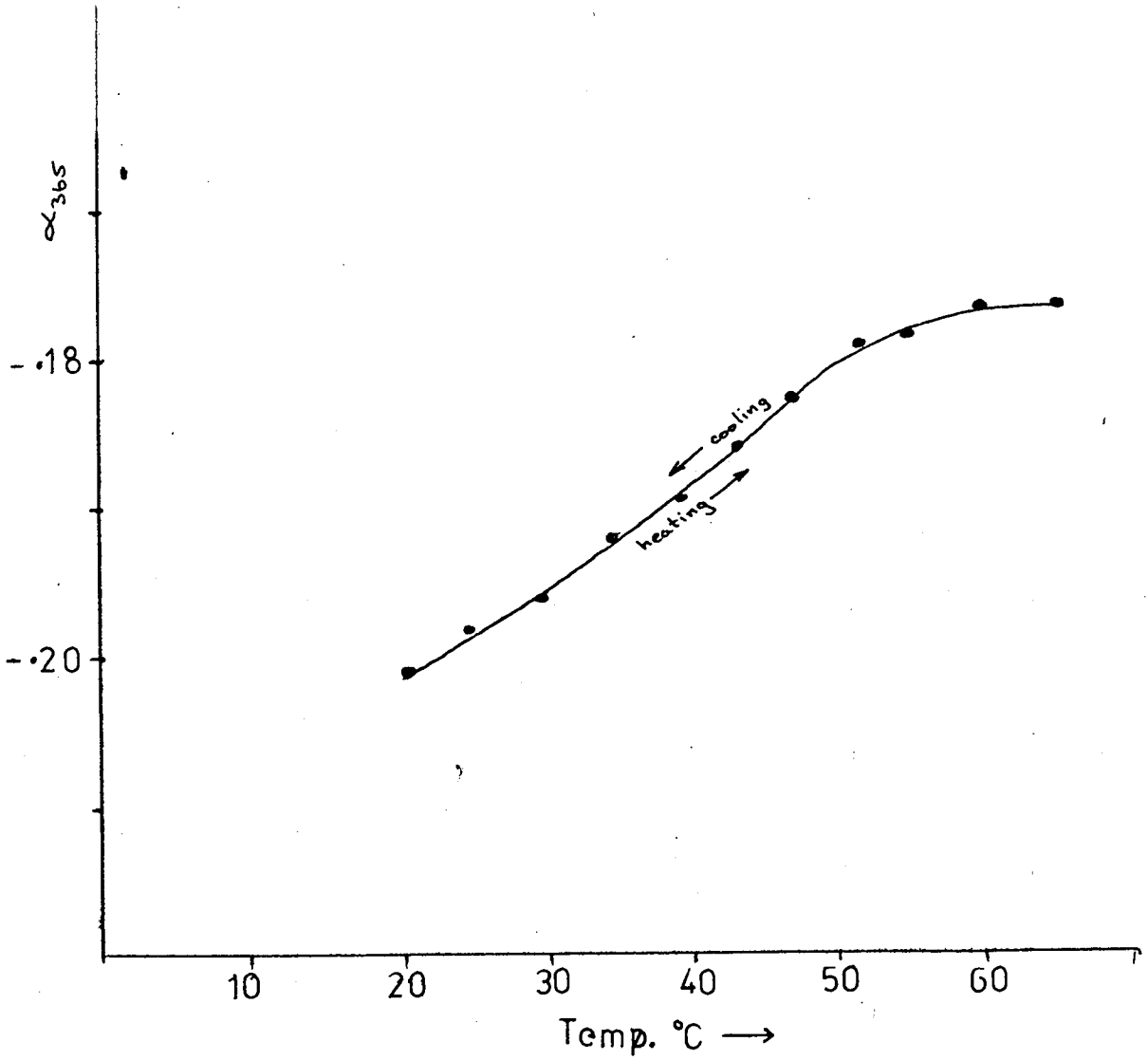

Fig. 3.5 Variation of optical rotation with temperature of a 0.7% solution of hyaluronate.

To consider this difference further, values corresponding to the optical rotations for the selected wavelengths were calculated (by Dr. E.R. Morris) using the Kronig-Kramers transform (Moscowitz, 1960), from circular dichroism spectra measured over the normal carbonyl $n \rightarrow \pi^*$ transition range, at temperatures between 6°C and 78°C. This showed that the change in optical rotation could be completely allowed for by the change in circular dichroism. This strongly suggests increased mobility of the carboxyl or acetamido chromophores on heating and that there is no significant change in backbone conformation.

It is difficult to put forward a definitive explanation of why we cannot observe the sigmoidal transition reported by Balazs and Chakrabarti. The discrepancy cannot be explained in terms of sample to sample variation because the optical rotation vs. temperature changes obtained are of greater magnitude than the reported changes for low molecular weight material. Further the samples used that were provided by Balazs, particularly Batch # 1119, were of comparable purity.

Variation of Optical Rotation with Urea concentration (Hirano and Kando, 1973)

Urea is used extensively as an effector of protein denaturation. At high concentrations of urea (8M) many proteins adopt an unfolded conformation in solution, as the noncovalent bonding systems holding them together are disrupted. The exact mechanism involved is uncertain.

The work of Hirano and Kando was repeated for our materials as it seemed to offer a good possibility of observing an order-disorder transition. However, this could not be confirmed for our system.

The specific rotations $[\alpha]_D^{21}$ of hyaluronate at the same concentration, path length of cell and temperature are set out below.

Urea concentration M.	$[\alpha]_D^{21}$		
		corrected	reported values*
0	-61°	-61°	-62°
2	-58°	-58°	-60°
4	-62°	-61°	-25°
6	-60°	-59°	-18°
8	-58°	-57°	-17°

* estimated from Fig. 3.2 (reproduced from Hirano and Kando, 1973).

From these results the following conclusions can be made;

(i) The observed change in $[\alpha]_D^{21}$ observed is 4° (Hirano and Kando claim 45°).

(ii) Allowing for an error of $\pm$ 0.002 in reading α, equivalent to $[\alpha]_D$ of 4°, then the change observed is zero within experimental error.

(iii) Previous experience with hyaluronate and with other polysaccharides indicates that optical rotations at 589 nm tend to be unreliable in that they are very susceptible to cloudiness and air bubbles. Hyaluronate at a concentration of 5 mg/ml is not obviously cloudy to the eye in a 1 cm pathlength cell although it clearly is in a 10 cm cell. It should be

mentioned however, that optical rotation readings at other wavelengths, particularly 436 nm and 365 nm, also failed to show a substantial change.

(iv) Without a side by side comparison of sample materials and a knowledge of instrumental techniques, it is not possible at this time to say categorically that the conformational change reported never occurs. It can be said however, that this repeated work shows no evidence for a sigmoidal transition in a sample of high molecular weight and low protein content. The protein content of the Hirano sample is not known.

2. Circular Dichroism Studies

Consideration of molar ellipticities reported for the monomeric units of hyaluronate shows that the molar ellipticity of the hyaluronate polymer is greater than a combination of their true values. This is in agreement with previous work (Stone, 1971) and our observations. By contrast Chakrabarti and Balazs (1973) report molar ellipticity values of -6.0×10^{-3} and -6.4×10^{-3} for the tetra and hexasaccharide fragments of hyaluronate, in good agreement with the linear sum of the monomer spectra. For the intact polymer at pH 7 an enhanced molar ellipticity of -11.5×10^{-3} is reported. This they interpret in terms of a 'degree of preferred order'. Subjectively this would suggest evidence of long range order in the solution causing the molecular environment of the chromophores to be more dissymetric, rather than simple steric interactions of adjacent residues that already exist in oligomers. Alternatively one could interpret the differences between oligomers and polymer

in terms of the properties of acetamido chromophores in a chemically different environment, i.e. on reducing terminal residues which exist in anomeric equilibrium, rather than in the chain interior.

To distinguish between these possibilities it was desirable to study the molar ellipticity at various temperatures, at pH 2.5 and pH 7 (as had Chakrabarti and Balazs) and further to study the change in molar ellipticity with a wide range of chain lengths. For the latter course of experiments it seemed reasonable to follow the course of the enzymic degradation of hyaluronate in the circular dichroism cell. This would provide a whole range of chain lengths down to dimer, the precise size of which could be later defined by, for example, gel chromatography. An advantage of this approach is that it removes errors in concentrations of polymer and oligomer for comparison purposes. Further, if a preferred conformation exists that is seen by circular dichroism, it will require an optimum chain length to persist, therefore once this is passed a sharp change in the ellipticity should be observed.

Validity of low wavelength circular dichroism band (Chakrabarti and Balazs, 1973)

Initial experiments using hyaluronate solutions at pH 7 immediately showed that while the spectra were essentially the same as those of Chakrabarti and Balazs (1973), the UV penetration of the Cary 61 became suspect at around 190-185 nm. The last reliable reading obtained using the sample supplied by Balazs was at 195 nm, below this there was loss of transmission. Since the reported circular dichroism band below this level was interpreted in terms of an order-disorder transition, this was surprising particularly as the

Cary 61 is generally recognised to have better UV penetration than the Jasco J20 used by the others. Investigations, by a colleague Dr. E.R. Morris, have shown that for both machines it is possible to obtain reproducible spectra below 200 nm by allowing the machine to drift in an 'out of light' (low transmission) state.

Since optical rotatory dispersion and circular dichroism are related by the Kronig-Kramers transform this provides a method of testing the validity of the reported low wavelength band. By taking a pH 2.5 circular dichroism spectra (Fig. 3.6a) obtained by Chakrabarti and Balazs (unpublished), Morris was able to resolve it into two Gaussian bands (Fig. 3.6b) and compute the corresponding optical rotatory dispersion spectra (Fig. 3.7). A comparison was then made of reported and observed optical rotatory dispersion curves calculated from the circular dichroism due to the normal 210 nm band alone and that from the two resolved bands. Neither gave an exact fit, although the spectra calculated from the 210 nm band alone was close to the observed spectra. Inclusion of the low wavelength band lifts the 200 nm optical rotatory dispersion lobe far above the reported curve.

Variation of molar ellipticity with temperature and pH

The change in the circular dichroism on acidification of hyaluronate is very similar in overall magnitude and form to that for the constituent uronic acid monomer, as shown in Fig. 3.8. Thus the observed pH dependence of the spectrum above 200 nm may simply be due to changes in the degree of ionisation of the carboxyl chromophores.

The effect of temperature on the circular dichroism is illustrated in Fig. 3.9. The change in ellipticity when

Fig. 3.6a Circular dichroism of pH 2.5 hyaluronate, showing low wavelength peak.

Fig. 3.6b Resolution of circular dichroism spectra into Gaussian bands.

The dotted lines show the two simple resolved bands for subsequent Kronig-Kramers transform.

Fig. 3.7 Comparison of observed and computed ORD spectra for hyaluronate at pH 2.5.

The centre curve (- - - -) shows the ORD spectrum at pH 2.5 observed by Chakrabarti and Balazs (unpublished). The upper curve (————) shows the combined ORD curve from both Gaussian components in Fig. 3.6b. The lower curve (-.-.-.) represents the ORD contribution of the normal 210 nm $n \rightarrow \pi^*$ band alone.

It is evident that inclusion of the low wavelength band makes the generated ORD contribution far less consistent with the observed spectrum.

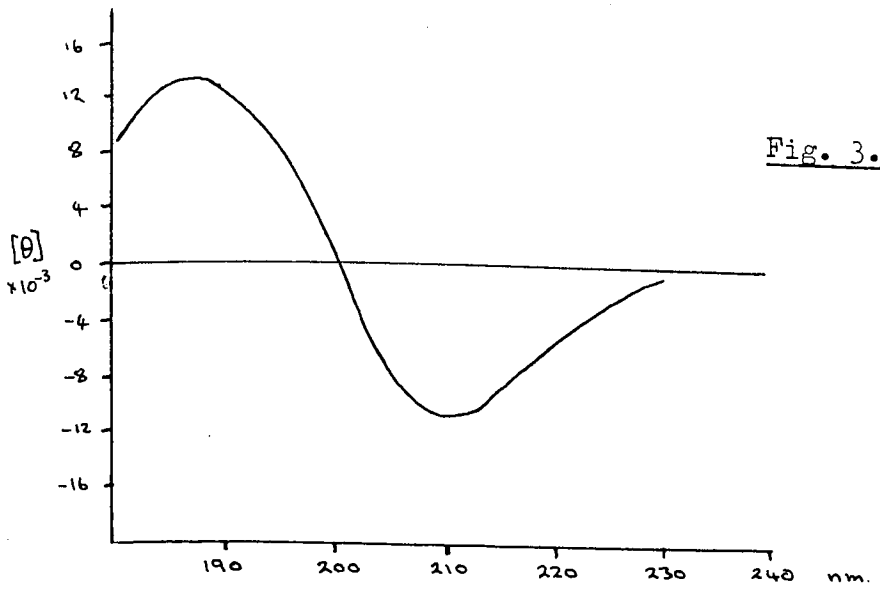

Fig. 3.6a

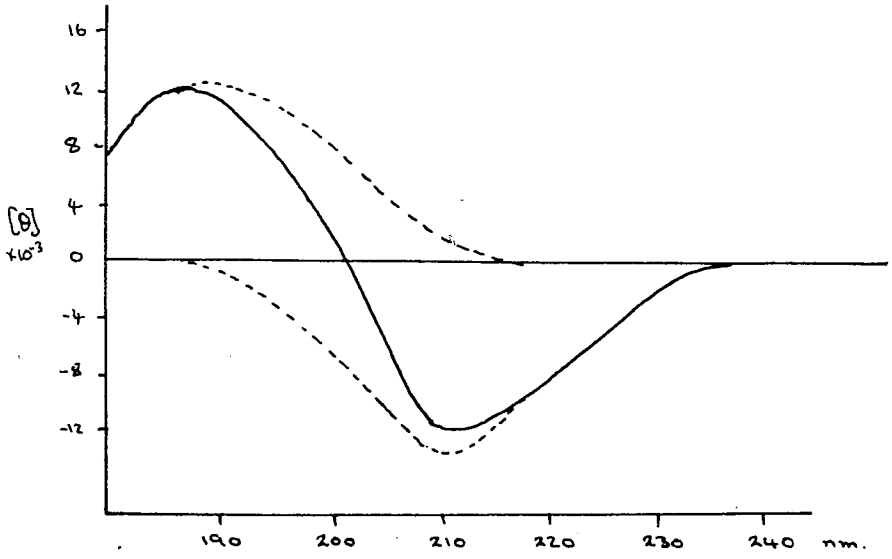

Fig. 3.6b

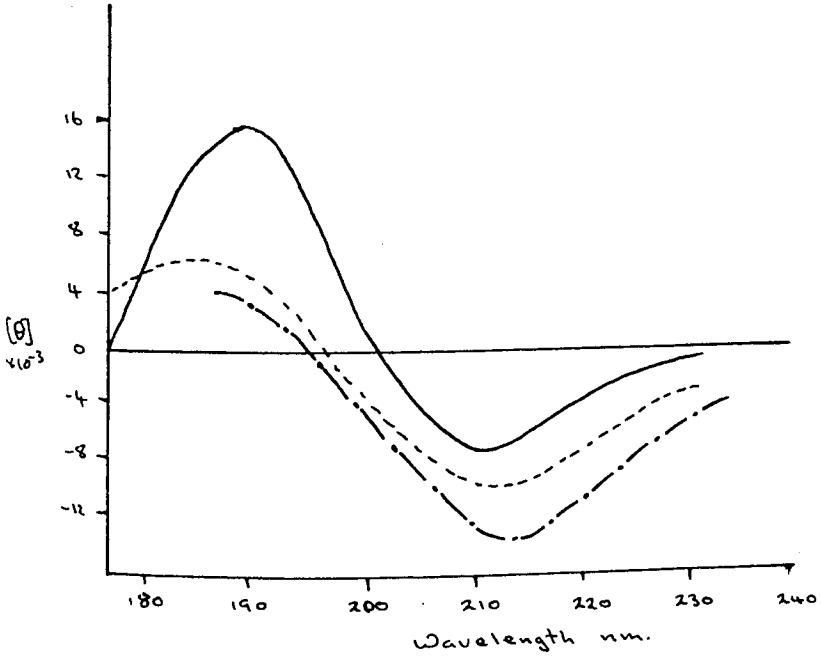

Fig. 3.7

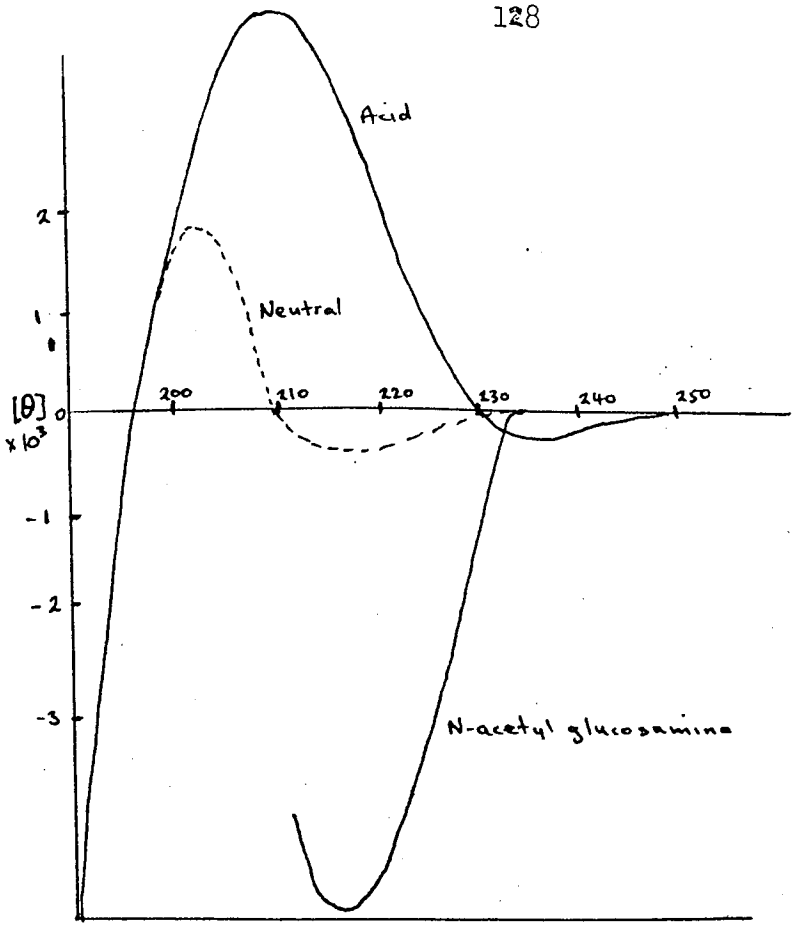

(a)

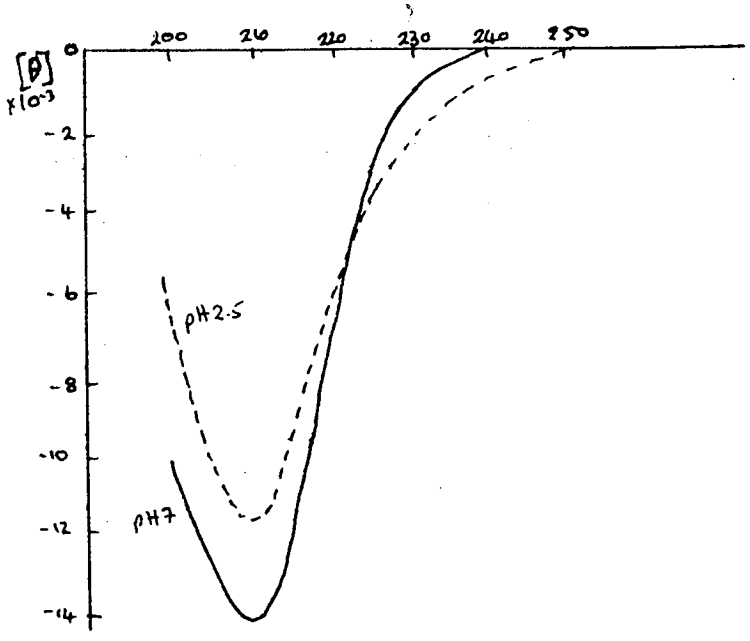

(b)

Fig. 3.8 (a) Hyaluronate monomer spectra showing the positive $[\theta]$ change in the 1-O-β-D-glucuronic acid upon acidification.

(b) A similar change is shown for the conversion of a pH 7 hyaluronate solution to pH 2.5.

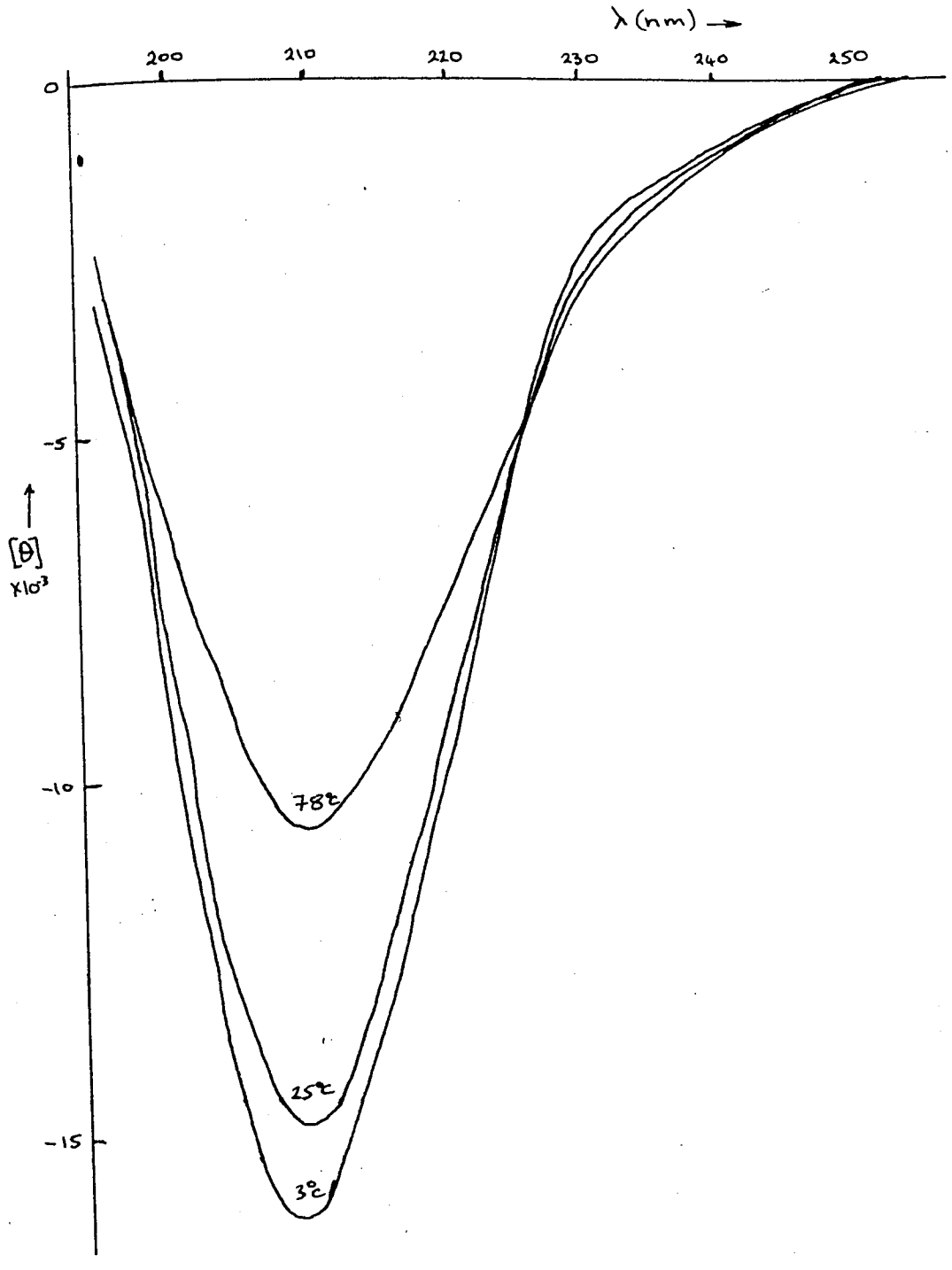

Fig. 3.9 Variation of the circular dichroism of hyaluronate with temperature.

hyaluronate solutions are heated from 5° to 75°C are (as for the pH changes above) entirely consistent with quantitative predictions made from the behaviour of the constituent monomers arising from an increased mobility of the carboxyl or acetamido chromophores. This variation of pH and temperature appears to give no evidence of any substantial additional perturbation that could indicate a fundamental change in chain conformation.

Circular Dichroism of Hyaluronate Oligomers

Two mixed samples were used:

a) hexa- and tetrasaccharide (60:40)

b) hexa- and octasaccharide (50:50)

Elemental analysis gave:

		Carbon	Hydrogen	Nitrogen
		%	%	%
(a)		37.6	5.32	2.63
(b)		37.6	5.14	2.53
Theoretical		41.9	5.0	3.5
Disaccharide) weight based) on element)	(a)	447	377	534
	(b)	447	390	555

Circular dichroism spectra at 25°C and pH 6-7 gave molar ellipticities calculated on the basis of the analytical results that were approximately double those previously reported (Chakrabarti and Balazs, 1973) and close to the values obtained for the intact polymer. (Table 3.3.)

Calculated Molar Ellipticities $[\theta]$

	Oligomer (a) x10^{-3}	Oligomer (b) x10^{-3}	Intact hyaluronate* x10^{-3}
$[\theta]$ carbon	-11.1	-11.5	-13.0
$[\theta]$ hydrogen	- 8.9	- 9.2	- 9.6
$[\theta]$ nitrogen	-13.8	-14.3	-13.5
$[\theta]$ theoretical	-10.0	-10.3	-10.7

Balazs tetrasaccharide -6.0×10^{-3}

hexasaccharide -6.4×10^{-3}

* C34 hyaluronate

(a) 0.88 mg/ml

(b) 0.95 mg/ml

1 mm pathlength cell

Table 3.3

This is as expected since the influence of the glycosidic oxygen on the accessible chromophores becomes minimal as the degree of polymerisation increases beyond 5 or 6.

As the enhancement of ellipticity of intact hyaluronate in relation to that of the oligomers was a major point in favour of some degree of long range order, this work was extended by a consideration of oligomers of various chain length.

Hyaluronidase treatment of hyaluronate

The mode of action of hyaluronidase has already been described. Initial experiments on a variety of samples using the same level of enzyme showed that the samples were apparently hydrolysed to different extents, as seen by circular dichroism (Table 3.4).

Changes in [θ] after hyaluronidase treatment

Hyaluronate sample	Decrease in peak height at 210 nm %	Analysis			Molar Ellipticity [θ]	
		Carbon	Hydrogen	Nitrogen	before incubation	after incubation
BDH	5	35.12	4.92	2.97	9.03	8.59
Miles 100A	26	29.42	4.36	2.70	13.01	9.7
Balazs C34	10	34.35	5.53	2.77	16.1	14.5
" C32/2	26	33.13	5.36	2.71	16.0	11.9
Miles 80A	10	35.19	5.05	3.04	16.4	14.6
Rooster comb	35	33.79	4.77	2.80	16.4	10.9

Conditions: Concentration 2 mg/ml

0.5 mm pathlength cell

Incubated for 48 hrs at 37° at pH 6-7 with no added NaCl

Table 3.4

The conditions used were not the optimum for the enzyme, although no additional salt was added there was probably some present in the samples.

Preliminary conclusions from these results were:

(i) The hyaluronate samples are in some way different, since it seems unlikely that each should behave differently with the same amount of enzyme.

(ii) The varying extents of change may be influenced by some structural differences within each sample. One example (for which there is as yet no evidence)

could be L-iduronate residues replacing D-glucuronate which would inhibit the enzyme and prevent the cleavage of that part of the molecules (Fransson and Roden, 1967).

(iii) Samples may contain varying amounts of salt or alternatively varying amounts of some inhibitor.

(iv) Over the time of incubation an enzyme blank also showed a small but significant change in peak height at 210 nm.

Overall from these preliminary experiments it seemed that controlled enzyme hydrolysis might indicate the type of conformational change occurring i.e. a gradual trend towards the $[\theta]$ of the oligomers would indicate no 'locked in order'. Alternatively a sharp change in $[\theta]$ at some degree of hydrolysis (probably low) could indicate the release of 'locked in order'.

Subsequent experiments using varying amounts of enzyme both with and without additional salt at pH 6, were monitored by both circular dichroism and Morgan Elson N-acetyl glucosamine end group determination.

Initial conclusions were:

(i) Proportionality does not exist between release of N-acetyl glucosamine end group (or chain length) and the apparent ellipticity at 210 nm, whether hydrolysis is carried out with or without added salt, and with various enzyme levels (Fig. 3.10).

(ii) In the early stages of hydrolysis, in the presence of salt, the apparent ellipticity change occurs much more slowly than the release of end group (Fig. 3.11).

Fig. 3.10 CD change vs. end-group release showing proportionality not present

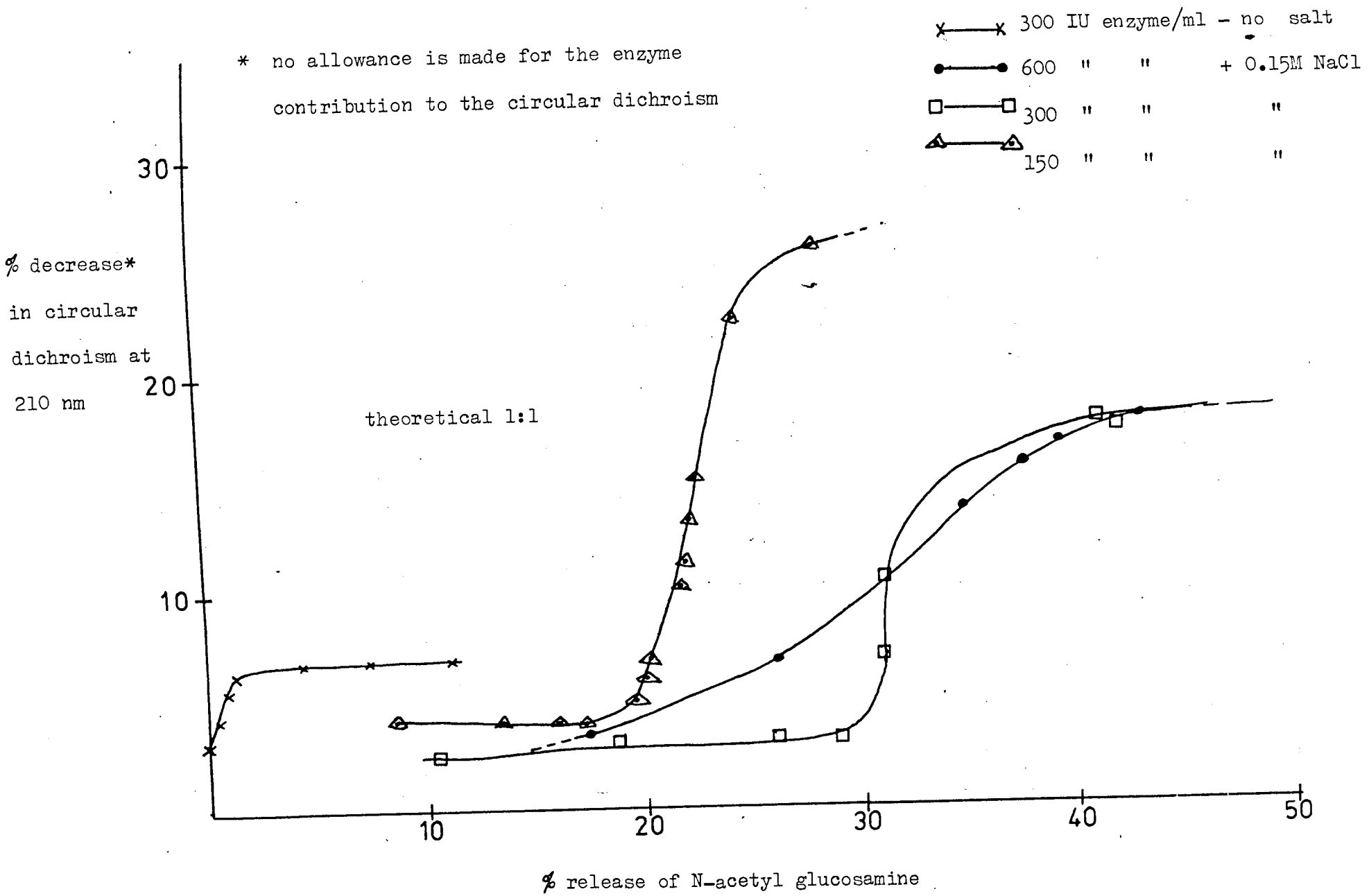

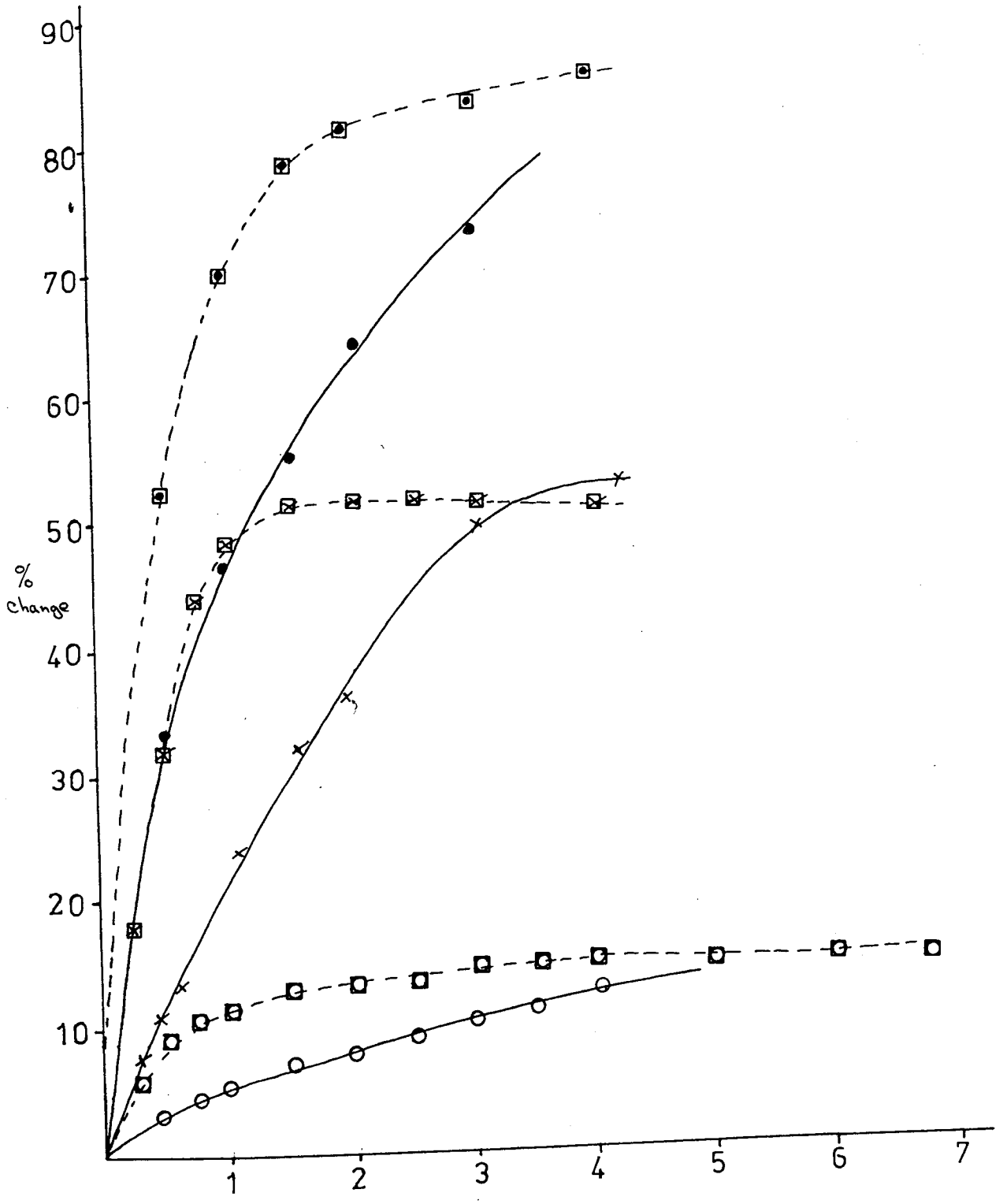

Fig. 3.11 Curves for CD decrease and end-group release at various enzyme levels. Showing that the CD apparently lags behind the end-group release (no correction is made for the enzyme in the CD.

	CD	End-group
600 IU enzyme/ml 0.15M NaCl	●—●	■- - -■
300 IU " "	×—×	⊠- - -⊠
150 IU " "	○—○	⊡- - -⊡

(iii) A rapid decrease in viscosity occurs during the initial chain cleavage. The viscosity change is effectively too fast to follow. A sample of hyaluronate alone (0.84 mg/ml) has a flow time of 490 sec. in a capillary viscometer. A similar sample after the addition of enzyme has reduced its flow time to about 85 sec. (water 78 sec.) in the time taken to set up the viscometer (about 5 mins).

(iv) It is difficult to allow for the enzyme in the circular dichroism spectra.

(v) The change in rate of release of N-acetyl glucosamine with changing amounts of enzyme is as expected (Fig. 3.12).

(vi) If the apparently sharp decrease in circular dichroism at 210 nm is true (Fig. 3.13), then there is an indication of some kind of ordered conformation.

This apparent sharp transition for a small increase in N-acetyl glucosamine release, which seems to be repeated for various enzyme levels, was initially considered as a mechanism in which random chain regions were destroyed more rapidly than (or before) ordered regions.

Subsequent experiments with a purified enzyme preparation did not confirm this initial interpretation. The change observed may therefore be due to some undefined behaviour of the Boehringer enzyme.

Since the enzyme alone has a circular dichroism at 210 nm (Fig. 3.14) which changes when incubated under identical conditions but without substrate, the question arises as to how

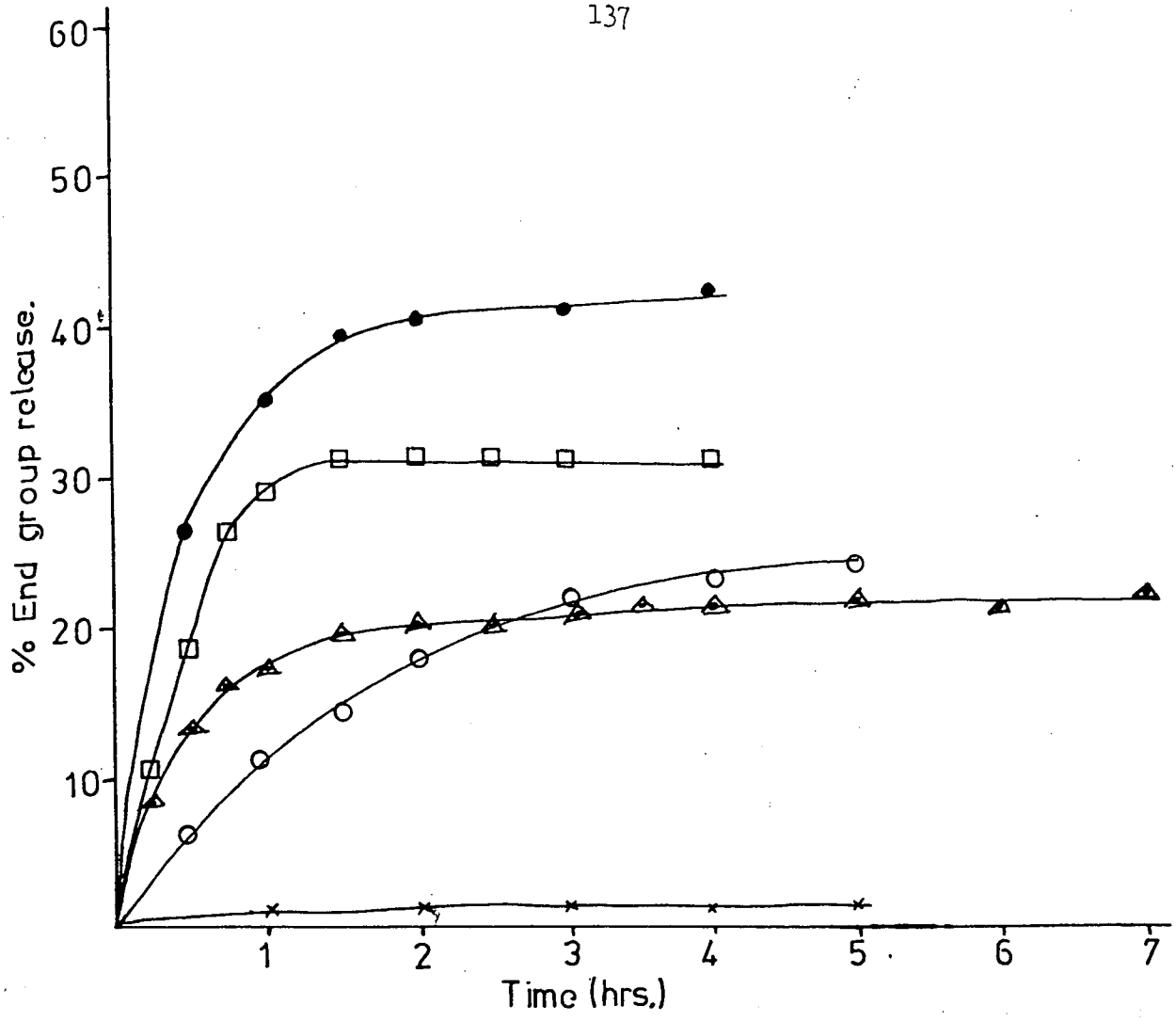

×—×	2.1 mg/ml hyaluronate	+ 300 IU enzyme/ml	– no salt	
●—●	1.6 mg/ml	"	+ 600 IU "	+ 0.15M NaCl
□—□	1.76 mg/ml	"	+ 300 IU "	"
△—△	1.58 mg/ml	"	+ 150 IU "	"
○—○	1.75 mg/ml	"	+ 800 IU Leo enzyme/ml	0.15M NaCl

Fig. 3.12 End-group release from C34 hyaluronate for various enzyme levels

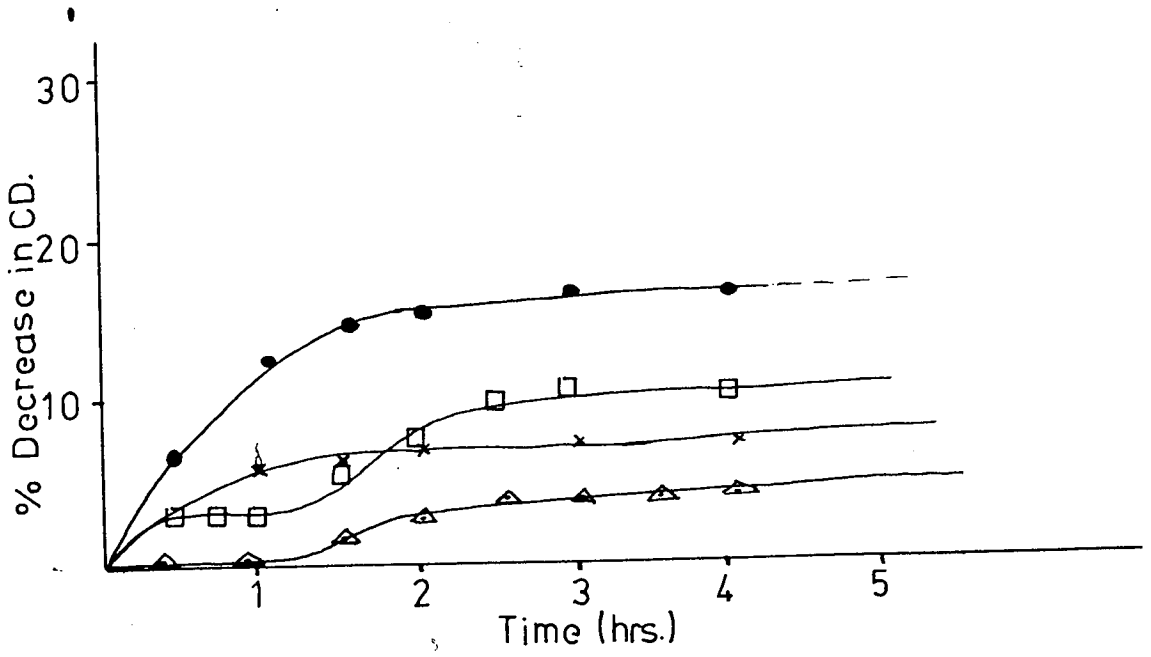

300 IU enzyme/ml – no salt.
600 IU " + 0.15M NaCl
300 IU " "
150 IU " "

Fig. 3.13 Apparent decrease in circular dichroism with time during enzyme hydrolysis.

this can be taken into account. The simplest way to allow for this change would be to subtract the contribution due to the enzyme at the corresponding time intervals. However, for this to be meaningful the following assumptions would have to be made:

(i) The enzyme circular dichroism changes at the same rate with and without substrate.

(ii) The conformation of the enzyme is the same both in the presence and absence of hyaluronate.

(iii) The change that is seen in the enzyme blank is due entirely to the enzyme and not due to other factors, such as binding of low molecular weight oligomers or a conformational change due to some protein impurity in the enzyme.

These assumptions gave considerable cause for concern as to the validity of the results presented above. Therefore, to reduce the probability that the circular dichroism changes observed were artefacts or changes in protein conformation it was essential to reduce or eliminate the contribution to the overall spectra by the enzyme, while retaining activity. It was found that the highly purified Leo enzyme gave a very small circular dichroism spectra, that hardly changed with time, even at much higher enzyme activity (Fig. 3.15). However, although this was supposed to be a highly active preparation, its activity was in fact several orders of magnitude lower, possibly caused by the sensitivity and inactivation of hyaluronidase, particularly very pure preparations, by glass (Rasmussen, 1954).

The experiment was to treat the hyaluronate with an amount of enzyme that was estimated to give an intermediate rate

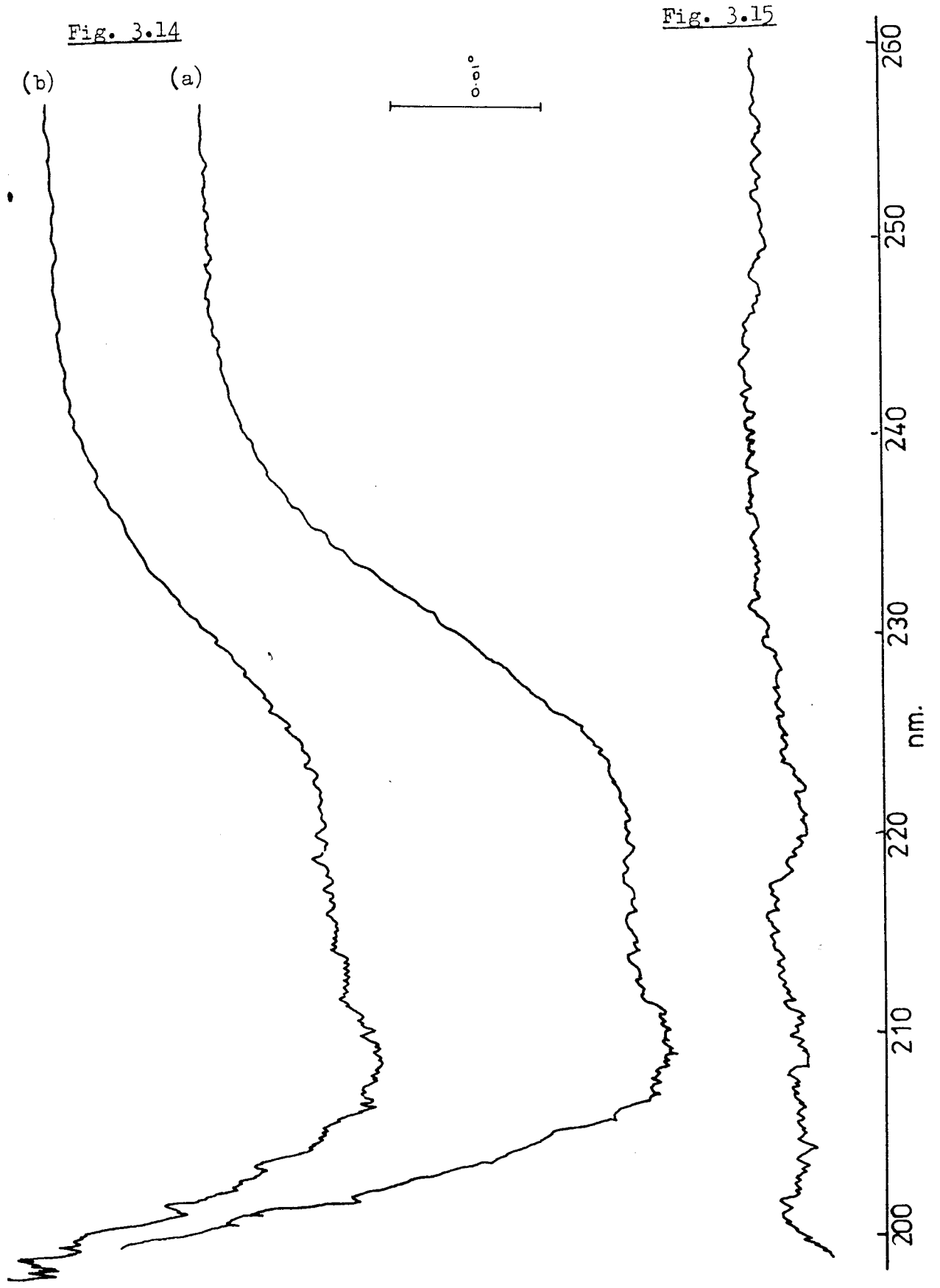

Fig. 3.14 Circular dichroism spectra of 600 IU/ml Boehringer enzyme (a) at start, and (b) after 24 hours.

Fig. 3.15 Circular dichroism spectrum of 3000 IU/ml Leo enzyme, the spectrum is identical after 24 hours.

N-acetyl glucosamine end group release, following the hydrolysis for 24 hrs. by Morgan-Elson assay and a continuous single wavelength circular dichroism run. The corresponding end group change with time is shown in Fig. 3.12. From the circular dichroism spectrum it was apparent that a slow linear change had taken place resulting in an overall 15% decrease in peak height at 210 nm. No trace of the previously observed sharp decrease in circular dichroism was apparent. The continuous spectra of the enzyme alone was a straight line.

To ensure that the incubation had reached completion, it was left at 37°C for 72 hrs. and the spectra rerun; it was identical. In case the conformation of the enzyme was changing, additional enzyme was added to the incubation mix. Allowing for the enzyme contribution both initially and after 24 hrs., no change was observed. Thus it was assumed that the binding of oligomers to the enzyme active sites does not alter the conformation of the enzyme as far as circular dichroism is concerned.

The molar ellipticities of the hyaluronate before and after hydrolysis are consistent with previous results (Table 3.5). Additionally the molar ellipticity of incubations that exhibited 70% end group release (average chain length between tetra- and disaccharide - probably a mixture) were consistent with the values obtained for our oligomers (Table 3.3). This is taken as further evidence that the values quoted by Chakrabarti and Balazs (1973) are apparently incorrect from our comparison, and that no cooperative transition can be detected. However, the nmr studies to be reported below suggest that this apparent inconsistency could be more complex.

	$[\varsigma]$ x 10^{-3}	
	no allowance for enzyme	deduction of enzyme contribution
Hyaluronate alone (C34)	-13.0	-
+ enzyme - at start	-13.3	-12.7
- after 24 hrs.	-11.5	-10.8
+ more enzyme - at start	-11.8	-11.0
- after 24 hrs.	-11.7	-10.9

Conditions: Hyaluronate 1.6 mg/ml

Enzyme (Leo) 0.05 mg/ml

0.5 mm pathlength cell at 37°C

Table 3.5

3. NMR studies

Nmr relaxation studies have been used little on polysaccharide systems. Perlin et al. (1970) in a survey of glycosaminoglycans at 220 MHz reported a poorly resolved spectrum for hyaluronate in which it was difficult to assign the protons, except for the well separated peak due to the N-acetyl methyl resonance.

Using 60 and 100 MHz nmr equipment it has been possible to obtain spectra of comparable quality, particularly when employing the Fourier Transform facility. The N-acetyl resonance at δ 1.93 ppm (Fig. 3.17) clearly lends itself to integration and line width measurement. Consequently the quantitative results reported here are based on this peak.

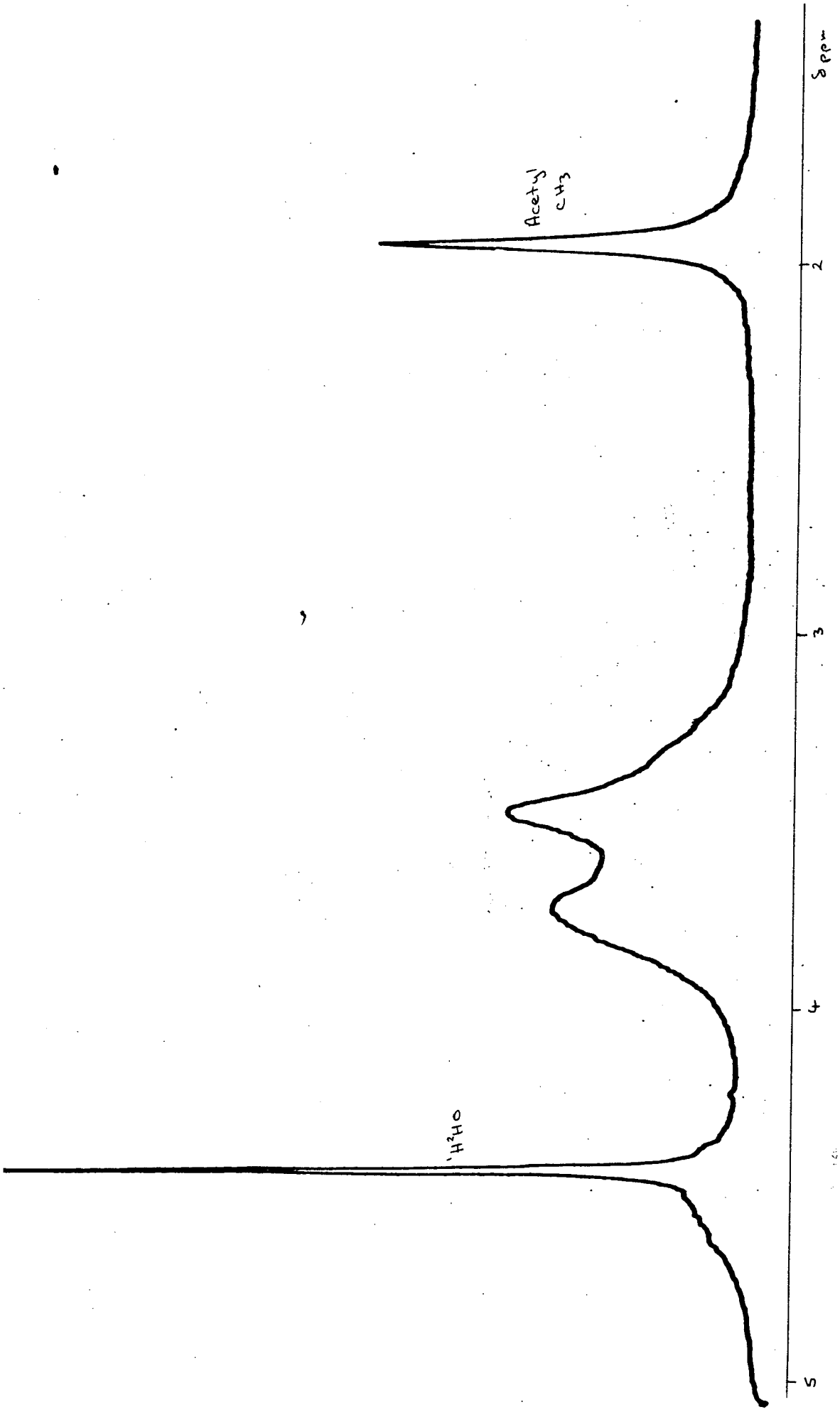

Fig. 3.17 100 MHz ^1H nmr spectrum of a D_2O solution of hyaluronate at 30°C

For quantitative measurements to be meaningful it is necessary to have an accurate knowledge of the theoretical amount of N-acetyl group present in each sample. Carbon, hydrogen and nitrogen analyses enabled the corrected disaccharide molecular weight and degree of hydration to be calculated. The average hydration calculated for the hyaluronate sample C34 used in this work was 4.3 ± 1.7 moles water/mole disaccharide, leading to a disaccharide weight of 479 ± 13. On the basis of this figure the fraction of N-acetyl protons having sufficient mobility to give a high resolution ^{1}H nmr signal could be calculated.

Effect of pH and temperature

Using single scans at 60 MHz to provide a rough estimate, it was clear that approximately 40 ± 10% of the sample was mobile enough to give a high resolution spectra. Further heating to 90°C did not seem to cause an appreciable increase in this value.

Reinvestigation at 100 MHz showed that the fraction of mobile species was 43 ± 5% and that this value was independent of salt content, concentration and temperature up to 90°C. Maintaining the sample at 90°C for 12 hours caused the figure to increase by only 4%. At 90°C the broad underlying peak whose protons do not contribute to the high resolution signal is narrowed slightly (i.e. the 'immobile' or 'ordered' species) but is not apparent on recooling to 30°C. This is consistent with the drop in viscosity at 90°C effectively allowing more mobility of the whole molecule, consequently sharpening the broad underlying peak.

The 4% increase in the proportion of 'mobile' species after prolonged heating is probably due to bond hydrolysis and/or some irreversible loosening of the 'immobile' or ordered regions.

This may parallel the undefined change in viscosity and optical activity noted when hyaluronate is heated above 70°C (Swann, 1969; Balazs and Chakrabarti, 1972). It follows that 90°C must be considerably below the transition temperature of the structured regions since no sharp increase in the proportion of mobile or random species is apparent. Consequently, at ambient temperatures (26°C) the dissociation of ordered regions to disordered must be minimal, indicating that a barrier exists between these two regions that is insensitive to temperature and salt. The 'putty' form (Balazs, 1966), which is prepared by adjusting the pH and salt concentration to enhance the viscoelastic properties of hyaluronate, is an exception. At 26°C the putty showed evidence of some extra structure (order) in that only 30% of the sample was mobile enough to give a high resolution spectra. However, this additional structure is very labile showing 38% signal at 40°C and returning to the "normal" figure of 43% at 50°C.

Alterations in the pH from 7 to 2.6 (putty) have shown that the major influence on the stability of the structured regions is some very stable barrier. It has, however, been possible to disrupt this feature by the presence of NaOH. Colleagues, Dr. E.G. Finer and Mr. A. Dark have shown that on addition of 0.1M NaOH the viscosity dropped drastically immediately (visual observation) and the nmr signal measured after 5 minutes showed 95% of the signal was now mobile or non-structured (the spectra is almost identical to Fig. 3.22, p 154). This increased slightly to 98% after 85 minutes, and remained essentially the same (93%) on neutralisation to pH 7 (may be slightly low due to small volume changes on neutralisation). This would be consistent with the involvement of an ester cross-link in the hyaluronate structure.

Pulse nmr measurements confirmed the presence of 57% of a component having T_2 short enough not to give a high resolution signal. The T_2 values obtained are shown in Table 3.4.

T_2 values for 3% hyaluronate at pH 6-7

Temperature °C	Mobile component		Less mobile component	
	T_2 ms.	% signal	T_2 ms.	% signal
27	6.5	46	0.9	54
47	10.6	42	1.9	58
60	13.3	41	2.7	59
77	14.7	42	2.4	58
27	6.8	43	0.9	57

Table 3.4

There are essentially two components or two types of protons, those having a long T_2 equivalent to a resolvable high resolution peak and those having a short T_2 corresponding to a broad unobservable high resolution peak (a much longer relaxation time due to considerable water, with $T_2 \simeq 1$ sec. has been eliminated). In fact the broad peak is just visible in the high resolution spectra but immeasureable due to its width and shallow height.

The data from pulse and high resolution spectra are related by:

$$\Delta\nu_{\frac{1}{2}} = {}^{1}/\pi\, T_2 \qquad - \quad 1.$$

where $\Delta\nu_{\frac{1}{2}}$ = peak width at half height in the high resolution

spectra. Thus from Table 3.4 the short component having a $T_2 \simeq$ 2 ms. corresponds to $\Delta\nu_{\frac{1}{2}}$ = 160 Hz, which is too wide to be observable on the high resolution spectra i.e. the 'immobile' component. The measured line width $\Delta\nu_{\frac{1}{2}}$ of 13.5 Hz for the high resolution spectra corresponds to a $T_2 \simeq$ 24 ms. for the mobile component. This is longer than the T_2 observed from the pulse measurements but can be accounted for by the fact that T_2 is a measure or average for all the protons in the disaccharide unit thus the ring protons will be considerably less mobile having a shorter T_2 than the N-acetyl methyl protons on the same ring. In addition it is difficult to allow fully for the mobile species in the other composite peak in the high resolution spectra (Fig. 3.17).

However what Table 3.4 does confirm is that the fraction of 'mobile' groups is ca. 43% and that it is independent of temperature.

Plotting the variation of T_2 in Arrhenius form against temperature shows that the plot for T_2 (long) is curved probably due to this being an average measure for several different types of proton. The ideal Arrhenius type behaviour that is often observed in nmr studies (Bloembergen et al, 1948) is demonstrated by the high resolution line width for the N-acetyl corresponding to an activation energy of 12.4 $\pm$ 1.6 kJ mole^{-1} which is consistent with a situation in which local viscosity is impeding the random motion of the N-acetyl protons. The average activation energy for T_2(long) is similar. In the case of T_2(short) the Arrhenius plot is highly curved showing two distinct activation energies; about 30 kJ mole^{-1} at ambient temperatures falling to small values at higher temperatures (Fig. 3.18a). A similar plot for the viscosity at the same

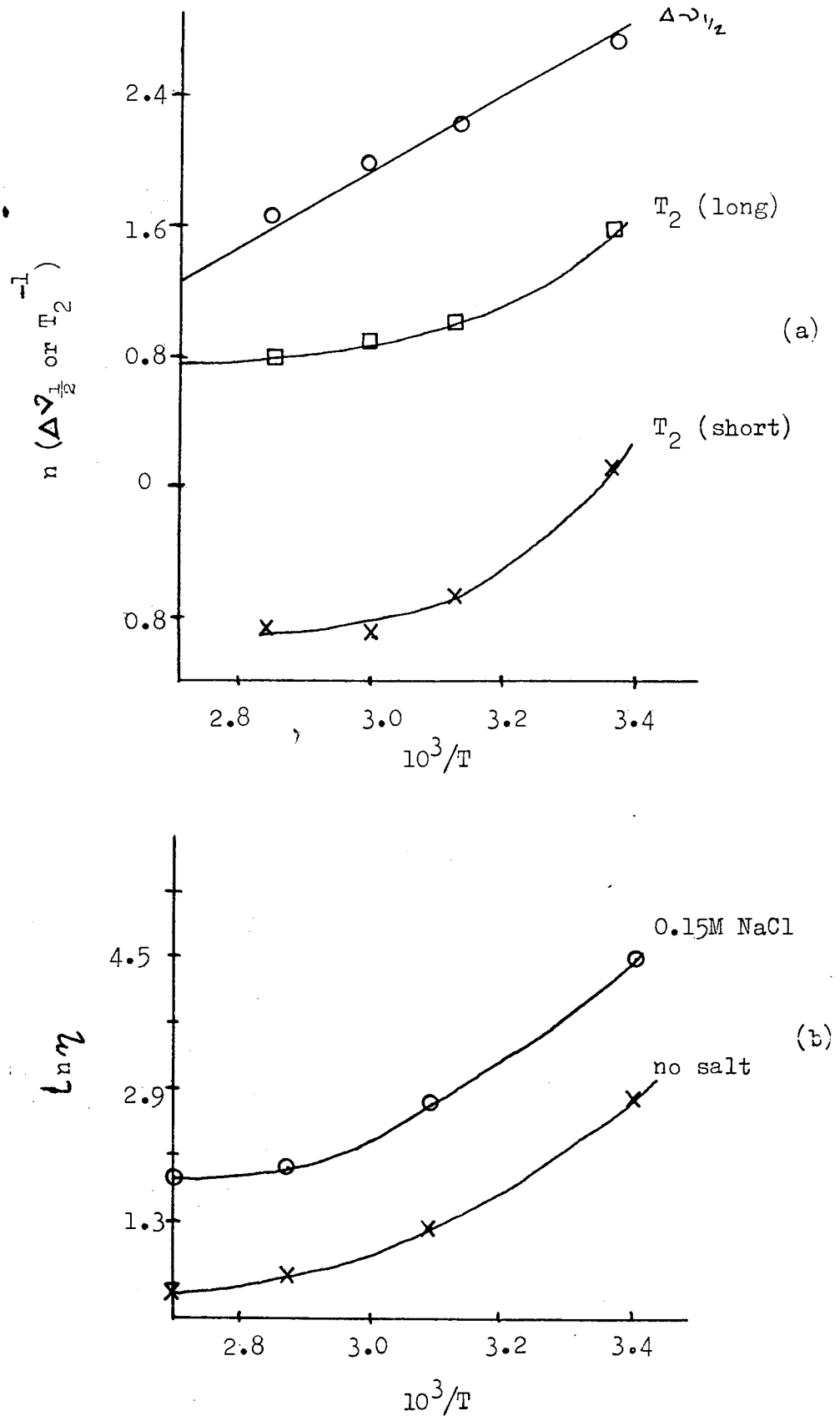

Fig. 3.18 Arrhenius plots for a 1.5% solution of hyaluronate, showing the temperature dependence of (a) high resolution linewidth($\Delta\nu_{\frac{1}{2}}$), relaxation rates T_2^{-1}, and (b) viscosity(η). (Taken from plots drawn by Dr. E.G. Finer)

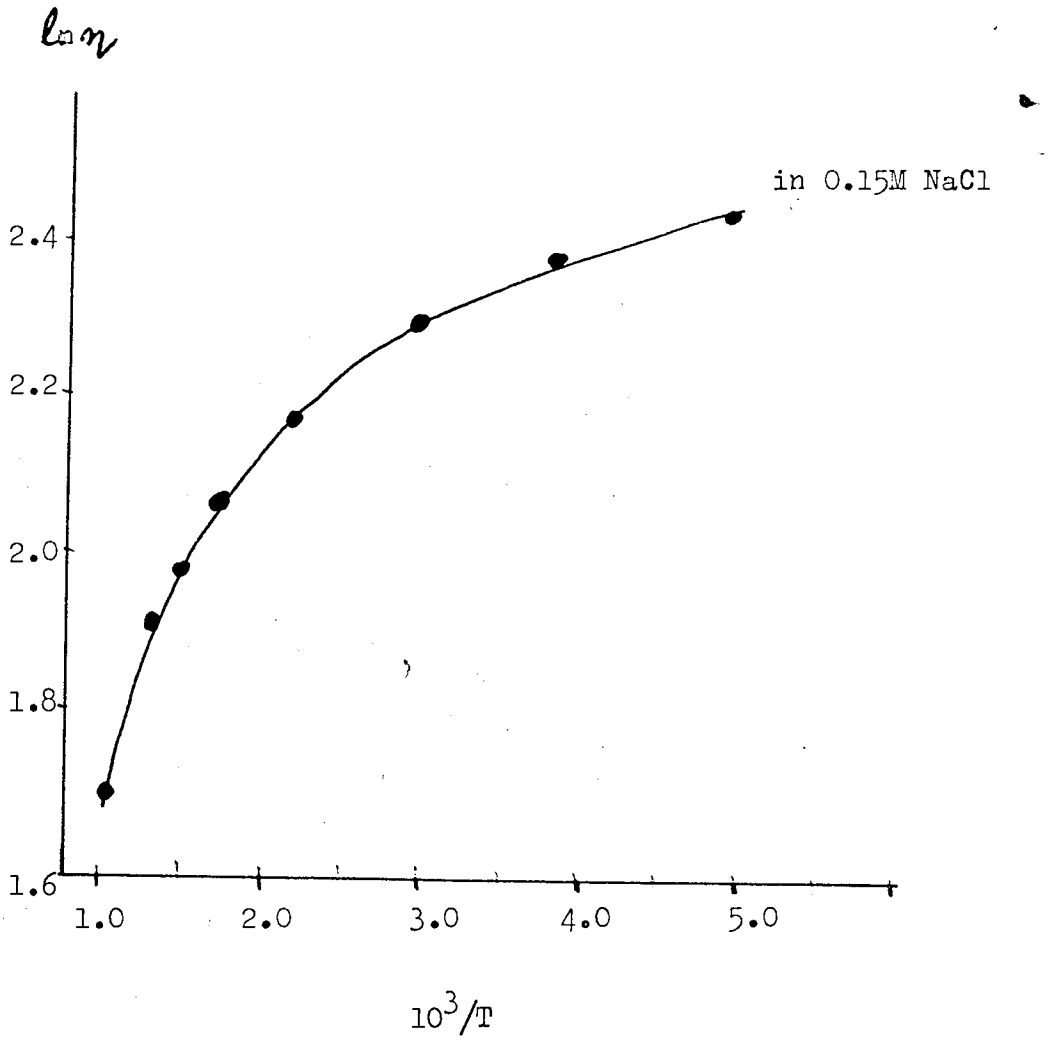

Fig. 3.19 Arrhenius plot for a 0.08% hyaluronate solution; showing the concentration dependence of the viscosity when compared with Fig. 3.18b.

concentration, followed by timing the fall of a ball bearing in the nmr tube, showed an activation energy of about 45 kJ $mole^{-1}$ at ambient temperatures decreasing to about 10 kJ $mole^{-1}$ at higher temperatures. Plots are shown in Fig. 3.18b of the results obtained by Mr. A. Darke, which although based on a crude estimate of viscosity seem to suggest some similarity of shape in the presence and absence of salt. As the viscosity of hyaluronate is concentration dependent and the curves take different forms (Fig. 3.19) it is not possible to extrapolate from low concentration. Therefore, the viscosity results should be considered as a qualitative indication only at this stage. It does however, appear that viscosity and mobility of the structured regions are interrelated in that they result from similar restrictions. The local motions of the unstructured regions does not appear to experience any similar restriction.

The ^{13}C spectrum of hyaluronate is shown in Fig. 3.20 with tentative peak assignments by Dr. E.G. Finer. The behaviour of this spectrum with temperature is consistent with the ^{1}H nmr results confirming that the processes already described apply equally to the ring carbons and the N-acetyl group.

A survey has been carried out on a variety of hyaluronate samples from various sources. This has shown that while the proportion of immobile species does vary from sample to sample it is always in the range 55-70% (Table 3.5). It is possible to separate the samples into two groups, those in A are mainly of commercial origin and/or lower purity than those in B, and may contain less structured regions.

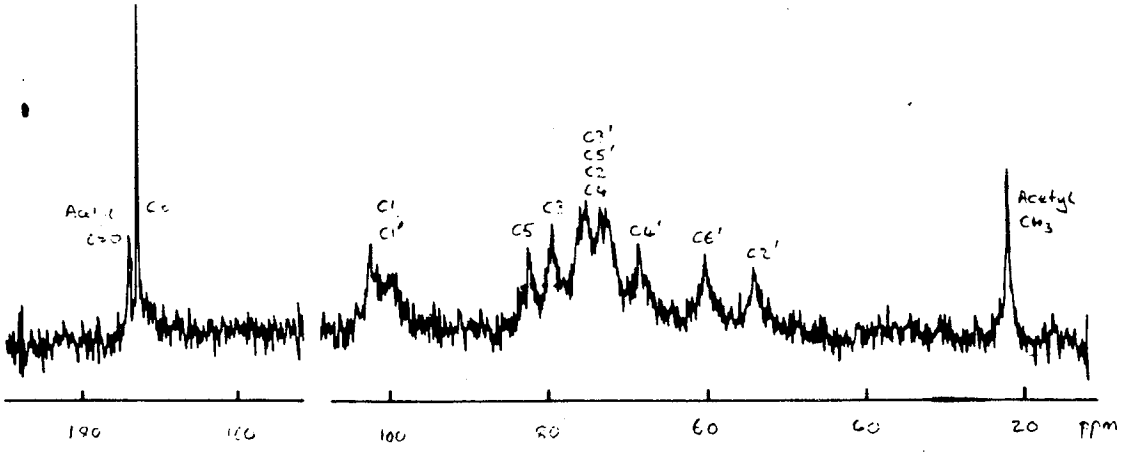

Fig. 3.20 22.63 MHz ^{13}C spectrum (40,000 scans) of 3% hyaluronate in D_2O at 80°, with tentative assignments by Dr. E.G. Finer. Primed atoms are on the N-acetyl glucosamine ring. Unprimed atoms are on the glucuronic acid ring.

Sample			Analysis				
Source	Batch	Salt	Carbon	Hydrogen	Nitrogen	% mobile residues	
A.							
Miles	101B*	K^+	32.87	4.74	2.69	45	)
"	100A*	K^+	28.76	4.18	2.50	36	)
BDH	1500740*	K^+	34.38	4.97	2.90	42	)
Sigma	920-0470*	K^+	29.96	4.30	2.79	40	) Av. 41±4
"	330-2450*	Na^+	31.84	4.65	3.20	39	)
Balazs	COM1†	Na^+	34.27	5.36	2.89	41	)
	Non-fibrous	"					)
"	C34	"	34.35	5.53	2.77	43	)
Miles	117A	20% C-4S$^+$	31.58	4.41	2.97	41	)
	80A	"	32.06	4.67	3.09	32	?
B.							
Sigma	12C-2730*	K^+	29.02	4.12	2.66	30	)
Balazs	Rooster	Na	33.83	5.0	3.03	32	)
"	C32/2	"	31.85	5.57	2.85	33	) Av. 31±2
"	~~//~~1119*	"	32.63	5.34	2.71	31	)
"	COM1†	"	34.27	4.70	2.79	30	)
	Fibrous						
N-acetyl glucosamines			43.72	6.9	6.27		

* from umbilical cord - those unmarked from rooster comb

† the fibrous preparation is claimed (Balazs personal communication) to have significantly more ordered structure as noted by viscosity and optical methods and that the average molecular size is the same in both cases.

\+ Chondroitin 4-sulphate

Table 3.5

On storing the samples having 31% of mobile regions for one week at 0-4°C, the 'extra' 10% order is lost and all the samples are now 41% mobile. It is possible that more 'native' preparations inherently have that extra labile order that is also shown by the 'putty' preparation.

Treatment with hyaluronidase

It has already been mentioned that initial chain cleavage of hyaluronate is accompanied by a large apparent decrease in viscosity. The nmr spectra show an analogous immediate narrowing of the N-acetyl proton linewidth from 12 Hz to 6 Hz when hyaluronate is treated with testicular hyaluronidase at 10°C.

The hydrolysis was followed at 10°C in order that the rate would be sufficiently slow to enable the early stages to be followed closely. During the first hour of incubation, release of end groups was undetectable (i.e. less than 1% release) while the proportion of mobile N-acetyl protons had rapidly increased. The time course of the fraction of mobile protons and of the release of end groups, is shown in Fig. 3.21. It is useful to note that for hyaluronate of 10^6 molecular weight containing approximately 2500 disaccharides (hence β1,4 linkages), a 1% release of end group is equivalent to the cleavage of 25 β1,4 linkages yielding fragments of average length 100 disaccharides.

After the initial linewidth narrowing due to the viscosity change no further substantial changes occur in the nmr spectra apart from the overall intensity increasing. This means that the hydrolysis is two state, i.e. residues are either structured or not, otherwise the linewidth would show a gradual change. When the end group release is approximately 15% (i.e. about 1 in 6 of available β1,4 linkages cleaved) the proportion of mobile protons has reached a limiting value of 88 ± 6% at ambient temperatures. Increasing the temperature to 92°C causes an increase of mobile protons to 96 ± 7%. The difference presumably represents about 8% of the sample which never becomes fully mobile no matter how far the digestion proceeds, but which gives a resonance narrow enough to be integrated at 92°C (Fig. 3.22).

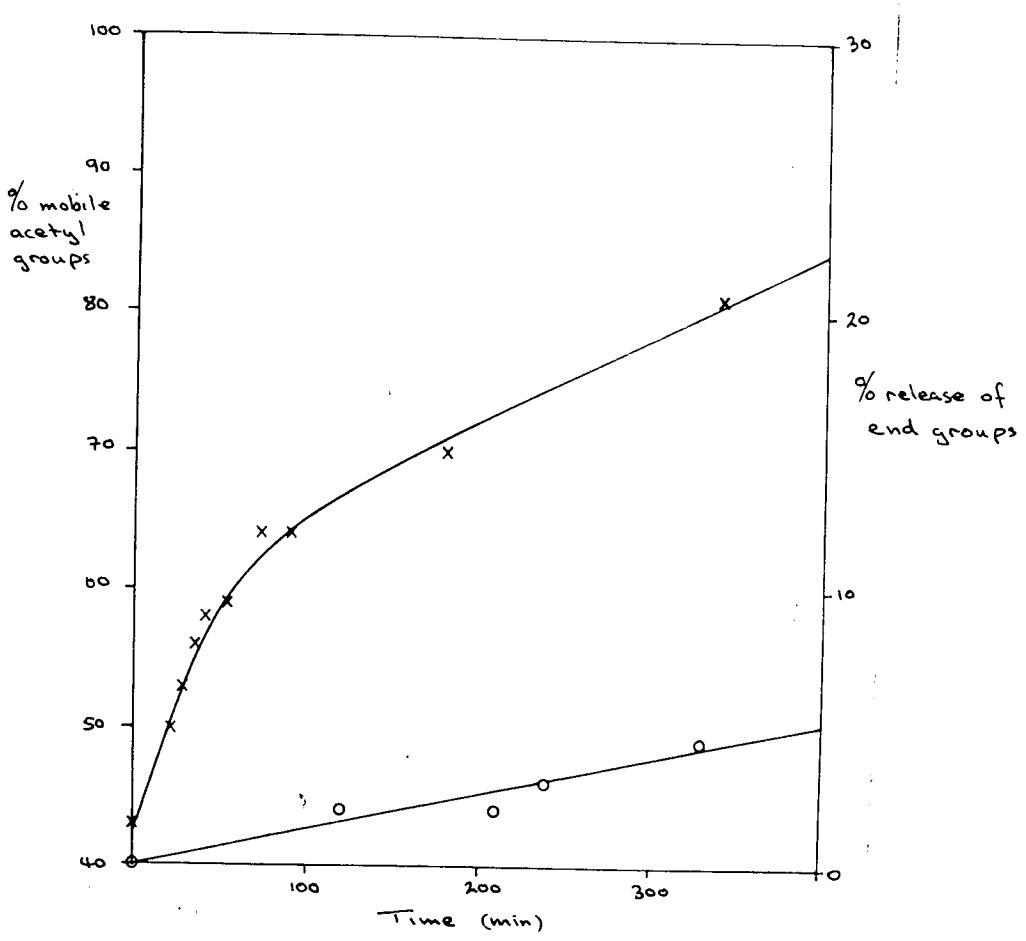

Fig. 3.21 The time course of digestion of hyaluronate (1.5%) dissolved in D_2O containing 0.15M NaCl at 10°C, by hyaluronidase (1900 IU/ml)

X——X, % mobile acetate groups (the end point is marked.-.-.-)

O——O, % end group release (reached 16% after 24 hours)

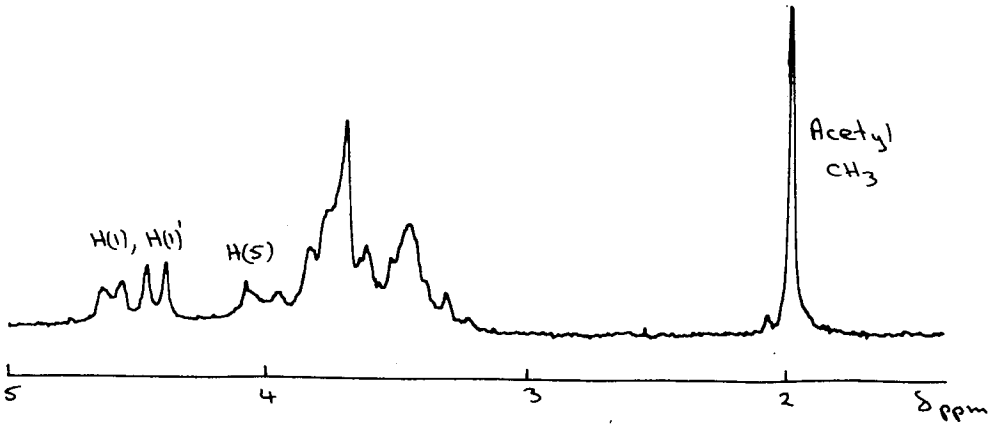

Fig. 3.22 100 MHz 'H nmr spectrum for 1.5% hyaluronate after enzyme digest. Part of the spectrum never becomes fully mobile.

This sudden conversion of structured to unstructured species by the cleavage of one or more linkages can be considered in terms of the cooperative unlocking of a region of order. Thus a disruption of some part of the structure within the heat insensitive regions could be sufficient to cause that particular segment of order to fly apart. This and the fact that ordered and disordered parts of the native hyaluronate are not in equilibrium must mean that the hyaluronate contains some covalent feature, as yet undetermined, capable of initiating a strong cooperative interaction between adjacent parts of the chain. The regions of order do not 'melt' completely as shown by the fact that 8% of the sample never becomes fully mobile under the hydrolysis conditions used here. This 'residual order' could perhaps exist in close proximity to the covalent barriers. This feature need only be present in small amounts and may be modified during analytical studies hence escaping detection. Therefore the 43% mobile species observed probably represent those unstructured regions of the polymer chain linking the structured regions that are terminated by this undetermined feature. A clue to its identity may be given by the non ideality of the carbon, hydrogen, nitrogen analyses.

Origin of the ordered regions in solution

The results from the nmr experiments show that hyaluronate has a partly ordered conformation in solution. Calculations show that the degree of rigidity of the ordered species is higher than can be accounted for by locking all the bonds in a single residue and requires that several consecutive residues be locked simultaneously in a cooperative structure. Elevated temperatures fail to melt out the structure as do additions of salt, pH changes (2.6-7) and the action of enzyme.

The model suggested by these results is one in which the hyaluronate chains possess regions of ordered immobile segments terminated by some covalent irregularity and that these regions exist within the same chain rather than in different chains. Such a system could account for the viscoelastic characteristics of hyaluronate. The ordered regions have a fixed and permanent existence, whereas intermolecular effects such as disruption of non-covalent interchain forces give rise to the make and break rheological character (Gibbs et al. 1968). Thus the ordered regions must be stabilised intramolecularly or perhaps within aggregates that involve a limited number of chains rather than involving aggregates of large size or upon aggregation phenomena that extends to form a network throughout the solution.

From Fig. 3.21 it has been possible to estimate the number of units in the structured regions (E.G. Finer et al. unpublished) as 60 disaccharides on average, and that cleavage of one band in such a region causes almost complete loss of structure. The evaluation of this parameter is shown in Appendix 2.

The action of alkali (pH 13) in disrupting the ordered structure is consistent with the covalent irregularity, that may nucleate these structured regions, being an ester linkage.

4. Conformation in solution

It is apparent that the wide variations in rheological properties, from a stiff viscoelastic putty to a solution having a relative viscosity close to unity, are not associated with the degree of conformational order or with conformational transitions. This contrasts with other polysaccharide systems whose rheological characteristics are able to be related to conformational transitions

(Arnott et al. 1974c; Rees, 1972; Morris et al. 1973). The important difference is that in hyaluronate the rheological properties arise from interactions between the preformed ordered entities rather than within.

Existing evidence for the Conformation in solution

In the past the conformation in solution has been interpreted by many workers as a random coil with some stiffness, based on hydrodynamic studies. The random character clearly exists but as will be shown later is entirely compatible with the proposed model.

The evidence for random coil character is:-

(i) The light scattering envelope shows that hyaluronate has a somewhat stiff random coil structure and the radius of gyration of the molecule is very large such that the chain extends over a solvent domain 10^3-4^4 times larger than the volume of the chain itself (Laurent, 1966; Preston et al. 1965).

(ii) Hyaluronate acts as a molecular sieve towards the diffusion of macromolecules both in vivo and in vitro. Various aspects of the exclusion phenomenon have been reviewed by Laurent (1967) and have been demonstrated by equilibrium dialysis, gel filtration, osmometry, light scattering and solubility measurements. This can be explained in terms of an expanded structure, rather than a compact conformation (Laurent, 1967; Preston et al. 1965).

(iii) Measurements of the variation of intrinsic viscosity with velocity gradient and temperature, streaming birefringence and variation of sedimentation coefficient with concentration, indicate a low axial ratio (of the order of 1) that is

consistent with nearly spherical particles that are highly solvated (Ogston and Stanier, 1951). This view is supported by later light scattering measurements (Preston et al. 1965). The variation of viscosity with molecular weight shows that the exponent in the modified Staudinger equation is 0.78, which is consistent with a random coil structure (Laurent, 1966).

(iv) The radius of gyration from light scattering measurements is in agreement with the intrinsic viscosity only if a random coil structure is assumed. A rod-like structure consistent with the viscosity would require a substantially larger radius of gyration (Preston et al. 1965). This is also in agreement with the observed sedimentation coefficient.

(v) The sensitivity of the viscosity to ionic strength and the shrinkage of the molecule on acidification supports the random coil model suggesting expansion of the molecule in the interaction between anionic groups is increased (Preston et al. 1965).

(vi) The sedimentation volume of hyaluronate as a function of concentration shows that due to its large hydrated volume it forms a more voluminous shape than do for example, globular proteins (Balazs, 1966).

Such randomness could easily exist within the mobile chain segments in the proposed model. The above evidence only indicates that the hyaluronate conformation has sufficient flexibility to exhibit the general characteristics of a random coil.

Evidence also exists for ordered regions that would correspond to the 'immobile' species:-

(i) Although the variation of viscosity with ionic strength supports the random coil model, no parallel change in the radius of gyration is observed by light scattering. Additionally the effect of added protein on the viscosity is inconsistent with a random coil configuration in that the viscosity is apparently unchanged. Both facts indicate that the structure lacks the complete flexibility of a random coil with respect to expansion or contraction. The apparent discrepancy could perhaps be reconciled in terms of a structure similar to that proposed having rigid junction zones which determine the shape and size of the molecular domain with flexible mobile cross-links that determine the viscosity and degree of internal 'free draining' (Preston et al. 1965; Silpananta et al. 1968).

(ii) The viscoelastic behaviour of hyaluronate changes in relaxation rates but not in nature with variation in temperature, concentration and ionic strength. The transition from viscous to elastic behaviour under these conditions is much sharper than for other systems in which viscoelastic properties depend on random coil entanglements (Gibbs et al. 1968) or than is predicted theoretically for such systems (Aklonis et al. 1972). This suggests that the transition from a relatively rigid elastic system to a viscous fluid does not involve extensive relaxations and uncoiling of the hyaluronate chain (Gibbs et al. 1968).

(iii) Although it has been stated (Ogston and Stanier, 1951) that the streaming birefringence of hyaluronate is consistent with an axial ratio of near unity, the value estimated for various

concentrations fall within the range 5-22, the more accurate values being in the range 14-22. This does not contradict the original contention of Ogsten and Stanier (1951) but might suggest a conformation that is neither a rigid rod nor a random coil, i.e. a conformation having characteristics of both.

A possible solution conformation

Literature evidence together with the results reported here from nmr experiments indicates that hyaluronate exists in solution as a mixture of ordered and disordered conformations. Probably a structure similar to that proposed by Preston et al. (1965) in which a cross-linked network is formed. We must now ask the question: What is the nature of the ordered regions?

The most attractive choice would be double helical regions similar to those known to exist in carrageenan and agarose gel networks. This would be an ideal source of cooperative stabilisation that could readily explain the apparent intramolecular stability and intermolecular instability of ordered regions in terms of the different types of contacts involved. Thus the viscoelastic viscosity could be accounted for by the inter-double helical contacts being sufficiently weak to break and reform. A priori a double helix must be formed intramolecularly to be consistent with Xray evidence for antiparallel structure (Dea et al. 1973; Atkins and Sheehan, 1973).

However, the latest Xray refinement by our colleagues at Purdue (Guss et al. 1974) shows convincingly that an antiparallel single helical structure is a more accurate interpretation of the Xray data. Thus so it must be in solution, for no obvious mechanism can be envisaged that will allow double helices to unwind during a gentle crystallisation process yet prevent them unwinding during

the pH, salt concentration and temperature changes experienced during nmr experiments.

All evidence therefore, points to a single helical conformation in solution, a conformation that must have some form of cooperative mechanism to preserve its rigidity in solution. A model that is consistent with the nmr data is one in which hyaluronate chains have 'rod and flexible chains' or 'plates and chains' (Fig. 3.23).

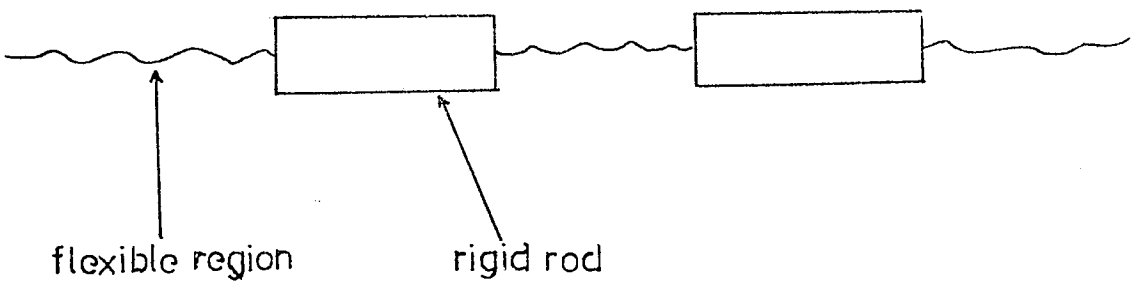

Fig. 3.23 Rod and chain model for hyaluronate

The nature of the 'rods' or 'plates' is unknown, some possibilities are:-

(i) a single hairpin-like structure (Fig. 3.24a)

(ii) a multiple folded structure (Fig. 3.24b)

(iii) a composite chain made of short segments joined by ordered regions (Fig. 3.24c)

Evidence in the literature could be considered to support these postulates.

It is reported that hyaluronate strands have been seen under the electron microscope as wide hairpins folding back upon each other (Fig. 3.24a) (Balazs 1974). Fessler and Fessler (1966) have also visualised hyaluronate by electron microscopy but although the individual chains can be seen in an apparently folded state (like Fig. 3.24b) no clear evidence is available about the fine structure of the ordered domains. Since about 50–60% of the hyaluronate chain is expected to be involved in such regions, the folds observed in the electron micrographs are possibly memories of part of the folded regions.

Swann (1969) suggests on the basis of ascorbate depolymerisation, that hyaluronate is a heterogeneous molecule containing subunits of molecular weight 65,000. Repeated treatment with ascorbate failed to decrease the size of the molecule further therefore, the reaction could not be described as a random depolymerisation process. Swann states that, "when hyaluronate is degraded, constituents and/or covalent linkages (which have not been identified) are cleaved by the ascorbate". Possibly these linkages are the same ones that have to be shown by nmr to be sensitive to alkali.

For such models to be consistent with the antiparallel structure derived by Xray diffraction (Guss et al. 1974) it is necessary that:

(i) folded regions have intrachain folds conferring and 'up-down' nature.

(ii) sub-units are joined by chains running in opposite directions

(iii) alternatively adjacent 'rods' or 'plates' formed by type (ii) could pack in an antiparallel fashion.

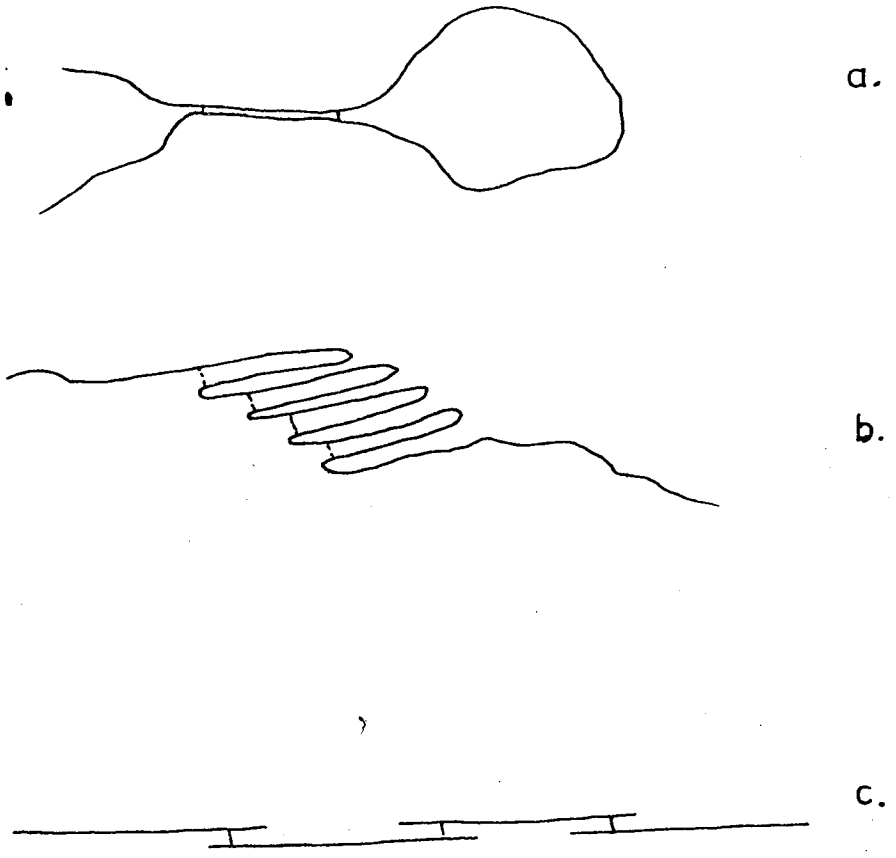

Fig. 3.24 Possible types of ordered regions in hyaluronate chains

(a) a single hairpin
(b) a multiple folded structure
(c) a composite chain consisting of several short segments joined covalently

Clearly this is somewhat speculative and further work is in progress to elucidate the nature of the covalent feature and form of the molecule in solution.

Preliminary nmr studies indicate that other glycosaminoglycans may possess similar ordered and disordered regions to hyaluronate. Three samples of Chondroitin 4- and 6- sulphate examined show 45±10% of immobile species that do not give a high resolution spectra. These results could be consistent with similar models to those proposed for antiparallel hyaluronate since Xray structures are related (Atkins et al. 1972b; Isaac and Atkins, 1973; Arnott et al. 1973). However, a folded chain model is probably less likely because of the lower molecular weights of the chondroitins (40–120 disaccharide units on average).

These results were surprising in the light of the existing model for proteoglycans. When the chondroitins are attached to the protein backbone in the supposedly characteristic 'bottlebrush' model, the chains are parallel and there is no reported evidence for two or more 'bottlebrushes' interpenetrating (Mathews and Lozaityte, 1958; Partridge et al. 1961). Thus the ordered antiparallel structures must be formed during or after cleavage from the protein backbone.

Similar phenomena may also occur for other glycosaminoglycans. Jaques et al. (1966) in an nmr study of heparins, noted variations in the relative intensities of given proton signals from one sample to another, that were independent of chemical composition. This was interpreted in terms of"substantial differences in the ratios of component sugar units" but could well be varying extents of ordered species in the light of the nmr results reported here.

Physical and Biological Implications

(i) The rheological properties of hyaluronate *in vitro* and *in vivo* can now be explained in terms of temporary cross-links between ordered domains. The aggregated regions having loose or weak bonds that break rapidly enough to allow ordered domains to slide past each other under low imposed strain, resulting in viscous flow. While under high strain, the ordered regions cannot adjust so rapidly and are thus deformed elastically (Balazs and Gibbs, 1970). This proposal is in good agreement with that of Gibbs *et al.* (1968), who postulated a relaxation mechanism consisting of a breakdown of a highly elastic hydrogen-bonded network, followed by viscous flow due to long range cooperative segmental motions. Alterations in pH, concentration and salt content are considered to alter the degree of aggregation rather than the nature of the aggregate (Balazs and Gibbs, 1970).

(ii) Studies on synovial fluid in arthritic joints (Balazs and Gibbs, 1970) have shown that the fluid is viscous rather than elastic, thus showing less rigidity. It has been proposed (Balazs and Gibbs, 1970) that one of the main functions of the intercellular matrix of connective tissue is to provide a system that absorbs mechanical stress, thereby protecting the cells from mechanical shock and vibration. At the interfaces between solid and liquid matrices, such as the surfaces of tendons, hyaluronate serves as the primary isolating and lubricating agent. Hyaluronate and proteoglycans are trapped in a collagen gel in solid matrices such as the vitreous (Balazs, 1955). The primary

mechanical stress is supported by the collagen fibrils and a large part of the energy is transferred to the viscoelastic macromolecules for storage and dissipation. Cellular damage or defective biosynthesis may release enzymes capable of disruption of the covalent features holding the hyaluronate chains together. Removal or reduction of the hyaluronate network will cause a breakdown of the collagen/hyaluronate matrix, hence reducing its protective ability.

(iii) Various solid state fibre structures are known for hyaluronate with antiparallel chains (none are known with parallel chains). The 0.84 nm projected residue height squat structure is expected to be the most important or natural form, because this appears to be obtained most readily by gentle crystallisation processes on samples of high molecular weight i.e. close to native polymer weight. The apparent polymorphism that does occur may suggest that the geometry within the ordered domains in solution is perhaps biologically controlled.

CHAPTER 4

Preliminary Xray diffraction studies on some Bacterial Polysaccharides

A. INTRODUCTION

Microorganisms synthesise a variety of polysaccharides that fulfil a variety of functions such as:-

(i) structural components providing rigidity to cell walls (e.g. bacterial and actinomycete peptidoglycan, chitin, mannan)

(ii) intracellular storage (glycogen)(Slodki,1967)

(iii) extracellular polysaccharides that can enhance virulence in plant and animal pathogens (e.g. capsules of Xanthomonas and Pneumococcus species and Meningococcus).

The extracellular polysaccharides, the subject of this Chapter can be further classified (McNeely and Kang 1973):

(i) capsules that are integral with the cell wall (Sharon, 1965), as well as structurally demonstrable micro-capsules. For example, hyaluronic acid from Group A hemolytic streptococci (Sharon, 1965) and the type specific heteropolysaccharides from Pneumococcus (Stacey and Barker, 1960; Sharon, 1965). These microorganisms, like many other encapsulated species are pathogens in man and other animals.

(ii) Slimes that accumulate outside the cell wall and diffuse constantly into the culture medium. Microorganisms producing slimes may or may not be encapsulated.

When both capsular and slime polysaccharides are produced, the chemical composition of both is essentially similar (Jeanes, 1968).

The function of extracellular polysaccharides and their relation to cell survival is not clear (Sutherland, 1972). However,

the suggestion of an ordered conformation in solution for Xanthomonas species and a synergistic interaction with a β1,4 mannan (Morris and Rees, unpublished) similar to that proposed for plant polysaccharides (Dea et al. 1972) may be open to interpretation as a model for parasitic host recognition and adhesion between bacterial and plant cells.

In this chapter preliminary models will be proposed for the extracellular polysaccharide from Xanthomonas phaseoli in the solid state from Xray diffraction data which may provide support for the solution characteristics observed by Morris and Rees for Xanthomonas campestris, a chemically similar member of the Xanthomonas species

In addition a preliminary solid state model for the extracellular polysaccharide from Arthrobacter viscosus B1973 will be described.

1. Origin, Role and Uses

A major factor determining the occurrence in nature of extracellular microbial polysaccharides is the availability of carbon-containing substrate material, such as carbohydrates or hydrocarbons, under conditions that permit microbial growth. A Pseudomonas species isolated from jet fuel produces a high molecular weight glucose polymer when grown on n-alkanes (Jones and Colasito, 1963).

Numerous plant diseases result from the mechanical blocking of water movement by extracellular polysaccharides produced by an invading phytopathogen. Partly by this mechanism, X. campestris produces vascular disease in cabbages and related plants. X. phaseoli behaves similarly, attacking its natural host, the common bean plant (Lesley and Hochsler (1959)).

The polysaccharide of *X. campestris* (NRRL B1459) is produced commercially by continuous fermentation from dextrose and finds considerable use in Industry by virtue of its unusual rheological properties; which provide a basis for its many uses as a thickening, suspending, emulsifying and stabilising agents in the Food Industry (Rocks, 1971; Kelco, 1972) and numerous applications such as in the pharmaceutical, paint, paper and oil drilling industries. In the latter case it provides the drilling fluid with low water loss properties thus keeping friction losses low.

Arthrobacter viscosus B1973 is a microorganism isolated from soils which produces large amounts of extracellular polysaccharide using various carbon sources, usually glucose. This polysaccharide has not yet found any commercial use.

Extracellular polysaccharides probably protect microorganisms against various adverse environmental factors (Wilkinson, 1958). For example, the thick capsule associated with extracellular polysaccharide production provides definite protection against bacteriophages, simply by serving as a physical barrier against the agent (Wilkinson, 1958). In general, extracellular polysaccharides do not appear to function as a reserve energy source.

2. Rheological Properties

Literature from manufacturers of *X. campestris* polysaccharide emphasize its unusual rheological characteristics, in particular claiming stability to heat, acid and salt, together with pseudoplastic viscosity and synergistic interactions with certain substituted mannans. The variations in viscosity caused by these parameters are described below.

a) Temperature

Most workers in the literature proclaim the stability

of the viscosity with temperature (Fig. 4.1a) (e.g. McNeely and Kang, 1973; Kelco Co., 1966). Strictly in the context of commercial applications this may well be true in that, for example, the viscosity at high temperature (say 100°C) may be very close to that at low temperature (say 10°C). However, the early paper by Jeanes et al. (1961) shows a sharp sigmoidal fluctuation in viscosity in an intermediate temperature range (Fig. 4.1b).

b) pH

The viscosity of aqueous solutions is nearly independent of pH between pH 6 and 9 and shows only minor variations over a pH range of 1 to 11. At pH 9 or above gradual deac ylation takes place but has little effect on the solution properties.

c) Salt

A sharp decrease in the viscosity of aqueous solutions of polyelectrolytes upon the introduction of electrolyte is considered a general characteristic. It appears however, that a number of microbial polysaccharides, including those from X. campestris and A. viscosus, either do not have this property or show it to a lesser extent than do synthetic or plant polyelectrolytes under similar conditions.

Important variables in such behaviour are concentrations of both polymer and electrolyte and pH. For example, electrolytes may produce a decrease in viscosity of X. campestris at concentrations of less than about 0.3% but show an increase at higher polysaccharide concentrations (Fig. 4.2). Solutions of deactylated X. campestris

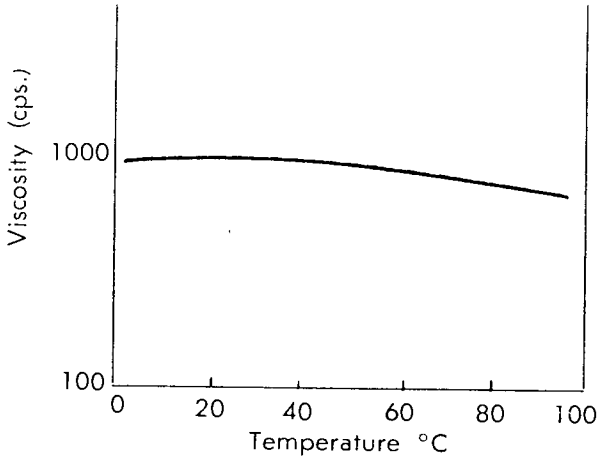

(a)

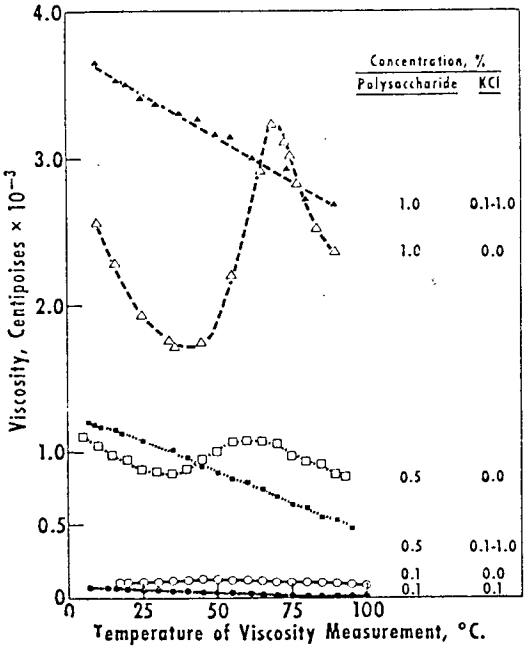

(b)

Fig. 4.1 Variation of viscosity with temperature for X. campestris.

(a) Often quoted curve, almost stable with temperature.

(b) Sigmoidal transition reported by Jeanes et al. (1961).

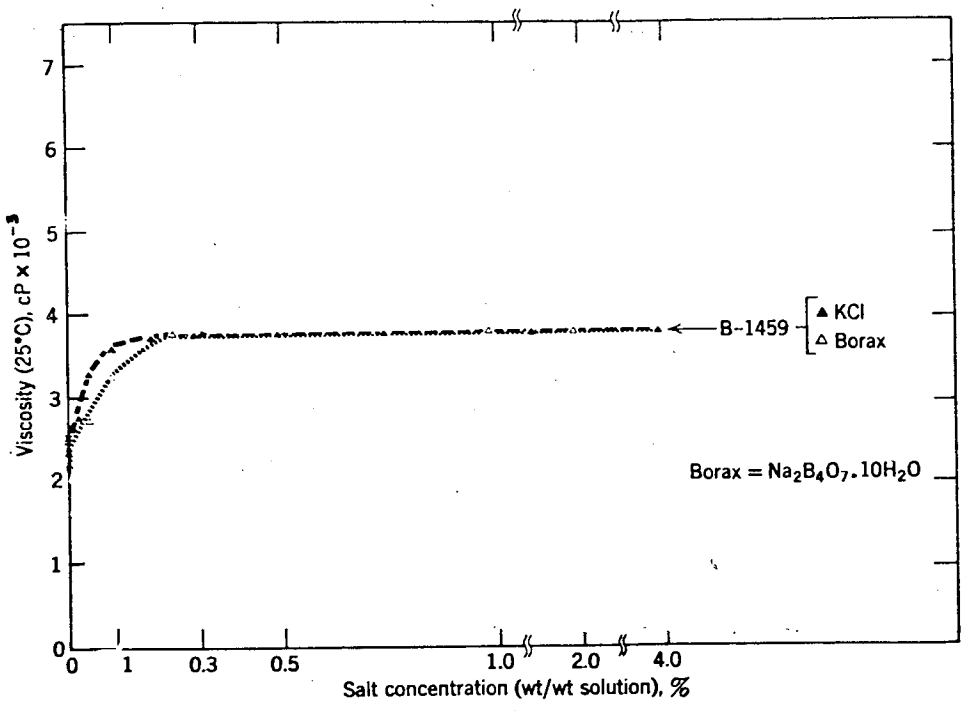

Fig. 4.2 Effect of added salt (KCl) on the viscosity of X.campestris

polysaccharide show a greater percentage increase in viscosity than those of the native polysaccharide upon addition of salts (Jeanes and Sloneker, 1961).

X. campestris polysaccharide is also stable to heat in the presence of KCl. Under comparable conditions of pH and salt, alginate and gum tragacanth show sharp decreases in viscosity; locust bean gum shows little change.

d) General viscosity characteristics

In a comparison of the viscosity profiles of various extracellular anionic polysaccharides, Jeanes and Pittsley (1973) considered the resistance of solutions to shearing forces, and characterised two general categories

(i) solutions that were pseudoplastic and appeared to be continuously deformable under shear stress, and

(ii) solutions that were plastic i.e. at or below a definite shear stress they do not continue to flow and the rate of shear decreases rapidly towards zero.

Furthermore, they interpreted (i) as indicative of flexible macromolecules possessing approximately linear backbone structure having a random coil solution conformation,(ii) was interpreted as corresponding to macromolecules that were relatively stiff or involved in cross-linked networks or other structured aggregates that can resist shearing stress. (Fig. 4.3.)

Deacetylated A. viscosus B1973 polysaccharide and guar gum are in accord with pseudoplastic substances while native B1973 polysaccharide follows a curve characteristic of plastic substances.

X. campestris polysaccharide appears to have characteristics of both extremes thus in at least this respect it is similar to

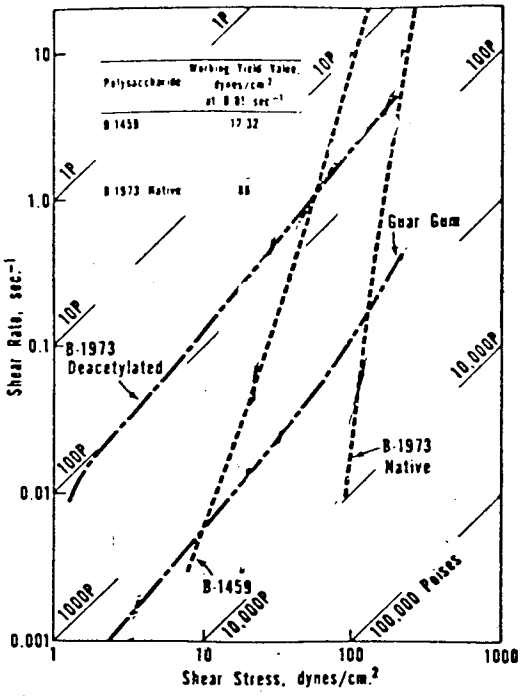

Fig. 4.3 Shear stress – shear rate – viscosity relations at 25°C for X. campestris (B1459), A. viscosus (B1973) and Guar Gum.

Deacetylated B1973 and guar gum are pseudoplastic; native B1973 is plastic; X.campestris (B1459) has characteristics of both.

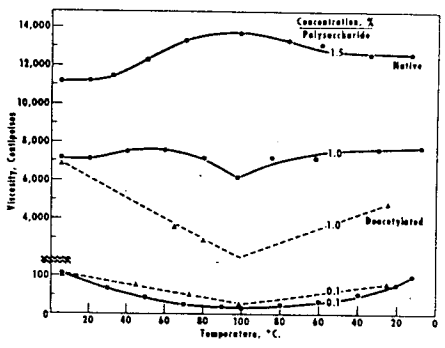

Fig. 4.4 Variation of viscosity of A.viscosus with temperature.

hyaluronate (Chapter 3) in exhibiting the character of a random coil with some stiffness.

In the presence of 0.5% KCl, the yield values for X. campestris and A. viscosus polysaccharides increase 4-5 fold. After being heated to 80°C and tested at 25°C, the value for X. campestris polysaccharide increases slightly, if KCl is present but decreases if absent (a useful property in food applications).

Upon deac ylation both polysaccharides become predominately pseudoplastic.

All microbial polysaccharides, with the exception of deac ylated A. viscosus, show a rapid decrease in viscosity with increased shear stress that is regained immediately upon removal of shear. Thus ease of thinning (thixotropy) while under shear is frequently cited as an unusual property of X. campestris polysaccharide (e.g. McNeely, 1967; Rocks, 1971) and A. viscosus polysaccharide (Floyd and O'Connor, 1969).

For A. viscosus polysaccharide, both deacetylated and autoclaved native polymer show higher viscosity than the native material. In general, the viscosity increases in the presence of salt. This polysaccharide is said to be also unaffected by heating as far as viscosity is concerned although the published curves (Fig. 4.4) show a suggestion of sigmoidal character.

3. Structure

A variety of constituent sugars and linkages appear in the extracellular polysaccharides, yet in some aspects there are similar common features. One unit long side chains appear to be a common form of branching and in many cases they possess uronic acid residues and alkali labile O-acetyl residues.

Xanthomonas species

Extracellular polysaccharides are produced by several species of the bacterium Xanthomonas (Lilly et al. 1958), that from X. phaseoli being the first to be characterised (Lesley and Hochster, 1959). This was claimed to be composed of D-glucose, D-mannose, and D-glucuronic acid in the approximate ratio 1:1:1 by the isolation of the crystalline derivatives of these sugars. However, no information is presented about the linkage configuration and the authors do suggest that the results are "subject to some error in view of the fact that some unknown amount of destruction of sugars occurs during hydrolysis". Recent work in this laboratory (Mindt and Sanderson, unpublished) suggests that the structure is in fact very similar to X. campestris polysaccharide, based on methylation analysis. This proposition is supported by Orentas et al. (1963), who indicate that the sugar compositions are similar for most of the Xanthomonas species.

Until recently it has been common belief that the X. campestris polysaccharide contained a basic repeating unit consisting of 16 sugar units, of which 13 were present in a main linear chain and 3 attached as single unit side chains (Sloneker et al. 1964)

i.e.

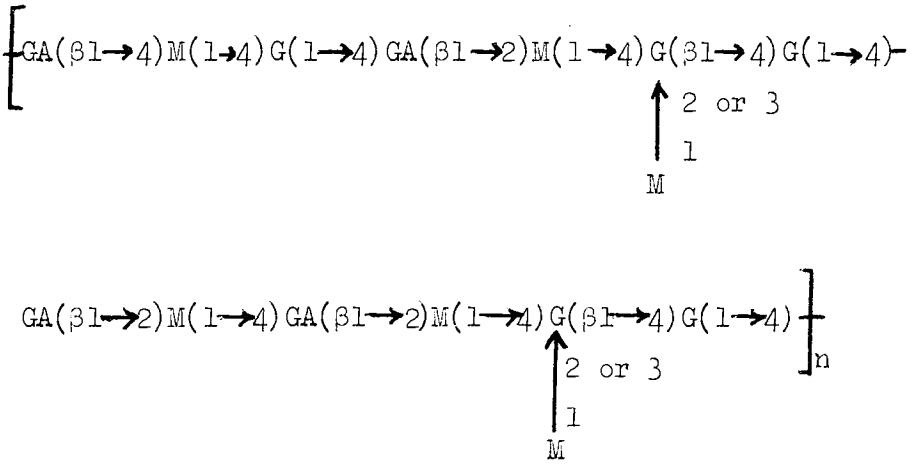

Also present: O-Acetyl (3.4 mole)

4,6-O-(1-Carboxyethylidene)-D-Glucose (1 mole)

The sugars present D-glucose (G), D-mannose (M) and D-glucuronic acid (GA) were in the ratio 2.8:3.0:2.0 together with acetic and pyruvic acid substituents, based on periodate oxidation and acid hydrolysis studies (Sloneker et al. 1964; Sloneker and Jeanes, 1962).

Methylation studies by Siddiqui (1967) lead to a slightly different sugar ratio (glucose:mannose:glucuronic acid 3.8:3.7:2), that is interpreted in terms of a structure containing 10 backbone sugars with 3 mannose side chains

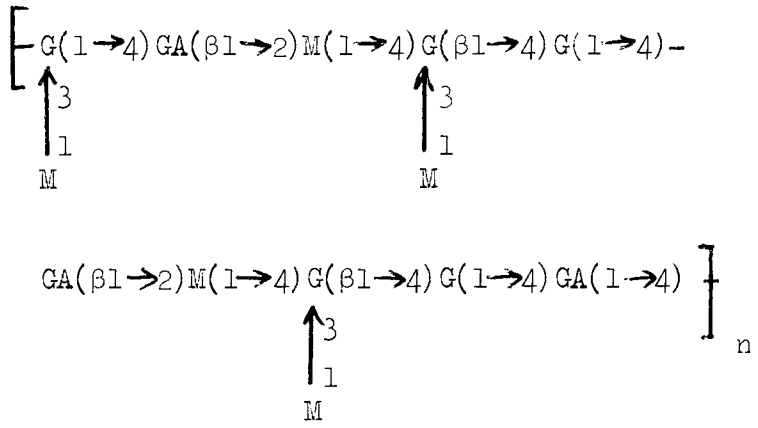

Also present: O-Acetyl

4,6-O-(1-carboxyethylidene)-D-glucose (1 mole)

Pyruvic acid appears every 16th (Sloneker et al. 1964) or 14th (Siddiqui, 1967) sugar residue as a single unit side chain on glucose (or possibly mannose) as a 4,6-O-(1-carboxyethylidene) substituent

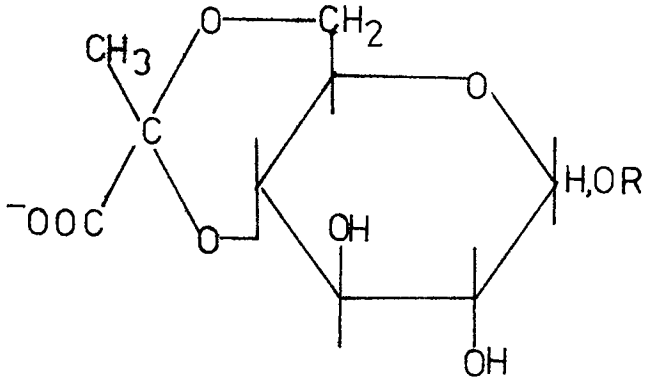

where R = polymer chain.

Work in this laboratory on the polysaccharides from both X. campestris and X. phaseoli (Melton et al. 1974) suggested at first that the structure could be interpreted in a simpler way having glucose:mannose:glucuronic acid in the approximate ratio 2:2:1 and proposing the structure:

$$\left[\text{GA}(\beta 1\rightarrow 2)\text{M}(\alpha 1\rightarrow 4)\,\text{G}(\beta 1\rightarrow 4)\,\text{G}(\beta 1\rightarrow 4)\right]_n \qquad \text{A.}$$

$$\uparrow \begin{matrix} 3 \\ 1 \\ \text{M} \end{matrix}$$

in which every third side unit on average carries a 4,6-O-(1-carboxyethylidene) substituent.

In the structures proposed by Sloneker et al. (1964) and Siddiqui (1967) the undefined anomeric configurations are assumed to be β. because the polysaccharide has a low optical rotation ($[\alpha]_D^{25}$ 0°). Calculations by Rees (unpublished), based on the optical rotation of various characterised oligomers and using the concept of 'linkage rotation' (Rees, 1970; Rees et al. 1970), suggest that the undefined linkages are probably

M(α1→4)G and G(β1→4)GA.

At the commencement of this work the above structure was considered to be a good approximation to the truth, bearing in mind that irregularities consistent with the other proposed structures could exist side by side. However, more recent work by Kenne, Svensson and Lindberg (personal communication from Professor Lindberg) indicates that the structure may have a glucan backbone with a 3 unit side chain

i.e. 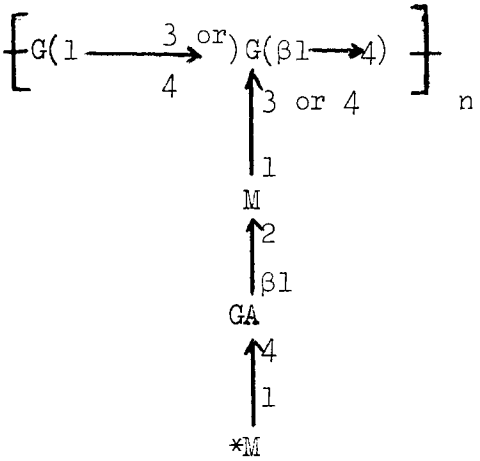 B.

* contains 4,6-O-(1-carboxyethylidene) substituent.

These findings are based on:

(i) Methylation analysis which gives products similar to those noted by Melton et al.(1974).

(ii) Chain cleavage by β-elimination at the uronic acid residue, followed by mild acid hydrolysis to remove the modified sugar residue gave a high molecular weight product. Thus assuming total loss of glucuronic acid then this residue must be on a side chain otherwise loss of molecular weight would be apparent.

(iii) The same β-elimination treatment with mild acid hydrolysis, when followed by CD_3 methylation gave;

2,3,6-tri-O-methylglucose

2,6-di-O-methylglucose

2[^{2}H],3,4,6-tetra-O-methylmannose

in the ratio 1:1:1.

The key result is (ii) above which if true eliminates all other structures. Neither (i) nor (iii) distinguish on their own between this structure and that of Melton et al. (1974).

In view of the uncertainty about the nature of the linkage mannose ($1 \xrightarrow[4]{3}$ or) glucose in the Lindberg structure, Melton (unpublished) has reinvestigated the methylation products from the isolated oligomer glucuronic acid - mannose - glucose, and finds that the linkage is probably mannose ($1 \longrightarrow 3$) glucose, thus throwing further doubt on Structure A.

In view of the preliminary nature of all these investigations, however, it has been considered prudent to include in this study preliminary models based on the various structures.

Arthrobacter viscosus

The structure of Arthrobacter viscosus D1973 has been well characterised (Siddiqui, 1967; Sloneker et al. 1968) as having a linear structure consisting predominantly of repeating trisaccharide units, --- O-β-D-mannopyranosyluronic acid-(1→4)-O-β-D-glucopyranosyl-(1→4)-D-galactose(1→4)---, in which 50% of the available hydroxyl groups are acetylated.

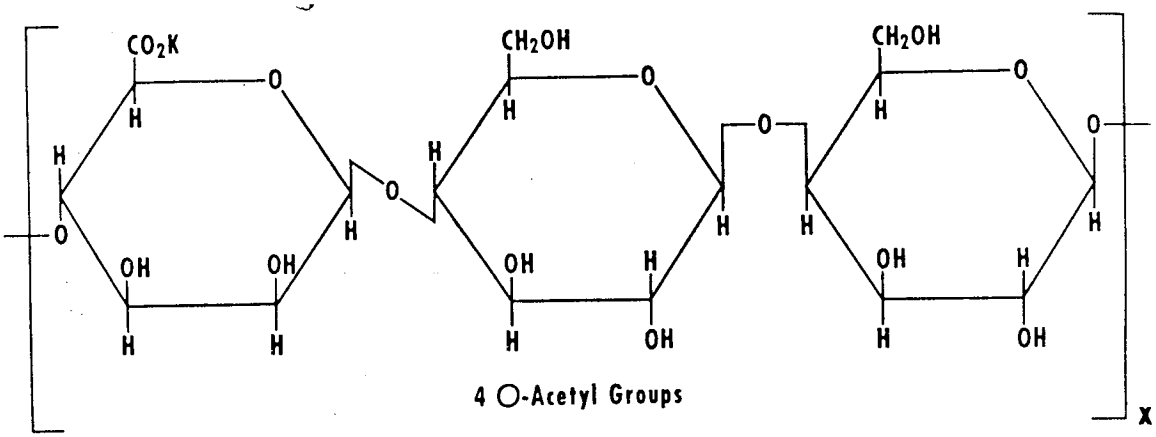

It is proposed that the majority of the linkages are β based on the negative specific rotation ($[\alpha]_D$ - 50°) for the non-methylated polysaccharide and isolation of characterised oligomers only the galactose-mannuronic acid linkage is undecided.

4. Structural similarity of the Xanthomonas species

Of the Xanthomonas species studied, most appear to produce polysaccharides of similar sugar composition (Orentas et al. 1963) containing varying amounts of 4,6-O-(1'-carboxyethylidene) substituent. The reported exceptions are X. vesicateria and X. stewartii (Gorin and Spencer, 1961), having galactose instead of mannose.

The extracellular polysaccharide from X. oryzae

(Misaki et al. 1962) shows methylation products almost identical to those derived from X. campestris (Siddiqui, 1967). Similarly Gorin and Spencer (1963) in a study of the structural relationships of Xanthomonas polysaccharides found essentially similar products from X. hyacinthi, X. translucens and X. maculofoliigardiae. Interestingly, acid and enzyme hydrolysis showed the presence of the four unit sequence;

$$\underline{\underline{D}}\text{-GA}(\beta 1\longrightarrow 2)\text{-}\underline{D}\text{-M}(1\longrightarrow 3)\text{-}\underline{\underline{D}}\text{-G-}(\beta 1\longrightarrow 4)\text{-}\underline{\underline{D}}\text{-G.}$$

which could be consistent with the recent findings of Melton.

It is therefore considered that the structures of the polysaccharides from the Xanthomonas species are essentially similar, in particular the structures of X. campestris and X. phaseoli (Melton et al. 1974).

B. METHODS

1. Materials

(i) Xanthomonas campestris polysaccharide was a commercial sample obtained from ABM Industrial Products Ltd. Cheshire, Batch No. KTL 21494, that had been dialysed against distilled water to remove excess salts.

(ii) Xanthomonas phaseoli polysaccharide was prepared in this laboratory from the supernatant of a culture grown by Mr. W.L. King using a X. phaseoli strain from the Northern Regional Laboratory (also (iii) below). Conditions used were those set down by Lesley and Hochster (1959).

(iii) Arthrobacter viscosus B1973 was a kind gift from Dr.Allene Jeanes, Northern Regional Laboratory, US Dept. of Agriculture, Peoria Illinois USA.

2. Preparation of samples for Xray diffraction

0.5-1% solutions of the polysaccharide in deionised water were prepared by stirring with slight heat. The polysaccharide from X. phaseoli readily dissolved but that from X. campestris was more difficult. Autoclaving was avoided to prevent any degradation of the samples.

Drops of the warm solution were placed between glass beads that were slowly drawn apart in a closed cell (Fuller et al. 1967). Constant humidity was maintained (about 58%) by means of a saturated sodium bromide solution. The fibre was allowed to 'dry' over 24-48 hrs at room temperature. No improvement in the quality of the diffraction patterns was observed by drawing fibres at higher humidities.

3. Xray diffraction, indexing and density measurement

Procedures already described in Chapter 2 were used.

4. Computer model building

In constructing a model in the computer the side chains can be ignored in the first stages. Therefore, the problem is to take each of the alternative covalent structures and systematically vary the torsion angles shown (Fig. 4.5) to match the values of n and h which were obtained from the diffraction pattern.

From Fig. 4.5, the disaccharide (i) can be dealt with as was hyaluronate (Chapter 2), but because of the extra residues in the trisaccharide (ii) and tetrasaccharide (iii), it was necessary to modify the original Rees program (Anderson et al. 1969).

The program was rewritten by Dr. D.A. Rees to handle polysaccharides of the types

(A-B-)n

(A-B-C-)n

(A-B-C-D-)n

Initially the program was written to calculate helix parameters and atomic coordinates for the individual chain conformations, when glycosidic torsion angles and residue coordinates are supplied. It has been subsequently elaborated to allow systematic exploration of glycosidic torsion angles between predetermined limits.

For a disaccharide repeat it was possible to readily determine the glycosidic angles from n - h graphs (Ramachandran et al. 1963) by holding two of the four torsion angles constant at a time. However, six and eight torsion angles cannot be derived in this way since many alternative solutions are possible. In addition the systematic variation of all the torsion angles would require formidable computing time e.g. the variation of six torsion angles

(a)

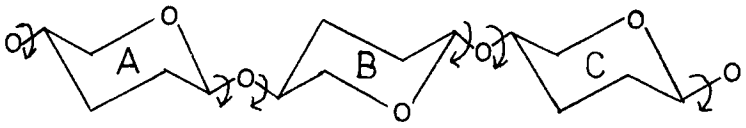

(b)

(c)

Fig. 4.5 Variable torsion angles for:

(a) disaccharide (4 variables)
(b) trisaccharide (6 variables)
(c) tetrasaccharide (8 variables)

in 10° steps would require 36^{6} (2×10^{9}) calculations. Hence, some extra assumptions were required.

(i) For each linkage in the repeating unit a hard sphere map was produced. The starting point was taken as near as possible to the centre of the map.

(ii) For the Xanthomonas polysaccharide backbone, the cellobiose link was fixed as in its crystal structure i.e. $\Delta\phi = 42^{\circ}$ and $\Delta\psi = 18^{\circ}$ (see following section for definitions of $\Delta\phi$ and $\Delta\psi$). Therefore, four of the eight angles were not initially explored.

(iii) Spacefilling models were constructed with torsion angles adjusted so that the repeat unit had approximately the calculated projected residue height. These in conjunction with (i) were taken as starting points.

These assumptions helped considerably with the problem of computing time particularly for the tetrasaccharide repeat. Additionally, the program was later modified to search for a fit to n and h using the Rosenbrock Hillclimb minimisation routine rather than the systematic exploration used initially.

5. Definition of torsion angles

In this work ϕ and ψ are the variations from $\phi = \psi = 0$ which is the conformation in which C(g), C(1), O(g), C(g)' and C(1)' are coplanar, C(g), C(g)' and O(g) are the relevant glycosidic carbons and the glycosidic oxygens as shown in the example below. (Fig. 4.6.)

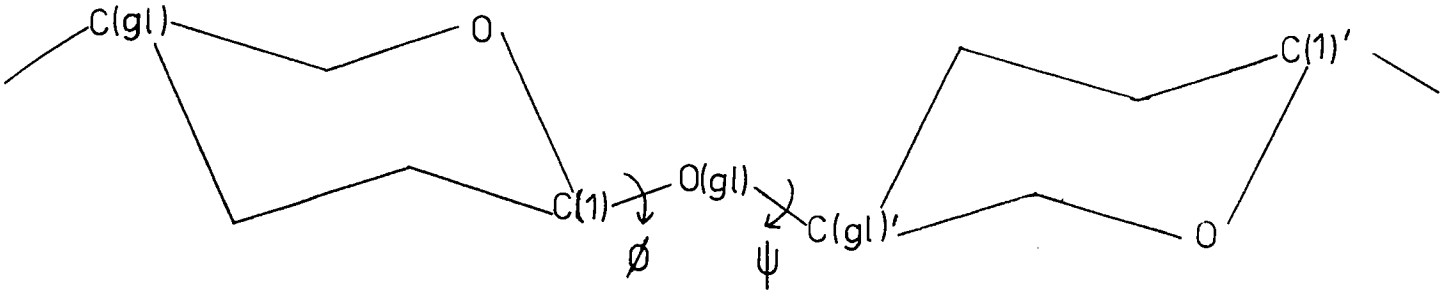

Fig. 4.6 Atoms defining ϕ and ψ.

$\Delta\phi$ and $\Delta\psi$ are related to ϕ and ψ merely by a shift of origin such that $\Delta\phi = \Delta\psi = 0$ is the conformation in which the

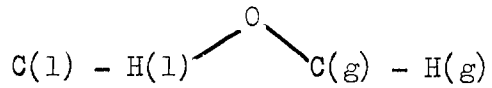

system is eclipsed (Rees, 1970) Table 4.1

Linkage	Approximate origins				Approximate* relations between ϕ, $\Delta\phi$ and ψ, $\Delta\psi$.
	ϕ	$\Delta\phi$	ψ	$\Delta\psi$	
β1,4	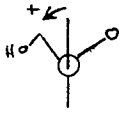	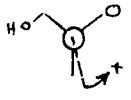	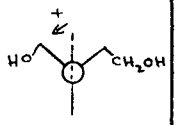	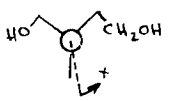	$\phi = \Delta\phi + 180^\circ$ $\psi = \Delta\psi + 180^\circ$
β1,3	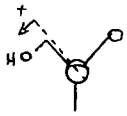	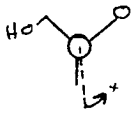	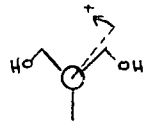	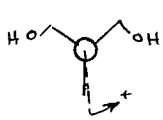	$\phi = \Delta\phi + 120^\circ$ $\psi = \Delta\psi + 240^\circ$
β1,2$^+$	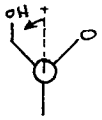	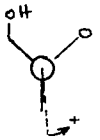	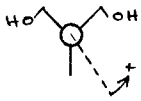	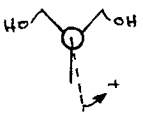	$\phi = \Delta\phi + 180^\circ$ $\psi = \Delta\psi + 300^\circ$
α 1,2$^+$	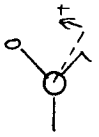	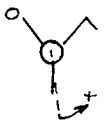	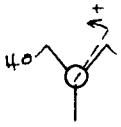	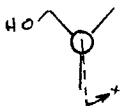	$\phi = \Delta\phi + 240^\circ$ $\psi = \Delta\psi + 240^\circ$
β1,4†	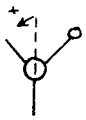		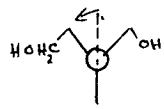	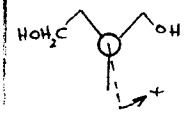	$\phi = \Delta\phi + 180^\circ$ $\psi = \Delta\psi + 180^\circ$

* These are for idealised sugar residues - real sugar residues are somewhat distorted so accurate correction factors need to be calculated for each set of coordinates.

\+ for mannose

† for galactose

Table 4.1 Definition of torsion angles for various linkages

6. Residue coordinates

Coordinates used were either derived from the standard Arnott and Scott (1972) β-D- or α-D glucose coordinates or already existed in Arnott and Scott form (Table 4.2).

In particular, coordinates for 2-linked α-D-mannose were derived using existing computer programs written by Smith (1972). This involved:

(i) adding an axial oxygen atom and equatorial hydrogen atom on C(2) the position of which are defined by
   a) the bond length from the atom to the ring atom
   b) the angles between this bond and the ring bonds backwards and forwards
   c) whether the atom is axial or equatorial.
   Values for these parameters were obtained from Arnott and Scott (1972).

(ii) orientation of the molecule with respect to defined axes:
   a) O(1) is set as the origin
   b) C(1) is set to lie on the -x semi-axis, and
   c) C(g) lies in the quarter plane formed by the -x, +y semi-axes.

X	Y	Z	NAME
-1.3890	0.0	0.0	C1
-1.8697	0.6651	1.2830	C2
-3.3826	0.8208	1.2686	C3
-3.8283	1.5360	0.0	C4
-3.2446	0.8433	-1.2268	C5
-3.5578	1.5746	-2.5150	C6
0.0	0.0	0.0	O1
-1.4521	-0.1112	2.4006	O2
-3.7987	1.5671	2.4136	O3
-5.2504	1.5236	-0.1042	O4
-1.8140	0.7751	-1.1228	O5
-4.7755	1.7197	-2.7574	=O1
-2.5588	1.9398	-3.1715	=O2
-1.8140	-1.0121	-0.0704	H1
-1.3997	1.6548	1.3818	H2
-3.8543	-0.1718	1.3155	H3
-3.4869	2.5813	0.0286	H4
-3.6560	-0.1739	-1.3047	H5

β-D-glucuronic acid linked 1 → 4.

X	Y	Z	NAME
-1.4150	0.0	0.0	C1
-1.8958	1.4451	0.0	C2
-1.4908	2.1407	1.2906	C3
-1.9654	1.3413	2.4969	C4
-1.5002	-0.1066	2.3850	C5
-2.0639	-0.9877	3.4795	C6
0.0	0.0	0.0	O1
-3.3088	1.4707	-0.1659	O2
-2.0589	3.4513	1.3274	O3
-1.4384	1.8968	3.6999	O4
-1.9355	-0.6635	1.1350	O5
-3.4898	-1.0303	3.4439	O6
-1.7658	-0.5037	-0.9128	H1
-1.4580	1.9777	-0.8572	H2
-0.3960	2.2422	1.3250	H3
-3.0639	1.3712	2.5480	H4
-0.4023	-0.1449	2.4415	H5

α-D-mannose linked 1 → 2

Table 4.2 Arnott and Scott coordinates for the variously linked residues used in model-building studies.

C. RESULTS AND DISCUSSION

1. Xanthomonas phaseoli polysaccharide

It has already been indicated that the exact chemical structure of the polysaccharides from X. campestris and X. phaseoli is incompletely characterised. As a consequence, while the Xray diffraction patterns are of good quality, fitting computer built models to the patterns can only be considered tentative based on the assumptions:

(i) X. phaseoli has a similar backbone structure to X. campestris, although variations in side groups may exist. To some extent this is confirmed by the similarity of the Xray patterns - see below.

(ii) The repeating unit has a tetrasaccharide backbone i.e.

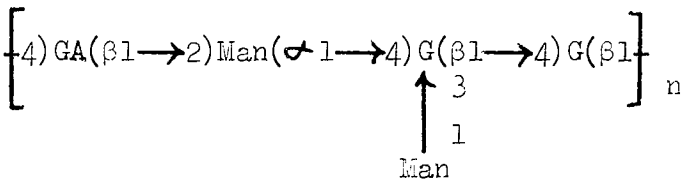

-1.

(iii) an alternative interpretation based on recent evidence (Kenne et al, unpublished) contains the same sugars as in (ii) but arranged with a cellulose-like backbone i.e.

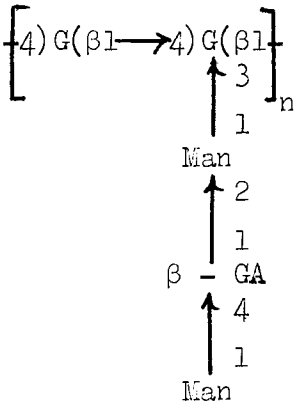

-2.

Possible models derived from the repeating structures above that correlate with the parameters derived from the diffraction pattern, have been investigated.

Diffraction Patterns of X. phaseoli and X. campestris

Xray diffraction patterns were obtained for the polysaccharide from both of these Xanthomonas species. That from X. campestris was of poorer quality than that from X. phaseoli but both showed similar characteristics. In particular, the axial periodicity and spacing of the equatorial Bragg reflection were identical. It is believed that the basic interpretations based on the analysis of the better diffraction pattern from X. phaseoli will be equally applicable to X. campestris, with the proviso that the assumptions above are valid. Typical diffraction patterns are shown in Fig. 4.7 a,b.

General characteristics of the diffraction pattern from X. phaseoli

Fibres stretched at 50-60% relative humidity gave diffraction patterns (Fig. 4.7a) having the features:

(i) meridional reflections occur when $\ell = 5n$, consistent with a five-fold helical repeating structure having an axial periodicity (fibre repeat) of 4.75 ± 0.05 nm

(ii) layer lines $\ell = 1 \rightarrow 7$ are apparent, with spacings of 0.95 ± 0.02 nm.

(iii) off the meridian, the diffraction pattern is essentially a continuous intensity distribution which could be a molecular transform on each layer line. Thus intensity maxima, for example on the first, second and fourth layer lines are not sharp Bragg reflections but parts of layer line streaks.

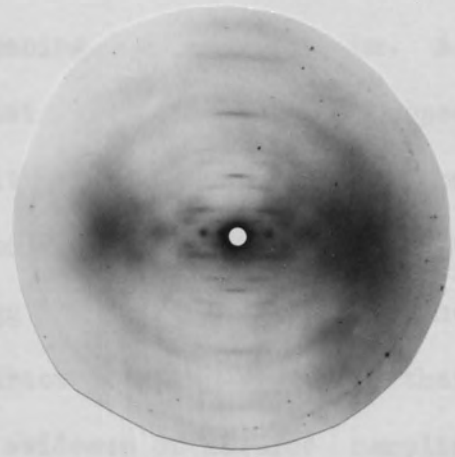

(a)

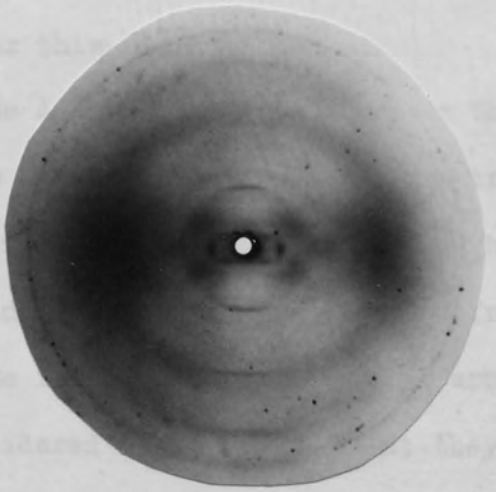

(b)

Fig. 4.7 (a) Xray diffraction pattern from X. phaseoli polysaccharide, and (b) that from X. campestris polysaccharide.

(iv) the only sharp Bragg reflection appears on the equator close to the centre of the pattern, at a spacing of 1.66 ± 0.05 nm. A possible second Bragg that is weak and diffuse appears at 0.86 ± 0.06 nm.

Although the pattern is predominantly the Arnott (1973) 'oriented' type, the possible presence of a second equatorial Bragg suggests that the specimen may have some crystalline character. It is possible that the higher layer lines also show some evidence of lattice sampling of the transform. The diffraction maxima are however, too broad to measure the spacings accurately since the crystalline character is not great enough for this.

The Arnott 'oriented' type is the least ordered situation, that gives rise to a continuous molecular transform everywhere except in that region of the equator where the Bessel function component provides single crystal-like diffraction, i.e. a Bragg reflection close to the centre of the pattern. The polymer chains are considered 'oriented' in that they have a common axial direction but are not crystalline and have no lateral order. In such a case the diffraction pattern would be characteristic of equally spaced, helical molecules packed 1.66 nm apart.

Without a comparison of observed and calculated intensity distributions for the various layer lines, it is impossible to say with certainty that the pattern is entirely 'oriented' and does not contain some low degree of crystallinity. Therefore, from a consideration of the density of the specimen and the possible presence of a second equatorial Bragg, tentative unit cells have been proposed.

Density

The density of fibres measured by flotation in chloroform/carbon tetrachloride showed some variation probably due to the difficulty in removing air bubbles from the sample. This was overcome to some extent by degassing the sample under vacuum.

The average density obtained was 1.5 ± 0.05 gm/cc.

Possible Unit Cells corresponding to the Bragg reflection at 1.66 nm

The layer line spacings together with the meridional reflections define the fibre axis repeat distance or c axis of the cell as 4.75 ± 0.05 nm.

The equatorial Bragg reflection at 1.66 nm could be consistent with:

(a) Hexagonal cell in which the Bragg corresponds to,

(i) the d_{100} or d_{010} spacing, with a = 1.92 nm

(ii) the d_{110} spacing, with a = 3.32 nm

(b) Tetragonal cell in which the Bragg corresponds to,

(i) the d_{100} and d_{010} spacing, with a = 1.66 nm

(ii) the d_{110} spacing, with a = 2.35 nm.

These are the simplest cases, an orthorhombic cell having one of its base parameters defined by 1.66 nm is another possibility but has not been considered further (more assumptions are required to define the second cell base parameter).

For the hexagonal system, the interplane spacing on the equator is given by:

$$d_{hko} = \frac{a\sqrt{3}}{2(h^2 + hk + k^2)^{\frac{1}{2}}} \qquad -3.$$

and for a tetragonal system

$$d_{hko} = \frac{a}{(h^2 + k^2)^{\frac{1}{2}}} \qquad -4.$$

where h, k are the indices of the reflection, and a, c are the cell sides.

The calculated d spacings for the various cells are shown in Table 4.3 and the number of chains passing through each consistent with the density are shown in Table 4.4.

On the basis that there is no evidence at the present for a unit cell containing several chains in some way related to each other, the larger hexagonal and tetragonal cells are rejected.

At this stage it is impossible to distinguish between the hexagonal cell (a = 1.92 nm) and the tetragonal cell (a = 1.66 nm) containing three and two chains per cell respectively (Fig. 4.8). Some support for them comes from the possible second Bragg reflection which is in close agreement with the expected reflection spacing. Since helices often pack hexagonally unless side chains have some influence (not known here) perhaps a relationship exists between trimerised sets of chains. Alternatively, for the tetragonal cell, the two chains could be antiparallel, packed randomly and hence giving rise to additional streaking on the diffraction pattern and disorder.

More detailed interpretation must await the comparison of the observed intensity distribution and that calculated from the cylindrically averaged molecular transform for the proposed helical structure.

Cell Type	Side, a nm	Reflection	Spacing . nm Calculated	Observed
a) Hexagonal	1.92	100,010	1.66	1.66*
		110	0.83	0.86?
		200,020	0.72	a
		210,120	0.42	a
	3.32	100,010	3.32	a
		110	1.66	1.66*
		200,020	1.44	a
		210,120	1.09	a
		220	0.83	0.86?
b) Tetragonal	1.66	100,010	1.66	1.66*
		110	1.17	a
		200,020	0.83	0.86?
		210,120	0.74	a
	2.35	100,010	2.35	a
		110	1.66	1.66*
		200,020	1.18	a
		210,120	1.05	a
		220	0.81	0.86?

* Cell side (a) calculated from this reflection.

Table 4.3 Calculated d spacing for various cells

Cell dimensions & Type	No of chains/cell* assuming density = 1.5 grm/cc		
	Water Content		
	0	10%	20%
a) Hexagonal			
$\underline{a}$ = 1.92 nm, $\underline{c}$ = 47.5 nm	3.6	3.3	3.0
$\underline{a}$ = 3.32 nm, $\underline{c}$ = 47.5 nm	10.7	9.7	8.9
b) Tetragonal			
$\underline{a}$ = 1.66, $\underline{c}$ = 47.5 nm	2.7	2.4	2.2
$\underline{a}$ = 2.35, $\underline{c}$ = 47.5 nm	5.4	4.9	4.5
	886	975	1063
	Repeat Unit Weight+		

* Number of chains/cell = $\frac{dvn}{nM}$ (See Chapter 2. p)

where n = Number of repeating units/fibre repeat = 5

+ Repeat assumed to contain: K^+ glucuronate, mannose, glucose O-acetyl in the ratio 1:2:2:1

Table 4.4 Possible number of five-fold helical chains passing through the various unit cell possibilities.

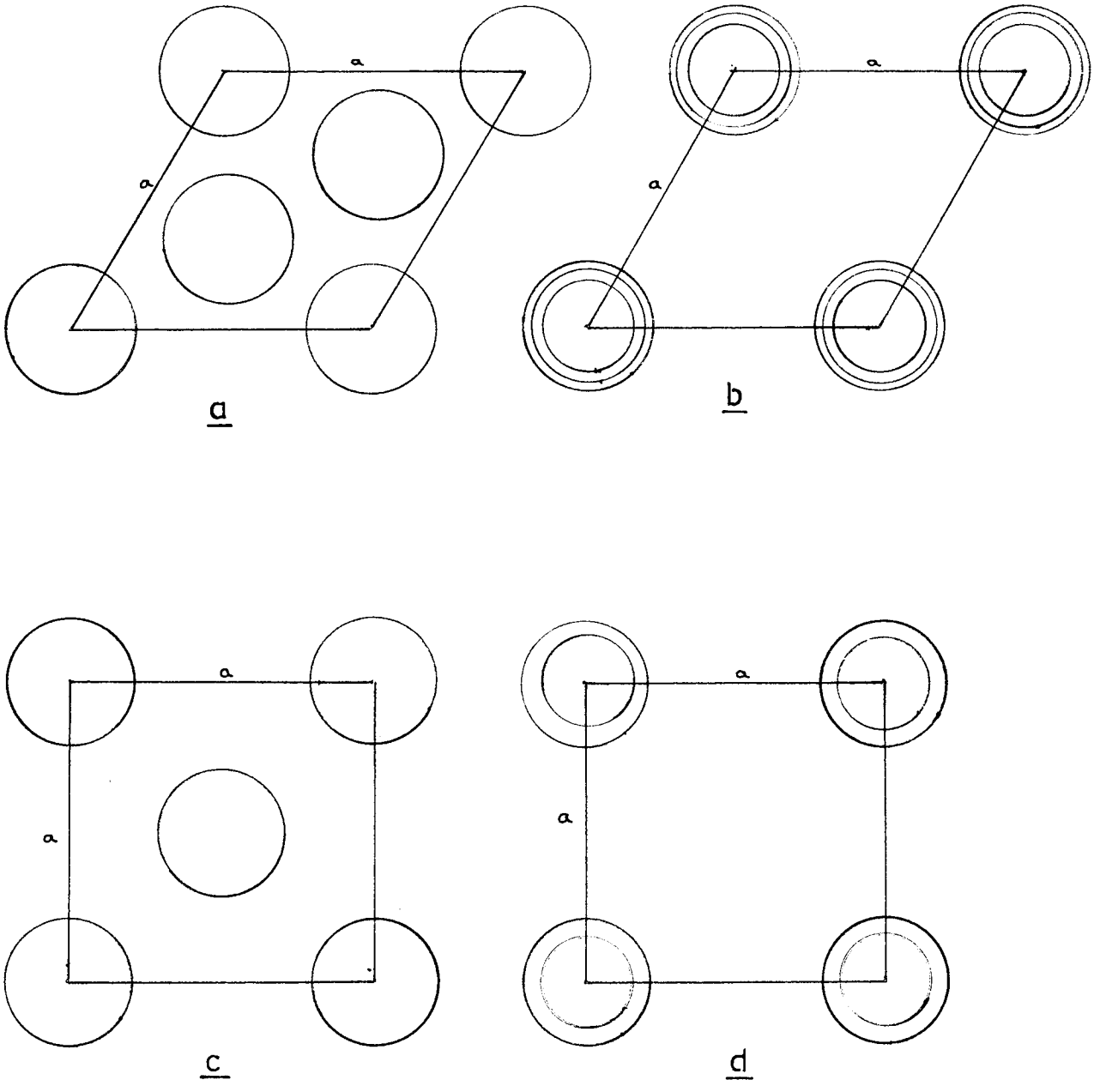

Fig. 4.8 Possible unit cell types

(a) Hexagonal a = 1.92 nm containing 3 single helices.
(b) Hexagonal a = 1.92 nm " 1 triple helix.
(c) Tetragonal a = 1.66 nm " 2 single helices.
(d) Tetragonal a = 1.66 nm " 1 double helix.

Geometrical parameters of the helix

If the diffraction pattern were as simple as that shown in Fig.4.9, which shows the optical transform of a helix with five points per turn, then measurement of the position of the

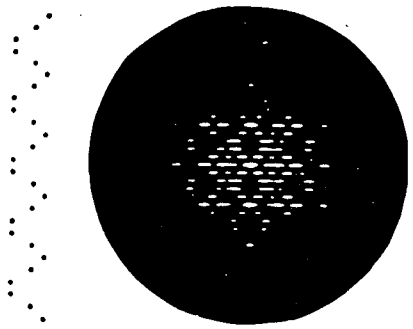

Fig. 4.9 Optical transform of a helix with 5 points per turn. (from Holmes and Blow, 1965)

first maximum of each Bessel function on each layer line would give the helix radius from,

$$r = \frac{J_n(x)}{2\pi \xi_{max}} \qquad -5.$$

where $J_n(x)$ = Bessel function maxima of the order n

ξ_{max} = reciprocal lattice coordinate of the particular intensity maximum.

For the diffraction pattern being considered here the intensity maxima cannot be treated accurately, consequently any radius calculated can only be a rough estimate. However, using the orders of Bessel function that should give maxima for the various layer lines (see later this section), the radius of the helix appears to vary between 0.5 and 1.0 nm. This compares with 0.55 nm calculated from the hexagonal cell and 0.41 nm or less for the tetragonal cell (Fig. 4.8).

There are several possible helical structures with a five-fold repeat.

(a) 5/1 (left or right handed) helices, that can have the form of:

(i) a single wide Type B (Rees, 1972) helix ($\underline{h}$ = 0.96 nm)

(ii) a multiple, antiparallel Type B helix, that is sinuous enough to accommodate two or more additional chains.

(b) 5/2 (left or right handed) helices can have the form:

(i) a single, less sinuous helix having $\underline{h}$ = 0.96 nm

(ii) a multiple, antiparallel helix.

Construction of an n-ℓ plot (Klug et al. 1958) can help to distinguish between the two sets of helical forms.

Helical symmetry imposes selection rules such that:

$$\ell = nt + um \qquad -6.$$

where,

ℓ = layer line number

n = an integer = Bessel function order

t = number of turns of helix in repeat distance

u = number of repeating units in $\underline{t}$ turns

m = positive or negative integer.

The selection rule (6) predicts:

(i) A meridional reflection when n=0, i.e. when ℓ = um;

thus for a five-fold helix (u=5) there will be meridionals on the 5th, 10th, 15th layer lines etc.

(ii) A strong layer line when $n=\pm 1$, i.e. when $\ell = um \pm t$.

The five-fold helices under consideration are governed by the selection rules shown below.

Helix Type	Helix Sense	Selection rule	u	t	turn/repeat
5/1	right	$n = \ell - 5m$	5	1	$+72^\circ$
	left				-72°
5/2	right	$n = \frac{\ell - 5m}{2}$	5	2	$+144^\circ$
	left				-144°

The integral values of n calculated from the selection rules above are shown in the corresponding $n-\ell$ plots in Fig. 4.10.

From Fig. 4.10a for the 5/1 helices it is expected that the second and third layer lines will involve relatively high orders (n) of Bessel function and hence no intensity is expected close to the meridian. The first and second layer lines involve lower order Bessel functions and will have intensity near to but not on the meridian for these layers.

A consideration of the diffraction pattern (Fig. 4.7a) shows that the intensity distribution does not fit, thus ruling out 5/1 helices.

Conversely for the 5/2 helices (Fig. 4.10b) the second and third layer line Bessel functions have low values. The expected strong intensity close to the meridian on the second

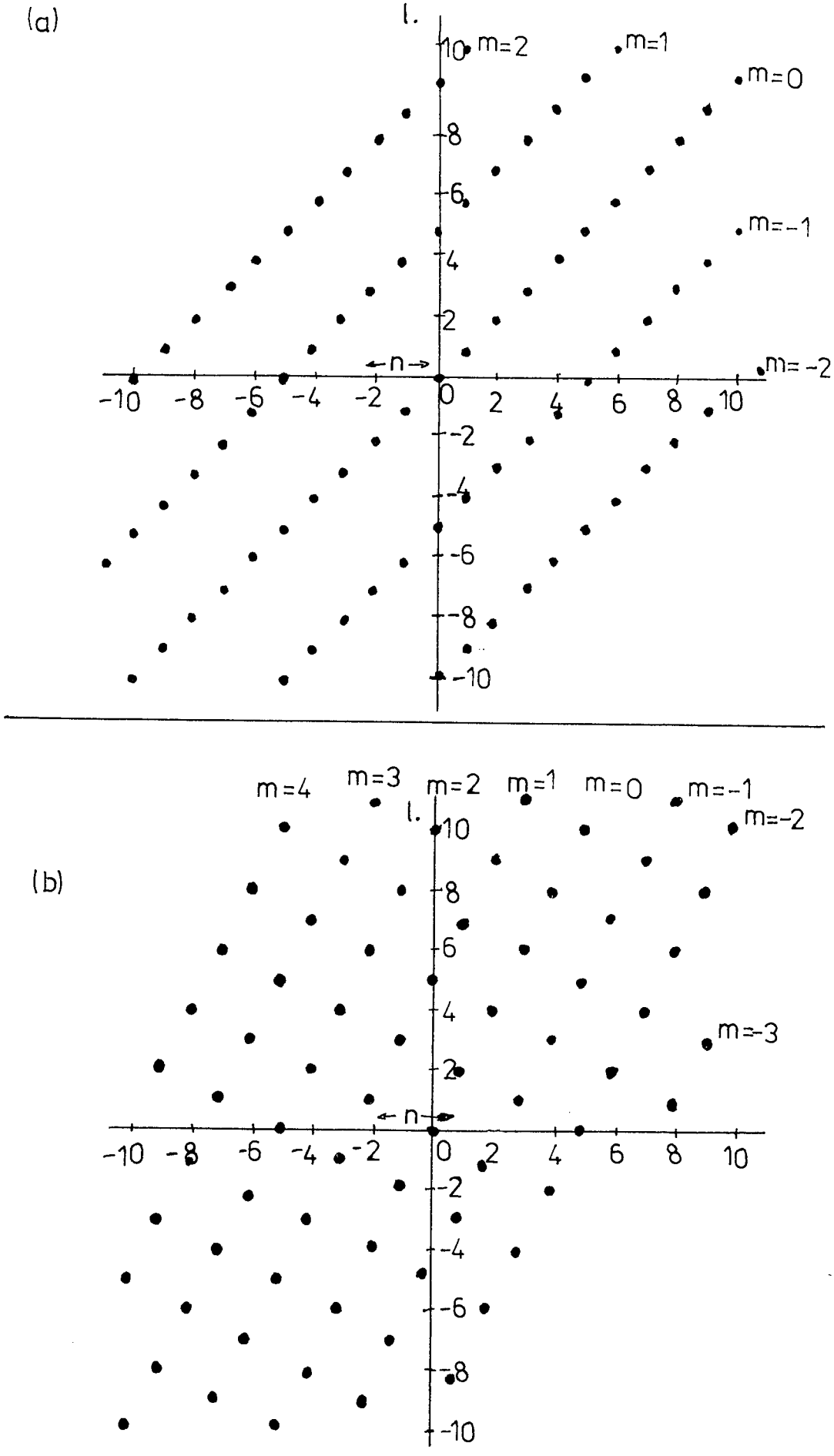

Fig. 4.10 n-ℓ plots for (a) 5/1 helices and (b) 5/2 helices.

layer line is apparent (Fig. 4.7a) but only a weak intensity appears on the third probably due to some accidental cancellation. The first and fourth layer line orders are somewhat higher and the corresponding intensities are away from the meridian as predicted.

Thus the diffraction pattern appears to be consistent with a 5/2 non-integral helix. On the basis of this conclusion various computer model-building studies were carried out.

Preliminary model building studies

Due to the recent uncertainty about the type of backbone repeat in Xanthomonas it has been necessary to consider several possible models.

(i) Structure 1A

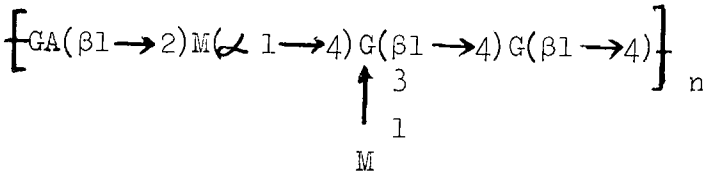

(ii) Structure 1B

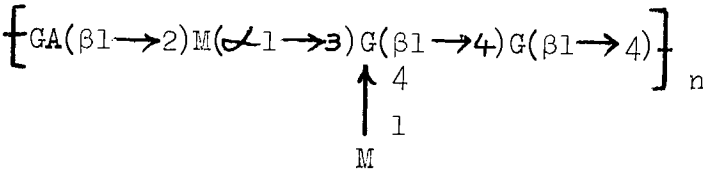

(iii) Structure 2A

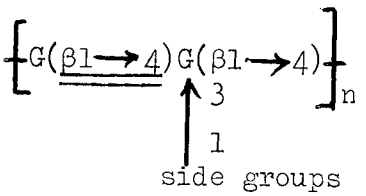

(iv) Structure 2B

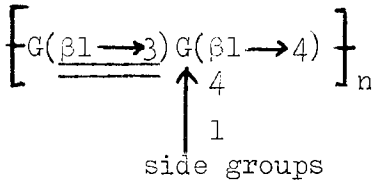

Structures 1A, 1B due to Melton et al. (1974)

Structures 2A, 2B due to Kenne et al. (unpublished).

Several observations can be made at the outset:

(i) The density measurement does not differentiate between single or multiple helical structures.

(ii) Structures 2A and 2B are almost fully extended (0.95 nm / disaccharide) therefore would be unlikely to be double or triple helices.

(iii) Spacefilling models of Structure 1A indicate that a left-handed helix would be necessary to accommodate a single unit side chain, which can only be on the outside of the helix to avoid steric clashes.

From the Xray data the screw symmetry is 2.5 (number of residues/turn of helix) and the projected residue height is 0.95 nm. The torsion angles were therefore varied within ranges that were shown to be possible by the relevant hard sphere linkage maps. In this preliminary study it was not necessary to include side chains in the calculations, nor to distinguish multiple helical structures separately. For all models the torsion angles were numbered 1—— 8 as shown below

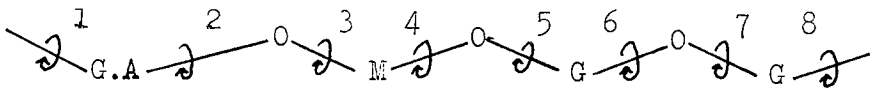

and explored in the ranges shown in Table 4.5. If possible the

Angle Number	Hard sphere map linkage		Range lower	upper
1	G	GA	130	200
2	GA	M	140	250
3	GA	M	200	280
4	M	G	170	280
5	M	G	140	240*
6	G	G	150	250
7	G	G	140	210
7a	G	G	190	270
8	G	GA	150	260

* spacefilling models suggested a model with an angle in this region might be possible although the hard sphere map (Fig. 4.11) disallowed linkages in this region.

Table 4.5

Ranges of Torsion angles used

cellobiose conformation angles were maintained near $\Delta\phi = 42^{\circ}$ and $\Delta\psi = -18^{\circ}$ (Chu and Jeffrey, 1968; Ham and Williams, 1970).

Structure 1A

Initial experiments using angles derived from a consideration of a space-filling model of the repeating unit showed that any possible models would be close to the edge of some of the allowed regions on the hard sphere maps. Applying the minimisation search procedure it was possible to obtain models with the required n and h using different starting angle sets. These models were broadly similar in their chain contour but, not surprisingly since there is no unique solution to this problem, they differed in detail depending on the starting point that was used. The torsion angles derived for two typical models are shown below.

Angle number (see above)	Model 1	Model 2
1	140°	133°
2	159°	145°
3	281°	280°
4	283°	260°
5	231°	151°
6	*230°	156°
7	*166°	206°
8	235°	255°

* these are close to the cellobiose angles of 222° and 162°.

Table 4.6

It is interesting to note that when the torsion angles for the cellobiose-like part of the repeat are close to those of crystalline cellobiose (Model 1 above) then the remaining

torsion angles tend to be in or close to the allowed regions of the respective hard sphere maps (Fig. 4.11). Those for Model 2 are more disallowed.

Although some of the torsion angles do lie outside allowed regions they are within the range $\Delta\phi = \pm 60^{\circ}$ and $\Delta\psi = \pm 60^{\circ}$ and therefore close to the bounds of steric possibility (Rees and Scott, 1971).

A typical plot of one model having near cellobiose angles is shown in Fig. 4.12 from which it can be seen that a side group on $O(3)^{c}$ (glucose residue c) points away from the centre of the chain.

Structures 1B, 2A, 2B

Preliminary calculations suggest that models having sets of torsion angles close to the allowed regions are possible for all these structures. The approximate torsion angles of possible models are shown in Table 4.7 and marked on their respective hard sphere maps (Fig. 4.11).

Additionally for Structure 2A (the cellobiose backbone) the possible models are marked on a potential energy map for β1,4-D-glucose dimers (Fig. 4.13) (Smith, 1972). Although the models are not at the energy minimum their relative closeness tends to show that models having the particular linkage conformations (Table 4.7) are not unreasonable. Some deviation from the cellobiose norm is expected due to the proposed models having $n = 2.5, h = 0.95$ nm compared with, say, the 'bent' chain of cellulose which has $n = 2$, $h = 1.03$ nm (for dimer), which will probably also remove the stabilising hydrogen bond present in cellulose.

Conclusions

This preliminary survey shows that models can be

Angle number	Structure 1B	Structure* 2A		Structure* 2B	
1	162°	210	210	160	180
2	150°	250	250	190	220
3	262°	200	210	210	240
4	278°	250	250	120	150
5	289°				
6	209°				
7	243°				
8	256°				

* angle numbering is

Structure 2A

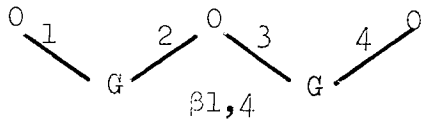

Structure 2B

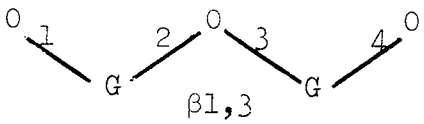

Table 4.7

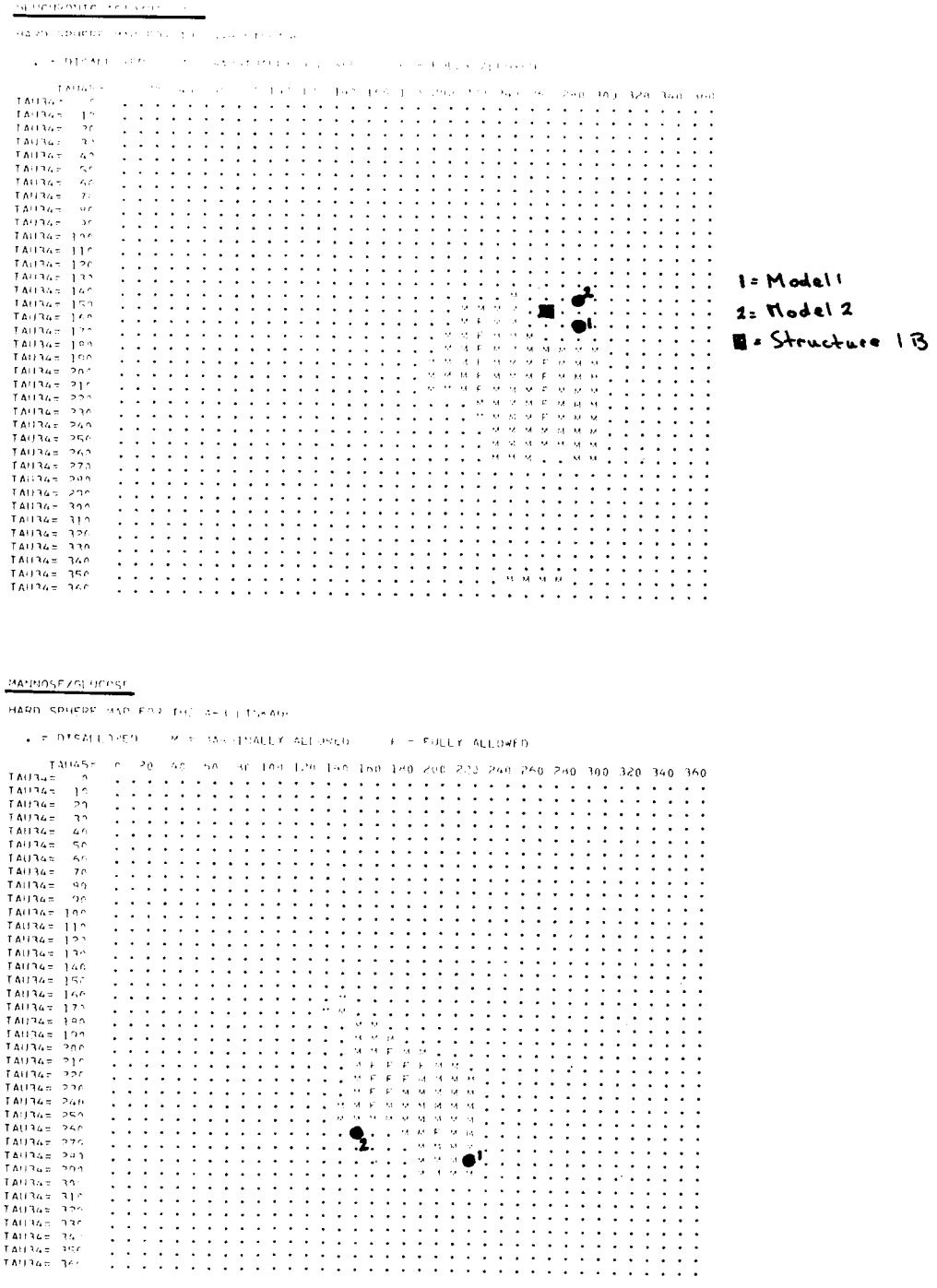

Fig. 4.11 Hard sphere maps for the various inter-residue linkages of X.phaseoli polysaccharide detailed in text. The positions corresponding to proposed

GLUCOSE/GLUCURONIC ACID

HARD SPHERE MAP FOR THE A-B LINKAGE

. = DISALLOWED M = MARGINALLY ALLOWED F = FULLY ALLOWED

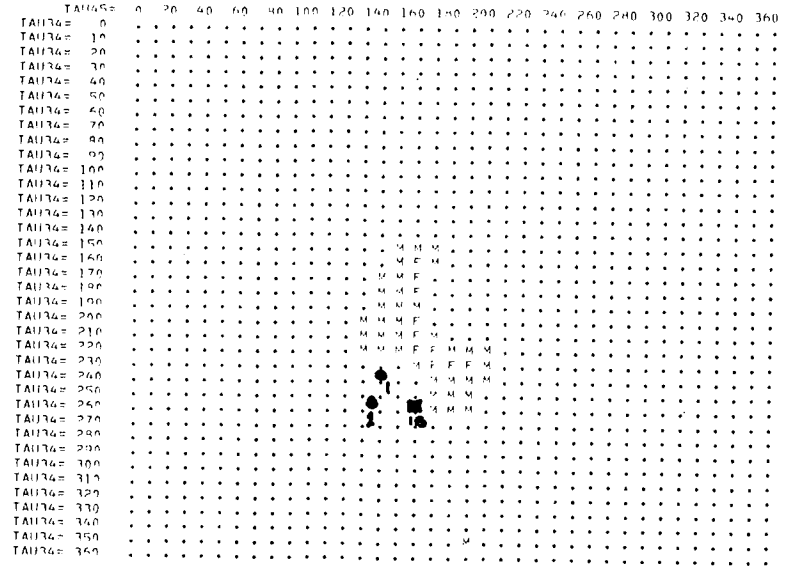

■ Structure 1B

GLUCOS/GLUCOSE

HARD SPHERE MAP FOR THE B-A LINKAGE

. = DISALLOWED M = MARGINALLY ALLOWED F = FULLY ALLOWED

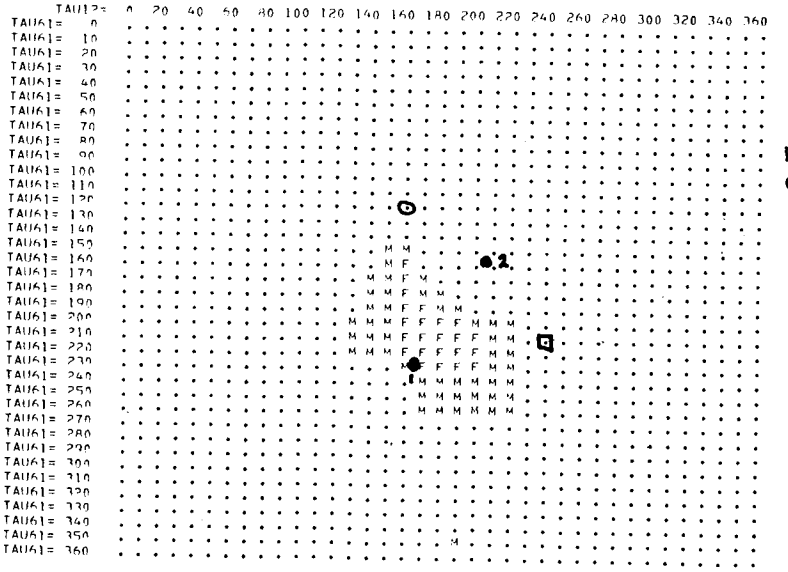

□ Structure 2A

○ Structure 2B

Fig. 4.11 cont'd.

MANNOSE A1-2--1,3 Glucose

HARD SPHERE MAP FOR THE [illegible]

. = DISALLOWED M = MARGINALLY ALLOWED F = FULLY ALLOWED

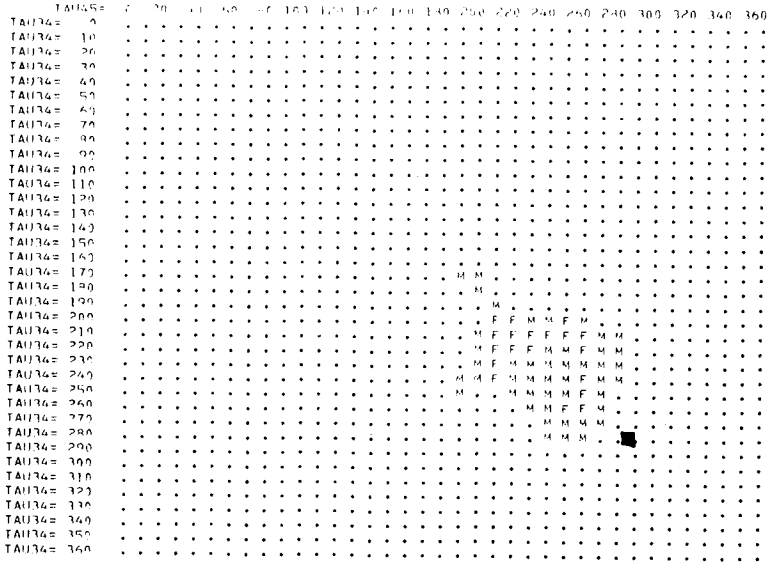

■ Structure 1B

BETA 1,4/1,3 GLUCOSE

HARD SPHERE MAP FOR THE A-B LINKAGE

. = DISALLOWED M = MARGINALLY ALLOWED F = FULLY ALLOWED

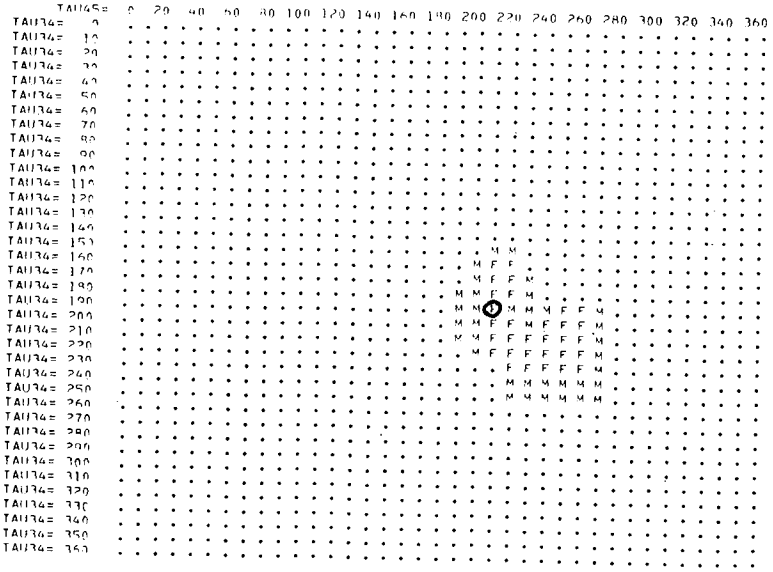

O Structure 2B

Fig. 4.11 cont'd

Fig. 4.12 Coordinate plot of typical 5_3 helix for X. phaseoli polysaccharide.

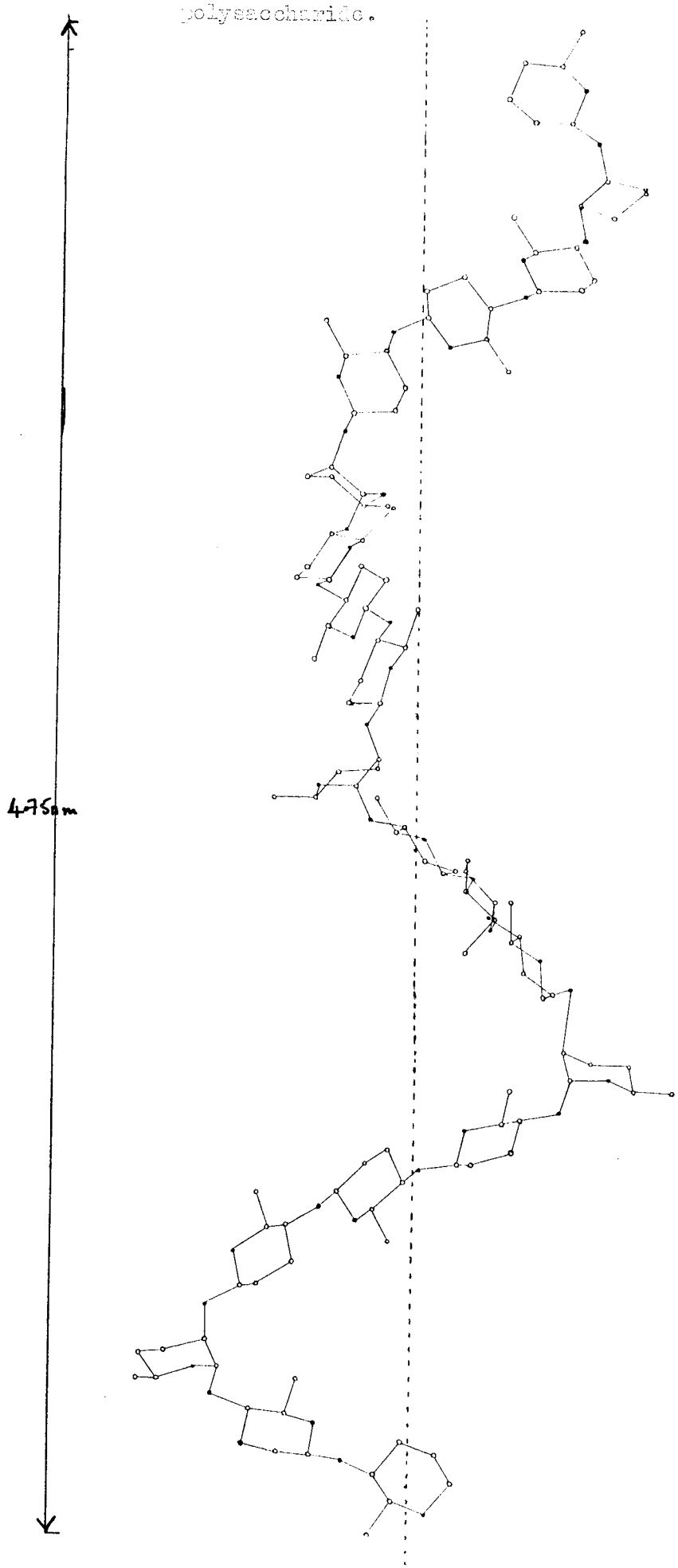

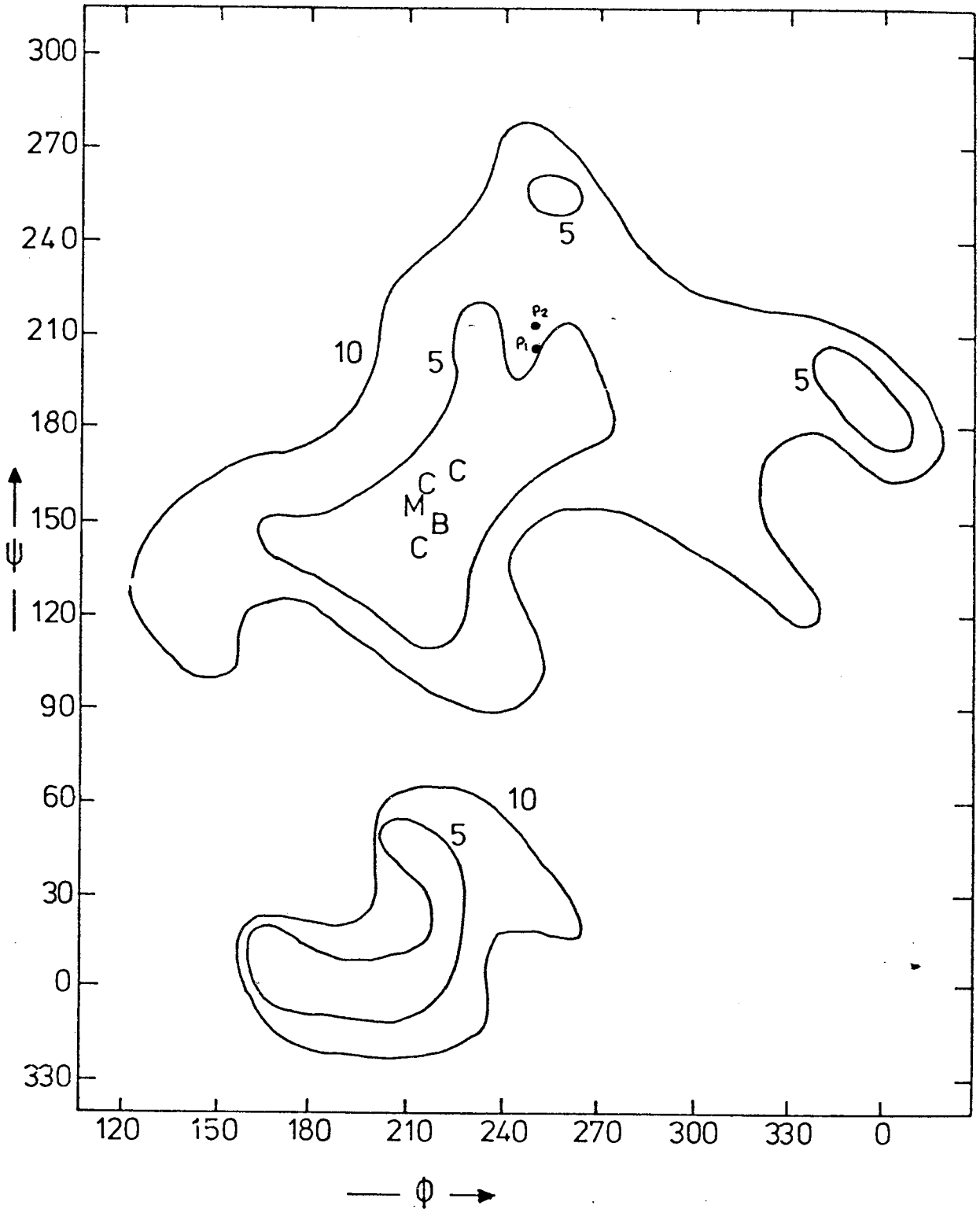

Fig. 4.13 Potential energy map for cellobiose. Contours are 5 and 10 kcal/mole above the minimum

M - the minimum, C - crystal structures,
B - bent chain conformation of cellulose (n=2, h=0.515 nm)
P_1/P_2 - Structure 2A models.

proposed that are in agreement with the Xray data and that the computed linkage angles are within or close to 'allowed' regions (no steric compression) on the relevant hard sphere maps.

From a consideration of possible chain packing arrangements (Fig. 4.8) the tetragonal single chain arrangement is the most likely although the hexagonal triple and tetragonal double would be attractive if multiple helices were sterically possible. This is based on:

(i) Special relationships between chains other than multiple helices or up and down pointing chains are hard to imagine.

(ii) Multiple helices are impossible for the most likely 'cellobiose-like' covalent structure.

(iii) Therefore the tetragonal single chain arrangement is favoured by elimination (Fig. 4.8c).

Further work will depend on the rigorous characterisation of the covalent structure. If, as now seems likely, the polysaccharide is indeed a modified cellobiose chain (Structure 2A) it is interesting that the conformation requires that alternate glucose units be sterochemically non-equivalent, which in turn suggest that the side chains occur regularly on alternate residues.

2. Arthrobacter viscosus B1973

Diffraction Pattern - Preliminary interpretation

Fibres of a 1% solution in deionised water were drawn as already described. The highest quality diffraction patterns were obtained when the fibres were allowed to dry at > 90% relative humidity (saturated K_2SO_4).

General characteristics of diffraction pattern

A typical diffraction pattern is shown in Fig. 4.14.

(i) meridional reflections occur on the 3rd, 6th, 9th, 12th layer lines (i.e. when $l = 3n$), consistent with a three-fold helical repeating structure having an axial periodicity of 4.2 ± 0.05 nm.

(ii) weakly defined layer lines can be seen having spacing 1.4 ± 0.02 nm.

(iii) off the meridian, the diffraction pattern in a continuous intensity distribution (cf. the pattern from Xanthomonas).

(iv) the only Bragg reflection appears on the equator close to the centre of the pattern with a spacing of 1.10 ± 0.05 nm.

The diffraction pattern can be classified as an "oriented type" (Arnott, 1973).

Geometrical characteristics of helix

From the layer line spacing it is apparent that the trisaccharide repeating unit is almost fully extended. The maximum extension for three β1,4 linked sugars is 1.62 nm (for glucose), the presence of 4-linked α- or β-D-galactose alters this to:

α-D-Galactose - 1.53 nm

β-D-Galactose - 1.53 nm

Consequently it is unlikely that a second chain could intertwine to form a double helix.

Three-fold helices are governed by the selection rule

$$n = l - 3m$$

Both right-handed 3_1 and left-handed 3_2 helices are theoretically possible. Without good sterochemical packing evidence it will be impossible to distinguish between these possibilities. The n-ℓ plot corresponding to the selection rule (7) is shown in Fig. 4.15.

From the n-ℓ plot it is expected that the diffraction pattern will have intensities close to the meridian on layer lines 1, 4 and 7 where the Bessel functions have low values. Close examination of the diffraction patterns reveal intensity streaks close to the meridian on layer lines 1 and 4 as predicted from the n-ℓ plot so confirming the interpretation.

Preliminary model building studies

Since the anomeric configuration of the galactose residue has not been defined models were built in the computer using both configurations. A possible right-handed model for both D-galactose configuration was readily obtained having the required n=3.0, h=1.40nm it is equally probable that left-handed models could be produced (Table 4.8).

Angle number*	Model 1 α-Galactose configuration	Model 2 β-Galactose configuration
1	228	153
2	170	158
3	230	201
4	200	185
5	190	143
6	211	184

* angles are numbered:

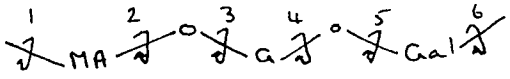

Table 4.8

Fig. 4.14

Diffraction pattern from

A. viscosus polysaccharide

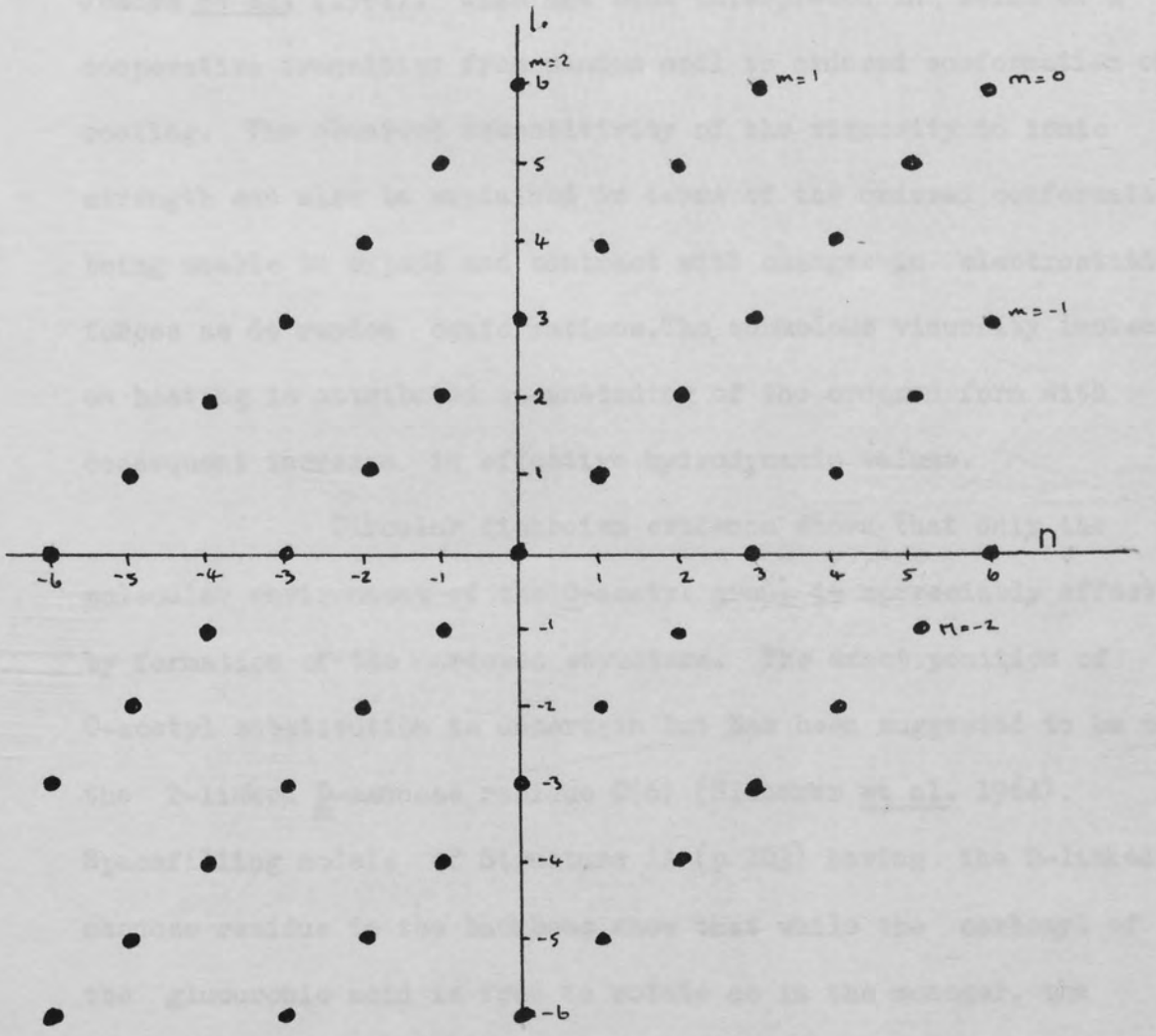

Fig. 4.15 n-ℓ plot for 3_1 helix corresponding to A. viscosus pattern above.

The positions of these angles are shown on the respective hard sphere maps in Fig. 4.16.

Most likely models are ribbon-like. Again, it would be wise to obtain definitive structural information about the covalent structure before attempting further refinement.

3. General Discussion

The change of optical rotation of X.campestris polysaccharide with temperature has been followed (Morris and Rees, unpublished) and shows a sigmoidal transition which is exactly coincident with the anomolous viscosity increase reported by Jeanes et al. (1961). This has been interpreted in terms of a cooperative transition from random coil to ordered conformation on cooling. The observed insensitivity of the viscosity to ionic strength can also be explained in terms of the ordered conformation being unable to expand and contract with changes in electrostatic forces as do random conformations.The anomolous viscosity increase on heating is attributed to unwinding of the ordered form with consequent increase in effective hydrodynamic volume.

Circular dichroism evidence shows that only the molecular environment of the O-acetyl group is appreciably affected by formation of the ordered structure. The exact position of O-acetyl substitution is uncertain but has been suggested to be on the 2-linked D-mannose residue C(6) (Sloneker et al. 1964). Spacefilling models of Structure 1A (p 203) having the 2-linked mannose residue in the backbone show that while the carboxyl of the glucuronic acid is free to rotate as in the monomer, the O-acetyl is more sterically restricted and may possibly hydrogen bond with O(6) of the adjacent 4-linked glucose residue. Models based on the Lindberg structures 2A/ 2B are less restrictive for an

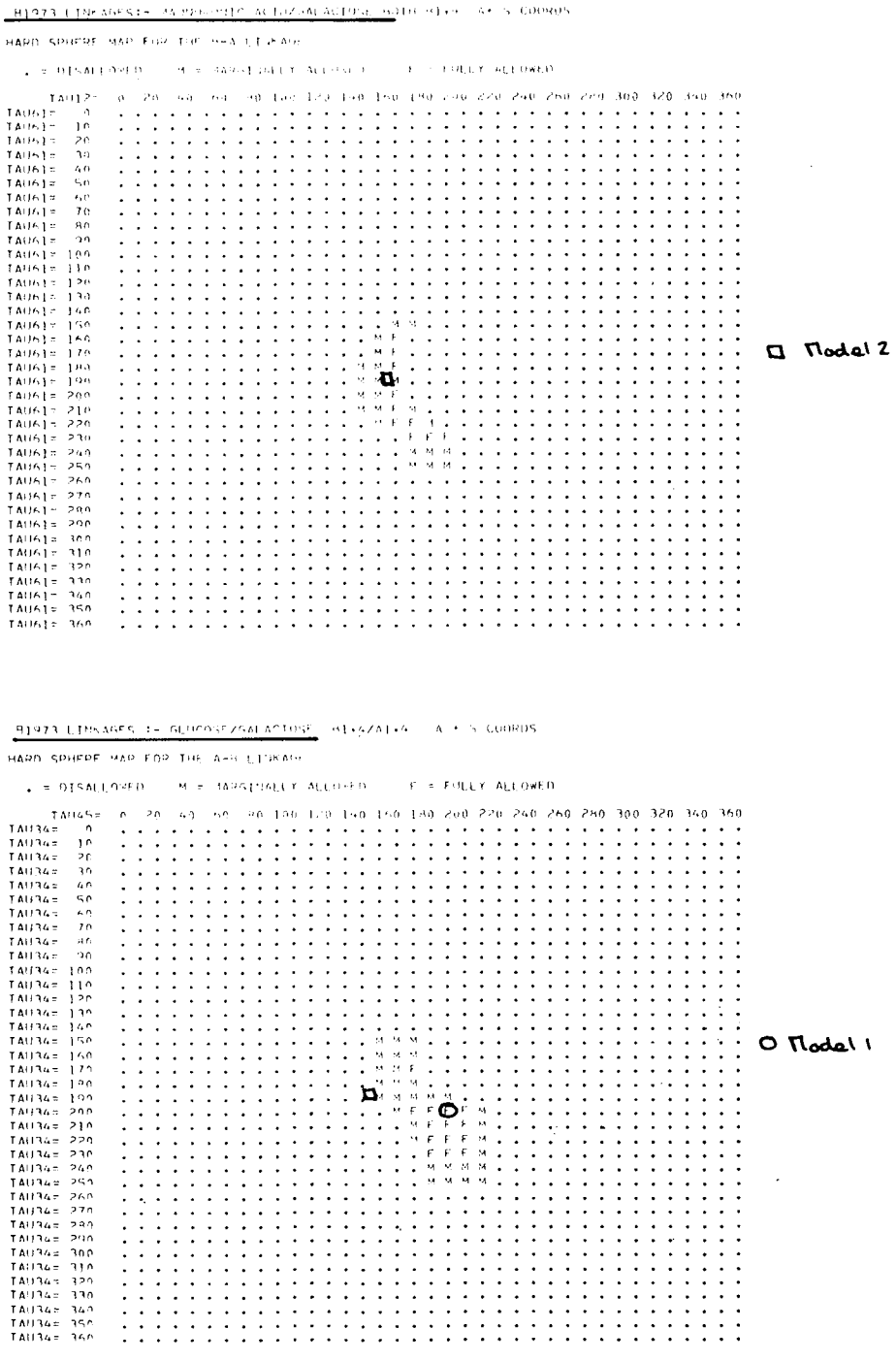

Fig. 4.16 Hard sphere maps for various inter-residue linkages detailed in text for A.viscosus polysaccharide. The positions corresponding to possible models are marked.

B1973 LINKAGES:- MANNURONIC ACID/GLUCOSE -- BOTH B1→4 A + S COORDS

HARD SPHERE MAP FOR THE A-B LINKAGE

. = DISALLOWED M = MARGINALLY ALLOWED F = FULLY ALLOWED

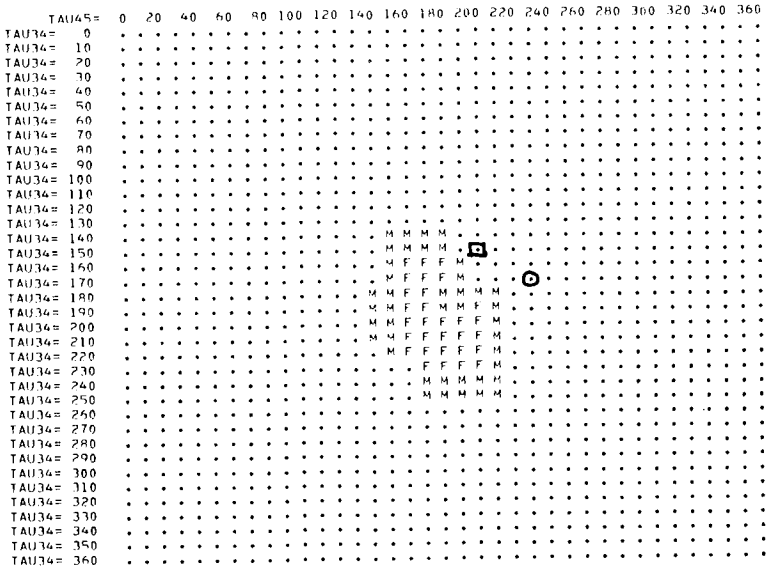

O Model 1

□ Model 2

B1973 LINKAGES:- MANNURONIC ACID/GALACTOSE B1→4--A1→4 A + S COORDS

HARD SPHERE MAP FOR THE B-A LINKAGE

. = DISALLOWED M = MARGINALLY ALLOWED F = FULLY ALLOWED

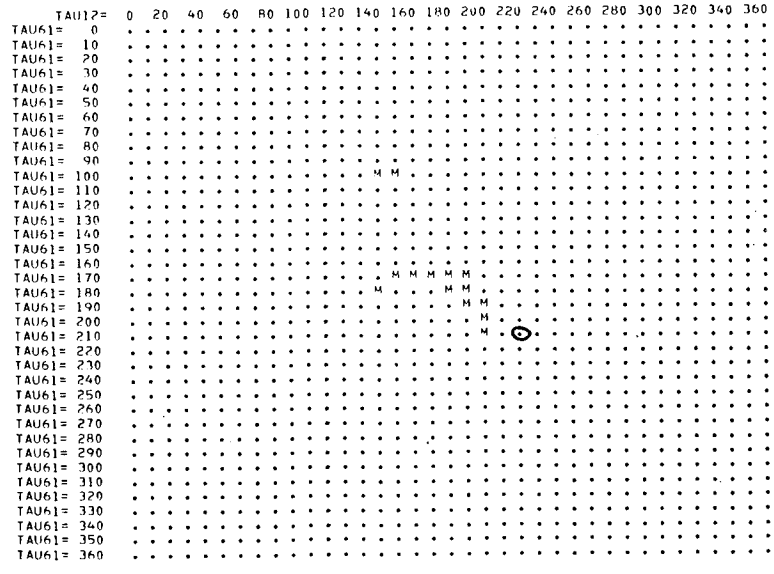

O-acetyl on C(6) so, at the present stage it is difficult to envisage how such structures could 'lock-in' this residue.

X.campestris polysaccharide and some galactomannans (e.g. locust bean gum, guar gum) gel or exhibit increased viscosity when mixed i.e. show synergistic cooperative associations. The characteristics shown are similar to the binding of galactomannans to agarose and carrageenan helices (Dea et al. 1972), such as the need for an ordered rather than disordered form of Xanthomonas polysaccharide.

Binding occurs by the formation of mixed aggregates of Xanthomonas polysaccharide helices and mannan ribbons. It is possible that this mechanism is mimicking the biological function of these polysaccharides in which the bacterial cell attaches to plant cell surfaces that are identified by specific hemicellulose compositions in the plant vascular system. Since Xanthomonas species are plant pathogens such a process of recognition would be an important step in the invasion and colonisation of plant tissues (Morris and Rees, unpublished).

Such rather elaborate functions for the extracellular polysaccharides of bacteria would explain why it is that considerable regulatory and genetic mechanisms exist to produce complex polysaccharides. The need for such complex structures is not obvious other than as a means of protecting the bacterial cell physically (Sutherland, 1972).

It is interesting to note that the Lindberg structure having the cellobiose backbone repeat is similar to carboxymethyl cellulose CMC (chemically modified cellulose).

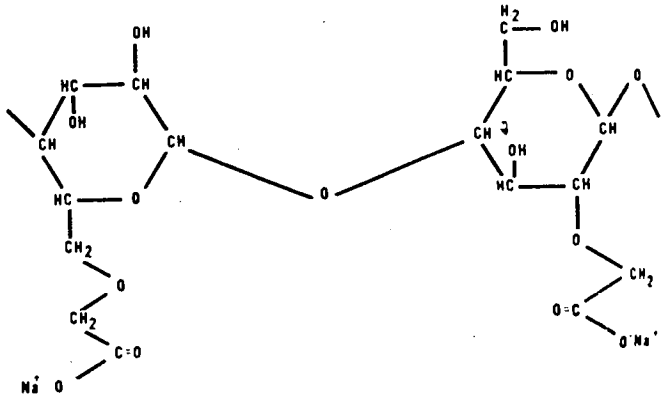

Although CMC does not contain a three unit long side branch it does have a terminal carboxyl group as does the Lindberg structure (pyruvic acid). Furthermore, the rheological properties are also similar i.e.

(i) Both show non-Newtonian viscosity in solution.

(ii) The viscosity varies with the rate of shear.

(iii) Both are pseudoplastic (Gauz, 1969).

(iv) The apparent viscosity decreases with increasing shear rate.

REFERENCES

Aklonis, J.J., MacKnight, W.J. and Shen, M. (1972). In Introduction to Polymer Viscoelasticity, p. 170, Wiley-Interscience, New York.

Alexander, L.E. (1969). Xray Diffraction Methods in Polymer Science, New York, Wiley-Interscience.

Anderson, N.S., Campbell, J.W., Harding, M.M., Rees, D.A. and Samuel, J.W.B. (1969). J. Mol. Biol., 45, 85.

Araki, C. and Arai, K. (1967). Bull. Chem. Soc. Japan, 40, 1452.

Arnott, S. (1970). Progr. Biophys. Mol. Biol., 6, 267.

Arnott, S. (1973). Trans. Amer. Crystallog. Assoc., 9, 31.

Arnott, S. and Wonacott, A. (1966). Polymer, 7, 157.

Arnott, S. and Scott, W.E. (1972). J. Chem. Soc. Perkin II, 324.

Arnott, S., Guss, J.M. and Hukins, D.W.L. and Mathews, M.B. (1973). Biochem. Biophys. Res. Comm., 54, 1377.

Arnott, S., Scott, W.E., Rees, D.A. and McNab, C.G.A. (1974). J. Mol. Biol., in press.

Arnott, S., Hukins, D.W.L., Whistler, R.L. and Baker, C.W. (1974a). Carbohyd. Res., 35, 259.

Arnott, S., Fulmer, A., Scott, W.E., Dea, I.C.M., Moorhouse, R. and Rees, D.A. (1974c). J. Mol. Biol., in press.

Atkins, E.D.T., Parker, K.D. and Preston, R.D. (1969). Proc. Roy. Soc. B., 173, 209.

Atkins, E.D.T., Phelps, C.F. and Sheehan, J.K. (1972). Biochem. J., 128, 1255.

Atkins, E.D.T., Gaussen, R., Isaac, D.H., Nandanwar, V. and Sheehan, J.K. (1972b). J. Polymer. Sci. (Sect. B.), 10, 863.

Atkins, E.D.T. and Isaac, D.H. (1973). J. Mol. Biol., 80, 773.

Atkins, E.D.T. and Sheehan, J.K. (1973). Science, 179, 562.

Atkins, E.D.T., Isaac, D.H., Nieduszynski, I.A., Phelps, C.F. and Sheehan, J.K. (1974). Polymer, 15, 263.

Balazs, E.A. (1955). Acta XVII Concil. Ophthalmol. (New York 1954), II, 1019.

Balazs, E.A. (1958). Fed. Proc. 17, 1086.

Balazs, E.A. (1966). Fed. Proc., 25, 1817.

Balazs, E.A. (1974). Personal communication.

Balazs, E.A. and Jeanloz, R.W. (1965). The Amino Sugars, vol. II-A., Academic Press, New York.

Balazs, E.A., Watoson, D., Duff, I.F. and Roseman, S. (1967). Arthrit. Rheum., 10, 357.

Balazs, E.A. and Gibbs, D.A. (1970). In Balazs 1970a, p.1241.

Balazs, E.A. ed. (1970a). Chemistry and Molecular Biology of the Intercellular Matrix, Academic Press, New York.

Balazs, E.A. (1970b). In Balazs 1970a, p.401.

Balazs, E.A. and Chakrabarti, B. (1972). 3rd Europ. Symp. on Connective Tissue Res., Turku, Finland, Abs. p.32.

Becker, E.D. and Farrar, T.C. (1972). Science, 178, 361.

Benz, F.W., Feeney, J. and Roberts, G.C.K. (1972). J. May. Res., 8, 114.

Bettleheim, F.A. (1959). J. Phys. Chem., 63, 2069.

Bhavanandan, V.P. and Meyer, K. (1967). J. Biol. Chem., 242, 4352.

Bhavanandan, V.P. and Meyer, K. (1968). J. Biol. Chem., 243, 1052.

Blackwell, J. (1969). Biopolymers, 7, 281.

Blackwell, J., Sarko, A. and Marchessault, R.H. (1969). J. Mol. Biol., 42, 379.

Bloembergen, N., Purcell, E.M. and Pound, R.V. (1948). Phys. Rev., 73, 679.

Blumberg, B.S., Ogston, A.G., Lowther, D.A. and Rogers, H.J. (1958). Biochem. J., 70, 1.

Bovey, F.A., Tiers, G.V.D. and Filipovich, G. (1959). J. Polymer Sci., 38, 73.

Brant, D.A. and Dimpfl, W.F. (1970). Macromols., 3, 655.

Brewster, J.H. (1959). J. Amer. Chem. Soc., 81, 5483.

Brimacombe, J.S. and Webber, J.M. (1964). The Mucopolysaccharides, B.B.A. Library Vol. 6, Elsevier.

Brown, C.J. (1966). J. Chem. Soc. A, 927.

Bryce, T.A., McKinnon, A.A., Morris, E.R., Rees, D.A. and Thom, D. (1974). In press.

Bumb, R.R. and Zaslow, B. (1967). Carbohyd. Res., 4, 98.

Bunn, C.W. (1961). Chemical Crystallography, Oxford Univ. Press, London.

Carlström, D. (1962). Biochim. Biophys. Acta, 59, 361.

Casu, B., Reggiani, M., Gallo, G.G. and Vigevani, A. (1966). Tetrahedron, 22, 3061.

Casu, B. and Reggiani, M., Gallo, G.G. and Vigevani, A. (1968). Tetrahedron, 24, 803.

Chakrabarti, B. and Balazs. E.A. (1973) J. Mol. Biol., 78, 135.

Chu, S.S.C. and Jeffrey, G.A. (1968). Acta Cryst. B, 24, 830.

Cifonelli, J.A. and Mayeda, M. (1957). Biochim. Biophys. Acta, 24, 397.

Cleland, R.L. (1970). In Balazs 1970a, p.733.

Cochran, W., Crick, F.H.C. and Vand, V. (1952). Acta Cryst., 5, 581.

Cohen, J.S. (1969). In Experimental Methods in Molecular Biology, (Nicolau, C. ed.), New York, Wiley.

Crabbé, P. (1971). An Introduction to the Chiroptical Methods in Chemistry. (Mexico).

Dea, I.C.M., McKinnon, A.A. and Rees, D.A. (1972). J. Mol. Biol., 68, 153.

Dea, I.C.M., Moorhouse, R., Rees, D.A., Arnott, S., Guss, J.M. and Balazs, E.A. (1973). Science, 179, 560.

Diamond, R. (1966). Acta Cryst., 21, 253.

Dintzis, F.R. and Tobin, R. (1969). Biopolymers, 7, 581.

Engel, J. and Schwarz, G. (1970). Angew. Chem. Int. Ed., 9, 389.

Ernst, R.R. (1966). Advances in Magnetic Resonance, 2, 1. (Waugh, J.S. ed.) Academic Press.

Ernst, R.R. and Anderson, W.A. (1966). Rev. Sci. Instrum., 37, 93.

Fessler, J.H. (1960). Biochem. J., 76, 124.

Fessler, J.H. and Fessler, L.I. (1966). Proc. Nat. Acad. Sci., U.S.A., 56, 141.

Finer, E.G., Henry, R., Leslie, R.B.and Robertson, R.N. (1974). Biochim. Biophys. Acta, in press.

Flory, P.J. (1969). Statistical Mechanics of Chain Molecules. (John Wiley:New York).

Flory, P.J. (1972). In Polymerisation in Biological Systems, Ciba Foundation Symposium, 7, 109. Amsterdam, Elsevier.

Flowers, H.M. and Jeanloz, R.W. (1964). Biochemistry, 3, 123.

Floyd, J.D. and O'Connor, M.J. (1969). U.S. Pat. 3,484,229 (Dec. 16).

Fransson, L.A. (1970). In Balazs 1970a, p.823.

Fransson, L.A. and Roden, L. (1967). J. Biol. Chem., 242, 4161.

French, D. (1969). In Symposium on Foods: Carbohydrates and their Roles, (Schultz, H.W., ed.), 26. (Westport, Connecticutt: AVI Publishing Co.).

French, D., Pulley, A.O. and Whelan, W.J. (1963). Staerke, 15, 349.

French, A. and Zaslow, B. (1972). Chem. Commun., 41.

Fuller, W., Hutchison, F., Spencer, M. and Wilkins, M.H.F. (1967). J. Mol. Biol., 27, 507.

Ganz, A.J. (1969). Food Product Dev., 3, 65.

Gibbs, D.A., Merrill, E.W., Smith, K.A. and Balazs, E.A. (1968). Biopolymers, 6, 777.

Good, T.A. and Bessman, S.P. (1964). Anal. Biochem., 9, 253.

Gorin, P.A.J. and Spencer, J.F.T. (1961). Can. J. Chem., 39, 2282.

Gorin, P.A.J. and Spencer, J.F.T. (1963). Can. J. Chem., 41, 2357.

Gorin, P.A.J., Ishikawa, T., Spencer, J.F.T. and Sloneker, J.H. (1967). Can. J. Chem., 45, 2005.

Grant, G.T. (1973). Ph.D. Thesis, University of Edinburgh.

Grant, F.T., Morris, E.R., Rees, D.A., Smith, P.J.C. and Thom, D. (1973). Febs. Letts., 32, 195.

Greenfield, N. and Fasman, G.D. (1969). Biochemistry, 8, 4108.

Guss, J.M., Hukins, D.W.L., Smith, P.J.C., Winter, W.T., Arnott, S., Moorhouse, R. and Rees, D.A. (1974b). J. Mol. Biol., In press.

Ham, J.T. and Williams, D.G. (1970). Acta Cryst. B., 26, 1373.

Hamerman, D. (1970). In Balazs (1970a), p.1259.

Hardingham, T.E. and Muir, H. (1972). Biochim. Biophys.Acta, 279,401.

Harris, M.J., Herp, A. and Pigman, W. (1972). J.Amer.Chem.Soc.,94,7570.

Hascall, V.C. and Heinegard, D.K. (1974). J.Biol.Chem., 249, 4232.

Hermans, P.H. (1943). Kolloid. Z., 102, 169.

Hermans, P.H. (1949). In Colloid Science, (Kruyt, H.R. ed.), 2, 483 (Amsterdam: Elsevier).

Hirano, S. and Meyer, K. (1971). Biochem. Biophys. Res. Comm., 44, 1371.

Hirano, S. and Kondo, S. (1973). J. Biochem., 74, 861.

Holmes, K.C. and Blow, D.M. (1965). The use of Xray diffraction in the study of protein and nucleic acid structure. Interscience Reprint, Wiley, New York.

Hudson, C.S. (1909). J. Amer. Chem. Soc., 31, 66.

Hybl, A., Rundle, R.E. and Williams, D.E. (1965). J. Amer. Chem. Soc., 87, 2779.

Inoue, S. and Inoue, Y. (1966). Biochem. Biophys. Res. Comm., 23, 513.

Isaac, D.H. and Atkins, E.D.T. (1973). Nature New Biol., 244, 252.

Iverius, P.H. (1972). J. Biol. Chem., 247, 2606.

James, R.W. (1965). 'The Optical Principles of the Diffraction of Xrays', p.400, Cornell. University Press, Ithiaca.

Jaques, L.B., Kavanagh, L.W., Mazurek, M. and Perlin, A.S. (1966). Biochem. Biophys. Res. Comm., 24, 447.

Jeanes, A. (1968). In Encyclopedia of Polymer Science and Technology, Vol. 8, p.693, John Wiley.

Jeanes, A., Pittsley, J.E. and Senti, F.R. (1961). J. App. Polymer Sci., 5, 519.

Jeanes, A. and Sloneker, J.H. (1961). U.S. Pat. 3,000, 790 (Sept. 19).

Jeanes, A. and Pittsley, J.E. (1973). J. Appl. Polymer Sci., 17, 1621.

Jeanloz, R.W. (1956). Proc. 3rd. Intern. Congr. Biochem., Brussels, p.65, Academic Press, New York.

Jeanloz, R.W. and Jeanloz, D.A. (1964). Biochemistry, 3, 121.

Johnson, L.N. (1966). Acta Cryst., 21, 885.

Jones, R.J. and Colasito, D.J. (1963). Am. Soc. Microbiol., Abst., 63rd Ann. Meet., Cleveland, p.23, A.89.

Kauzmann, W., Clough, F.B. and Tobias, I. (1961). Tetrahedron, 13, 57.

Kelco Co., (1966). Chem. Eng. News 44, 71, 83, 89.

Kelco Co. (1972). Xanthan Gum/Kellrol/Kelzan/a natural biopolysaccharide for scientific water control. Kelco Co., San Diego, Calif.

Kirtley, M. and Koshland, D.E. (1967). J. Biol. Chem., 242, 4192.

Kotowycz, G. and Lemieux, R.U. (1973). Chem. Rev., 73, 669.

Langridge, R., Wilson, H.R., Hooper, C.W., Wilkins, M.H.F. and Hamilton, L.D. (1960). J. Mol. Biol., 2, 19.

Laurent, T.C. and Gergely, J. (1955). J. Biol. Chem., 212, 325.

Laurent, T.C. (1957a). Arkiv Kemi, 11, 487.

Laurent, T.C. (1957b). Physico-Chemical Studies on Hyaluronic Acid, Almqvist and Wiksell, Uppsala.

Laurent, T.C. (1957c). Arkiv Kemi, 11, 503.

Laurent, T.C., Ryan, M. and Pietruszkiewicz, A. (1960). Biochim. Biophys. Acta, 42, 476.

Laurent, T.C. (1966). Fed. Proc., 25, 1037.

Laurent, T.C. (1967). In The Chemical Physiology of Mucopolysaccharides, (Quintarelli, G., ed.) p.153, Little, Brown and Company Inc.

Laurent, T.C. (1970). In Balazs (1970a) p.703.

Lemieux, R.U. and Stevens, J.D. (1966). Can. J. Chem., 44, 249.

Lesley, S.M. and Hochster, R.M. (1959). Can. J. Biochem. Physiol., 37, 513.

Liang, C.Y. and Marchessault, R.H. (1959). J. Polymer Sci., 37, 385.

Lilley, V.G., Watson, H.A. and Leach, J.G. (1958). Appl. Microbiol, 6, 105.

McKinnon, A.A. (1973). Ph. D. Thesis, University of Edinburgh.

McKinnon, A.A., Rees, D.A. and Williamson, F.B. (1969). Chem. Commun., 701.

McNeeley, W.H. (1967). In Microbiol Technology, (Peppler, H.J. Ed.) p.381, Reinhold, New York.

McNeeley, W.H. and Kang, K.S. (1973). In Industrial Gums 2nd Edition (Whistler, R.L. and BeMiller, J.N. eds.) p.473. Academic Press, New York and London.

Mathews, M.B. and Cifonelli, J.A. (1965). J. Biol. Chem., 240, 4140.

Mathews, M.B. and Lozaityte, I. (1958). Arch. Biochem. Biophys., 74, 158.

Melton, L.D., Mindt, L., Rees, D.A. and Sanderson, G.R. (1974). To be published.

Messelson, M. and Stahl, F.W. (1958). Proc. Natl. Acad. Sci. U.S.A., 44, 679.

Meyer, K. (1958). Fed. Proc., 17, 1075.

Meyer, K. (1970). In Balazs 1970a, p.5.

Meyer, K. (1972). In The Enzymes, Vol. V, p.307. Boyer, P.D. ed.

Meyer, K., Davidson, E., Linker, A. and Hoffmann, P. (1956). Biochim. Biophys. Acta, 21, 506.

Meyer, K.H. and Misch, L. (1937). Helv. Chim. Acta, 20, 232.

Misaki, A., Kirkwood, S., Scaletti, J.V. and Smith, F. (1962). Can. J. Chem., 40, 2204.

Miyazawa, T. (1961). J. Polymer Sci., 55, 215.

Mizushima, S. and Shimanouchi, T. (1961). Advan. Enzymol., 23, 1.

Moffit, W., Woodward, R.B., Moscowitz, A., Klyne, W. and Djerassi, C. (1961). J. Amer. Chem. Soc., 83, 4013.

Monod, J., Wyman, J. and Changeux, J.P. (1965). J. Mol. Biol., 12, 88.

Morris, E.R. and Sanderson, G.R. (1972). In New Techniques in Biophysics and Cell Biology, (Pain, R., Smith, B. eds.) p.113 (Wiley, London).

Morris, E.R., Rees, D.A. and Thom, D. (1973). JCS Chem. Comm.,245.

Moscowtiz, A. (1960). In Optical Rotation Dispersion. (Djerassi, C. ed.), p.150, McGraw Hill.

Némethy, G. and Scheraga, H.A. (1965). Biopolymers, 3, 155.

Ng Ying Kin, N.M.K. and Yaphe, W. (1972). Carbohyd. Res., 25, 379.

Ogston, A.G. and Stanier, J.E. (1951). Biochem. J., 49, 585.

Orentas, D.G., Sloneker, J.H. and Jeanes, A. (1963). Can. J. Microbiol., 9, 427.

Partridge, S.M., Davis, H.F. and Adair, G.S. (1961). Biochem. J., 79, 15.

Pauling, L. and Corey, R.B. (1953). Proc. Nat. Acad. Sci. U.S.A., 39, 253.

Perlin, A.S., Casu, B., Sanderson, G.R. and Johnson, L.F. (1970). Can. J. Chem., 48, 2260.

Perlin, A.S., Ng Ying Kin, N.M.K., Bahattacharjee, S.S. and Johnson, L.F. (1972). Can. J. Chem., 50, 2437.

Pessac, B. and Defendi, V. (1972a). Science, 175, 898.

Pessac, B. and Defendi, V. (1972b). Nature New Biol., 238, 13.

Preston, B.N., Davies, M. and Ogston, A.G. (1965). Biochem. J., 96, 449.

Ramachandran, G.N., Ramakrishna, C. and Sasisekharan, V. (1963). In Aspects of Protein Structure, (Ramachandran, G.N., ed.) (New York: Academic Press).

Rao, V.S.R., Sundararajan, P.R., Ramakrishnan, C. and Ramachandran, G.N. (1967). In Conformation of Biopolymers, (Ramachandran,G.N. ed.) p.721 (Academic Press: London).

Rasmussen, P.S. (1954). Acta Chem. Scand., 8, 633.

Rees, D.A. (1969). J. Chem. Soc., B., 217.

Rees, D.A. (1970). J. Chem. Soc., B., 877.

Rees, D.A. (1972). In MTP International Review of Science: Organic Chemistry series 1, 7, (Aspinall ,G.O. ed.) Butterworth's, London.

Rees, D.A. and Skerrett, R.J. (1968). Carbohyd. Res., 7, 334.

Rees, D.A., Steele,I.W. and Williamson, F.B. (1969). J. Polymer Sci., C., 28, 261.

Rees, D.A., Scott, W.E. and Williamson, F.B. (1970). Nature, 227, 390.

Rees, D.A. and Skerrett, R.J. (1970). J. Chem. Soc., B., 189.

Rees, D.A. and Scott, W.E. (1971). J. Chem. Soc., B., 469.

Reeves, R.E. (1949). J. Amer. Chem. Soc., 71, 215.

Reeves, R.E. (1951). Advan. Carbohyd. Chem., 6, 107.

Rocks, J.K. (1971). Food Technol., 25, 476.

Roden, L. (1970). In Balazs 1970a, p.797.

Sathyanarayana, B.K. and Rao, V.S.R. (1970). Biopolymers, 10, 1605.

Schellman, J.A. (1966). J. Chem. Phys., 44, 55.

Scott, J.E. (1960). Methods of Biochem. Anal., 8, 145.

Scott, J.E. (1970). In Balazs 1970a, p.1105.

Seifter, S. and Gallop, P.M. (1966). In The Proteins, 2nd ed., Vol. 4, (Neurath, H., ed.) Academic Press, New York.

Sharon, N. (1965). In The Amino Sugars, Vol. IIA, p.1 (Balazs, E.A. and Jeanloz, R.W., eds.) New York, Academic Press.

Siddiqui, I.R. (1967). Carbohyd. Res., 4, 284.

Siddiqui, I.R. (1967a). Carbohyd. Res., 4, 277.

Silpananta, P., Dunstone, J.R. and Ogston, A.G. (1968). Biochem. J., 109, 43.

Sheard, B. and Bradbury, E.M. (1970). Progr. Biophys. Mol. Biol., 20, 187.

Slodki, M.E. (1967). In McGraw-Hill Yearbook Science and Technology, p.315.

Sloneker, J.H. and Jeanes, A. (1962). Can. J. Chem., 40, 2066.

Sloneker, J.H. and Orentas, D.G. (1962). Can. J. Chem., 40, 2188.

Sloneker, J.H., Orentas, D.G. and Jeanes, A. (1964). Can. J. Chem., 42, 1261.

Slonaker, J.H., Orentas, D.G., Knutson, C.A., Watson, P.R. and Jeanes, A. (1968). Can. J. Chem., 46, 3353.

Smith, P.J.C. (1972). Ph. D. Thesis, University of Edinburgh.

Srinavasa, S.R., Dolan, P., Radhakrishnamurthy, B. and Berenson, G.S. (1972). Prep. Biochem., 2, 83.

Stacey, M. and Barker, S.A. (1960). Polysaccharides of Micro-organisms, Oxford University Press, London.

Stone, A.L. (1969). In Structure and Stability of Biological Macromolecules (Biological Macromolecules Series), Vol. 2. (Fasman, G. and Timasheff, S. eds.) Dekker, New York.

Stone, A.L. (1971). Biopolymers, 10, 739.

Sugeta, H. and Miyazawa, T. (1967). Biopolymers, 5, 673.

Sundararajan, P.R. and Marchessault, R.H. (1972). Can. J. Chem., 50, 792.

Sutherland, I.W. (1972). Advances in Microbial Physiology, 8, 143.

Swann, D.A. (1968). Biochim. Biophys. Acta, 156, 17.

Swann, D.A. (1969). Biochem. Biophys. Res. Comm., 35, 571.

Sylvén, B. and Ambrose, E.J. (1955). Biochem. Biophys. Acta, 18, 587.

Thom, D. (1973). Ph. D. Thesis, University of Edinburgh.

Varga, L. (1955). J. Biol. Chem., 217, 651.

Watson, J.D. and Crick, F.H.C. (1953). Nature (London), 171, 737.

Wellman, K.M., Briggs, W.S. and Djerassi, C. (1965). J. Amer. Chem. Soc., 87, 73.

Whittington, S. (1971). Macromols., 4, 569.

Wiffen, D.H. (1956). Chem. and Ind., 964.

Wilkinson, J.F. (1958). Bacteriol. Rev., 22, 46.

Williamson, F.B. (1970). Ph. D. Thesis, University of Edinburgh.

Wolfrom, M.L., Vercellotti, J.R., Tomamatsu, H. and Horton, D. (1964). J. Org. Chem., 29, 540.

Zimm, B.H. and Bragg, J.K. (1958). J. Chem. Physics, 28, 1246.

APPENDIX 1

Construction of Beevers Model of Hyaluronate

Computer model building yields a set of Cartesian coordinates for each atom in one strand of the double helix. A two dimensional representation of one strand of the helix can be obtained graphically (e.g. Fig. 2.17 , p. 86).

Strand 1 (rising from non reducing end)

Take an atom, usually a glycosidic oxygen as an origin e.g. O(3)', the glycosidic oxygen in the 1 β 3 linkage. The next O(3)' up the strand is displaced by 0.84 nm (projected length of one disaccharide residue) and rotated through 90° in a left-handed sense (since four fold repeat). Thus looking down the strand

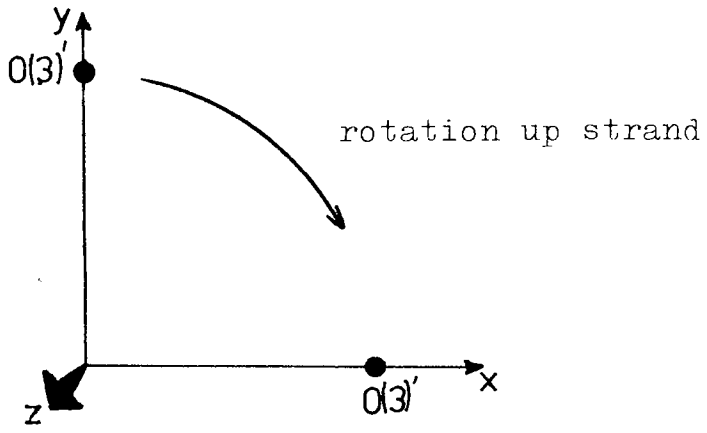

In between is O(4) (the glycosidic oxygen in the 1 β 4 linkage) displaced from the preceding O(3)' atom by 0.422 nm and rotated in a LH sense by 33° relative to O(3)'.

The rotation and displacement of O(4) are obtained from the coordinates of O(3)' and O(4).

For example:

	x	y	z
O(3)'	4.0669	0	0
O(4)	2.5292	-1.6064	4.2152

Displacement = $^{z}(04') - {}^{z}(03')$

= 4.2152Å i.e. 0.422 nm

Rotation = $\tan^{-1} \frac{x(04)}{y(04)}$

= $\tan^{-1} \frac{1.6064}{2.5290}$ = 33°

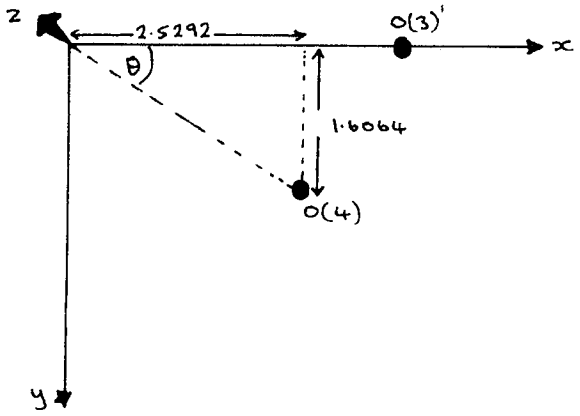

Thus for O(3)' - O(4) d = 0.422 nm

$\theta = 33^{\circ}$

O(4) - O(3)' d = 0.418 nm

$\theta = 57^{\circ}$

repeated up the length of the strand.

Strand 2 (falling from non-reducing end)

The coordinates of the second anti-parallel strand are generated by the formulae:

$x' = x \cos \theta - y \sin \theta$

$y' = -(x \sin \theta + y \cos \theta)$

$z' = -(z + d)$

where x, y, z are the Cartesian coordinates of any atom in Strand 1, x', y', z' are the coordinates of the equivalent atom in Strand 2.

Θ = rotation in anticlockwise sense of the second strand with respect to the first (looking from the reducing to non-reducing end of the first strand).

d = displacement of an atom in the second strand from an identical atom in the first strand.

For example

Consider glycosidic oxygen O(3)'(in the 1 β 3 linkage)

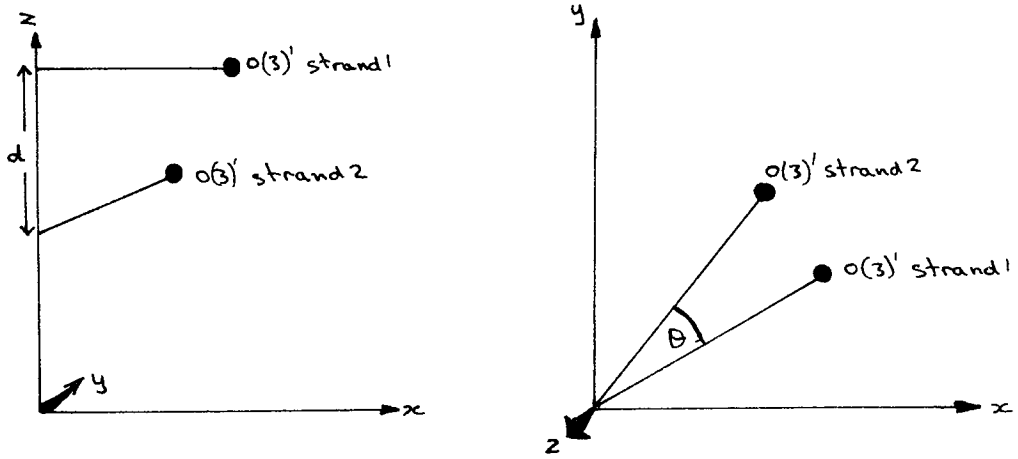

Θ and d are obtained from the hard sphere map produced by the computer (Fig.). This shows allowed regions for a double helix in terms of displacement along helix axis and rotation about this axis.

From the hard sphere map for inter-strand contacts a reasonable fit is when:

d = 14.0Å and Θ = +5° but other possibilities do exist in the same region.

Translation to the physical model

Beevers ball and spoke models (scale 1 cm = 0.1 nm) of the glucuronic acid and N-acetyl glucosamine residues were obtained pre-assembled. However, it was necessary to have the glycosidic oxygen atoms specially drilled at the correct calculated angles and fitted with bonds of the correct length. Thanks are due to Dr. Beevers for the speed and efficiency with which he supplied these specially drilled atoms during the construction of several possible models.

The model can be conveniently supported on a central 9 mm clear perspex rod by metal rods of calculated length running from the glycosidic oxygen atoms. A procedure was evolved for simply and rapidly drilling the support for the two chains.

1. Looking down the rod the rising strand rotates clockwise for an LH helix.

2. A card template fitting over the end of the rod is marked with the angles between O(3)' and O(4) i.e.

looking down model

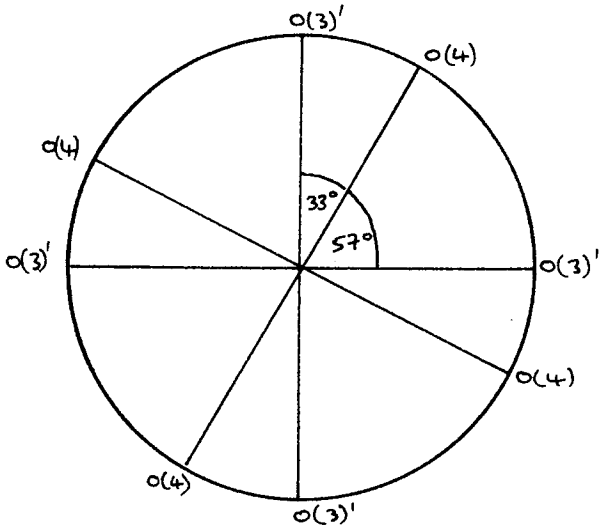

3. The first hole is drilled to half the thickness of the rod, let this be O(3)'. A O(3)' bond is inserted and the angle template aligned with the rod covering the O(3) line.

4. The O(3)' - O(4) distance (4.22 cm) is measured up the rod.

5. The rod is rotated through 33° i.e. in an anticlockwise direction looking down the rod, lining up the drill with the O(4) line on the template.

6. The O(4) - O(3)' distance (4.18 cm) is measured, the rod rotated through 57° and drilled.

7. Continue up the rod for the length of helix required.

8. It is then necessary to fix the position of the second strand with respect to the first. Pick a bond atom say O(3)' in strand 1 near the non-reducing end. Measure the calculated displacement 14 cm towards the reducing end of strand 1. Using a template with the rotation angle marked, line up with O(3)' on strand 1 and rotate clockwise through 5°. This gives O(3)' on strand 2.

9. Using an angle template the second strand is built up from here in reverse i.e. from reducing to non-reducing end.

10. Insert all the glycosidic oxygens and attach the sugar ring between to complete the model. Correct alignment of the residues can be checked with a helix plot (e.g. Fig. 2.17, p 86).

Appendix 2

The number of disaccharide units in the structured regions of hyaluronate

From Fig. 3.21 (p 153) the number of disaccharide units in each structured region can be estimated, as follows:

Consider the first 40 min of the reaction. The probability of a bond undergoing cleavage is 1.3×10^{-4} min $^{-1}$ (slope of lower curve in Fig. 3.21). It can be assumed that this applies equally to bonds in structured and unstructured regions because the cleavage rate is independent of the proportion of structured regions during the first 24 hours. The probability that a disaccharide unit will change its environment from structured to unstructured is the initial slope of the upper curve in Fig. 3.21, viz. 3.8×10^{-3} min^{-1}. Allowing for the fact that only 50% (on average) of the units are structured during this period it follows that cleavage of one bond in a structured region causes $(3.8 \times 10^{-3}/0.5 \times 1.3 \times 10^{-4}) \sim 60$ disaccharide units to change their environment from structured to unstructured. The reaction is two-state, i.e. residues are either structured or unstructured - this is shown by the fact that the high resolution nmr spectrum grows in intensity without gradual linewidth changes. This observation renders unlikely the possibility of structured regions containing 60 n disaccharide units and requiring the cleavage of n bonds to release the structure, since then the cleavage of $n - 1$ bonds would be expected to cause partial release. ~~It follows that the structured regions containing 60 n disaccharide units and requiring the cleavage of n bonds simultaneously to release the structure, since then the cleavage of n - 1 bonds would be~~

~~expected to cause partial release.~~ It follows that the structured regions contain about 60 disaccharide units, on average, and that cleavage of one bond in a structured region causes complete loss of structure.